IntechOpen

Flow Cytometry

Select Topics

Edited by Ingrid Schmid

FLOW CYTOMETRY - SELECT TOPICS

Edited by **Ingrid Schmid**

Flow Cytometry - Select Topics
http://dx.doi.org/10.5772/59733
Edited by Ingrid Schmid

Contributors

Gary Warnes, Gerardo Barroso, Maria Schönberg, Denise Schlorke, Juergen Arnhold, Tulay Kilicaslan Ayna, Maria De Lourdes Pereira, Helena Oliveira, Henrique M.A.C. Fonseca, Fernando Garcia E Costa, Conceição Santos, Hassan Kassassir, Karolina Siewiera, Tomasz Przygodzki, Magdalena Labieniec-Watala, Cezary Watala, Francesco Mannelli

Notice

First published in Croatia, 2016 by INTECH d.o.o.
eBook (PDF) Published by IN TECH d.o.o.
Place and year of publication of eBook (PDF): Rijeka, 2019.
IntechOpen is the global imprint of IN TECH d.o.o.
Printed in Croatia

Legal deposit, Croatia: National and University Library in Zagreb

Additional hard and PDF copies can be obtained from orders@intechopen.com

Flow Cytometry - Select Topics
Edited by Ingrid Schmid

p. cm.

Print ISBN 978-953-51-2550-1

Online ISBN 978-953-51-2551-8

eBook (PDF) ISBN 978-953-51-5445-7

Meet the editor

Ingrid Schmid, Mag. Pharm. is an Academic Research Specialist in the Department of Medicine at the University of California at Los Angeles and the technical director of the UCLA Flow Cytometry Resource which she established in 1989 in conjunction with Dr. Janis Giorgi. She received her Pharmaceutical Sciences degree from the University of Vienna, Austria. Ms. Schmid has a broad perspective on applications of various flow cytometry techniques and has developed numerous flow cytometry methods. She has published twenty-seven first-author papers, reviews, and book chapters, has co-authored an additional thirty-one publications, and has edited two books. Ms. Schmid is a member of the International Society for the Advancement of Cytometry Biosafety Committee and has served as its Chair between 1997 and 2007.

Contents

Preface XI

Chapter 1 **Sperm Flow Cytometry: Beyond Human Fertilization and Embryo Development 1**
Gerardo Barroso, Alexia Alvarez and Carlos Valdespin

Chapter 2 **The Role of Cytometry for Male Fertility Assessment in Toxicology 13**
Maria de Lourdes Pereira, Helena Oliveira, Henrique M.A.C. Fonseca, Fernando Garcia e Costa and Conceição Santos

Chapter 3 **Only the Truth Would Enlighten Us—The Advantages and Disadvantages of Flow Cytometry as a Method of Choice in the Study of Mouse and Rat Platelets 31**
Hassan Kassassir, Karolina Siewiera, Tomasz Przygodzki, Magdalena Labieniec-Watala and Cezary Watala

Chapter 4 **The Multiplexing of Assays for the Measurement of Early Stages of Apoptosis by Polychromatic Flow Cytometry 85**
G. Warnes

Chapter 5 **Effects of WF10 on Glycosaminoglycan Sulphation in Proinflammatory Monocytes and Macrophages 101**
Maria Schönberg, Denise Schlorke and Jürgen Arnhold

Chapter 6 **Immunophenotyping of Acute Leukemias – From Biology to Clinical Application 115**
Francesco Mannelli

Chapter 7 **Detection of Anti-HLA Antibodies by Flow Cytometer 131**
Tülay Kılıçaslan Ayna and Aslı Özkızılcık Koçyiğit

Preface

Advances in cell biology have always been closely linked to the development of critical quantitative analysis methods. Flow cytometry is such a pivotal methodology. It can be applied to individual cells or organelles allowing investigators interested in obtaining information about the functional properties of cells to assess the differences among cells in a heterogeneous cell preparation or between cells from separate samples. It is characterized by the use of a select wavelength of light (or multiple ones) to interrogate cells or other particles one at a time providing statistically relevant, rapid correlated measurements of multiple parameters with excellent temporal resolution. These intrinsic attributes, as well as advances in instrumentation and fluorescent probes and reagents, have contributed to the tremendous growth of applications in flow cytometry and to the world-wide expansion of laboratories which use this technology since its inception in the late 1960s.

This publication titled Flow Cytometry - Select Topics reflects these facts as indicated by the global author panel and the range of sample types, assays, and methodologies described. The book will give readers an opportunity to refresh or up-date their knowledge in specific subject areas of flow cytometry.

Ingrid Schmid, Mag. Pharm
University of California at Los Angeles
Los Angeles, USA

Chapter 1

Sperm Flow Cytometry: Beyond Human Fertilization and Embryo Development

Gerardo Barroso, Alexia Alvarez and
Carlos Valdespin

Additional information is available at the end of the chapter

http://dx.doi.org/10.5772/64344

Abstract

Male infertily is a contributing factor in up to 50% of all infertility cases, a solo cause in about 30% of them. Therefore, new and improved diagnostic methods that reduce operator variability regarding sperm defects that are not accesible by the conventional microscope scoring should be evaluated. Assisted reproductive technology (ART) has been involved in the description of alternative pathways in basic cellular functions. it is important to know that it is also related to the peri-implantatory processes that involve the sperm-oocyte interaction, cellular changes observed during fertilization, and the early and late embryo development. Several pathways have been involved at the early stages of human gametogenesis. The spermatozoon has demonstrated an intricate correlation during the fertilization process, as a transfected vector on genetic material, and as interacting with other inner components (RNAm, mitochondrial organelles, etc.). Spermatogenesis is affected by programmed death cell pathways from its packaging process through the elongated cytoplasmic structures during spermiogenesis. Flow cytometry (FC) has been an outstanding tool with the capability to select human gametes to achieve a better reproductive condition. It has been applied as a diagnostic and therapeutic tool allowing a measurable and objective selection and discrimination of spermatozoa from subfertile subjects. Using FC, we are able to know that early distribution of organelles such as mitochondria has an impact in embryo quality before genetic activation on the eight-cell stages occurs. This chapter will let the readers know the current knowledge on sperm fertilization and the relation between the embryo development and the offspring and all the tools now available for an early diagnosis and to identify therapeutic options with FC.

Keywords: sperm, spermatozoa, flow cytometry, fertilization, embryo development, apoptosis, DNA fragmentation

1. Introduction

During the previous decades, the understanding of human reproductive processes has been newly addressed since the implementation of assisted reproductive technology (ART). In twenty-first century, novel data from cellular and molecular diagnostic techniques in the reproductive field play a primary role. ART has been involved in the description of alternative pathways in basic cellular functions not only in early reproductive processes as gametogenesis but also in peri-implantatory processes involving the sperm-oocyte interaction, cellular changes observed during fertilization and the early and late embryo development. The implementation of the flow cytometry (FC) in this field has contributed to the understanding of all of these processes as well as to the standardization of a growing number of both diagnostic techniques and therapeutic approaches.

Several processes have been involved at the early stages of human gametogenesis; the spermatozoon has demonstrated an intricate correlation during the fertilization process, not just as transfected vector on genetic material, but also in the interaction of other inner components (RNAm, mitochondrial organelles, etc.). Spermatogenesis is affected by programmed death cell pathways, from its packaging process through the elongated cytoplasmic structures during spermiogenesis. Flow cytometry has been applied as a diagnostic and therapeutic tool allowing a measurable and objective selection and discrimination of spermatozoa from subfertile subjects. Nowadays, the use of *in-vitro* fertilization including micromanipulation techniques as the intracytoplasmic sperm injection (ICSI) has demonstrated a better embryo outcome, applying the use of these discriminating tools.

The acrosome reaction is a primary step during the sperm/oocyte interaction where the content of several enzymes will be delivered into the egg cytoplasm. The scoring of acrosome-reacted human sperm allows a more accurate, faster, and simpler method using FC. The process of sperm chromatin decondensation occurs when a spermatozoon enters an ovum where the interaction between male and female pronuclei has shown to be prognostic during the early stages of embryo development. Today, by using FC we know that early distribution of organelles as mitochondrial has an impact on embryo quality before genetic activation on stages of eight cells occurs. Furthermore, polarity and blastocyst development may be affected by the egg/sperm condition during the peri-implantatory process.

The potential of producing offspring of a predetermined sex has been a goal that exercised the imagination of mankind over many generations. A desire to predetermine sex is generally based on social values or a wish to avoid the potential conception of a child with an X-linked recessive disorder. This is now possible by the selection of spermatozoa using FC.

The main objective of this chapter is to address the current knowledge on sperm fertilization and its relationship with the embryo development and the offspring, showing the diagnostic and therapeutic opportunities using FC as an accurate and objective tool. The chapter is divided in three main subjects: the fertilizing spermatozoa, fertilization assessment, and evidence from ART.

http://dx.doi.org/10.5772/64344

2. Flow cytometry to explore human spermatozoa: reproductive impact

During the last decades, adverse, male reproductive health condition has been associated with an increase of testicular cancer, hypospadias, anatomical dysfunction, and abnormal semen parameters, together with an increased demand for ART [1, 2]. Male infertility diagnosis includes a visual assessment of semen analysis referred by the World Health Organization guidelines [3], which is not standardized and variability has been demonstrated among technicians and laboratories worldwide [4, 5]. Additionally, this subjective evaluation of sperm morphology, viability, motility, and number does not evaluate the entire sperm biological characteristics that may play a critical role during the egg-spermatozoa interaction, and no molecular or functional tests are applied routinely. As male infertility contributes up to 50% of the dysfunction reproductive process [6], development of new and improved diagnostic methods that reduce operator variability reflecting sperm defects not accessible by the conventional microscope scoring [1], becomes critical. The use of FC in this field represents an automated, rapid, sensitive, objective, multiparametric, and reproducible approach for the assessment of male infertility, especially in candidates for ART [7]. Because a flow cytometer can acquire thousands of events in seconds at a fixed flow rate, it could be used to determine sperm concentration [8]. Assessing cell number with FC is frequently performed using DNA dyes to differentiate between haploid mature cells, haploid round spermatids and diploid cells, in order to determine the total number in a known volume while assessing spermatogenesis [7, 9]. Good flow adjustment and the use of fluorospheres as internal control improve the reliability of spermatozoa numbers [10].

Sperm motility has been evaluated by FC using mitochondrial membrane potential markers to test the effects of cell sorting, swim-up, cryopreservation, and attempts to create populations enriched in highly motile spermatozoa [11–13]. Studies of cell viability have used a wide variety of vital stains as propidium iodine (PI) and ethidium homodimer [7–9]. These dyes enter cells with a broken plasmalemma, emitting red florescence when binding to nucleic acids [8]. Other viability probes as fluorescein diacetate and SYBR-14 emit green fluorescence upon entering metabolically active cells. The combination of PI/SYBR-14 is probably the most widely used to evaluate sperm viability [8].

3. Acrosome reaction: fertilizing spermatozoa-oocyte binding

It is generally accepted that to fertilize the egg, ejaculated spermatozoa must undergo capacitation, recognize and bind to the zona pellucida, and undergo the acrosome reaction. The most significant changes experienced by sperm during capacitation are plasma membrane changes, increase in certain intracellular messengers, and increased phosphorylation of a set of proteins by different kinases [14, 15].

The acrosome reaction is an exocytic process of spermatozoa and an absolute requirement for fertilization [16]. Numerous sperm plasma membrane candidates for zona pellucida-sperm

binding have been described [17], but only some of them have been shown to be involved in the induction of the acrosome reaction. *In vivo*, the acrosome reaction is induced by a zona pellucida glycoprotein (ZP3), which may act as a ligand for one or more sperm plasma membrane receptor(s), while a second protein, ZP2, facilitates the secondary binding of acrosome-reacted spermatozoa to the zona matrix penetration [18]. Several studies have found that sperm responsiveness to acrosome reaction inducers was reduced in infertile patients [19, 20] therefore, evaluation of acrosome reaction can be used to predict fertilization success and can be a great help in choosing the most appropriate technique of ART [16]. Acrosome intactness has been traditionally examined by using phase-contrast, fluorescent, or even electron microscopy. However, the FC can be used instead of microscopy allowing determination of acrosome reaction and its temporal occurrence, and the examination of large sperm numbers [21]. The probes labeled with fluorescent agents bind to mannose and galactose moieties of the acrosomal matrix. As probes cannot penetrate an intact acrosomal membrane, only acrosome-reacted or damage spermatozoa will stain [22]. The double staining for membrane integrity and acrosomal integrity is relatively reliable for fresh and *in vitro* capacitated sperm.

Additionally, the potential of FC to study the molecular and physiological changes that render the sperm able to fertilize has been demonstrated in different studies. For example, the function of CD46 on human sperm inner acrosomal membranes is to protect the spermatozoa from complement-mediated lysis. Carver et al. demonstrated that it is feasible a high fertilization prediction by flow cytometric analysis of the CD46 antigen [23]. Moreover, there is a recent study that shows that the capacitation-associated hyperpolarization of the sperm plasma membrane potential involves a decrease in Na^+ mediated by inhibition of epithelial Na^+ channels, and regulated by PKA [24].

4. The ubiquitin-proteasome pathway

The ubiquitin is a protein present in all cells with a nucleus. This protein forms covalent bonds to other proteins with an isopeptide that binds the C-terminal glycine of ubiquitin and the E-amino group of a lysine in substrate proteins. This phenomenon is called ubiquitination. The ubiquitination has been related to several fertilization processes, for example, during spermatogenesis, there is a replacement in the spermatid's nuclear histones by transition proteins and permanent protamines [25]. This process is also present in the spermatid elongation with a drastic reduction of the sperm centrosome. The ubiquitination normally occurs in the cell cytosol or nucleus, but sometimes, when there is a defective spermatozoa, it occurs on their surface during posttesticular sperm maturation in the epididymus [26]. The detection of the surface-ubiquitin helps to identify defective spermatozoa and has the potential to become a biomarker for infertility diagnostics [1]. Detecting and measuring ubiquitin expression can be as easy as getting a single semen sample [26].

http://dx.doi.org/10.5772/64344

5. Human spermatozoa related to abnormal fertilization and embryo development: evidence from ART

In-vitro fertilization (IVF) facilitates the interaction between gametes, but beyond the resolution of fertility dysfunction, it has been shown its biological diagnostic qualities in the fertilization process. Intracytoplasmic sperm injection (ICSI) is a technique where the mature spermatozoon is injected into a metaphase II oocyte, it is regularly used in cases of male factor infertility. With this technique, the impact of the microinjection should be established to determine the safety of the process, and also the long-term possible consequences. This is because in ICSI many processes from natural fertilization are skipped.Although successful fertilization is unequivocally dependent upon multiple inherent qualities of the oocyte [27, 28], in the last two decades, several lines of evidence resulting from the use of ART provided initial support for the concept of paternal contribution to faulty fertilization and abnormal embryogenesis. The first days, the new zygote depends on the oocyte's endogenous information, initiating the cleavage divisions. Afterward, when the embryo is in a four to eight cell stage, the transcription starts. That is why the sperm nuclear defects are not regularly detected before an eight-cell stage embryo, time when a bigger expression of sperm genes started.

Sperm cytoplasm deficiencies can be detected in the single-cell zygote and then throughout the preimplantation development [29]. It is supposed that the early paternal effect may include sperm abnormalities related to activation of the oocyte (no sperm delivery or dysfunctional oocyte-activating factor) and aberrations of the centrosome-cytoskeletal device. Moreover, it is seen that the late paternal effect is connected to sperm alterations in the DNA chromatin and also probably in sperm mitochondrial or mRNAs delivery abnormalities.

The abnormalities related to genomic imprinting alterations can be presented in early and late paternal effects. Strong evidence associates the presence of abnormal sperm parameters (particularly teratozoospermia, but also oxidative damage and DNA fragmentation) with failed or delayed fertilization and, importantly, to aberrant embryo development.

Ejaculated human spermatozoa may present various degrees of DNA damage. Different theories have been proposed to explain its origin [30–32]:

(1) Harm could occur at the moment of DNA packing or can be the result of it during the transition of histone to protamine complex in toe spermiogenesis process; (2) the DNA fragmentation could be the consequence as well of direct oxidative damage that has been associated with xenobiotics, antioxidant depletion, smoking, heat exposure, presence of ions in sperm culture media, leukocyte contamination of semen, and (3) DNA damage that could be the consequence of apoptosis. The evidence of apoptosis in ejaculated spermatozoa could be the effect of several types of injuries [31, 32]. *In vivo*, apoptosis could be triggered at the testicular (hormonal depletion, irradiation, toxic agents, chemicals, and heat have been shown to induce apoptosis), epididymal (the result of signals released by abnormal and/or senescent spermatozoa or by leukocytes, such as reactive oxygen species and other mediators of inflammation/infection), or seminal (reactive oxygen species, lack of antioxidants, or other causes) levels. In addition, apoptosis could be triggered by factors present in the female tract.

In vitro, apoptosis is induced by incubation with inadequate culture media or different kind of manipulation procedures. Independently of the stimulus, spermatozoa that goes through apoptosis is not recognized by current methods. On the other hand, this spermatozoa could have the risk to transfer a damaged genome into the egg, and as a consequence having a poor embryo development, miscarriage, or birth defects [31].

For many years, it has been known that the chromatin of the mature sperm nucleus can be abnormally packaged [33]. In addition, abnormal chromatin packaging and nuclear DNA damage appear to be linked, and there is a strong association between the presence of nuclear DNA damage in the mature spermatozoa and poor semen parameters [31, 34, 35]. Endogenous basis in DNA are regularly expressed at particular stages of spermiogenesis in different animal species; these endogenous basis are present during spermiogenesis but they are not evident once chromatin packaging is completed. It is known that topoisomerase 11, an endogenous nuclease, forms and binds nicks to release torsional stress and fix chromatin rearrangement during protamination [36–38].

Several studies have demonstrated that sperm DNA quality has a robust power to predict fertilization *in vitro* [39–41]. Tomlinson et al. show that the only parameter that presented a significant difference between pregnant and nonpregnant groups in IVF was the amount of DNA fragmentation assessed by *in situ* nick translation.

The sperm chromatin structure assay (SCSA) has been considered as a diagnostic option to define fertilization by the evaluation of DNA stability. SCSA criterion is related to fertilization, blastocyst formation, and ongoing pregnancy in *in vitro* fertilization and ICSI cycles [42]. This assay measures susceptibility to DNA denaturation *in situ* in sperm exposed to acid for 30 s followed by acridine orange staining, and the use of FC in the SCSA increases its dependability [43, 44]. Moreover, evaluation of chromatin condensation with FC has demonstrated that swim-up and percoll gradient centrifugation methods improve the percentage of spermatozoa with normal chromatin structure in some samples with poor initial quality [45].

The expression of sperm apoptotic-like markers can be rapidly evaluated using FC and differences have been found in individuals with normal and abnormal sperm parameters [46–49]. One of the early steps of apoptosis is the translocation of phosphatidylserine from the inner to the outer leaflet of the plasma membrane, which can be detected by sperm annexin V labeling. Currently, annexin V is available conjugated with a wide variety of fluorochromes to perform sperm FC analysis. Increased membrane permeability is another indicator of apoptosis and there are several dyes that are combined to identify membrane-undamaged spermatozoa with increased membrane permeability. The combination of annexin V with PI permits the identification of apoptosis-like changes and spermatozoa with compromised plasma membrane. This two parameters identify four categories of sperm: live, live early "apoptotic", dead and late "apoptotic", and late "necrotic" cells using FC [21]. Flow cytometric analysis of DNA fragmentation evaluated by terminal deoxynuceotidyl transferase-mediated UTD nick-end labeling (TUNEL) measures changes at the later stage (late apoptosis), while annexin V/PI measure early sperm apoptosis-like changes [21].

Caspases are the central components in the apoptosis signaling cascade. Members of this family of cysteine proteases have been found in their inactive and active states in spermatozoa [50]. The detection of activated caspases in living spermatozoa can be performed by using fluorescence labeled inhibitors of caspases, which are cell permeable and noncytotoxic [50]. Active caspases will form a covalent bond with the reagent, so retain the fluorescent signal within the cell and can be easily detected by FC. Any unbound inhibitor leaves the sperm [51].

6. Gender DNA-based spermatozoa sex selection

Evidence of regular methods of preconceptional gender selection show that *in vivo* methods such as timed intercourse, ovulation induction, and artificial insemination do not affect the sex ratio in a clinically significant percentage. *In vitro* separation of X- and Y-bearing spermatozoa by gradient methods change significantly the sex ratio at birth. Nevertheless, these trials were non controlled, and molecular biological techniques were not able to prove that these methods changed the Y- to X-bearing spermatozoa ratio significantly for clinical use. However, recent scientific studies have made reliable preconceptional sex selection possible by using preimplantation diagnosis or sperm separation by FC combined with IVF. Actually, these methods are used to avoid sex-linked disorders. The two of them include in vitro fertilization as an invasive procedure and most of them do not have a medical and therapeutical indication. Both involve the invasive procedure of IVF and thus are held by most as inappropriate for non-medical indications. The improvement in FC output of selected X and Y spermatozoa could bring in the future sufficient selected gametes for artificial insemination. This technique will provide a viable noninvasive technique for the selection of sex for social purposes.

FC for gender selection is based on the variability of chromatin staining by DNA-binding fluorescent dye Hoechst 33342, detecting the fluorescence from individual cells, and classifying individual cells based on fluorescence. Afterward, selected spermatozoa are used for based on polymerase chain reaction (PCR) or FISH on treated spermatozoa, or by biopsy of the developing embryo (preimplantation genetic diagnosis, PGD).

Main concerns regarding safety of sorting technique are the possible hazards imposed especially on the DNA of the spermatozoa. A chemical compound is used that binds to DNA and emits energy in form of light when hit by a laser beam. Also the laser beam transmit energy to the atoms inside and around DNA. This excessive energy with the combination of many chemical compounds, and water, may create molecular species that can break other molecular junctions and cause damages in DNA. In the mature sperm head, there are no mechanisms to fix the damaged DNA; this situation only takes place in the egg after fertilization. The higher the number of disruptions of the DNA, the higher number of the error probabilities.

In 1998, Fugger et al. presented births of normal female after sperm sorting techniques and subsequent IUI, IVF, or ICSI. Indications were sex-linked disorders or family balancing. From 27 patients that were treated in 33 cycles with X-sorted spermatozoa, seven pregnancies were after IVF or ICSI treatment. IUI was performed in 208 cycles in 92 patients. The results were 22 clinical pregnancies, of which seven ended in spontaneous miscarriage, one of them was an ectopic pregnancy, and 12 of them were still ongoing when the study was published. Nine of

the pregnancies terminated in eleven healthy children. In 17 cases where the sex was known at the time of publication 15 were female. In a subsequent report on 332 patients, 96 pregnancies were achieved in 663 cycles; desired gender was obtained in 94% (37/39) of cases for parents desiring females and in 73% (11/15) of cases for those desiring males. At publication, 47 pregnancies were ongoing.

7. Perspectives for sperm flow cytometry

In the last two decades, FC has revolutionized the perspective of reproductive biology. Several dogmas have changed not just in the understanding of sperm-oocyte interaction, but mainly in the fertilization process. Assisted reproductive technology has provided to be efficient helping infertile couples and to raise this reproductive goals, we have to understand the molecular network related to the human model. Flow cytometry has been an outstanding tool with the capability to select human gametes to achieve a better reproductive condition. Moreover, FC has made clear these processes under the molecular understanding, but primarily for the clinical application. Human fertilization and embryo development are a wide field where for the next years, we will be witnesses of the offspring modulation and the FC will still being an outstanding resource.

Author details

Gerardo Barroso[1,2*], Alexia Alvarez[3,2] and Carlos Valdespin[3,2]

*Address all correspondence to: barrosog@me.com

1 Medical Director, Center for Reproduction and Clinical Research, Nascere, Mexico City, Mexico

2 Obstetrics and Gynecology Department, American British Cowdray Hospital, Mexico City, Mexico

3 Medical Associated, Center for Reproduction and Clinical Research, Nascere, Mexico City, Mexico

References

[1] Cordelli E, Eleuteri P, Leter G, Rescia M, Spanò M. Flow cytometry applications in the evaluation of sperm quality: semen analysis, sperm function and DNA integrity. Contraception. 2005;72(4):273–9.

[2] Jensen TK, Carlsen E, Jørgensen N, Berthelsen JG, Keiding N, Christensen K, Petersen JH, Knudsen LB, Skakkebaek NE. Poor semen quality may contribute to recent decline in fertility rates. Hum Reprod. 2002;17(6):1437–40.

[3] World Health Organization. WHO Laboratory Manual for the Examination of Human Semen and Sperm-cervical Mucus Interaction. 4th Ed: Cambridge University Press, 2010.

[4] Barroso G, Mercan R, Ozgur K, Morshedi M, Kolm P, Coetzee K, Kruger T, Oehninger S. Intra- and inter-laboratory variability in the assessment of sperm morphology by strict criteria: impact of semen preparation, staining techniques and manual versus computerized analysis. Hum Reprod. 1999;14(8):2036–40.

[5] Ferrara F, Daverio R, Mazzini G, Bonini P, Banfi G. Automation of human sperm cell analysis by flow cytometry. Clin Chem. 1997;43(5):801–7.

[6] Barroso G, Morshedi M, Oehninger S. Analysis of DNA fragmentation, plasma membrane translocation of phosphatidylserine and oxidative stress in human spermatozoa. Hum Reprod. 2000;15(6):1338–44

[7] Garrido N, Meseguer M, Remohi J, Pellicer A, Simón C. Flow cytometry in human reproductive biology. Gynecol Endocrinol. 2002;16(6):505–21.

[8] Martínez-Pastor F, Mata-Campuzano M, Alvarez-Rodríguez M, Alvarez M, Anel L, de Paz P. Probes and techniques for sperm evaluation by flow cytometry. Reprod Domest Anim. 2010;45 Suppl 2:67–78.

[9] Levek-Motola N, Soffer Y, Shochat L, Raziel A, Lewin LM, Golan R. Flow cytometry of human semen: a preliminary study of a non-invasive method for the detection of spermatogenetic defects. Hum Reprod. 2005;20(12):3469–75.

[10] Eustache F, Jouannet P, Auger J. Evaluation of flow cytometric methods to measure human sperm concentration. J Androl. 2001;22(4):558–67.

[11] Kramer RY, Garner DL, Bruns ES, Ericsson SA, Prins GS. Comparison of motility and flow cytometric assessments of seminal quality in fresh, 24-hour extended and cryopreserved human spermatozoa. J Androl. 1993;14(5):374–84.

[12] Troiano L, Granata AR, Cossarizza A, Kalashnikova G, Bianchi R, Pini G, Tropea F, Carani C, Franceschi C. Mitochondrial membrane potential and DNA stainability in human sperm cells: a flow cytometry analysis with implications for male infertility. Exp Cell Res. 1998;241(2):384–93.

[13] Auger J, Leonce S, Jouannet P, Ronot X. Flow cytometric sorting of living, highly motile human spermatozoa based on evaluation of their mitochondrial activity. J Histochem Cytochem. 1993;41(8):1247–51.

[14] Storey BT. Interactions between gametes leading to fertilization: the sperm's eye view. Reprod Fertil Dev. 1995;7(4):927–42.

[15] Visconti PE, Bailey JL, Moore GD, Pan D, Olds-Clarke P, Kopf GS. Capacitation of mouse spermatozoa. I. Correlation between the capacitation state and protein tyrosine phosphorylation. Development. 1995;121(4):1129–37.

[16] Patrat C, Serres C, Jouannet P. The acrosome reaction in human spermatozoa. Biol Cell. 2000;92(3–4):255–66.

[17] Wassarman PM. Mammalian fertilization: molecular aspects of gamete adhesion, exocytosis, and fusion. Cell. 1999;96(2):175–83.

[18] Aitken RJ. Sperm function tests and fertility. Int J Androl. 2006;29(1):69–75

[19] Baldi E, Luconi M, Bonaccorsi L, Krausz C, Forti G. Human sperm activation during capacitation and acrosome reaction: role of calcium, protein phosphorylation and lipid remodelling pathways. Front Biosci. 1996; 15;1:d189–205.

[20] Tomlinson MJ, Moffatt O, Manicardi GC, Bizzaro D, Afnan M, Sakkas D. Interrelationships between seminal parameters and sperm nuclear DNA damage before and after density gradient centrifugation: implications for assisted conception. Hum Reprod. 2001;16(10):2160–5.

[21] Hossain MS, Johannisson A, Wallgren M, Nagy S, Siqueira AP, Rodriguez-Martinez H. Flow cytometry for the assessment of animal sperm integrity and functionality: state of the art. Asian J Androl. 2011;13(3):406–19.

[22] Cross NL, Morales P, Overstreet JW, Hanson FW. Induction of acrosome reactions by the human zona pellucida. Biol Reprod. 1988;38(1):235–44.

[23] Carver-Ward JA, Jaroudi KA, Hollanders JM, Einspenner M. High fertilization prediction by flow cytometric analysis of the CD46 antigen on the inner acrosomal membrane of spermatozoa. Hum Reprod. 1996;11(9):1923–8.

[24] Escoffier J, Krapf D, Navarrete F, Darszon A, Visconti PE. Flow cytometry analysis reveals a decrease in intracellular sodium during sperm capacitation. J Cell Sci. 2012;125(Pt 2):473–485

[25] Baarends WM, Hoogerbrugge JW, Roest HP, Ooms M, Vreeburg J, Hoeijmakers JH, Grootegoed JA. Histone ubiquitination and chromatin remodeling in mouse spermatogenesis. Dev Biol. 1999;207(2):322–33.

[26] Sutovsky P. Ubiquitin-dependent proteolysis in mammalian spermatogenesis, fertilization, and sperm quality control: killing three birds with one stone. Microsc Res Tech. 2003;61(1):88–102

[27] Van Blerkom J. Intrafollicular influences on human oocyte developmental competence: perifollicular vascularity, oocyte metabolism and mitochondrial function. Hum Reprod. 2000;15 Suppl 2:173–88.

[28] Swain JE, Pool TB. ART failure: oocyte contributions to unsuccessful fertilization. Hum Reprod Update. 2008;14(5):431–46.

[29] Tesarik J, Greco E, Mendoza C. Late, but not early, paternal effect on human embryo development is related to sperm DNA fragmentation. Hum Reprod. 2004;19(3):611–5.

[30] Sakkas D, Mariethoz E, St John JC. Abnormal sperm parameters in humans are indicative of an abortive apoptotic mechanism linked to the Fas-mediated pathway. Exp Cell Res. 1999;251(2):350–5.

[31] Aitken RJ, De Iuliis GN. Value of DNA integrity assays for fertility evaluation. Soc Reprod Fertil Suppl. 2007;65:81–92.

[32] Oehninger S, Morshedi M, Weng SL, Taylor S, Duran H, Beebe S. Presence and significance of somatic cell apoptosis markers in human ejaculated spermatozoa. Reprod Biomed Online. 2003;7(4):469–76.

[33] Evenson DP, Darzynkiewicz Z, Melamed MR. Relation of mammalian sperm chromatin heterogeneity to fertility. Science. 1980;210(4474):1131–3.

[34] Cayli S, Sakkas D, Vigue L, Demir R, Huszar G. Cellular maturity and apoptosis in human sperm: creatine kinase, caspase-3 and Bcl-XL levels in mature and diminished maturity sperm. Mol Hum Reprod. 2004;10(5):365–72.

[35] Sun JG, Jurisicova A, Casper RF. Detection of deoxyribonucleic acid fragmentation in human sperm: correlation with fertilization in vitro. Biol Reprod. 1997;56(3):602–7.

[36] McPherson S, Longo FJ. Chromatin structure-function alterations during mammalian spermatogenesis: DNA nicking and repair in elongating spermatids. Eur J Histochem. 1993;37(2):109–28.

[37] Sakkas D, Manicardi G, Bianchi PG, Bizzaro D, Bianchi U. Relationship between the presence of endogenous nicks and sperm chromatin packaging in maturing and fertilizing mouse spermatozoa. Biol Reprod. 1995;52(5):1149–55.

[38] Chen JL, Longo FJ. Expression and localization of DNA topoisomerase II during rat spermatogenesis. Mol Reprod Dev. 1996;45(1):61–71.

[39] Duran EH, Morshedi M, Taylor S, Oehninger S. Sperm DNA quality predicts intrauterine insemination outcome: a prospective cohort study. Hum Reprod. 2002; 17(12): 3122–8.

[40] Larson KL, DeJonge CJ, Barnes AM, Jost LK, Evenson DP. Sperm chromatin structure assay parameters as predictors of failed pregnancy following assisted reproductive techniques. Hum Reprod. 2000;15(8):1717–22.

[41] Chan PJ, Corselli JU, Patton WC, Jacobson JD, Chan SR, King A. A simple comet assay for archived sperm correlates DNA fragmentation to reduced hyperactivation and penetration of zona-free hamster oocytes. Fertil Steril. 2001;75(1):186–92.

[42] Virro MR, Larson-Cook KL, Evenson DP. Sperm chromatin structure assay (SCSA) parameters are related to fertilization, blastocyst development, and ongoing pregnancy

in in vitro fertilization and intracytoplasmic sperm injection cycles. Fertil Steril. 2004;81(5):1289–95.

[43] Evenson D, Darzynkiewicz Z, Jost L, Janca F, Ballachey B. Changes in accessibility of DNA to various fluorochromes during spermatogenesis. Cytometry. 1986;7(1):45–53.

[44] Evenson DP. Flow cytometric analysis of male germ cell quality. Methods Cell Biol. 1990;33:401–10.

[45] Golan R, Shochat L, Weissenberg R, Soffer Y, Marcus Z, Oschry Y, Lewin LM. Evaluation of chromatin condensation in human spermatozoa: a flow cytometric assay using acridine orange staining. Mol Hum Reprod. 1997;3(1):47–54.

[46] Oosterhuis GJ, Mulder AB, Kalsbeek-Batenburg E, Lambalk CB, Schoemaker J, Vermes I. Measuring apoptosis in human spermatozoa: a biological assay for semen quality?. Fertil Steril. 2000;74(2):245–50

[47] Ricci G, Perticarari S, Fragonas E, Giolo E, Canova S, Pozzobon C, Guaschino S, Presani G. Apoptosis in human sperm: its correlation with semen quality and the presence of leukocytes. Hum Reprod. 2002;17(10):2665–72.

[48] Sakkas D, Moffatt O, Manicardi GC, Mariethoz E, Tarozzi N, Bizzaro D. Nature of DNA damage in ejaculated human spermatozoa and the possible involvement of apoptosis. Biol Reprod. 2002;66(4):1061-7.

[49] Wang X, Sharma RK, Sikka SC, Thomas AJ Jr, Falcone T, Agarwal A. Oxidative stress is associated with increased apoptosis leading to spermatozoa DNA damage in patients with male factor infertility. Fertil Steril. 2003;80(3):531–5.

[50] Grunewald S, Sharma R, Paasch U, Glander HJ, Agarwal A. Impact of caspase activation in human spermatozoa. Microsc Res Tech. 2009;72(11):878–88.

[51] Vaux DL, Korsmeyer SJ. Cell death in development. Cell. 1999;96(2):245–54.

Chapter 2

The Role of Cytometry for Male Fertility Assessment in Toxicology

Maria de Lourdes Pereira, Helena Oliveira,
Henrique M.A.C. Fonseca,
Fernando Garcia e Costa and Conceição Santos

Additional information is available at the end of the chapter

http://dx.doi.org/10.5772/62965

Abstract

Infertility is nowadays a major concern, affecting approximately 8–12% of the couples and the male factor accounts for about 50% of the cases. Occupational and/or environmental exposure to heavy metals and other pollutants is the main cause of male infertility. Lead, cadmium and chromium are heavy metals widely used in industry and quite persistent in the environment, raising major concerns over the possible effects on the reproductive health of workers and the general population. Sperm DNA integrity is essential for the accurate transmission of paternal genetic information, and normal sperm chromatin structure is important for sperm fertilizing ability. Flow cytometry can be to characterize multiple physical characteristics of the population of spermatozoa in the sperm, including sperm concentration, viability, mitochondrial mass and function, acrosome integrity, capacitation, membrane fluidity, DNA content and status, etc. This chapter elucidates the role of cytometry in the study of male fertility under toxicological insult by pollutants such as chromium, cadmium and lead. Some representative examples are presented using in vivo studies with rodents. In addition, complementary techniques to cytometry and future perspectives will be mentioned in an interdisciplinary point of view to gain knowledge on this subject.

Keywords: cytometry, male fertility, sperm analysis, heavy metals, toxicology

1. Introduction

Extensive use of heavy metals in some sectors of industry and its long persistence in the environment has been taken as an important factor affecting male fertility. The male infertility results from a combination of factors that include sperm DNA integrity. Spermatozoa may contain a variety of nuclear alterations including chromosome aberrations, DNA sequence modifications, DNA chemical modifications and DNA strand breaks. DNA breaks can arise spontaneously during chromatin remodeling on spermiohistogenesis and are usually repaired under normal circumstances. However, multifactorial pressures may lead to the occurrence of abnormal sperm DNA breaks.

Flow cytometry (FCM) is a powerful technique which allows the simultaneous measurement and analysis of multiple physical characteristics of single particles, usually cells, as they flow in a fluid stream through a beam of light tuned at a particular wavelength. FCM is used to determine sperm concentration, viability, mitochondrial mass and function, acrosome integrity, capacitation, membrane fluidity, DNA content and status, etc. DNA fragmentation assessed by the terminal deoxylnucleotidyl transferase-mediated deoxyuridine triphosphate nick-end labelling (TUNEL) assay and chromatin integrity evaluated by sperm chromatin structure assay (SCSA) are extremely important flow cytometry–based tools to evaluate the impact of toxicants on male fertility.

In the field of male reproductive health, the role of cytometry, among other techniques for semen analysis, was reported by several authors [1–3]. Some elegant reviews focus on the relevant role of FCM on animal and human spermatology [4, 5]. They give an insight into FCM as a useful tool in the analysis of semen so indispensable for the artificial insemination of livestock and breeding programs in industry, as well as its application in assisted human reproductive technology. These authors not only discuss the potential of FCM in the diagnosis of fertility potential, but also elaborate on the development of current technologies of reproduction, such as sperm freezing, sperm selection and sperm sorting.

This chapter discusses the role of cytometry in the study of male infertility exposed to toxicants such as chromium, cadmium and lead. Representative example using in vivo rodent studies will be presented to demonstrate the applicability of flow cytometry techniques.

2. General concepts of analytical cytology

Analytical cytology, or quantitative cytometry, is a discipline that allows an innovative vision of the cell. Despite being recent, it is closely linked to the long history of microscopy and to the historical development of FCM and image cytometry. The evolution of cytometry (and cytomics) relies on advances of disciplines such as dye chemistry (allowing the development of new fluorochromes), electronics and software (allowing more powerful computer-based analyses).

The study of cytomes within an -omics perspective combines a multiparametric and statistics-based approach. Eventually, cytomics may be considered an ultimate expression of functional

genomics. This emerging and multidisciplinary discipline can and should bridge the gap between quantitative disciplines of molecular/-omics biology and other disciplines of cyto-histology, cell biology and physiology.

Analytical cytology is strongly based on two major approaches: FCM and microscopy-associated cytometry (image cytometry/analysis and imaging flow cytometry). In each of these research techniques, cells can be measured one at a time in an automated device. In FCM, measurements are taken in a flow cytometer, as particles pass one by one in a narrow liquid stream through an illuminated flow chamber. Thus, FCM offers unique advantages, particularly its statistical potential, as it allows multi-parametric analysis of a large number of individuals in a given population and the objective detection and characterization of (sub)populations. However, when using FCM, one loses the three-dimensional perspective of the structure where the cells are inserted. Recently, new technology has been developed by combining in a single instrument the speed and sample size of FCM with the resolution and sensitivity of microscopy. This hybrid technology, often called of image stream, offers the advantages of both image and flow cytometry, particularly in studies, for example, of cell morphology or internalization and trafficking.

In the image cytometry/analysis method, slides containing cells are scanned and each cell image is analyzed on an electronic imaging and analysis system, which with appropriate software allows the measurement of physical/chemical cell features of interest. These analytical imaging techniques offer huge potential for dimensional and spatial organization, but they usually allow only restricted number of sampling.

Imaging flow cytometry introduced a quantum leap to cytometry flow analysis by adding the resolution and sensibility of light microscopy with robust statistical analysis of FCM. This technology allows the development of gating strategies where morphological characteristics (including those enhanced by multicolor staining), fluorescence, advanced fluidics control and the power of statistical analysis are used to resolve details that normally fall within the noise of FCM machines. In the literature, there are many examples of the use of imaging flow cytometry applied to diverse areas of research showing gains compared with the FCM [6–8].

Equipping a FCM laboratory requires high initial investment, but nowadays more affordable flow cytometers can be found in the market. In addition to the general advantages described above for FCM (e.g., speed, statistical potential, rare subpopulation detection), sample preparation is extremely simple and rapid, the cost of consumables is very low, and the rapidity of analyses allows that several samples to be run within a short period. Furthermore, small amounts of material are required (e.g., 50 mg or less), different tissues are suitable for analyses (e.g., for DNA analyses, there is no need for mitotically active cells), and although fresh samples are always recommended, often good results can be achieved with few days old samples or even using fixed or dried material.

3. Flow cytometry and flow cytometers

The first primitive equipment for FCM was developed in the years 1940–1950 by Wallace Coulter initially for aerosol analyses or blood cell counting. Later, Mark Fulwyler (US Los

Alamos National Laboratories) added to the Coulter principle for cell size analyses, an ingenious idea of sorting electric charged droplets that contained the desired cells [9].

The advances in fluorescence from the late 1960s broadened the research applications enabling multiparametric analysis of cells, and the first commercial fluorescence flow cytometers appeared in 1970s. Since then, several and increasingly powerful and sensitive flow cytometers have been developed (for example, BD Biosciences® CA, USA; Coulter Beckman Coulter CA, USA; Sysmex Partec GmbH, Germany), together with devices with specific applications, such as portable and marine flow cytometers. Simultaneously, the first commercial cell sorter (fluorescence-activated cell sorter) was developed.

A FCM is composed of several components, namely optical, fluidic, electronic, computational and mechanical systems. In the fluidic system, the suspension of particles flowing at high speed are hydrodynamically focused to flow one by one in the flow chamber (or flow cell) where they are intersected by the light source. This hydrodynamic focusing is achieved by one of two methods: using another fluid (sheath fluid) that surrounding the sample stream at a different speed but does not mix with the sample (laminar flow); or by acoustic focus (acoustic-assisted hydrodynamic focusing) using the ultrasonic radiation pressure (>2 MHz) to transport the particles into the center of the sample stream.

An alternative to the enclosed stream and hydrodynamic focus is the "jet-in-air" design, common in most cell sorters, where the sample stream exits the flow chamber into open air through narrow orifices.

The optical system consists of narrow very stable laser beams that illuminate the particles, and each particle response (light scatter and/or fluorescence) is used to measure their physical-chemical characteristics. The most common light sources are argon ion lasers (emitting at 488 nm) and helium-cadmium lasers usually emitting in the blue (442 nm) or in the UV (325 nm) regions. More recent cytometers are equipped with more efficient light-emitting diodes and solid-state lasers, which give greater accuracy within a wither spectral range [10, 11].

In response to the incidence of the laser beam, particles scatter the light both as *forward scatter*, FS (light scattered at narrow angles to the laser beam axis) and *side scatter*, SS (light scattered at approximately a 90° of the laser beam). These are two important characterization parameters: FS gives rough information of the particles size, while the SS informs on the internal granularity and the surface roughness.

Particles may also emit fluorescent light at specific wavelengths that can be separated by appropriate optical filters. Several filters may be used: the *long-pass* and *short-pass* filters transmit light, respectively, above and below a specific wavelength, while the *band-pass* filters transmit light within a certain range of wavelengths. Dichroic mirrors are also used to selectively pass light within a small range of wavelengths while reflecting others.

Light emitted from particles is collected by photodiodes (typically used for forward scatter channel detection) and photomultiplier tubes (they are two different photon collection devices), which convert the light they receive into a proportional voltage pulses.

These pulses are then amplified, integrated, and analyzed by a computer-based electronic system. Amplified signals are linearly or logarithmically transformed and then converted from analog continuous voltages into discrete digital data through an analog-to-digital converter. Typically, conventional instruments had 10-bit ADCs, but more recent instruments are equipped with higher 14-bit ADCs, resolution that is divided into 1024 channels scale. Data are then displayed, analyzed and stored by the computational system in list modes that contain all measurements of each particle. The resulting histograms or cytograms provide a global and easy-reading information of all particle (sub)populations; diverse software are also available for further FCM data analysis (e.g., gating, histogram/cytogram overlay) and statistics.

FCM is constantly evolving. For example, to circumvent the problematic correlation of FS with particle size, which often is not true, new FCM equipment provide an *electronic volume* parameter, instead of the classical FS parameter, which is more accurate for the particle size range. Also, in order to combine the statistical advantages of FCM and the image analyses of microscopy systems, new equipments have CCD cameras integrated.

Currently, most flow cytometers compute and directly provide, for example, histograms (univariate for single parameters or bivariate histograms/cytograms when multiparametric parameters are simultaneously analyzed); and the ratios of a distinct subpopulation of cells in relation to others and/or to the total. If suitable markers are used, resolving specific types of fluorescence, rare subpopulations may be separated in a proportion as low as 1 cell in 10^7.

4. Most relevant parameters in toxicological assays

The main parameters in toxicological assays are DNA content, DNA ploidy and cell cycle analyses; cell viability and death; mitochondrial membrane potential and oxidative stress and ROS.

4.1. Quantification of DNA, ploidy and cell cycle analyses

Both ploidy and genome size determinations are important in clinical and biological sciences. In general, FCM genome sizes are usually expressed in picogram of DNA (pg) per 2C (or C) or as the number of base pairs (Mbp) assuming that 1 pg = 0.978×10^9 bp. DNA ploidy and, less often, the quantification of DNA are one of the most widely used applications in FCM. The quality of a DNA histogram, given by the coefficient of variation which depends on the peak width of the G_0/G_1 peak of DNA cycle, is crucial to estimate the DNA content.

Several aspects must be considered when performing DNA analyses by FCM, as they may condition the quality of the results. Particularly important are the source and preservation of the biological material, the use of a reliable standard, the selection of an adequate buffer solutions, the selection of suitable fluorochromes and the proper exclusion of clumped cells/nuclei.

Fluorochromes such as propidium iodide (PI, stoichiometrically intercalates with nucleic acids; excitation at 530 nm and emitting at 620 nm) or DAPI (diaminophenylindole, stains

regions rich in A/T; excitation 360 nm in the ultraviolet region, and emission 460 nm) are the most widely used DNA fluorochromes, not only to quantify DNA content (only PI is suitable as a stoichiometric stain), but also for studies on DNA ploidy and cell cycle dynamics.

4.2. Cell viability and death

Viability vs. apoptotic vs. necrotic cells are among the most used analyses in flow cytometry. A main difference between apoptotic and necrotic cells is that the former have intact plasma membrane, whereas the later have lack of membrane integrity. Therefore, PI fluorochromes, which are excluded by integral membranes, as in cells undergoing apoptosis can enter the necrotic cells. Other fluorochromes are retained by intact membranes, as, for example, the fluorescein diacetate (FDA, excitation 488 nm, emission 530 nm) that penetrates the membrane and inside the cell is converted by viable cells to fluorescein. Thus, the combination of multiple fluorochromes will allow separate different subpopulations according to their staining profiles.

FCM also allows to discriminate between early and late apoptotic subpopulations in addition to necrotic cells. A particularly useful technique for assessing early apoptosis is the use of phosphatidylserine (PS) residues (typical of the cytoplasmic side of the plasma membrane) that during apoptosis are exposed to the external side of the membrane. By adding fluorescently labeled Annexin V, which binds to PS, only those cells with externalized PS will stain as positive. It is common to combine Annexin V with PI and/or with other fluorochromes.

It should be noted that in late apoptosis, cells become increasingly permeable to fluorochromes as PI or Hoechst 33342 (excitation 352 nm, emission 461 nm), such as with necrotic cells, late apoptosis can be marked as positive for these staining (which, however, will decrease as DNA is also degraded). Other parameters include detecting proteins as caspases, using fluorochrome-conjugated probes (e.g., anti-PARP antibodies, fluorogenic substrate for the detection of activated caspases).

Another parameter widely used to monitor apoptosis, DNA fragmentation, is determined by TUNEL assays. This technique uses an enzyme, terminal deoxynucleotidyl transferase (TdT) that adds labelled nucleotides to the 5′ ends of the fragments of DNA in apoptotic cells. These labeled nucleotides, often BrdUTP, are proportional to the amount of fragmented DNA present in the apoptotic cells.

4.3. Mitochondrial membrane potential

Mitochondrial assays by flow cytometry allow to determine mitochondrial changes often associated with apoptotic pathways. Several fluorochromes are retained by mitochondria, being the most widely used the rhodamine 123 (common excitation at 507 nm and emission 529 nm) and MitoRed (common values of excitation around 560 nm, and of emission around 580 nm). When the mitochondrial membrane potential decreases by loss of integrity, the fluorochrome redistributes resulting in signal loss. Alternatively, some fluorochromes, for example, 5,5′,6,6′-tetrachloro-1,1′,3,3′-tetraethylbenzimidazolylcarbocyanine iodide (JC-1), may shift from red (in healthy cells; excitation ~535 nm, emission ~595 nm) to green (excitation

~485 nm, emission ~535 nm) depending on the state of aggregation of the fluorochrome (e.g., [12]).

4.4. Oxidative stress and ROS

Another process closely associated with various events in the cell (e.g., stress, aging, apoptosis, etc.) is oxidative stress. Normal cells have basal levels of reactive oxygen species (ROS) in a complex homeodynamic balance. Using this oxidative potential, compounds such as 2′,7′-dichlorodihydrofluorescein diacetate (DCFH-DA) are used to study these key events. The cell-permeable DCFH-DA (nonfluorescent when reduced) is retained inside the cells and, when hydrolyzed by cellular esterases, emits fluorescence when oxidized by ROS.

5. Flow cytometry and other techniques: the case study of sperm analyses

Potential applications of flow cytometry for the evaluation of sperm functions and genetic integrity were reviewed by Oliveira et al. [13].

The following section outlines some examples of the application of flow cytometry to study the toxicity of chromium, cadmium and lead on mice spermatozoa.

5.1. Counts

FCM can be used to automatically evaluate sperm concentrations based on sperm suspension mixture with a known concentrations of fluorospheres [14]. Another approach combines gating sperm cells based on light scattering proprieties, forward scatter and side scatter, which are related with cell size and granularity, respectively (**Figure 1**), and DNA staining [15]. Sperm concentration is then calculated as the ratio of sperm cells to fluorosphere counts and fluorosphere concentration. This methodology allows a more accurate evaluation of sperm concentration than usual counts performed with a hemocytometer. Based on Oliveira

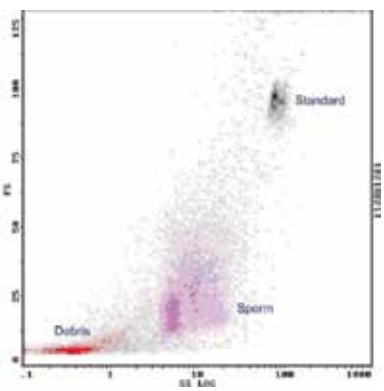

Figure 1. Flow cytometry cytogram showing the identification of a sperm cells population of ICR-CD1 mice based on light scatter. FS, particle size; SS LOG, internal granularity and surface roughness.

et al. [16], **Figure 2** shows an example of the effect of cadmium chloride exposure on male mice, obtained by FCM.

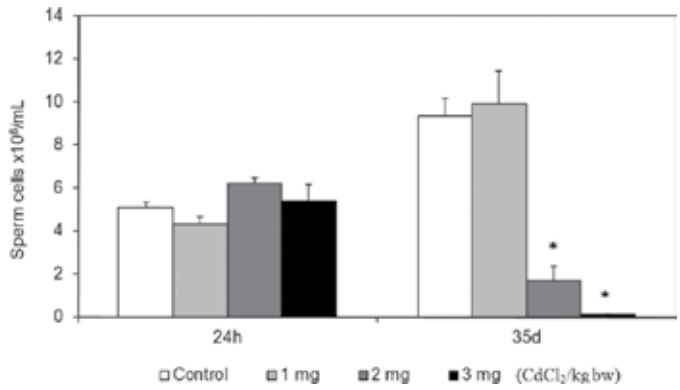

Figure 2. Effect of a single subcutaneous administration of cadmium chloride at 1, 2, or 3 mg/kg body weight (bw) to ICR-CD1 mice on the sperm concentration. Animals were sacrificed 24 h or 35 days after the administration. Values represent mean ± standard deviation. Symbol * indicates significant difference between the control and treated animals to $p < 0.001$.

5.2. Viability

Sperm viability is usually evaluated by assessing the status of the plasma membrane, based on the differential membrane permeability of damaged sperm cells to fluorescent probes. For a review on used dyes such as PI, ethidium bromide (EtBr), ethidium homodimer-1 (EthD-1) and YOPRO-1, see Oliveira et al. [13].

The fluorescent probes are excluded by intact cell membranes but can enter and stain nuclei of cell with damaged membranes. Dyes such as Hoechst 33342 and 33258 are cell permeant (the first has a slightly higher permeability than the latter) and are also used to assess membrane status [17].

Acylated dyes are amphipathic probes that can pass the intact membrane and enter live sperm. These probes are readily deacylated inside the cell by intracellular non-specific esterases producing a fluorescent compound. If the cell membrane is intact, these fluorescent probes are entrapped within cells, and as membrane damage allows leakage of the probes and signal loss [13].

SYBR-14 [18] is an example of acylated membrane permeant DNA fluorochrome, which labels viable cells with functional ion pumps.

Cell viability can be estimated in a more accurate way using membrane impermeant and permeant stains in combination, for example, the LIVE/DEAD® sperm viability kit that combines SYBR-14 and PI. The SYBR-14 stains living spermatozoa green, whereas the PI stains dead or membrane-damaged spermatozoa red. A third population is often detectable, which is stained with both fluorochromes, and represents dying spermatozoa [13]. **Figure 3A** shows

http://dx.doi.org/10.5772/62965

an example of a flow cytometry cytogram of mice sperm cells stained with SYBR-14/PI, and **Figure 3B** shows the effect of cadmium chloride exposure on sperm viability. Our results show that despite the apparent tendency to a decline in sperm viability after exposure to cadmium chloride, the differences did not reach statistical significance.

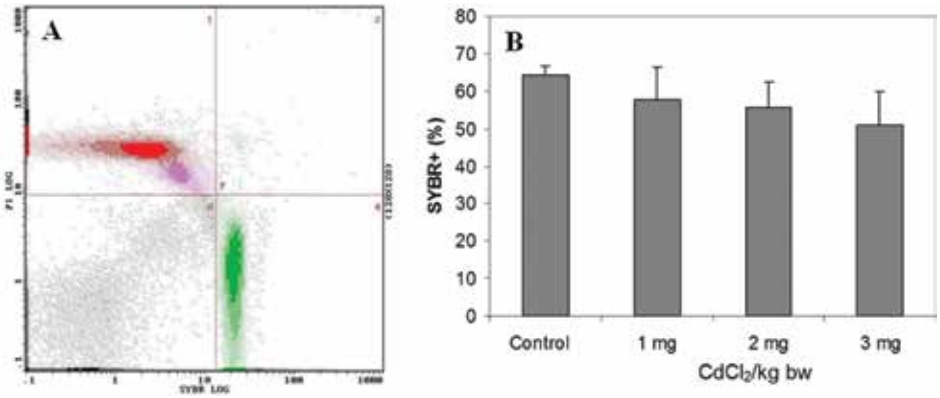

Figure 3. (A) Logarithmic flow cytometry cytogram of mice sperm stained with LIVE/DEAD sperm viability kit (SYBR-14/PI). SYBR-14 stains living spermatozoa green, whereas the PI stains red the dead or membrane damaged. A third population of dying sperm cells is represented in the cytogram in purple. (B) Effect of a single subcutaneous administration of cadmium chloride at 1, 2, or 3 mg/kg body weight (bw) to ICR-CD1 mice on the sperm viability. Mice were sacrificed 24 h after the administration. Values represent mean ± standard deviation.

5.3. Mitochondrial function

In sperm cells, mitochondria are arranged helicoidally in the midpiece of the sperm tail and are responsible for generating energy for the flagellar beat. Therefore, changes in mitochondrial membrane potential are a good indicator of functional impairment.

Mitochondria can be stained by specific fluorochromes for these organelles. Rhodamines and carbocyanines are the most usual compounds that are sensitive to mitochondria membrane potential (MMP). Rhodamine 123 (Rh123, excitation 507 nm, emission 529 nm) is a cationic fluorescent dye frequently used to indicate MMP [19]. However, Rh123 is not capable of distinguishing mitochondria with high and low membrane potential. The lipophilic cationic probe JC-1 is a special type of multimer of carbocyanine that in contrast to Rh123 is able to distinguish mitochondria with high and low membrane potential. In mitochondria with high membrane potential JC-1 forms multimers of J-aggregates that fluoresce orange (590 nm) when excited at 488 nm. In mitochondria with low membrane potential, JC-1 forms monomers that when excited at 488 nm emit in the green range (530 nm). MitoTracker fluorochromes, namely MitoTracker Green, MitoTracker Orange, MitoTracker Red 580, and MitoTracker Deep Red 633, are also used to evaluate sperm mitochondrial function [13]. Finally, 10-n-Nonyl Acridine Orange chloride (NAO), a mitochondrial-specific fluorochrome, which is MMP independent, is used to estimate mitochondrial mass in male germ cells [20]. An example is shown in **Figure 4A**, where mice sperm stained with Rh123/PI showed

that cells with functionally active mitochondria appear intensely stained in green for Rh123, whereas dead or membrane-damaged sperm cells satin red for PI. **Figure 4B** demonstrates the effect of a single subcutaneous administration of cadmium chloride at 1, 2 or 3 mg/kg body weight to ICR-CD1 mice on mitochondrial function. A significant decrease in sperm mitochondrial function was observed for the highest cadmium chloride dose.

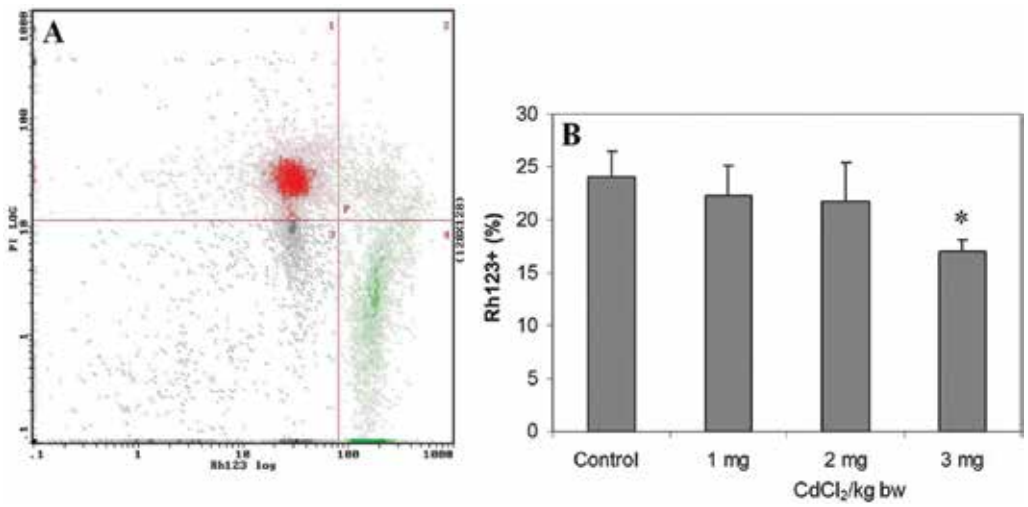

Figure 4. (A) Logarithmic flow cytogram of mice sperm stained with Rh123/PI. Functionally active mitochondria stain intensely for Rh123, whereas the PI stains red the dead or membrane-damaged sperm cells. (B) Effect of a single subcuteneous administration of cadmium chloride at 1, 2, or 3 mg/kg body weight (bw) to ICR-CD1 mice on mitochondrial function. Mice were sacrificed 24 h after the administration. Values represent mean ± standard deviation. Symbol * indicates significant difference between the control and treated animals to $p < 0.001$.

5.4. Flow cytometry for the evaluation of sperm DNA damage

Sperm DNA integrity is essential for the accurate transmission of paternal genetic information, and normal sperm chromatin structure is important for fertilizing capacity of spermatozoa [21–25].

Chromatin of mature sperm cells is highly condensed during spermatogenesis due to the replacement of nucleosomal histones by intermediate proteins and finally, by protamines [26]. Defects in sperm chromatin structure can be associated with abnormal nucleoprotein content and/or DNA strand breaks. However, it has been demonstrated that sperm with damaged DNA is able to fertilize the oocyte and form pronuclei [27], but embryonic development is dependent on the degree of DNA damage [28].

Several tests can be performed in order to evaluate sperm DNA integrity. The chromatin structure can be evaluated by the SCSA, AOT, CMA3, or toluidine blue assays. DNA fragmentation can be assessed by the TUNEL assay, the *in situ* Nick Translation assay, SCD or the comet assay as revised by Oliveira et al. [29].

5.5. Sperm chromatin structure assay—SCSA

5.5.1. $PbCl_2$/kg bw

Normal sperm development leads to a chromatin structure, which confers DNA resistance to denaturation; by contrast, DNA in regions within abnormal chromatin structure is susceptible to acid denaturation. The extension of DNA denaturation can be quantified by SCSA, which is a FCM assay developed by Evenson and co-workers [30] that measure the sperm DNA susceptibility to acid denaturation *in situ* [31].

SCSA is based on metachromatic proprieties of acridine orange that emits green fluorescence (515–530 nm) when intercalated to double-stranded native DNA and red fluorescence (630–640 nm) when bound to single-stranded denatured DNA. The DNA fragmentation index (DFI), which is the ratio of red fluorescence/(red + green) fluorescence, is calculated for each measured cell (usually 5–10,000). **Figure 5A** shows a typical SCSA cytogram of a sperm samples with low % DFI. Green fluorescence is from native DNA, whereas red fluorescence is from fragmented DNA. The effect of a daily administration of lead chloride at 74 and 100 mg/kg bw for four consecutive days to ICR-CD1 mice on % DFI is presented in **Figure 5B**. Results indicate that lead chloride treatment did not induce significant changes in DNA fragmentation assessed by the SCSA.

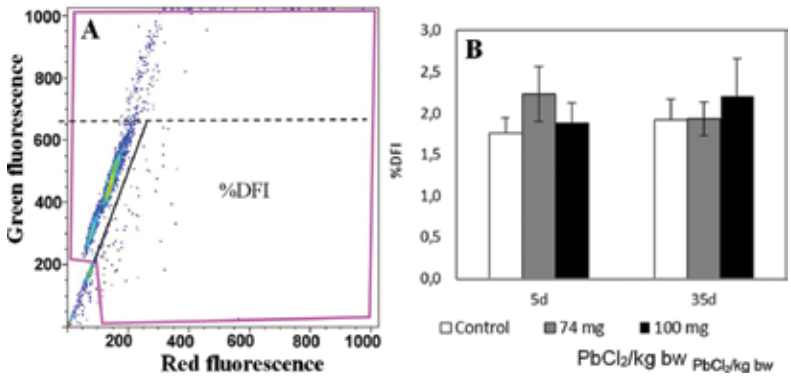

Figure 5. (A) Typical SCSA cytogram of a sperm samples with low % DFI. (B) Effect of a daily administration of lead chloride at 74 and 100 mg/kg body weight (bw) for four consecutive days to ICR-CD1 mice on sperm % DFI. Mice were sacrificed at day 5 and 35 of the assay. Values represent mean ± standard deviation.

5.6. Evaluation of DNA fragmentation-TUNEL assay

The TUNEL assay quantifies the incorporation of deoxyuridine triphosphate (dUTP) at free 3′-OH termini of single- and double-stranded DNA breaks in a reaction catalyzed by the template-independent enzyme, TdT. This assay allows simultaneous detection of both single- and double-strand breaks. The incorporated dUTP is chemically labelled so that breaks can be quantified either by fluorescence microscopy, light microscopy or flow cytometry, where sperm with DNA breaks shows positive after being subjected to TUNEL

reaction [32]. **Figure 6** shows an example of the effect of a daily administration of lead chloride at 74 and 100 mg/kg bw for four consecutive days to ICR-CD1 mice on percentage of sperm DNA fragmentation assessed by the TUNEL assay. Although the results show a trend towards an increase in sperm DNA damage in the presence of lead chloride, the differences did not reach statistical significance.

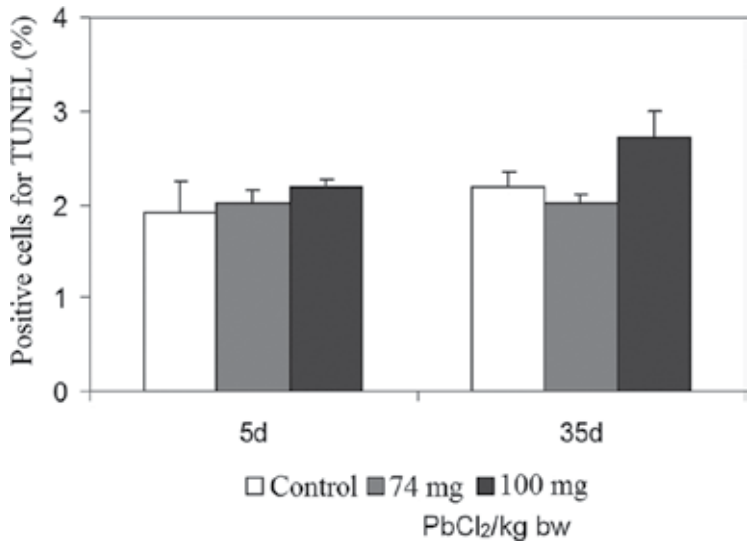

Figure 6. Effect of a daily administration of lead chloride at 74 and 100 mg/kg body weight (bw) for four consecutive days to ICR-CD1 mice on sperm % DNA fragmentation assessed by the TUNEL assay. Mice were sacrificed at days 5 and 35 of the assay. Values represent mean ± standard deviation.

5.7. Flow cytometry for the evaluation of the testicular subpopulations

The different populations of cells of testes can be isolated from fresh biopsies or from fixed and paraffin-embedded samples as described by Oliveira et al. [33]. Permeabilized cells or isolated nuclei are then stained with PI, or other DNA-staining dye, and then analyzed by flow cytometry. **Figure 7** represents a histogram of testes of control and exposed mice to $CdCl_2$ showing the distribution of subpopulation of cells. DNA histograms revealed four main peaks corresponding to different ploidy levels: the sub-haploid peak (HC) that consists of elongated spermatids and the haploid peak (1C) refers to round spermatids.

The discrimination of haploid nuclei into two peaks is due to differences in chromatin condensation. Elongated spermatids have highly condensed chromatin; therefore, PI intercalation with DNA is lower. Somatic cells, spermatogonia and secondary spermatocytes are recorded in the diploid peak (2C). Cells in the G2/M phase of the cell cycle and primary spermatocytes are included in the tetraploid peak (4C). The region between the diploid and the tetraploid peaks corresponds to cells actively synthesizing DNA (S phase). Administration of 3 mg $CdCl_2$/kg body weight decreased the number of haploid cells (round spermatids) and increased the percentage of diploid, tetraploid and cells in S phase (**Figure 7**).

http://dx.doi.org/10.5772/62965

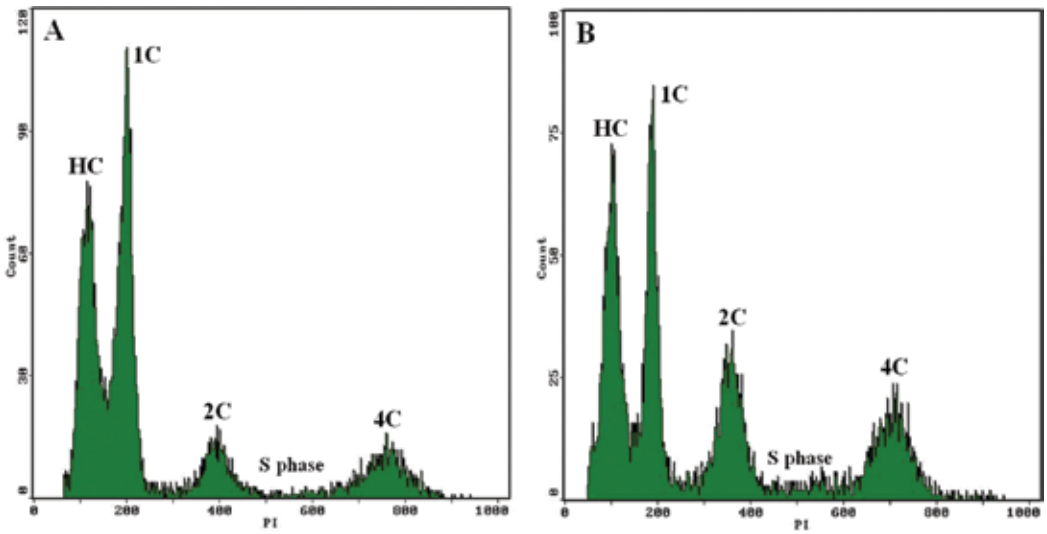

Figure 7. Flow cytometry histograms of nuclei isolated from ICR-CD1 mice testis from paraffin embedded tissue as described by Oliveira and co-workers [33]. Initially, to set up the instrument's acquisition conditions, chicken red blood cells were used as standards (not shown); thereafter, samples were run without the standard. (A) control, (B) exposed to 3 mg $CdCl_2$/kg body weight by subcutaneous injection for 24 h. PI, propidium iodide assay. HC, sub-haploid; 1C, haploid; 2C, diploid; and 4C, tetraploid peaks. Doublets were excluded in the cytogram linear fluorescence pulse integral versus linear fluorescence pulse height as described in Oliveira and co-workers [16, 33].

6. Conclusions and final remarks

In this chapter, we address some of the latest advances in functional cytometry applied to the analysis of sperm quality. Structural and functional cytometry has been a robust support for cellular functional analysis in numerous fields of biology and particularly in animal and human reproductive technologies. As outlined above, FCM comprises a set of technologies that enhance the potential of other fields and methods, namely does related to the reproductive management in animal husbandry, in specialized andrology laboratories, and in areas of reproductive toxicology.

FCM has enormous potential to explore complex biological matrices, such as semen through consistent evaluation of gamete quality. This will be achieved with the advances in hardware/instrumentation, reagent development and bioinformatics, allowing increasing automation and sophistication of polychromatic/multiple parameter data set analysis.

We reviewed here some recent applications of this technique in assessing fundamental endpoints in toxicological assays (including quantification of DNA, ploidy, cell cycle dynamics, cell viability and apoptosis/necrosis, mitochondrial membrane potential, or oxidative stress parameters). Moreover, we also demonstrated the validity of FCM in comparison with other techniques in assessing sperm analyses (counting, viability, sperm DNA damage, chromatin

structure, DNA fragmentation) and testicular subpopulations. Finally, we also stress that, in the foreseeable future, the expected developments in cytometry will produce major gains in the understanding of mechanisms of action of toxicants in animal models and in the field of toxicological diagnosis applicable to human clinical and will consolidate its value in providing cytological analytical data essential in a multidisciplinary approach (from genomics to functional biology).

Acknowledgements

This chapter was developed within the scope of the project CICECO-Aveiro Institute of Materials, POCI-01-0145-FEDER-007679 (Foundation for Science and Technology—FCT Ref. UID/CTM/50011/2013), financed by national funds through the FCT/MEC and when appropriate co-financed by FEDER under the PT2020 Partnership Agreement; and FCT Ref. UID/GEO/04035/2013. Also FEDER/COMPETE/POCI– Operacional Competitiveness and Internacionalization Programme, (POCI-01-0145-FEDER-006958) and FCT, UID/AGR/04033/2013. FCT awarded grant to Helena Oliveira (SFRH/BPD/111736/2015) is also acknowledged.

Author details

Maria de Lourdes Pereira[1*], Helena Oliveira[2], Henrique M.A.C. Fonseca[3], Fernando Garcia e Costa[4] and Conceição Santos[5]

*Address all correspondence to: mlourdespereira@ua.pt

1 Department of Biology and CICECO – Aveiro Institute of Materials, University of Aveiro, Aveiro, Portugal

2 Department of Biology and CESAM, University of Aveiro, Aveiro, Portugal

3 Department of Biology and GeoBioTec, University of Aveiro, Aveiro, Portugal

4 Department of Morphology and Function, CIISA Interdisciplinary Centre of Research in Animal Health, Faculty of Veterinary Medicine, University of Lisbon, Lisbon, Portugal

5 Department of Biology, GreenUP/Citab UP, University of Porto, Rua Campo Alegre, 4169-007 Porto, Portugal

References

[1] Niżański W, Partyka A, Rijsselaere T. Flow cytometry and state of the art in semen analyses in research and breeding management. Proceedings of the 7th International Symposium on Canine and Feline Reproduction—ISCFR, 2012. Whistler, Canada.

[2] Marchiani S, Tamburrino L, Olivito B, Betti L, Azzari C, Forti G, Baldi E, Muratori M. Characterization and sorting of flow cytometric populations in human semen. Andrology 2014; 2: 394–401.

[3] Sutovsky P. New Approaches to Boar Semen Evaluation, Processing and Improvement. Reproduction in Domestic Animals 2015; 50 (Suppl. 2): 11–19.

[4] Hossain MS, Johannisson A, Wallgren M, Nagy S, Siqueira AP, Rodriguez-Martinez H. Flow cytometry for the assessment of animal sperm integrity and functionality: state of the art. Asian Journal of Andrology 2011; 13: 406–419.

[5] Peña FJ. Multiparametric flow cytometry: a relevant tool for sperm function evaluation. Animal Reproduction 2015; 12(3): 351–355.

[6] George TC, Basiji DA, Hall BE, Lynch DH, Ortyn WE, Perry DJ, Seo MJ, Zimmerman CA, Morrissey PJ. Distinguishing modes of cell death using the ImageStream multispectral imaging flow cytometer. Cytometry A 2004; 59(2): 237–45.

[7] Basiji DA, Ortyn WE, Liang L, Venkatachalam V, Morrissey P. Cellular image analysis and imaging by flow cytometry. Clinics in Laboratory Medicine 2007; 27(3): 653–70.

[8] Headland SE, Jones HR, D'Sa ASV, Perretti M, Norling LV. Cutting-edge analysis of extracellular microparticles using ImageStreamX imaging flow cytometry. 2014; Scientific Reports 4: 05237-05237.

[9] Shapiro HM. Practical Flow Cytometry. New York: Wiley, 2005.

[10] Kapoor V, Karpov V, Linton C, Subach FV, Verkhusha VV, Telford WG. Solid state yellow and orange lasers for flow cytometry. Cytometry Part A 2008; 73A: 570–577.

[11] Lawrence WG, Varadi G, Entine G, Podniesinski E, Wallace PK. Enhanced red and near infrared detection in flow cytometry using avalanche photodiodes. Cytometry Part A 2008; 73A: 767–776.

[12] Christensen ME, Jansen ES, Sanchez W, Waterhouse NJ. Flow cytometry based assays for the measurement of apoptosis-associated mitochondrial membrane depolarisation and cytochrome c release. Methods 2013; 61(2): 138–145.

[13] Oliveira H, Spanò M, Santos C, Pereira ML. Flow Cytometric Analyses of Sperm Functions and Genetic Integrity. In: Glantz B. and Edquist K. (eds.) Male and Female Infertility: Genetic Causes, Hormonal Treatments and Health Effects, Edition: 1, Chapter: Nova Publishers, New York, 2009; pp. 1–32.

[14] Evenson DP, Parks JE, Kaproth MT, Jost LK. Rapid determination of sperm cell concentration in bovine semen by flow cytometry. Journal of Dairy Science 1993; 76: 86–94.

[15] Eustache F, Jouannet P, Auger J. Evaluation of flow cytometric methods to measure human sperm concentration. Journal of Andrology 2001; 22: 558–567.

[16] Oliveira H, Spanò M, Santos C, Pereira Mde L. Adverse effects of cadmium exposure on mouse sperm. Reproductive Toxicology 2009; 28(4): 550–555.

[17] Sutkeviciene N, Riskeviciene V, Januskauskas A, Zilinskas H, Andersson M. Assessment of sperm quality traits in relation to fertility in boar semen. Acta Veterinary Scandinavia 2009; 51: 53.

[18] Garner DL, Thomas CA, Joerg HW, DeJarnette JM, Marshall CE. Fluorometric assessments of mitochondrial function and viability in cryopreserved bovine spermatozoa. Biology of Reproduction 1997; 57: 1401–1406.

[19] Gravance CG, Garner DL, Miller MG, Berger T. Fluorescent probes and flow cytometry to assess rat sperm integrity and mitochondrial function. Reproductive Toxicology 2001; 15: 5–10.

[20] Petit JM, Ratinaud MH, Cordelli E, Spanò M, Julien R. Mouse testis cell sorting according to DNA and mitochondrial changes during spermatogenesis. Cytometry 1995; 19: 304–312.

[21] Collins JA, Barnhart KT, Schlegel PN. Do sperm DNA integrity tests predict pregnancy with in vitro fertilization? Fertility and Sterility 2008; 89: 823–831.

[22] Lewis SE, Agbaje I, Alvarez J. Sperm DNA tests as useful adjuncts to semen analysis. Systems Biology in Reproductive Medicine 2008; 54: 111–125.

[23] Zini A, Sigman M. Are tests of sperm DNA damage clinically useful? Pros and cons. Journal of Andrology 2009; 30: 219–229.

[24] Bungum M, Bungum L, Giwercman A. Sperm chromatin structure assay (SCSA): a tool in diagnosis and treatment of infertility. Asian Journal of Andrology 2011; 13: 69–75.

[25] Oleszczuk K, Giwercman A, Bungum M. Sperm chromatin structure assay in prediction of in vitro fertilization outcome. Andrology 2016. doi:10.1111/andr.12153

[26] Rathke C, Baarends WM, Awe S, Renkawitz-Pohl R. Chromatin dynamics during spermiogenesis. Biochimica and Biophysica Acta 2014; 1839(3): 155–168.

[27] Twigg JP, Irvine DS, Aitken RJ. Oxidative damage to DNA in human spermatozoa does not preclude pronucleus formation at intracytoplasmic sperm injection. Human Reproduction 1998; 13: 1864–1871.

[28] Ahmadi A, Ng SC. Developmental capacity of damaged spermatozoa. Human Reproduction 1999; 14: 2279–2285.

[29] Oliveira H, Spanò M, Santos C, Pereira ML. Lead chloride affects sperm motility and acrosome reaction in mice. Cell Biology and Toxicology 2009; 25: 341–353.

[30] Evenson DP, Darzynkiewicz Z, Melamed MR. Relation of mammalian sperm chromatin heterogeneity to fertility. Science 1980; 210: 1131–1133.

[31] Evenson D, Jost L. Sperm chromatin structure assay is useful for fertility assessment. Methods in Cell Science 2000; 22: 169–189.

[32] Takeda K, Uchiyama K, Kinukawa M, Tagami T, Kaneda M, Watanabe S. Evaluation of sperm DNA damage in bulls by TUNEL assay as a parameter of semen quality. Journal of Reproductive Development 2015; 61(3): 185–190.

[33] Oliveira H, Loureiro J, Filipe L, Santos C, Ramalho-Santos J, Sousa M, Pereira Mde L. Flow cytometry evaluation of lead and cadmium effects on mouse spermatogenesis. Reproductive Toxicology 2006; 22(3): 529–535.

Chapter 3

Only the Truth Would Enlighten Us—The Advantages and Disadvantages of Flow Cytometry as a Method of Choice in the Study of Mouse and Rat Platelets

Hassan Kassassir, Karolina Siewiera,
Tomasz Przygodzki,
Magdalena Labieniec-Watala and Cezary Watala

Additional information is available at the end of the chapter

http://dx.doi.org/10.5772/63473

Abstract

Increasing number of transgenic and knockout strains of laboratory rodents has been developed to provide reliable models of human cardiovascular diseases. Due to apparent differences in platelet physiology, morphology, biochemistry, etc. between rodents and men, methods employed to study blood platelets in rodents should always consider these differences in a reasonably critical way. Flow cytometry is a convenient tool that enables to easily cope with the minute amounts of the available biological material and providing an extremely versatile information. This review focuses on the practical and methodological aspects of flow cytometry, pointing to the key elements of the commonly used protocols for determining of multiple parameters of blood platelet (patho)physiology in mice and rats. We summarized and critically reviewed the available procedures, as well as figured out how to overcome possible obstacles, shortcomings, drawbacks or artefacts that a researcher may encounter when monitoring various phenomena intimately associated with blood platelet biology. Flow cytometry assays have been also collated with some alternative techniques (intravital fluorescence microscopy, *in vitro* platelet adhesion under flow conditions). We hope that our paper may further facilitate other researchers to study mouse and rat platelets with the use of the most optimal and the least artefact-prone procedures.

Keywords: flow cytometry, mouse, platelets, rat, rodents

1. Introduction

Among various laboratory animals, mice and rats offer several benefits that make them convenient tools for preclinical *in vitro* and *in vivo* studies. Considering the variety of available methods used to study blood platelet activation and/or reactivity, flow cytometry seems an attractive technique that largely counterbalances the constraints of using rodents and as such it enables outcomes of laboratory research to be transferred successfully to clinical practice. However, the use of flow cytometry in the study of platelet function in laboratory rodents, such as mice and rats, is a quite distinguished field in the methodology of cytometry research. Differences in relation to the studying of human platelets do not concern so much the equipment requirements, but the protocols for blood sampling and preparation of collected biological material. Simple and straightforward implementations of the procedures commonly employed in human platelet research for the investigating of rodent platelets usually do not bode a researcher a success in obtaining reliable and repeatable results. This is an important issue because the use of laboratory animals in preclinical studies has become almost a universal practice, and the results of animal tests are often considered as an incentive to start further clinical trials. In this chapter, the particular attention was paid to methodological and technical aspects of research protocols, and especially concerning the used mice and rats strains, methods of animal anesthesia, blood withdrawal, preparation and anticoagulation, cell fixation, selection of platelet agonists, and the last but not the least important - the choice of antibodies. All the above could potentially lead to distortions in the collected results and/or drive to obtain false conclusions. In this chapter, the results obtainable with flow cytometry assays have been collated with those obtained with the use of alternative techniques applied in scientific research of particular objects, such as intravital fluorescence microscopy or *in vitro* platelet adhesion under flow conditions. Also, protocols for estimating blood platelet viability —the parameter that can potentially interfere with functional assays and may have an impact on final conclusion of an experiment—are critically reviewed. Further, we describe the methods invented for measuring intraplatelet calcium mobilization during platelet activation and emphasize the risk of artifacts in the course of these procedures. Another important topic is the selection of a flow cytometry approach for studying possible nitric oxide generation in blood platelets. We also summarize the available procedures, [as well] as we present our experience in the overcoming of the troubles with setting up the alternative approaches and the least artifact-prone protocols for the quantification of platelet-derived microvesicles. Moreover, one of the chapters describes possibilities of using flow cytometry in some challenging research applications, which, at the first side, appear quite unusual for this technique—the investigations of subcellular and paracellular objects, such as mitochondria. In particular, the characterization of parameters explored in functional mitochondria and applications of such methods to study platelet activation are presented. Finally, we summarize studies focused on monitoring apoptosis in blood platelets of rodents with the use of flow cytometric approach.

http://dx.doi.org/10.5772/63473

2. From the beginning to the end—search for an optimal discriminative flow cytometric protocol for studying mouse and rat platelets

Because of the ethical limitations and restraints on human research, animal models, especially the ones involving rodents, constitute a convenient and recognized tool for studying platelet functioning. However, it should be pointed out that platelets from rodents differ in certain morphological characteristics from human platelets. For instance, murine platelets are much smaller than human (with a diameter in the range of 0.5 μm compared to 1–4 μm in human platelets), but they are more than two times abundant (0.7 to even 1.5 million cells per microliter of blood [1]). In the case of rat platelets, they are bigger (1.5–2.5 μm), but approximately equally abundant as in mice (ca. 1.3 million/μl of blood [2]). The commercially available beads, covered with a fluorescent label, of various diameters may be of a great convenience when determining the exact sizes of murine and rat platelets [3]. Such beads, added to the sample, may facilitate the determination of reference ranges and the estimation of platelet size at resting conditions and upon the *in vitro* stimulation of platelets with agonists (**Figure 1**).

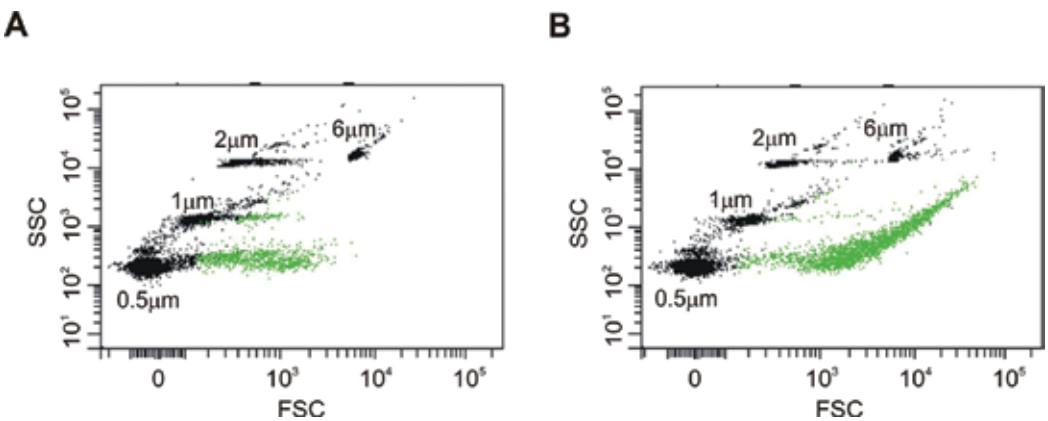

Figure 1. Scatter dot plots of polystyrene beads and resting and thrombin-stimulated isolated mouse platelets. The beads of the following sizes were applied: 0.5, 1, 2, and 6 μm. Mouse platelets were isolated by gel filtration and were labeled with FITC-conjugated anti-CD41/61 gating antibodies (green dots).

It should be noted that despite some similarities in terms of platelet surface antigens between men and rodents, it is crucial to use different antibodies for labeling human, murine, and rat blood platelets. Application of the same antibodies for these species is not indicated as any putative cross-reactivity of antibodies against human, murine, and rat platelet surface antigens is minimal or none [4]. The selection of proper antibodies can be a particular problem for the researcher, as the range of commercially available monoclonal antibodies against the rodent platelet antigens is quite limited, especially in the case of rat platelets. In such cases, it remains to use polyclonal antibodies, which are much less specific than monoclonal antibodies, because they recognize various nonspecific antigenic determinants. In the case of murine platelets, it should be noted that despite a significantly larger offer of commercially available antibodies,

they significantly differ from each other and hence are not equivalent in binding to target platelet surface antigens (**Figure 2**).

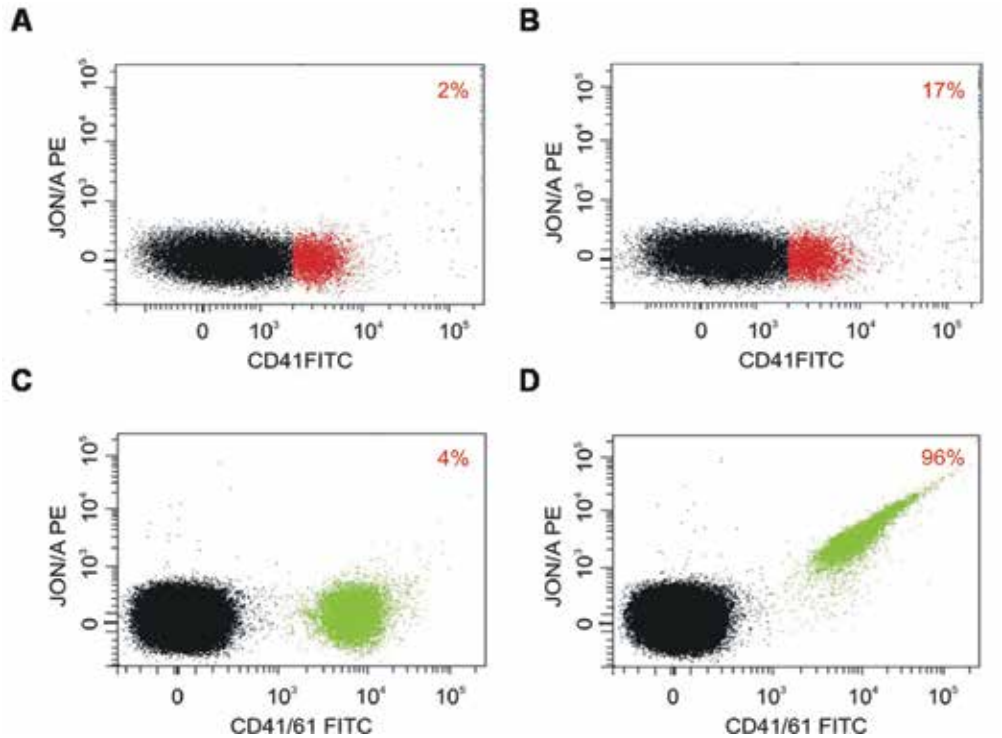

Figure 2. Fluorescence dot plots of resting and thrombin-activated mouse platelets labeled with FITC-conjugated anti-CD41 or anti-CD41/61 gating antibodies and with PE-conjugated JON/A (anti-theactivated form of integrin $\alpha_{IIb}\beta_3$) antibodies. Red dots represent the CD41-positive objects (A, B), whereas green dots represent the CD41/61-positive objects in samples of resting platelets (A, C) or platelets stimulated with 0.25 U/ml human thrombin (15 min, RT) (B, D). The percentage of JON/A-positive platelets was obtained after subtracting of nonspecific mouse IgG binding and was presented as a numerical value (in red).

As occasionally reported, merely the selected products are appropriate to identify the platelets without the interference from other cells [5]. Platelet reactivity is usually evaluated by the monitoring of the expressions of platelet surface membrane antigens after platelet stimulation with physiological or, rarely, nonphysiological agonists. Interestingly, while in the case of ADP and thrombin we receive the response of murine platelets similar to that observed in humans, platelet activation in mice after collagen stimulation is observed to be significantly lower than in human platelets (**Figure 3**).

When using flow cytometry, rodent platelets are usually identified in a whole blood according to the presence of a typical constitutive platelet surface membrane antigen (CD41, CD61, and CD41/61) on their surface [6, 7]. However, in some studies, the researchers used to rely only on the analysis of the FSC and SSC signals, which caused them to extract considerable pools

http://dx.doi.org/10.5772/63473

of other cellular components (erroneously regarded as blood platelets) of whole blood or plasma-free blood [8]. It has been proven that there are some advantages of platelet gating on the basis of the presence of a given pan-platelet surface antigen over the identification of platelets on the virtue of FSC/SSC images [9]. First, such an approach enables to "pick up" all platelet-originated objects and to further distinguish normoplatelets from other objects (small aggregates, microparticles, dust, etc.). Moreover, platelets can be visualized in different cohorts as single platelets or aggregates with other blood cells. It clearly indicates that gating of platelets based on FSC/SSC instead of a demarcation with the use of a common platelet-specific marker can lead to the increased risk of collecting artifacts (i.e., objects resembling blood platelets in size and/or light scattering, missing the platelets in aggregates) (**Figure 4**).

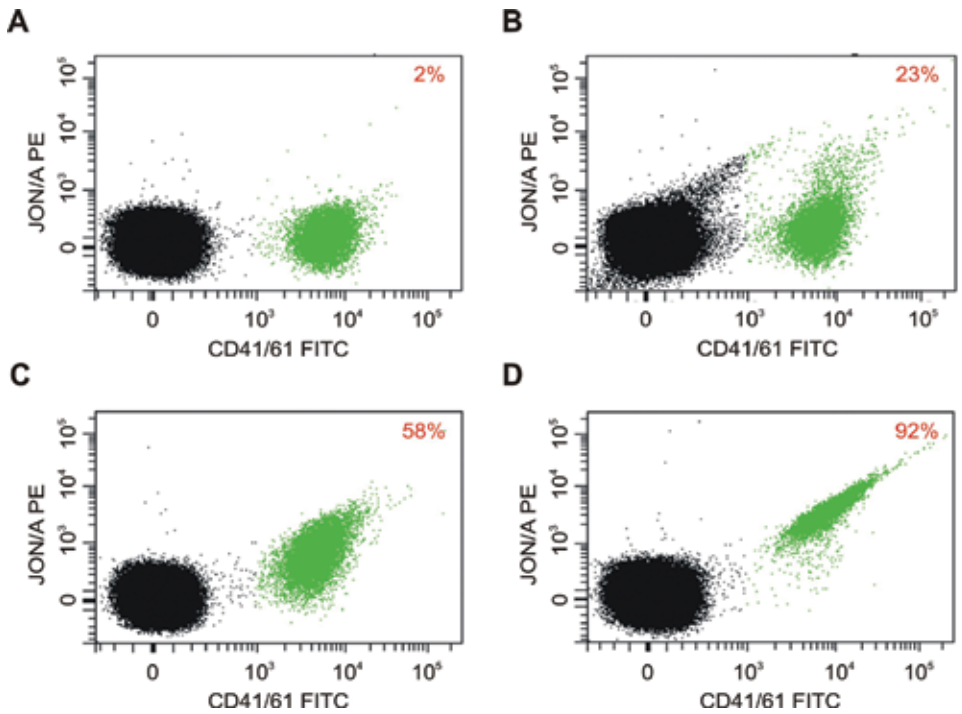

Figure 3. Fluorescence dot plots of resting mouse platelets and platelets stimulated with collagen, ADP, or thrombin. Platelets were labeled with FITC-conjugated anti-CD41/61 gating antibodies and with PE-conjugated JON/A (anti-the activated form of integrin $\alpha_{IIb}\beta_3$) antibodies. Green dots represent the CD41/61-positive objects in samples of resting platelets (A) and platelets stimulated with 20 μg/ml collagen (B), 20 μmol/l ADP (C), or 0.25 U/ml thrombin (D) (15 min, RT).). The percentage of JON/A-positive platelets was obtained after subtracting of nonspecific mouse IgG binding and was presented as a numerical value (in red).

The identification of platelets based on FSC/SSC images can be eventually made in the case of washed platelets. However, one has to keep in mind that in such an approach platelet aggregates still cannot be detected. Analyzing blood platelets from rodents, especially murine blood platelets, may be challenging due to some methodological restraints concerning the minute amount of blood available and the technical difficulties of collecting the blood, while

avoiding at the same time undesirable artifactual platelet activation. No uniform flow cytometry protocol has been recommended in the literature for studying mouse platelets. In the majority of the available reports, it has been demonstrated that none of the alternative methods of blood collection from mice (either from retrobulbar venous plexus, vena cava, by cardiac puncture or by tail bleeding) appear inferior with regard to artifactual platelet activation [10]. In contrast, some authors showed that blood withdrawal from retrobulbar venous plexus and inferior cava resulted in the least artifactual activation of platelets compared to blood collected directly from a heart, jugular vein, carotid artery, lateral saphenous vein, or tail vessels [11]. Moreover, the opinions on the effects of animal anesthesia on platelet artifactual activation vary a lot. In most studies, either inhalation or injected anesthesia has been utilized regardless of the likely effects of these methods on platelet functioning [12, 13]. However, some authors demonstrated that parenteral anesthesia reduced platelet reactivity in humans and various animal species and only a few studies on mice concerned this issue [14]. Also the effects of different blood anticoagulants on the outcomes of flow cytometric analysis have been compared. Heparin and citrate are the anticoagulants most widely used in the experiments with rodent blood samples [15, 16]. It has been proven, on the other hand, that the effects of these two compounds on the platelet functioning are quite dissimilar [10]. In this study, only the effects of citrate on platelet artifactual activation have been observed (**Figure 5**).

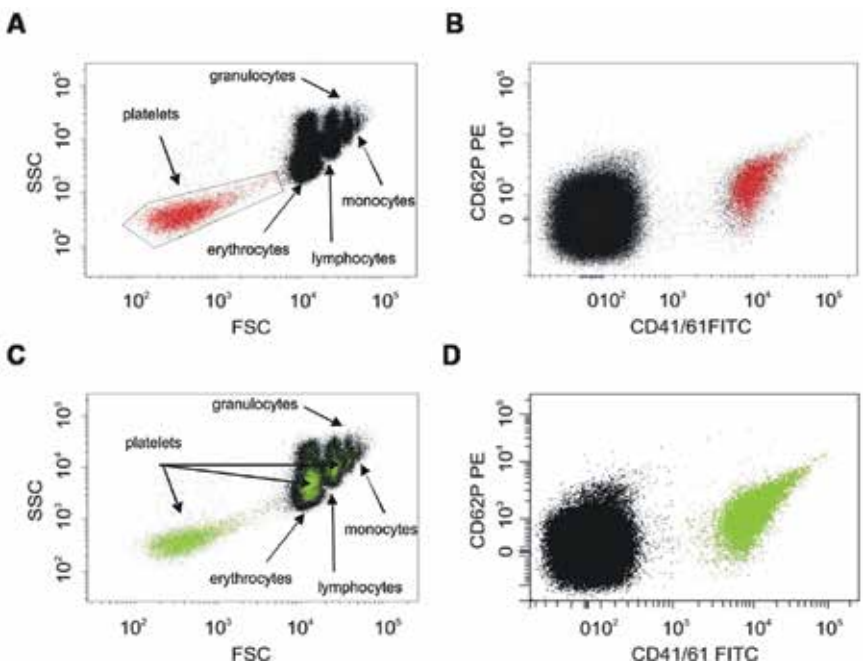

Figure 4. Fluorescence and scatter dot plots of thrombin-activated mouse platelets labeled with FITC-conjugated anti-CD41/61 and PE-conjugated anti-CD62P antibodies. Blood was incubated with 0.25 U/ml human thrombin (RT, 15 minutes). Green dots represent the CD41/61-positive objects (C, D), whereas red dots represent the objects referred to as "blood platelets" gated on the basis of the FSC/SSC scatter (A, B). Individual populations of blood cells and the aggregated platelets that are comprised in them were labeled.

http://dx.doi.org/10.5772/63473

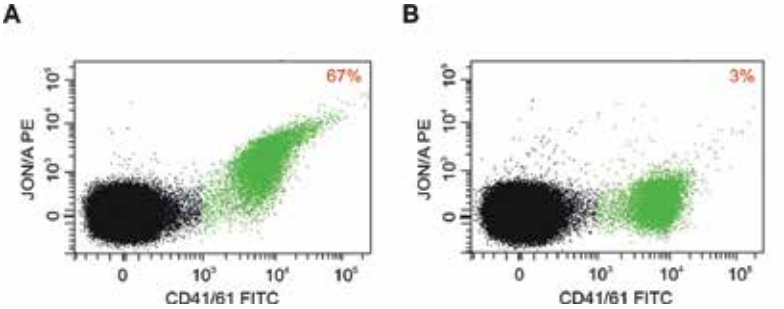

Figure 5. Fluorescence dot plots of resting mouse platelets in blood collected on citrate and low molecular weight heparin (LMWH). Platelets were labeled with FITC-conjugated anti-CD41/61 gating antibodies (green dots) and with PE-conjugated JON/A (anti-the activated form of integrin $\alpha_{IIb}\beta_3$) antibodies in blood collected on 3.2% sodium citrate (A) or 20 U/ml LMWH (B). The percentage of JON/A-positive platelets was obtained after subtracting of nonspecific mouse IgG binding and was presented as a numerical value (in red).

However, the contradictory reports have claimed that there is no firm evidence on the significance of different anticoagulants on platelet activation [11]. While working on optimizing the flow cytometry protocol, the impact of blood fixation on platelet functioning should certainly be evaluated. It has been proven that a fixation procedure may strongly affect the binding of antibodies to mouse platelets, thus supporting the conclusion that the flow cytometry protocols requiring shorter time of blood collection and preparation are preferential [10] (**Figure 6**).

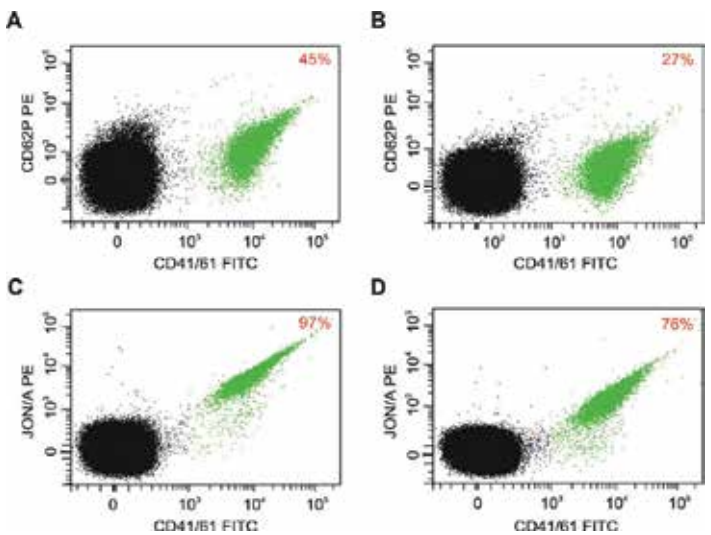

Figure 6. Fluorescence dot plots of thrombin-activated mouse platelets in unfixed and fixed blood. Platelets were labeled with FITC-conjugated anti-CD41/61 gating antibodies (green dots) and with PE-conjugated anti-CD62P (A, B) or JON/A (anti-the activated form of integrin $\alpha_{IIb}\beta_3$) (C, D) antibodies in unfixed blood(A, C) and in samples fixed with 1% paraformaldehyde (B, D). The percentages of CD62P-positive (A, B) and JON/A-positive (C, D) platelets were obtained after subtracting of nonspecific mouse IgG binding and presented as a numerical value (in red).

Furthermore, in the unfixed blood individual populations of blood cells seem to be better separated (**Figure 7**).

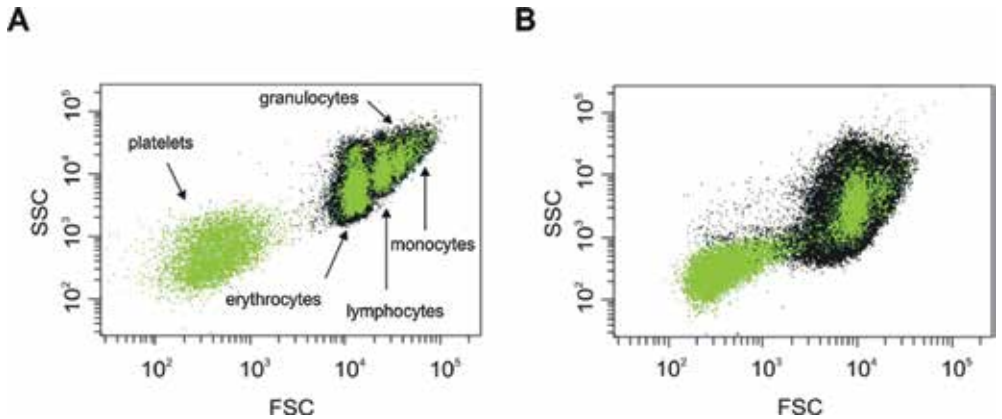

Figure 7. Scatter dot plots of resting mouse platelets in unfixed and fixed blood. Platelets were labeled with FITC-conjugated anti-CD41/61 gating antibodies (green dots) in unfixed blood (A) and in samples fixed with 1% paraformaldehyde (2 h, RT) (B).

In conclusion, it has been shown that in order to establish an optimal protocol for measuring rodent platelets, some crucial factors, including blood preparation or platelet fixation, a type of the anticoagulant, and methods of the anesthesia, should be considered.

3. Not only flow cytometry—alternative methods for studying the phenomena of platelet activation in laboratory mouse and rat models

Recently, very much attention is paid to the methods based on measuring of platelet adhesion under flow conditions. The idea behind this approach is to test the response of platelets under conditions resembling those to which platelets are exposed in blood vessels. It is accepted that a shear force, to which blood platelets are subjected in a bloodstream, strongly modulates platelets' activation and reactivity. The first studies performed under flow conditions were conducted with the use of artificial chambers assembled by researchers. Nowadays numerous companies provide systems combining capillaries of standardized dimensions and equipped with the pumps able to generate a flow of defined parameters. The combination of a flow rate chosen by the researcher and dimensions of the capillary define the shear rate generated by a flowing sample (expressed in cm^{-1}). Using an approximated viscosity of the sample, the shear force (expressed in $dyne/cm^2$) can be calculated based on the shear rate. Depending on the researcher intentions, the capillary can be coated either with a protein or with the cell monolayer. The most often used proteins for this purpose are fibrinogen, von Willebrand factor (vWf), and collagen. The interaction with fibrinogen results in a firm adhesion of platelets, which form a layer coating the surface, but no aggregate formation is observed. The adhesion

http://dx.doi.org/10.5772/63473

to vWf is unstable and platelets weakly interact with a capillary. In turn, in capillaries coated with a collagen the aggregate formation occurs, which can even lead to the occlusion of a capillary if the inhibitors of thrombin generation are not applied. The visualization and quantification of the adhesion can be performed using various approaches. One of the methods is to prestain the platelets prior to the experiment with a fluorescent dye and to record images at a very high frequency (more than 5 Hz) using a highly sensitive camera. The most often used dyes include $DiOC_6$, rhodamine 6G, and fluorescein derivatives. The biggest challenge of this approach is the reliable quantification of the results. Using a dedicated software, the researchers usually count the number of platelets that adhered to the surface in a defined period of time. The other parameter, often presented in publications, is the velocity of platelet "rolling" on the surface, which is calculated by measuring the trace left by a platelet within a given range of frames of the image. The other way is to image these blood platelets that formed stable contacts with a coating protein and remained adhered even after the perfusion of the capillary with a washing buffer. In this approach, we can evaluate either the number of firmly adhered platelets or the surface area covered by platelet aggregates. These adhering platelets can be additionally stained with antibodies against the active form of $\alpha_{IIb}\beta_3$ or P-selection in order to evaluate platelets' activation. In the case of a thrombus formation in capillaries coated with a collagen, the volume of thrombus is the mostly informative parameter. This can be measured with the use of a confocal microscopy.

3.1. *In vivo* methods

The *in vivo* methods can be categorized with respect to the way of inducing a specified platelet response. The most often used techniques are based on the experimental disruption of the endothelial layer, which inevitably leads to the exposure of the subendothelial matrix, thus triggering blood platelet activation and platelets' adherence to subendothelial matrix components, and in consequence the thrombus formation [17, 18]. The disruption of the endothelial layer is usually achieved by placing the vehicle saturated with $FeCl_3$ on the vessel. The diffusion of the highly reactive agents to the vessel wall results in a gradual endothelial denudation. The other approach is a disruption of the cells of a vessel wall by the applying of an electric impulse. A more sophisticated and a far more precise method utilizes the multiphoton excitation microscopy, which destroys the area covered by several endothelial cells with the use of a laser beam. The thrombus formation initialized by one of these methods can be subsequently quantified in one of the two manners. One is the measurement of the rate of cessation of blood flow resulting from the formation of the occlusive thrombus. Such a measurement utilizes Doppler flowmetry, based either on ultrasounds or a laser light. The probe of a dedicated device is usually located downstream from the site of an occlusion. The time required to achieve the flow cessation is accepted as the measure of the readiness of blood platelets to form the occlusive thrombus. The other way to quantify the extent of the *in vivo* thrombus formation is the microscopic visualization of the event. Usually, for this purpose the platelets are prestained with fluorescent dye or platelet-specific antibodies. Microscopic visualization with the use of a confocal microscopy allows to measure the volume of the thrombus. Moreover, the injecting of specific antibodies or fluorescent proteins to an animal provides the opportunity to monitor the structure of thrombus, its porosity, and functional architecture [19, 20].

The *in vivo* microscopy in animal models also allows the sight into the interactions between platelets and the intact endothelium (**Figure 8**).

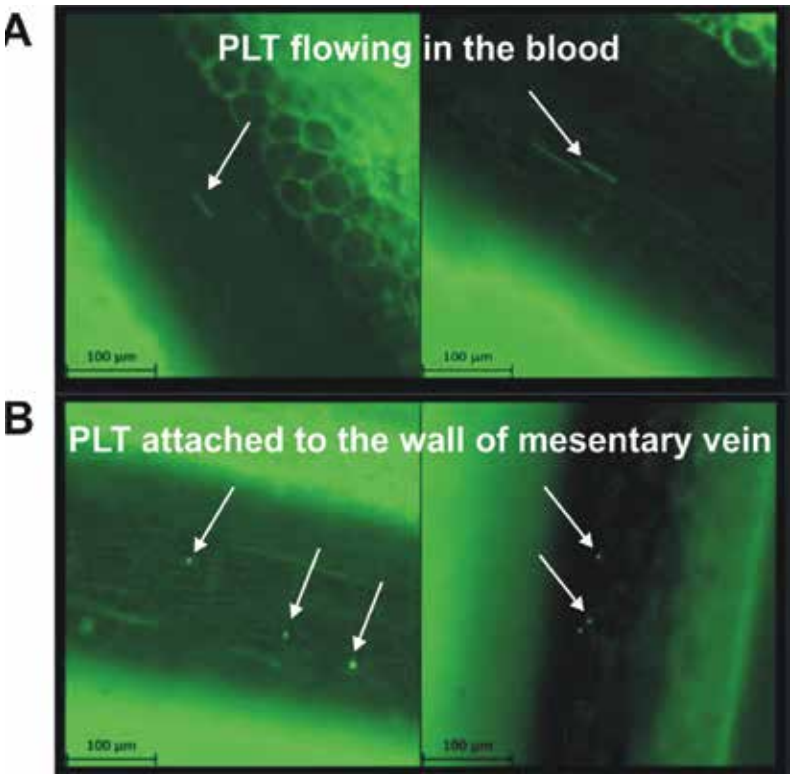

Figure 8. Platelet flow and adhesion in mesentery veins of healthy and diabetic mice. Anesthetized mice were injected with either DyLight488-conjugated anti-GPIbβ antibodies and placed on a stage of an upright microscope equipped with saline immersion objectives. Platelets flowing in the blood and those attached to the wall of a mesentery vein were evaluated in saline-injected (control) (A) and STZ-injected (diabetic) (B) mice.

Fluorescent-labeled platelets adhering transiently or firmly to the vessel wall are recorded and the interactions are quantified as described in the *in vitro* section of this paper. Another approach to test platelet reactivity *in vitro* is based on a systemic injection of a platelet agonist. In this case, the response of platelets can be quantified by two methods. In one of them, the measure of platelet reactivity is the death rate of animals, resulting from the agonist-induced thrombi formation in lungs [21]. The other method is based on the infusion of radiolabeled platelets to the animal's circulation and the monitoring of the rate at which radiolabeled platelets accumulate in lung vessels in response to nonlethal doses of an agonist [22]. We have recently proposed quite a novel approach to measure blood platelet aggregation in lungs induced by ADP injection. The protocol is based on the recording of the changes of blood flow in mesenteric vessels with the use of laser Doppler flowmetry [23].

http://dx.doi.org/10.5772/63473

4. Investigation of platelet viability—critical appraisal of flow cytometric assays

Due to the lack of nucleus the commonly used methods for assessing the viability of nucleated cells, including the methods based on the measurement of a metabolic activity of cells (e.g. MTT, XTT, WST-1, and PrestoBlue™ assays), those based on the damage of a plasma membrane (e.g. lactate dehydrogenase assays, trypan blue staining) or the methods based on the analysis of DNA fragmentation cannot be adapted for a reliable measuring of the viability of blood platelets [24, 25]. Therefore, the most encouraged method for assessing the viability of platelets is the staining of blood platelets with the ester of calcein and the monitoring of the fraction of stained cells with the use of flow cytometry [26]. This assay may be applied for either a whole blood or isolated platelets. The application of this procedure is similar for platelets obtained from humans, mice or rats. The acetomethoxy ester of calcein (calcein AM) is a nonfluorescent lipophilic compound that trespasses plasma membranes of living cells and gets into the cells, where it is hydrolyzed by cytoplasmic esterases to the hydrophilic, highly green fluorescent compound—calcein [27, 28]. The free calcein is well retained within living cells with the intact plasma membrane, while the leakage of calcein to the extracellular environment is observed in the case of the loss of the integrity of cellular membranes. The application of the acetomethoxy ester of calcein, when using various protocols of platelet viability detection, has certain limitations. The presence of Ca^{2+} and Mg^{2+} in a strongly alkaline environment affects the growth of calcein fluorescence intensity, while the ions of Co^{2+}, Ni^{2+}, Cu^{2+}, Fe^{3+}, or Mn^{2+}, when present in a medium at physiological pH, quench the fluorescence of calcein [29–31]. The latter phenomenon is apparent when assessing the viability of platelets in a whole blood with the use of calcein. It was observed that platelets exhibit significantly stronger fluorescence derived from calcein than other blood cells. The probable reason for this is the fact that red blood cells, which are the most numerous cellular components of blood, contain hemoglobin, and thus the Fe^{3+} ions become responsible for the quenching of the calcein-derived fluorescence. Interestingly, it was also shown that the fluorescence of platelets stained with calcein and stimulated under *in vitro* conditions with physiological platelet agonists was increased compared to resting platelets [32]. One explanation could be that the higher concentration of Ca^{2+}, released from intracellular stores into the cytoplasm after platelet stimulation, may false-positively increase the fluorescence of calcein. However, this hypothesis was undermined, as the chelator of calcium ions, BAPTA AM, reduced platelet activation due to the binding of the intracellular Ca^{2+}; however, it did not affect the calcein fluorescence in stimulated platelets. This indicates that the increased population of calcein-positive platelets upon their *in vitro* stimulation does not result directly from the mobilization of intracellular calcium ions. Thus, it seems particularly important to provide the optimum reliable positive and negative controls for the protocols with calcein. As a potential agent used for the damaging of platelets (at present considered as a good positive control), formaldehyde (at a concentration above 1%) may be used. The reported protocol is also applicable in the case of mouse platelets (**Figure 9**).

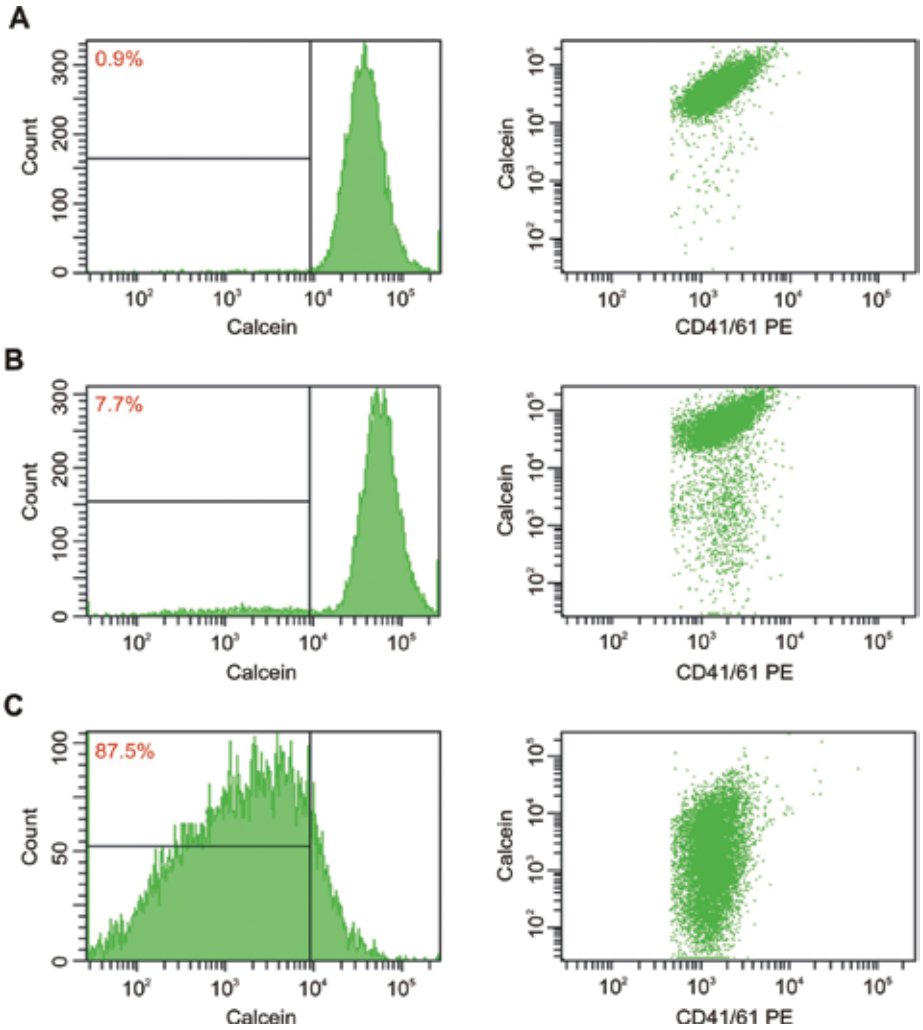

Figure 9. The viability of resting and collagen-activated mouse platelets. Platelets were labeled with calcein AM and PE-conjugated anti-CD41/61 gating antibodies. Platelets' viability was presented as percentage (numerical values in red) of calcein-negative objects in resting (A) and collagen-activated (20 μg/ml) platelets (B). Platelets incubated with 1% formaldehyde (2 h, RT) remain the positive control (C).

If we measure the viability of platelets in a whole blood, we have to use antibodies for gating the platelets. What is important is that they cannot be conjugated with the fluorochrome emitting a green fluorescence. The analysis of the changes in the intensity of a green fluorescence of gated platelets may become falsified due to the fact that in the case of platelet activation the objects showing the increased intensity of green fluorescence may be recorded, probably due to the formation of platelet aggregates. Therefore, the most convenient approach to distinguish between living platelet and those with damage cellular membrane is to set the appropriate cutoff on the histogram of green fluorescence and the subsequent recording of the appearance of calcein-negative objects [33].

http://dx.doi.org/10.5772/63473

5. Monitoring of the ion mobilization and transport in platelets—flow cytometry protocols for the release of calcium ions into a cytoplasm

Changes in platelet cytosolic concentrations of calcium ions are fundamental conditions for the transmission of signals within the cell and between the cytoplasm and the external environment of platelets. These ions can be released from intracellular resources stored in granules, mainly the dense tubular system, or they can penetrate into a cytoplasm through the cell membrane from the outside [34–36]. This process takes place in a similar manner in both human platelets and platelets derived from laboratory rodents, such as mouse or rat [37, 38]. It is known that the increased cytosolic free calcium is a key for early events that follow platelet activation, and it underlies several activation responses, including shape change, aggregation, and secretion [39, 40]. Thus, the changes in the concentration of platelet intracellular calcium can be seen as a characteristic sign of platelets' stimulation by an external stimulus. For the measurements of Ca^{2+} release into the cytoplasm of platelets, the calcium-sensitive dyes have been employed. These can be divided into two groups: (i) those for which the intensity of the fluorescence emission grows when the concentration of Ca^{2+} in the cytoplasm increases (e.g., Fluo-3, Quin-2, and Rhod-2) [41, 42] and (ii) those characterized by a shift in the excitation and emission spectra (e.g., respectively, Fura-2, and Indo-1) with the increasing calcium concentrations [43, 44]. The second group of the calcium-sensitive fluorophores is much more appreciated by the researchers, as their use minimizes the risk of artifacts due to nonuniform intracellular Ca^{2+} distribution. A common problem encountered with the application of these compounds is their high polarity that hinders the penetration through the cell membrane and prevents the entering of the label into the cells [45]. To overcome this obstacle, the electroporation of cells is often performed; however, for the platelet membrane perforation (also referred to as membrane permeabilization) this procedure carries the risk of the change/loss of some cell functions [46]. Another way to increase the ability of calcium indicators to penetrate cell membranes is a chemical modification of these labels, e.g., their esterification. The esterified forms of fluorescent labels are re-released in a free form due to the action of cytoplasmic esterases. Due to their reduced polarity the esterified indicators easily penetrate the lipid bilayer membranes of platelets, and their ionization in the cytoplasm, following the hydrolysis of ester bonds, permits the binding of divalent ions, such as calcium ions. It is important that the fluorescence of the ionized forms of ion indicators is several orders of magnitude greater than their esterified derivatives, therefore the efficient hydrolysis of the labels in a cell cytoplasm is the intimate condition of the usefulness of these compounds in examining the changes in the ion concentration in platelet cytoplasm [47]. Moreover, the efficient transport of these labels into cells is also an experimental evidence of the proper functioning of cells and a preservation of the integrity of cytoplasmic membranes. Since the conversion of a nonfluorescent indicator into its fluorescent derivatives requires the presence of some active enzymes in the cell (esterases, oxidases, etc.), the calcium flux assay also provides the information on the activity of some intracellular enzymes. The excessively rapid and facilitated transport of the label and its redistribution in the cell (e.g., due to its excessively high concentrations) may result in its penetration into the intraplatelet granules (where the cell reservoirs of calcium ions are accumulated). Under such conditions the label may easily turn out useless for the moni-

toring of the release of calcium from the granules into the cell cytoplasm. The requirement of the proper adaptation of this method for the testing of a particular type of cells is, therefore, the selection of the optimal fluorescent label concentration and the optimal incubation time of the label with cells. Too short incubation time and/or low label concentration slow down its transport into the cytoplasm and result in the incomplete hydrolysis. In addition, in the case of an inefficient label concentration the assay is poorly sensitive to large changes in the concentrations of calcium in the cytoplasm because the pool of the available ionized label becomes quickly saturated with the calcium ions present in the overwhelming concentration. On the other hand, the excessively long incubation time and/or high concentration of fluorescent label may lead to its uniform distribution in the cell. In that case, the changes in the fluorescence of the labeled calcium ions released from the intracytoplasmic granules might have not been recorded because the entire pool of the label (present also in the granules) would be uniformly saturated with calcium ions. A typical flow cytometry protocol for measuring the concentration of calcium in platelets involves several crucial steps (it is similar for mouse, rat, and human platelets [48]). First, platelets are labeled with the appropriate calcium indicator for 10 minutes at 37°C. The fluorescence intensity is then recorded for about 1 minute to establish the baseline. At 60 seconds, a given platelet agonist is added to the sample and the time-dependent changes in the fluorescence of calcium-sensitive dye are measured over a period of 5 minutes. Then, the magnitude of the calcium concentration change is represented by the alterations in the calcium concentration at every second divided by basal calcium level. The key factor in the case of flow cytometric determination of intracellular calcium mobilization is the selection of appropriate ion indicator. The use of the fluorescent probes that are characterized by a shift of either the excitation or emission spectrum along with varying Ca^{2+} concentrations is limited since such shifts are typically not big enough to be recorded in the different flow cytometer channels [47]. Therefore, more available and useful are labels characterized by the changes in a fluorescence intensity along with the increasing calcium concentration. These changes can be recorded either as changes in the relative fluorescence or changes in the fraction of fluorescing cells. The commonly used calcium indicator is Fluo-3 because its excitation and emission spectra make it suitable for the use in flow cytometers equipped with a standard 488 nm argon laser. Preferably, two different calcium indicators may be used in which the emission varies in the opposite direction (increases for one and decreases for the other) with the increasing calcium ion concentration. One of the labels is then a reference indicator. When deciding to study the ion transport in platelets with the use of flow cytometry, a researcher has to face a number of methodological problems. First, since the calcium indicators are present in the ionized form in the platelet cytoplasm, there is a risk of their removal by the cellular membrane anion transporters. Hence, the concentration of the "active" ion indicator decreases inside a cell, as the time passes, which makes it impossible to reliably monitor the fluctuations in calcium concentration in such cells. Under such circumstances, the use of ion transporter blockers (like probenecid) may guarantee a collection of the reliable results [49]. However, as it turns out, some current reports undermine the use of some of these blockers due to their negative effect on platelet functioning. The above-mentioned probenecid is a good example of such a compound. It was applied in numerous studies to prevent a leakage of the used calcium indicators [50, 51]. Unfortunately, probenecid was also found to markedly

http://dx.doi.org/10.5772/63473

hamper the increase in Ca^{2+} caused by physiological platelet agonists [52, 53]. Hence, paradoxically, a physiological event of calcium mobilization in activated platelets can be hardly monitored. Second, numerous ion indicators are characterized by a considerable toxicity and thus may cause a gradual leakage of fluorophores from the labeled cells due to cell membrane disruptions [54, 55]. A good way to confirm this kind of leakage may be the adding of Mn^{2+} ions to the buffer, in which the cells are suspended. These ions are capable of quenching the fluorescence of a variety of labels. If there is a leakage of ions through the damaged platelet membrane, Mn^{2+} ions may penetrate into the cytoplasm and—via competing with calcium ions—may bind to the molecules of indicator inside cells and quench its fluorescence [56]. Importantly, needless to emphasize, there are a few advantages of flow cytometry over the alternative classical spectrofluorometric plate- or cuvette-based methods for measuring Ca^{2+} release from the intracellular resources. First, sample preparation for flow cytometry measurement requires only a minute amount of blood. This fact is particularly important in the case of smaller laboratory rodent models, for which main methodological obstacle concerns the minimal portions of blood available (like in mice). Second, for plate- or cuvette-based methods, it is necessary to isolate platelets and separate them (wash out) from other cellular elements of blood [57]. In practice, it seems hardly possible to obtain a sufficient aliquot of isolated washed platelet suspension from the aforementioned small volume of blood withdrawn from small rodents. In the case of flow cytometry, we can monitor the process of calcium mobilization in platelets in whole blood samples. For this purpose, we have to use the antibodies against a common platelet-specific marker that discriminates between platelet-positive and platelet-negative blood cell subpopulations. This constitutes the guarantee that calcium concentration will be monitored only in these "gated" objects—platelets. Thus, the procedure of platelet "gating" truncates the calcium-specific signal originating from multiple cells types other than platelets, which possibly show differentiated responses to the same stimulus. As far as calcium mobilization constitutes one of the most initial stages of blood platelets, the protocols that allow to trace the phenomenon in a whole blood certainly minimizes the risk of artifacts due to sample preparation. Another advantage of flow cytometry may be that it enables the identification of varying extents of calcium-related responsiveness within a single population of platelets [58]. In turn, the possibility to record a high number of independent single cellular events provides a high statistical power of such analysis. In addition, in contrast to other methods, flow cytometry allows, with the use of the panel of appropriate antibodies, to distinguish between the fluorescent signals originating from either single platelets or platelet aggregates. It seems particularly important, and more even so, considering the fact that the total fluorescence of platelet aggregates appears artificially elevated compared to the fluorescence arising from single platelets, hence elevating the risk of collecting overestimated outcomes [58]. Finally, it should be remembered that for either plate- or cuvette-based methods the washing steps are required in order to cut off the background fluorescence [59, 60]. These washing steps can inevitably cause the artifactual platelet activation, and therefore, their further stimulation with an agonist may result in the apparently reduced response, also reflected in the extent of calcium mobilization. Immediate and continuous recording of a fluorescence wave upon platelet stimulation is very important since the oscillations of

cytoplasmic calcium levels occur rapidly within a few to several seconds from the occurrence of the stimulus (**Figure 10**).

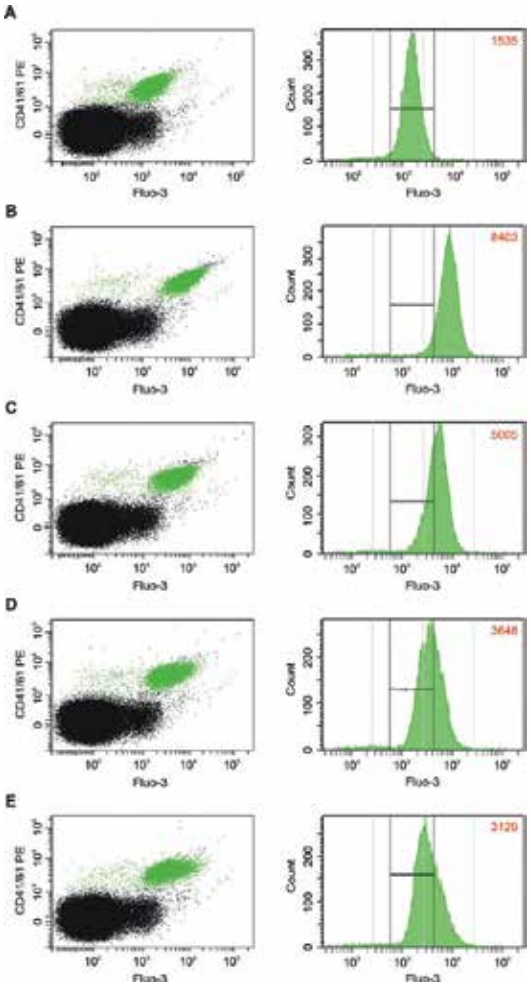

Figure 10. Calcium mobilization in resting and thrombin-activated mouse platelets. Platelets were labeled with calcium indicator, Fluo-3 AM, and PE-conjugated anti-CD41/61 gating antibodies. Changes in calcium concentration were monitored in resting (A) and thrombin-activated platelets at the following time points (starting from the addition of the agonist): 0 second (B), 30 seconds (C), 60 seconds (D), 90 seconds (E) and presented as mean fluorescence intensity (numerical values in red).

After this period there is usually a fast decrease in the calcium concentration to the level observed for the resting platelets [61]. This subsequent decrease in the calcium level results from the removal of Ca^{2+} ions from the cytosol into internal stores or their extrusion across the plasma membrane of cells. The main limitation of the flow cytometry method is that most flow cytometers have a pressurized system for aspirating the sample, and therefore, there is practically no opportunity for a continuous addition (within a certain period of time) of tested

http://dx.doi.org/10.5772/63473

compounds, such as agonists, in order to stimulate the calcium mobilization in platelets [62]. Resulting gaps in the recordings, as the consequence of the addition of these compounds, may result in the loss of some details of the recorded signal in the course of a rapid calcium response. This approach requires the researcher to keep in mind that the aspiration of the sample is paused for a really very short time to supplement the tube with a needed component and of course that the pause time should be the same in each experiment. Only then the accuracy and reproducibility of the results is ensured. Fortunately, the new generations of flow cytometers resolve this problem by the use of peristaltic pump which allows to add tested compounds to the cell suspension placed in open tubes [62]. This provides the continuous measurement of the kinetics of calcium mobilization in platelets in a relatively repeatable manner. Summing up, we argue that flow cytometry provides simple and sensitive tools to assess the time course and intensity of the signal transduction of calcium mobilization in platelets in response to different platelet agonists under near-physiological conditions.

6. Nitric oxide synthase activity in blood platelets—a fact or a myth? Is there a place for the use of flow cytometry?

Platelets, the major components of primary hemostasis, are regulated by both procoagulant and anticoagulant factors. One of the factors inhibiting the activation of circulating platelets is nitric oxide. NO (as well as its precursor, L-citruline) is produced from L-arginine by the catalytic action of NO synthase (NOS) isoforms in various types of cells [63–65]. Upon diffusion across the plasma membrane, NO binds to its intracellular receptor, soluble guanylyl cyclase (sGC), triggering the production of increased cGMP levels [66]. The cyclic nucleotide directly activates protein kinase G (PKG) and indirectly activates PKA through the inhibition of phosphodiesterase 3. The activation of PKG inhibits almost all the agonist-induced events in a platelet, including intracellular calcium mobilization [67], integrin activation [68], cytoskeletal reorganization [69], and platelet granule secretion [70]. In addition, NO is able to exert cGMP-independent functions, however, at much higher concentrations than those needed for sGC activation [71]. In addition to endothelial cells, where the NOS activity is crucial for the controlling of platelet activation [72], human blood platelets are also considered to express functional NOS. Therefore, nowadays it is believed that platelets may be regulated not only by exogenous endothelium-derived NO, but also by nitric oxide produced endogenously in platelets themselves. Two isoforms of NO synthase, endothelial (eNOS) and inducible (iNOS), seem to participate in that [73]. According to the opinions raised by some researchers, the endogenous activity of NOS present in platelets might act in an autocrine manner to stabilize platelets or to reduce the activation of resting platelets during the recruitment phase [74]. Nowadays, a major question in a scientific debate is whether platelets really express endogenous, functionally active NOS proteins. The data concerning the expression, regulation, and function of eNOS and iNOS in platelets remain contradictory. Since platelets do not have nuclei, and thus do not have the ability to regulate protein expression transcriptionally, the observed elevated NO generation upon platelets' stimulation with agonists most likely results from the increased activities of these enzymes [75]. Some older reports confirm the presence

of eNOS (also referred to as NOS3) and iNOS (also referred to as NOS2) in human platelets, with NOS3 being predominant [76]. Platelet NOS3 has been characterized as the Ca^{2+}-sensitive enzyme, and therefore, each stimulus that triggers intracellular calcium mobilization, such as e.g. physiological platelet agonists, should demonstrate the ability to activate NOS and induce NO generation [77, 78]. Some recent evidence also suggests the possible calcium-independent mechanism of NOS3 activation [79]. It has been reported that the NOS activity in human platelets increased via the cAMP/PKA pathway. The mediator is involved in the nitric oxide synthesis induced by adenosine, forskolin, and potentially also by any other antiaggregating substance enhancing the intraplatelet cAMP concentration either via the receptor-dependent or receptor-independent mechanisms [80]. The agonist-mediated activation is physiologically probably the most natural pathway of NO generation in platelets, we should be aware, however, that also other compounds of either natural or exogenous origin may affect NOS activity in human platelets. It has been proven that both aspirin and indomethacin decrease the activity of NOS in human platelets [81]. On the other hand, however, some most recent reports put the putative presence of eNOS and iNOS in human or mouse platelets into question [82]. First of all, the authors showed that platelets of the mentioned species did not contain mRNA for these proteins. The suggested lack of an active NOS of platelet origin was further confirmed by the fact that neither human platelets treated with the NOS substrate (L-arginine) nor those subjected to the action of the NOS inhibitor (L-NAME), and nor even platelets from mice with NOS deficiency (eNOS/iNOS knockout mice), produced detectable functional effects in blood platelets. These findings may collectively indicate either the presence of nonfunctional NOS in nonstimulated or stimulated platelets, or even the complete absence of NOS isozymes in these cells. To possibly reconcile, at least partly, these contradictory findings reported in this chapter, note that some reports have shown that a possible contamination of platelets with NOS-expressing cells may stimulate NO production in human platelets [83]. Otherwise, some contrary reports not only suggest the presence of NOS in mouse platelets, but also propose a biphasic role of NO in platelet activation—promoting platelet aggregation and secretion at low NO concentrations (of the order of that produced by platelet NOS) or the inhibition of platelet activation at the higher levels of NO [84]. Such a view has only occasionally been raised and several studies have even questioned the possible pathophysiologic role of platelet-derived NO because of the evanescent nature of this oxide and very small amounts of NO produced by platelets (estimated at about 5×10^{-17} mole per platelet stimulated with 5 μM ADP) [85]. So far, definitely much less publications relate to the expression and activity of NOS in platelets from mice or rats in comparison to human studies. Some earlier studies have suggested that the expression of NOS in murine platelets is possible, and thus, the lack of platelet-derived NO would alter the *in vivo* hemostatic response by increasing the recruitment of platelets [86]. Furthermore, it has been suggested that NO generated by murine platelets upon their activation at the site of arterial damage is more effective than that generated by endothelium-derived NO, probably because it acts at short distances, exactly in the place where platelets get activated [87]. However, the most current research confirms the findings gathered for humans, i.e., that also in the case of mice blood platelets do not express NOS, and hence, the endogenous production of NO inside these cells seems unlikely. Animal studies concern in particular the use of genetic models

http://dx.doi.org/10.5772/63473

of animals with the knockout NOS expression [88]. Under these conditions the potentiation of platelet response to agonists is observed to be similar to that recorded following the systemic NOS inhibition. The conclusion is that *in vivo* platelets are regulated primarily by NO originating from the outside of platelets, mainly from the vascular endothelium [89]. As for rat platelets, there is only a very few reports of possible expression and activity of NOS in these cells [90, 91]. The fact that there exist so many conflicting reports about the expression of NOS in platelets, also in rodent platelets, largely results from differences in experimental conditions and from nonspecific methods employed to detect NOS expression and activity. For example, the detection of platelet eNOS by Western blot and immunoprecipitation may provide false-positive results because of the variable specificity of commercially available eNOS antibodies [82]. A frequently used NOS activity assay is based on measuring of a radiolabeled L-citruline formed by the incubation of a radiolabeled L-arginine with intact or lysed platelets [73]. These methods seem not to be specific because platelets, as well as other cells, can utilize L-arginine in various pathways independent of NOS, including , for example, the urea cycle [73]. Undoubtedly, numerous reported findings apparently seem to be nothing more than artifacts, considering the fact that the reported platelet NOS activity, measured on the basis of the L-citruline production, ranged from 8 fmol [92] to 16 pmol/min/mg protein [93], which constitutes the difference of three orders of magnitude. In the collagen-stimulated platelets, the formation of 5 fmol/mg protein in 60 minutes was observed [94]. When we assume a protein content of 2.1 pg protein per platelet, this trace synthesis is equivalent to the formation of 6.3 molecules of NO per a single platelet per hour, and that minuscule amount simply seems negligible to cause any physiological effect [94]. Otherwise, this method does not provide the information on the concentration of NO produced from L-arginine. More specific GC-MS assay for NOS activity is based on the simultaneous measurement of nitrites and nitrates formed from the oxidized NO upon its NOS-catalyzed formation from L-arginine [95]. Remarkably, most studies did not verify NOS expression in platelets using stringent negative (NOS-deficient cells) or positive (endothelial cells, stimulated macrophages) controls [82]. There are also some doubts concerning the utilization of spectrophotometric, fluorescence-, and chemiluminescence-based assays to determine the level of NO production in platelets. The main objections concern the lack of a specificity of these methods. It has been suggested that such assays cannot discriminate between NO released by NOS-catalyzed oxidation of one of the guanidine nitrogen atoms of L-arginine and NO released by other sources [73]. The NO released by the oxidation of the α-NH_2 group of L-arginine or other amino acids and amines could falsely contribute to the measured NOS activity. As shown in the literature, despite the above-mentioned doubts, flow cytometry is still a widely used method for the monitoring of the intracellular NO production [96, 97]. The main advantage of this method is the fact that we can identify the selected population of cells, therefore, the presence of other cells does not interfere in the measurements of NO production. This aspect seems to be important since it has been suggested that the positive signs of the presence of NOS even in conventionally prepared, isolated platelets very likely result from the contaminants originating from other blood cells or their fragments [83]. The assessment of NOS activity by measuring NO concentration seems challenging because of its short half-life in a circulation and its high reactivity. It has been proven that the superoxide anion (O^{-2}) rapidly scavenges

NO to produce the cytotoxic peroxynitrite ($ONOO^-$) and this is one of the fastest chemical reaction occurring in the liquid phase ($k = 9.6 \times 10^9$ l/mol per s) [98]. Therefore, it is important to optimize the measurement conditions, especially the concentration and the incubation time with a fluorescent dye should be optimized and assessed using different concentrations and different incubation times with a probe. The most commonly used dye, DAF-FM (4-amino-5-methylamino-2'7'-difluorofluorescein) diacetate, is a pH-insensitive fluorescent dye that spontaneously penetrates the plasma membrane and is cleaved inside cells by esterases to generate the intracellular ionized form of DAF FM, which is subsequently oxidized by NO to the strongly fluorescing triazole product [99]. The fluorescence quantum efficiency increased more than 100 times after the transformation of DAF by NO. Typical flow cytometric protocol includes platelets labeling with DAF-FM diacetate for 30 minutes at 37°C. Following the addition of the NO donor (the NOS substrate, L-arginine) or the NOS inhibitor (L-NAME), the fluorescence intensity is measured at 515 nm upon the excitation at 494 nm [100]. Our own results are in line with other reports (**Figure 11**).

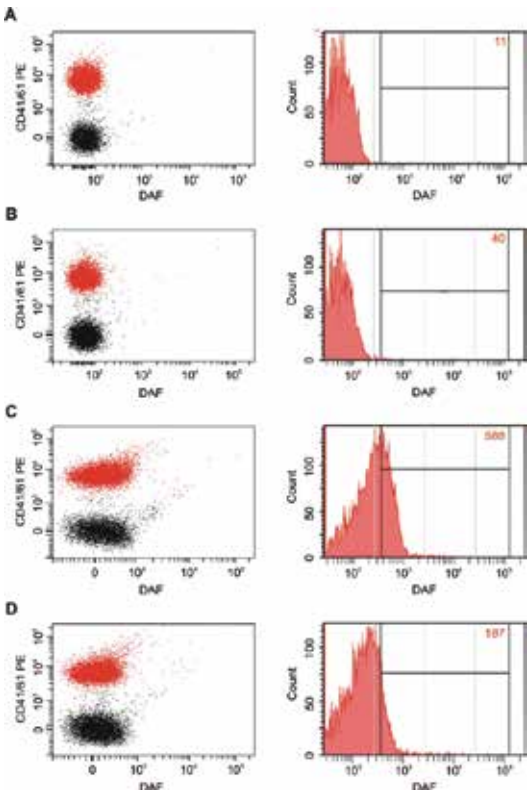

Figure 11. Monitoring of the presence of nitric oxide in mouse resting platelets. Platelets, labeled with PE-conjugated anti-CD41/61 gating antibodies, were incubated with NO indicator (DAF FM) alone (A) or with the addition of L-arginine (the substrate for NO synthase) (B), DEA/NO (the NO donor) (C), or both DEA/NO and L-NAME (the inhibitor of NO synthase) (D). Changes in DAF FM fluorescence were presented as mean fluorescence intensity (numerical values in red).

http://dx.doi.org/10.5772/63473

We confirm that there is no NO production in murine platelets (**Figure 11A**). Furthermore, even providing a substrate for nitric oxide synthase (L-arginine) did not increase the fluorescence derived from DAF FM (**Figure 11B**). Nitric oxide was detected in platelets only when the NO donor (DEA/NO) was applied to these cells (**Figure 11C**). Interestingly, the detection of nitric oxide derived from DEA/NO significantly decreased when we used L-NAME, the inhibitor of NO synthase (**Figure 11D**). This may confirm the hypothesis claimed by other authors for human platelets that the presence of exogenous NO in platelets may stimulate NO production in these cells [83]. What is worth emphasizing is that DAF-FM is rather an endpoint dosimeter and it is not a reversible equilibrium sensor. This may further constitute a certain limitation in the monitoring of rapid fluctuations in the intracellular NO concentrations in a real time. The reaction, in which DAF FM is converted into the fluorescent benzotriazole derivative, is a two-step process. In fact, first DAF-FM must be nonspecifically oxidized to an anilinyl radical, which then reacts with NO to form the fluorescent triazole product [101]. When interpreting experimental data, this mechanistic complication must be kept in mind. Specifically, the question of whether a nonspecific preoxidation or rather a subsequent reaction with NO is the dominant factor controlling the recorded DAF-FM fluorescence signals requires a critical scrutiny [102].

7. Platelet-derived microparticles—what we are really supposed to measure?

Extracellular vesicles (EV)[1] are small membrane vesicles derived from cells upon their activation or apoptosis. The classification of EV is mostly based on their size, composition, and the process of their release from cells. Exosomes (50–100 nm in diameter) are stored in cells and are extracted by exocytosis of multivesicular bodies. Apoptotic bodies (1000–5000 nm in diameter) are formed during apoptosis, while microparticles (100–1000 nm in diameter) are produced - for example, upon platelet activation [103]. In the circulating blood, in a physiological state platelet-derived microparticles are widely distributed and constitute up to 70–90% of the total pool of various microparticles present in plasma [104, 105]. They are a convenient marker of platelet exhaustion and/or damage, and the increased number of platelet-derived microparticles may be associated with certain diseases [106]. Therefore, they are often considered as the specific diagnostic markers [107]. Microparticles originating as the consequence of platelet membrane shedding can exhibit substantial biological (procoagulant) activity due to phosphatidylserine exposed on the surface (although not all microparticles have it), and thus, they provide a convenient indicator of the reactivity and/or sensitivity of platelets for various states of disease [108, 109]. Indeed, diabetes mellitus, collagen-associated vascular disorders, hypertension, and acute coronary syndromes are associated with increased

[1] For years they have been erroneously termed—and in the literature they are still most often referred to as— "platelet microparticles" (PMPs). However, according to the latest terminological trends, they should be rather called "platelet microvesicles" (PMVs).

levels of platelet-derived microparticles [110]. Microparticles are also considered to have an important effect on atherosclerosis, thrombosis, and cancer metastasis [110]. In comparison to studies on humans, there is noticeably less reports describing the formation of microparticles in laboratory rodents. Nevertheless, even these few studies confirm the significant role of these small vesicles in the thrombogenic process. Ramaciotii and colleagues showed that platelet-derived microparticles correlate with thrombus weight and tissue factor activity in an experimental mouse model of venous thrombosis in [111]. In another study by Chen and coauthors, the authors proved the elevated formation of platelet-derived microparticles in a murine AIDS model, which exhibited procoagulant activity to accelerate the coagulation cascade and caused platelet activation in autocrine manner [112]. Interestingly, it was shown that the generation of platelet-derived microparticles did not differ between commonly used laboratory mouse strains (C57BL/6, BALB/c, and 129Sv) and that it was not possible to efficiently inhibit microparticle formation by the potent antiplatelet inhibitor, aspirin [113]. Increased production of platelet-derived microparticles was also observed for various rat laboratory models, including diabetes [114] and hypertension [115]. Although the formation of microparticles can be monitored with the use of many methods, such as atomic force microscopy, electrochemical impedance spectroscopy, ELISA, or functional assays, the use of a standard flow cytometry has several advantages in the study of these objects. Obviously, the possibility of enumeration and the possibility of using multiple fluorochromes for a simultaneous detection of multiple markers of these cells seem the most important. Remarkably, the isolation of microparticles, as well as their counting, and finally staining pose a number of methodological/technical limitations. Since the detection of microparticles in a whole blood is not recommended, the initial and the most crucial steps involve the selection of the optimized centrifugal forces to obtain the microparticles from platelet-rich plasma. This is particularly important in the case of platelet-derived microparticles because the platelets are the smallest cells of all morphological blood elements. The situation becomes even difficult when we want to isolate murine microparticles since platelets (and microparticles derived from these platelets) are much smaller in mouse in comparison to human or rat blood [1]. Unfortunately, as it clearly emerges from the profound review of the available literature, there is no suitable uniform protocol to obtain microparticles from human or rodent blood [116]. Optimally, in order to obtain cell-free plasma, blood should be subjected to the two-step purification procedure, in which the platelet-poor plasma (PPP) is first obtained. Microparticles can be directly quantified in PPP; however, the better results may be obtained for isolated microparticles. Therefore, PPP should be centrifuged again at a much higher centrifugal forces (very often the ultracentrifugation may be a reasonable choice) in order to obtain platelet-free plasma (PFP) and to get rid of the remaining small platelets and to further purify the pool of microparticles [117]. However, it was shown that microparticles counts may be lower in PFP than PPP [118, 119]. The possible explanation is that probably in the course of this procedure large microparticles may also become depleted. Indeed, we have also confirmed these observations in our studies (**Figure 12**).

http://dx.doi.org/10.5772/63473

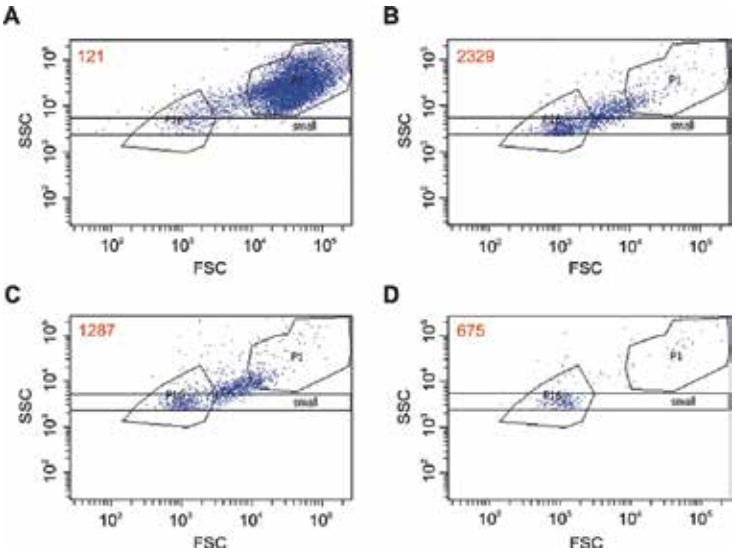

Figure 12. Detection of microparticles derived from thrombin-activated mouse platelets. Platelets and platelet-derived microparticles were labeled with FITC-conjugated anti-CD41/61 gating antibodies (blue dots). The gates P1 and P16 correspond to the areas where respectively the 1 μm and 0.2 μm beads (Megamix-Plus SSC beads) were found. The formation of microparticles was estimated in a whole blood (A), pellet obtained after centrifugation of PPP to PFP (B), PPP (C), and PFP (D). The number of CD41/61-positive objects in the size range of 0.2 μm was presented as a numerical value (in red).

We have recorded much smaller populations of platelet-derived microparticles in PFP (**Figure 12D**) than in PPP (**Figure 12C**). In that case, some part of the population of microparticles was found in the pellet resulting from the centrifugation of PPP to PFP (**Figure 12B**). When considering the measurement of platelet-derived microparticles using flow cytometry, first it is worthy to perform the analysis of FSC (with linear scale) vs. SSC (with logarithmic scale). Microparticles appear close to the electronic noise and may interfere with cellular debris and precipitates. Regrettably, the standard protocol of how efficiently discriminate between the objects of interest particularly with small dimensions and dust particles or cellular debris has not been established hitherto. One of the possibilities is to use the ultrapure saline solution (filtered twice through a filter with a pore size of 0.2 μm) and to set up the reference threshold value for objects registered in the background noise (per time unit) at a given flow rate [120]. It should be emphasized herein that the value of 0.5 μm has been commonly accepted for the minimum size of the microparticles that can be reliably measured by modern classical cytometry. Microparticles with sizes lower than 0.5 μm are practically impossible to be distinguished from cellular debris. This is because the lasers used in most cytometers excite at 488 nm and this wavelength is not suitable as a discriminator for the detection of microparticles of sizes less than 488 nm (i.e., 0.488 μm) [121, 122]. Multiple smaller microparticles can often be detected simultaneously and are erroneously considered as single objects. High-sensitivity flow cytometers have been recently developed and they provide sufficient size resolution for the identification of microparticle subtypes [123, 124]. However, as with the conventional flow cytometers, protein aggregates and potentially other factors present in

biological samples may also significantly interfere in a measurement performed using novel-generation flow cytometers. Neither conventional nor even the standard novel-generation cytometers are optimal for the evaluation of murine microparticles due to their extremely small sizes of less than 0.2 μm. Therefore, it is recommended to use a high-sensitivity flow cytometer with the small particle module equipped with a more powerful blue laser (100 mW rather than 20 mW) and a Fourier bar that provides a lower background and noise and increases the angle of light diffusion[125]. The best strategy to identify microparticles would be the simultaneous monitoring of the forward light scattering and fluorescence upon labeling of the microparticles with the antibody recognizing the antigen reflecting their cell of origin. An example of such a marker may be annexin V, which more strongly binds to the platelet-derived microparticles than to normal platelets (due to the strong procoagulant activity of the former) [126]. The identification of platelet microparticles can also be made on the virtue of the gating for one of the pan-platelet surface antigens (CD41, CD41/61, and CD42) or platelet surface activation markers (P-selectin, active form of GP IIb/IIIa complex). Alternatively, the CELLTracker (5-chloromethylfluorescein, CMFDA) can be used to determine the platelet-derived microparticles [125]. This compound freely passes through cellular membrane and is subsequently converted into a fluorescent cell-impermeant product product by cytosolic esterases. When activating the platelets preloaded with this reagent, the fluorescence gets encapsulated within microparticles, permitting their closer identification [127]. However, the uncritical application of such an approach may be associated with the collection of artifacts. First of all, we should use the simultaneous labeling of several platelet membrane antigens since various subpopulations of microparticles may carry on their different surface platelet antigens [128]. Otherwise, the number of microparticles largely depends on biological and individual variation depending on numerous factors, such as a strain, sex, age, and physiological or pathophysiological state of the organism. Therefore, it is impossible to establish any kind of standardization depending on the volume of body fluid or the volume of platelet suspension. In such circumstances, a good solution may be the enumeration of microparticles using fluorescently labeled beads [129] and the subsequent use of the relevant amount of antibodies or the relevant concentration of a fluorophore for the labeling of a known number of microparticles in a cell suspension [117]. On the other hand, it should be remembered that to work with the calibration beads of a size range similar to the size of microparticles is more troublesome due to the nonlinearity of FSC parameter vs. the diameter of the small-sized beads. Alternatively, the measurements of the appropriately calibrated flow rate with the use of Trucount™ beads can be applied [120, 130]. In general, the photomultiplier (PMTs) values should be validated for the sufficient resolution of the objects. Too low resolution makes the recording of the poor-light scattering objects difficult, whereas for too high PMT values the recording of noncellular objects is also risky. It should be kept in mind that the use of artificial beads for any size-related calibrations (FSCs) remains imprecise as far as beads and microparticles display different refractive indices. The development of "calibration vesicles," having a refractive index similar to that of cellular microparticles, seems challenging, but the correct determination of microparticle sizes and further, maybe, the comprehension of their physio(patho)logical functions may be possible only with this "tool." In summary, the proper determination of microparticles, especially those derived from murine platelets, requires not

http://dx.doi.org/10.5772/63473

only the advanced and suitable flow cytometric instrumentation, but also, mostly, the properly validated protocols and the experience in this field of cytometric analysis.

8. Mitochondria as a source of energy for platelets' activation—the applications of flow cytometry

Mitochondria are essential for the proper functioning of the cell. Their main role is to generate ATP and to regulate the metabolism of the cell [131], but they are also involved in a number of other biochemical processes, including the regulation of calcium homeostasis [132], the production of reactive oxygen species [133], and the control of apoptotic and necrotic cell death [134]. An increasing number of reports indicate the potential impact of changes in a mitochondrial bioenergetic on the activation and aggregation of blood platelets [135–138], and more even so, considering that both these physiological events definitely depend on the energy produced in platelet mitochondria [136–138]. Changes in blood platelet mitochondria mass, mitochondrial membrane potential (MMP), reactive oxygen species production (ROS), ATP level, or mitochondrial respiration were observed in pathological states and diseases, such as sepsis [139], diabetes [140–142], or major depressive disorder (MDD) [143]. Some studies revealed positive associations between the expressions of activation markers on the surface of blood platelets (like P-selectin) and the extent of mitochondrial respiration [144] or the value of mitochondrial membrane potential [143]. Moreover, the associations between the potentiated collagen-stimulated platelet aggregation and mitochondrial membrane hyperpolarization and/or the overproduction of mitochondrial ROS in blood platelets were observed [135]. Interestingly, it has also been revealed that the mechanism of the action of a strong inhibitor of platelet adhesion and aggregation, nitric oxide, can be associated with the inhibition of the complex IV of mitochondrial respiratory chain, thus implying a reduced mitochondrial energy production [138]. Therefore, more and more attention is paid to the mitochondrial functioning in blood platelets, and flow cytometry is certainly a well-suited technique often chosen for this purpose. The following examples help to understand the essence of the appropriate study design of the experiments in which the flow cytometry technique is used to study mitochondria and to show how our knowledge on the applied staining methods helps in assessing the reliability of the results.

8.1. Mitochondrial membrane potential

One of the most commonly evaluated parameters when studying these organelles is the mitochondrial membrane potential. This parameter is a sensitive indicator of the mitochondrial energetic state. The conventional techniques for MMP measurements are based on the potential-dependent movement of positively charged lipophilic dyes across biological membranes. This method can be applied in both isolated mitochondria and intact cells. Since the potential inside the cell is negative (about −60 mV for the majority of cells), the positively charged dye molecules freely pass through the cell membrane to get into the cytoplasm and negatively charged organelles. Due to the strong negative potential of the mitochondrial

matrix (approximately −160 mV), much more dye (by two or even three orders of magnitude) can accumulate in the mitochondria matrix than in the cytoplasm. Significant amounts of dyes also locate in the space between the two mitochondrial membranes. Therefore, the total amount of cationic dyes inside the cell highly depends on the mitochondrial potential [145]. Changes in mitochondrial membrane potential lead to the concentration-dependent alterations in a dye fluorescence. However, the use of cationic, lipophilic fluorescent probes is not devoid of traps regardless of whether we study cells derived from humans, animals, or cell cultures. Therefore, a careful selection of a probe and the knowledge about its limitations are extremely important.

8.2. Problems with the evaluation of MMP with the use of cationic, lipophilic fluorescence probes

The problems concerning the use of cationic lipophilic dyes to evaluate the MMP include (a) nonspecific binding of the dye, e.g., rhodamine 123 (Rh-123), which locates in a number of places regardless of the level of energetic level of mitochondria or (b) the need to use large amounts of biological material to record signals of sufficiently high intensity [146]. Moreover, numerous potential-sensitive fluorescent probes may nonspecifically inhibit mitochondrial respiration, and thus, indirectly contribute to the changes in mitochondrial potential. Such features are characteristic for carbocyanine dyes such as $DiOC_2$ (3), $DiOC_5$ (3), $DiOC_6$ (3), $DiOC_2$ (4) [147], or rhodamine 123 [148]. Due to the cytotoxicity of these compounds, it is recommended to avoid the use of these dyes at loading concentrations higher than 1 μM. In general, to restrain problems with fluorescent signal that is nonproportional to MMP, probe concentrations should not exceed 500 nM [149]. Therefore, the evaluation of a threshold concentration for the selected probe, above which a fluorescence quenching occurs, is always highly recommended. Otherwise, the accumulation of a probe used at the excessive concentrations may likely complicate the data interpretation [150, 151]. Furthermore, some literature reports indicate that rhodamine 123 has a high nonspecific fluorescence in the presence of the elevated level of reactive oxygen species in the sample (regardless of whether isolated mitochondria or whole cells are studied) and this type of fluorescence is not related to the mitochondrial membrane potential [152, 153]. Therefore, it may happen that inexperienced researchers may consider such a rhodamine 123-derived fluorescence as an indicator of high (or low) MMP, whereas in fact (usually unconsciously) they evaluate the level of ROS. Therefore, the best option, as far as we want to obtain the reliable results, is not to employ this dye in the measurements of MMP [154]. Unfortunately, relatively low cost of rhodamine vs. other more specific markers used to evaluate the MMP, the apparent ease of a "direct" interpretation of the obtained results and the widespread use of this dye, makes rhodamine still commonly used by many researchers to assess the potential of mitochondrial membrane in both the studies that use spectrofluorometry and those that employ flow cytometry.

8.3. The use of JC-1 to evaluate MMP with the addition of MP uncouplers: CCCP and FCCP

One of the most popular dyes to evaluate MMP is JC-1 (5,5',6,6'-tetrachloro-1,1',3,3'-tetraethylbenzimidazolylcarbocyanine iodide). It is also one the most commonly used indicators of MMP in human blood platelets [155–160]. Although the studies of MMP in rodent platelets are very

http://dx.doi.org/10.5772/63473

scarce, the occasionally collected data point out that JC-1 also remains the most commonly used probe for the evaluation of MMP in both rat [161, 162] and mouse [155, 163–167] blood platelets. At high concentrations, this dye forms aggregates. This change is accompanied by the shift in the emission wavelength from green fluorescence (FL1 channel), characteristic for the JC-1 monomers (occurring at low mitochondrial potential), to red fluorescence (channel FL2), characteristic for JC-1 aggregates (occurring at elevated mitochondrial potential) (**Figure 13**).

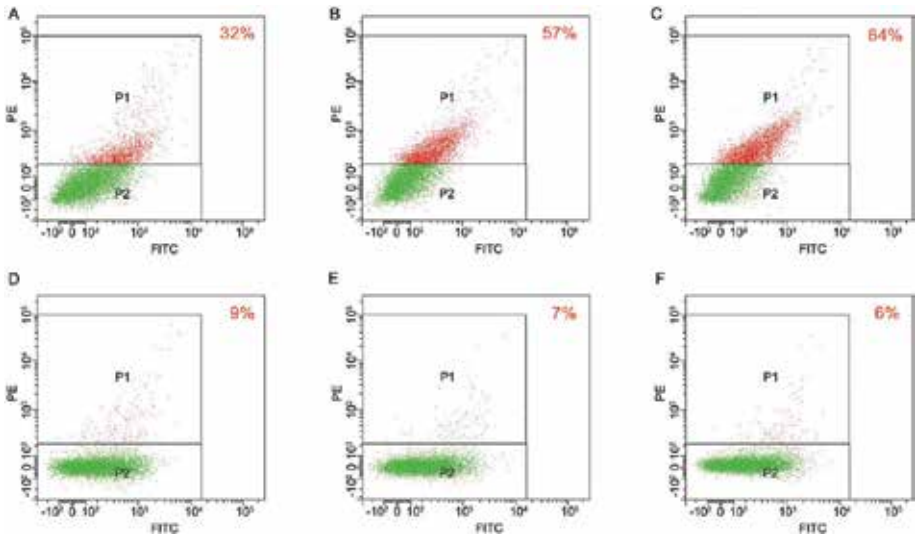

Figure 13. The flow cytometric analysis of MMP measured with the use of JC-1 in mitochondria isolated from rat hepatocytes. The fraction of JC-1 aggregates (region P1) in mitochondria (A, B, C) incubated with EtOH (solvent for FCCP) disappears after the incubation with 5 μM FCCP lasting for 1 minute (D), 6 minutes (E), and after 11 minutes (F). Green dots in the region P2 represent the fluorescence emitted by monomers, while red dots in the region P1 show the fluorescence emitted by JC-1 aggregates. The number of JC-1 aggregates was presented as a numerical value (in red).

In mitochondria with a high MMP, JC-1 spontaneously forms aggregates, which results in the intense red fluorescence dominating over a weak green fluorescence (**Figure 13A**, **B**, and **C**). With a decline in mitochondrial membrane potential, caused for example by the addition of a strong MMP uncoupler (such as CCCP or FCCP) to the sample, the dye concentration inside the mitochondrial matrix reduced, which is accompanied by the disintegration of JC-1 aggregates to monomeric forms. These changes lead to a distinct change in the color of the light emitted by JC-1, from red to green (**Figure 13C**, **D**, and **E**). A simple mechanism of action of this dye is based on changes in the fluorescence emitted by either monomers or aggregates or both. The use of JC-1 allows for a fast and direct assessment of the MMP without the considerable risk of committing interpretation errors compared to the protocols using rhodamine 123. In **Figure 13**, we can see that before the addition of the uncoupler FCCP, the mitochondrial potential is very high, which is reflected by a strong increase in the concentration of the tracer inside mitochondria and the efficient formation of JC-1 aggregates. FCCP leads to the uncoupling of mitochondria and causes a quick and drastic decrease in MMP so

that any later changes in MMP of the uncoupled mitochondria (from 1 to 11 minutes) are almost imperceptible. The ratio of red light to green fluorescence emitted by JC-1 is then a suitable indicator for the evaluation of the MMP because the resultant fluorescence ratio is not influenced by size, shape, or density of mitochondria inside the cells. Moreover, JC-1-staining can be used for both isolated mitochondria and whole cells [146, 168]. Advantages and disadvantages of the flow cytometry technique in the analysis of MMP with the use JC-1 probe are mainly derived by the characteristics of the probe. Like in the case of other cationic, lipophilic dyes, the use of JC-1 may also lead to collecting artifacts associated with too short time of incubation of cells or mitochondria with JC-1. Therefore, it is important to carry out preliminary tests to determine the optimal time of staining (**Figure 13**). To illustrate this problem, the mitochondria were incubated for 1 minute with JC-1 before measurement and then the samples were measured again 5 and 10 minutes after the first measurement. After 11-minute incubation of mitochondria with probe, the ratio of red to green fluorescence increased from 0.3 to 1.1 (**Figure 13A**, **B**, and **C**). Such an increase was not observed for FCCP-uncoupled mitochondria (**Figure 13D**, **E**, and **F**). This clearly shows that too short time designed for the dye accumulation results in the underestimation of the JC-1 aggregate/monomer ratio (and the misevaluation of MMP), and may lead to the blurring of the differences between mitochondria with different MMP. Hence, the rigorously controlled time of mitochondria incubation with the probe is essential. The recommended incubation time may vary depending on the studied sample and usually it is within the range of 1 and 15 minutes. Therefore, it seems highly desirable to evaluate the incubation time that would be appropriate to a given experimental protocol (which may differ in details since it closely depends on the type of examined mitochondria) and to stick to it faithfully. Due to the broad spectrum of JC-1 emissions, the additional staining of a sample with antibodies conjugated with FITC or PE may cause certain problems. This apparent obstacle, however, can be bypassed by choosing antibodies conjugated with fluorochromes emitting in the deep red (channel FL3). This creates additional opportunities for researchers, but it is not entirely devoid of drawbacks because such a choice may sometimes be quite problematic when setting up the compensation, e.g., in the case of simultaneous staining with propidium iodide and JC-1. Other commonly used indicators of MMP are TMRM (tetramethyl rhodamine methyl ester) and TMRE (tetramethyl rhodamine ethyl ester). However, TMRE was found to inhibit the mitochondrial respiration chain even stronger than Rh123 when used at approximately the same concentrations. Otherwise, TMRM has no effect on mitochondrial respiration, at least when used at low concentrations [151], and therefore, it became one of the most popular dyes to evaluate MMP in different cells [169–173]. TMRM is also very often used in the research of both human and rodents' blood platelets [174, 175]; according to the number of publications listed in PubMed, TMRM is actually the second most frequently used indicator of MMP in mouse blood platelet mitochondria [141, 176]. Both TMRE and TMRM exhibit a considerable fluorescence quenching upon their accumulation in mitochondria, and the characteristic red shifts in both the maximum excitation and emission wavelengths [151]. These dyes can be used in both nonquenching (below 5 nM) [177] and quenching modes, keeping in mind, however, that the appropriate approach and suitable calculations should always be carefully elaborated [178]. Moreover, it is important to remember that very often mitochondrial preparations are not

http://dx.doi.org/10.5772/63473

homogeneous. They may significantly differ in both the number of mitochondria in cells (important for measurements in whole cells) and the level of mitochondrial membrane potential (important for measurements in whole cells or isolated organelles). Mitochondria are cellular organelles that are in a constant motion, undergoing fission and fusion, which are usually accompanied by the MMP changes passed on adjacent mitochondria [179]. The consequence of this is the difference in the accumulation of a tracer in the studied mitochondria preparation, which in turn affects the recorded differences in the fluorescence intensity of the probe [180]. The advantage of flow cytometry over spectrofluorometry lies in the fact that the fluorescence is collected from each object individually, thus allowing to calculate median or mean and to determine a variability for all objects in the sample. This gives an idea about the biological variation of mitochondria presented in the sample. Moreover, the possibility of multicolor staining, using different markers to study various parameters of mitochondrial function, seems the advantage hard to overestimate. However, since for the evaluation of mitochondrial parameters an ideal method has not yet been discovered, it is important to remember the limits of the presented methods.

9. Blood platelet apoptosis—do we need to bother with this?

Blood platelets are produced by megakaryocytes, then released into the bloodstream, where they circulate for around 10 days (anucleate human platelets) or much shorter—from a few hours to a few days (anucleate rodents' platelets). Afterward, platelets are destroyed by the reticuloendothelial system, mainly in spleen and liver [181]. While some mechanisms regulating the platelet biogenesis have been known very well [182], the factors that control their lifespan and death are still a subject of many speculations. Physiologically, the cells that are aged, redundant, damaged, or infected are eliminated by the organism in the course of a cell suicide mechanism termed apoptosis [183]. Nevertheless, apoptosis is thought to be unique to selected cells, and although the mechanisms controlling the lifespan of platelets is still not clear, a number of studies suggested that apoptosis may also concern blood platelets [184, 185]. Hence, some nontrivial questions may be raised. How do platelets undergo apoptosis living so shortly? Is it possible at all? Is it reasonable from the evolutionary point of view? What are the mechanisms of their apoptosis, if any? Willing to answer these questions, in this chapter we provide a brief insight into some peculiar and specific regularities of apoptosis in murine platelets. It has been evidenced quite well that platelets display all the typical events of apoptotic pathway. It suggests that we can consider the occurrence of apoptosis in platelets. Numerous studies have documented that apoptosis in platelets can be induced by various factors, such as (a) natural or artificial chemical agonists, i.e., ADP, collagen, thrombin, hydrogen peroxide, arachidonic acid, calcium ionophore-A23187, ionomycin, valinomycin, dibucaine, epinephrine, and cyclosporine A [186–188]; (b) oxidative-stress-associated factors, i.e., hyperlipidemia, altered cardiac functions, diabetes, and chronic uremia [189, 190]; (c) physical factors, i.e., hyperthermia, hypothermia, platelet storage, and shear stress [190–192]; and (d) others, i.e., resveratrol, doxorubicin, etc. [193, 194]. The majority of these proapoptotic factors have been identified when studying human platelets; however, it is likely that a

number of them may *per analogiam* also act in rodents' platelets (i.e., originating from rats or mice). Until now, to the best of our knowledge, merely very occasional papers related to this subject have been published. The first reports date back to the last decade, suggesting the possible mechanisms of apoptosis in blood platelets of these species [191]. Interestingly, at the very beginning of the researchers' interest focused on platelet apoptosis, different terms were used to define the phenomenon occurring specifically in these cells, e.g. "process that resembles apoptosis," "apoptosis-like events," "apoptosis-like process," or "constitutive death program" [191]. Most likely it happened because two intimately connected physiological phenomena, apoptosis and platelet activation, share common morphological and biochemical features. Nowadays, there is no longer doubt that anucleate platelets of higher vertebrates also have the ability to self-destruction in the course of the commonly known process of apoptosis. The symptoms of apoptosis concern the "bunch" of morphological changes, including the platelet shrinkage, plasma membrane scrambling, cytoplasm condensation, or phosphatidylserine (PS) redistribution to the outside leaflet of the surface membrane lipid bilayer. All of the above-mentioned alterations were found in murine platelets after the treatment with either thrombin or collagen [195]. Moreover, the other apoptosis markers, such as the enhanced depolarization of the mitochondrial membrane (reduced membrane potential), cytochrome c release from mitochondria, caspase pathway activation, and microparticle formation, have been well annotated to blood platelets from mice [196]. In the paper by Gyulkhandanyan et al., the authors indicated some murine models, in which the occurrence of apoptosis in platelets was studied. It was revealed that on exposure to various factors (antiplatelet antibodies, diabetes induction, aging processes, and genetic mutations), blood platelets of mice, rats, rabbits, or dogs exhibited all the hallmarks of classical apoptosis [196]. In another study, Zhao et al. demonstrated that lovastatin (a statin drug used for the lowering of plasma cholesterol) induced a dose-dependent apoptosis of murine platelets, and the revealed significant depolarization of mitochondrial membrane strongly suggested that apoptosis proceeded through the mitochondria-associated pathways. Furthermore, the authors demonstrated that lovastatin therapy lead to the upregulation of proapoptotic Bak protein, downregulation of antiapoptotic Bcl-X_L protein, and the activation of caspases-3 and 9, thus clearly indicating that these platelets were able to undergo the apoptosis using mitochondrial destruction [197]. The integrity of outer mitochondrial membrane (OMM) is regulated by proapoptotic and antiapoptotic members of Bcl-2 family proteins. Following proapoptotic treatment, the balance between Bcl-2 regulatory proteins shifts in a proapoptotic direction. Proapoptotic Bcl-2 proteins interact with the OMM, resulting in membrane permeabilization and release of apoptogenic factors [198, 199]. The investigations conducted by Leytin et al. have shown that *in vivo* administration of antiplatelet antibody, antiglycoprotein IIb (anti-GPIIb), causes apoptotic changes in murine platelets, involving the dissipation of mitochondrial transmembrane potential, the activation of caspase-3, and the augmented exposure of PS [200]. Other research demonstrated apoptosis of rabbit platelets exposed to the action of ßy-CAT (nonlens crystalline). The activation of caspase-3, augmented PS exposure, depolarization of mitochondrial membrane, cytochrome c release, as well as a strong expression of Bax and Bak proteins were recorded. Two of these phenomena, PS delocalization and mitochondrial membrane depolarization, appeared Ca^{2+} dependent [201]. Interestingly, it was

http://dx.doi.org/10.5772/63473

also revealed that aspirin (a widely used antiplatelet and inflammatory drug) administered in mice caused significant reduction in the half-life of circulating platelets. Moreover, following the treatment with aspirin platelets exhibited features of typical apoptosis, including the decrease in mitochondrial membrane potential, the increase in PS exposure, the rise in the cytosolic ROS concentrations, and the activation of caspase-3 [202]. The above findings, briefly reviewed herein, indicate that murine platelets are intrinsically programed to undergo cell death and that their lifespan in the circulation is circumscribed by the initiation of the pathway of apoptosis. Moreover, it also seems that mitochondria play a central role in mediating the phenomena associated with platelet life and death cycle. It appeared that diverse stimuli (e.g., thrombin, calcium ionophore A23187, or antiglycoprotein (GP) IIb antibody) are able to induce depolarization of transmembrane mitochondrial potential in blood platelets. Mitochondria-associated apoptotic markers (caspase-9 and proapoptotic members of Bcl-2 family, caspase-3) have also been shown to get induced in animal platelets on the appropriate stimulation, both under *in vitro* and *in vivo* conditions [188, 203]. Remarkably, the contribution of the extrinsic apoptosis pathway to the regulation of platelet lifespan and death has not been hitherto extensively explored. Probably because until now platelets had been reported to lack the death FAS receptors, suggesting that classical extrinsic activation of apoptosis by FAS ligand is unlikely in these cells [204]. However, recently Schleicher et al. have evidenced that both human- and mouse-activated platelets present the death receptor Fas ligand (FasL) on their surface, which is able to trigger platelet apoptosis [205]. These findings suggest that platelets are probably not "slavishly" dependent on mitochondrial signaling to undergo apoptosis, but can also use other pathways to induce process of the programed death. In the face of these reports, probably the role of the extrinsic pathway of apoptosis in regulating platelet survival, particularly in pathological states, will still be explored and new facts may soon appear on this intriguing topic. The above-mentioned pieces of evidence seem supportive for the belief that apoptosis may also concern platelets in mice or, more generally, in rodents. This in turn implies another question: how apoptotic platelets could be identified and further characterized using flow cytometric tools? In 2009 The Nomenclature Committee on Cell Death (NCCD) has formulated the recommendations for the determination of apoptosis in nucleated cells. Later, based on these guidelines, Gyulkhandanyn et al. have proposed the bunch of methods useful for the characterization of apoptosis in anucleate cells, such as platelets. Among them, the flow cytometric analysis of the increased caspase-3 activity with the use of a cell-penetrating carboxyfluorescein probe, FAM-DEVED-FMK (the executioner of caspase-3 activation), has been strongly encouraged. Staining of fixed permeabilized platelets with anti-Bax and anti-Bak antibodies demonstrated the increased binding of these antibodies to proapoptotic Bax and Bak proteins following thrombin treatment [196]. Rapid development of cytometric tools and protocols suitable for the monitoring of apoptosis in anucleate platelets has soon revived the interest in the use of fluorescently labeled annexin V for the determination of the symmetrization of platelet membrane lipid bilayer. The loss of a natural asymmetry of phospholipid distribution, with PS being preferentially located in the inner leaflet of membrane lipid bilayer, appeared so intimately associated with the apoptotic pathway that nowadays the use of annexin V became an integral part of the protocol for determining apoptosis [195, 196]. One particular methodological issue has to be addressed

herein. The protocol with annexin V works appropriately, provided the concentration of Ca^{2+} ions is sufficient [206, 207]. To ensure the efficient annexin V binding, samples are supplemented with exogenous calcium (intraplatelet [Ca^{2+}] increased up to 2.5 mM), which is of particular significance in blood samples anticoagulated with calcium chelators (e.g., sodium citrate) [116, 208]. However, what is good for annexin binding appears devastating for blood platelets. In the milieu rich with Ca^{2+} ions platelets undergo facilitated spontaneous activation, and thus, they become more procoagulant [209–211]. In turn, the enhanced platelet priming and accelerated activation drive to the augmented consumption of platelets and a massive formation of microparticles [212–214]. Thus, the protocol may appear to drive artifactual outcomes, as far as it perpetuates platelet activation, although, paradoxically, it has been designed to determine the extent of platelets' readiness to get activated. Remarkably, all the above hallmarks, presented in the course of platelets' staining with annexin V, are strictly convergent with those typical for apoptosis [215–218]. Then, it is of no wonder that merely the determination of annexin V binding might discriminate reliably apoptotic from nonapoptotic platelets. Occasionally, another protocol for the determination of PS exposure in blood platelets, devoid of the above-mentioned drawbacks, has been elaborated and validated, which uses merocyanine 540 instead of annexin V. This alternate or compounding protocol is based on the membrane charge redistribution and may be used in a whole blood flow cytometry for the monitoring of platelet membrane symmetrization. Platelet staining with MC540 does not require Ca^{2+}; however, it is sensitive to the fluctuations in the intraplatelet [Ca^{2+}] during platelet activation, required for the increased PS exposure and membrane bilayer symmetrization [219, 220]. Furthermore, it has been revealed that the third upstream marker of apoptosis, the expression of proapototic members of Bcl-2 protein family, and their translocation to mitochondria can be successfully quantified by flow cytometry, allowing the detection of these proteins in both the cytosol and in the outer mitochondrial membrane. Another apoptotic hallmark, the changes in platelet mitochondrial membrane potential, may also be detected with the use of flow cytometry. Several cell-penetrating fluorescence dyes, such as $DiOC_6(3)$ or JC-1, have been recommended for that, as we have already much more profoundly described in the previous chapter [154, 155]. Platelet shrinkage, the consequence of shear-induced shedding of MPs, can be investigated using forward light scatter (FSC) and side scatter (SSC) flow cytometric histograms since FSC and SSC light signal intensities have been shown to correlate with cell size and internal cellular structure [221]. In order to decide whether platelets are apoptotic in the tested platelet population (e.g., platelet-isolated animal models) and to evaluate the sensitivity of the tested population to stimulation with appropriate apoptosis trigger, it has been recommended to use not one but several apoptosis markers simultaneously to determine a whole spectrum and the magnitude of apoptotic responses. All assays should be performed in parallel with positive and negative controls. Platelets may be considered apoptotic if the level of the specific apoptotic response is statistically higher than that in respective negative control population, keeping in mind that the extent of apoptotic changes can be determined in comparison with positive controls. In accordance with the policy raised by the Nomenclature Committee on Cell Death, it has been recommended to employ the following methodology for the determination of apoptotic platelets: simultaneous quantitative determination of different apoptosis markers (e.g., mitochondrial membrane depolariza-

http://dx.doi.org/10.5772/63473

tion, MPTP formation, Bax and Bak expression, caspase-9 and caspase-3 activation, gelsolin and moesin cleavage, PS exposure, platelet shrinkage, and microplatelet formation) [196, 213, 222–225]. Healthy donor platelets treated with appropriate diluent buffer as a negative control and platelets treated with strong platelet agonists, such as calcium ionophore A23187 or thrombin or collagen, as a positive control, are strongly recommended [196]. In general, reviewing the literature related to the methodology employed for studying apoptotic events in blood platelets, flow cytometry seems one of the most often utilized and also one of the most universal for the confirmation of apoptosis. In summary, our literature review supports the argument that the phenomenon of apoptosis is not only theoretically possible, but that it really exists in murine platelets. Although it might seem unbelievable that platelets, the relatively short-lived cells, undergo apoptosis, there is quite a lot of data showing that apoptosis-like processes have been linked to these cells. Nevertheless, certainly the further studies on other apoptotic mechanisms could help in the understanding of the association between apoptotic pathway and platelets kinetics, platelet lifespan and their survival, and, as such, could add new insights into platelet biology.

Acknowledgements

The work was supported by the National Science Centre (grant number DEC-2012/06/A/NZ5/00069) and the National Centre for Research and Development (STRATEGMED 1/233226/11/NCBR/2015)

Author details

Hassan Kassassir[1], Karolina Siewiera[1], Tomasz Przygodzki[1], Magdalena Labieniec-Watala[2] and Cezary Watala[1*]

*Address all correspondence to: cezary.watala@umed.lodz.pl

1 Department of Haemostasis and Haemostatic Disorders, Medical University of Lodz, Lodz, Poland

2 Department of Medical Biophysics, University of Lodz, Lodz, Poland

References

[1] Schmitt A, Guichard J, Massé JM, Debili N, Cramer EM. Of mice and men: comparison of the ultrastructure of megakaryocytes and platelets. Experimental Hematology. 2001;29:1295–1302. DOI: 10.1016/S0301-472X(01)00733-0

[2] Takahashi O. Characteristics of rat platelets and relative contributions of platelets and blood coagulation to haemostasis. Food and Chemical Toxicology. 2000;38:203–218. DOI: 10.1016/S0278-6915(99)00155-6

[3] Al-Rubeai M, Welzenbach K, Lloyd DR, Emery AN. A rapid method for evaluation of cell number and viability by flow cytometry. Cytotechnology. 1997;24:161–168. DOI: 10.1023/A:1007910920355

[4] Ciaglowski RE, Martinez J, Ryan TJ, Lewandowski LJ, Barnhart MI, Weller MA, et al. Monoclonal antibodies to bovine platelet factor 4: species interactions to platelets and megakaryocytes using indirect immunocytofluorescence. Thrombosis Research. 1986;41:855–865.

[5] Dancis A, Ehmann C, Ferziger R, Grima K, Karpatkin S. GPIIIa-related PLA1 antigens with different molecular weights: studies in platelets, endothelial cells, and megakaryocytes. Blood. 1988;71:1056–1061.

[6] Ehrlich D, Hochstrasser T, Humpel C. Effects of oxidative stress on amyloid precursor protein processing in rat and human platelets. Platelets. 2015;24:26–36. DOI: 10.3109/09537104.2012.661104

[7] Nuytens K, Tuand K, Di Michele M, Boonen K, Waelkens E, Freson K, Creemers JW. Platelets of mice heterozygous for neurobeachin, a candidate gene for autism spectrum disorder, display protein changes related to aberrant protein kinase A activity. Molecular Autism. 2013;4:43. DOI: 10.1186/2040-2392-4-43

[8] Sintnicolaas K, de Vries W, van der Linden R, Gratama JW, Bolhuis RL. Simultaneous flow cytometric detection of antibodies against platelets, granulocytes and lymphocytes. Journal of Immunological Methods. 1991;142:215–222.

[9] McFarland DC1, Zhang C, Thomas HC, T L R. Confounding effects of platelets on flow cytometric analysis and cell-sorting experiments using blood-derived cells. Cytometry Part A. 2006;69:86–94. DOI: 10.1002/cyto.a.20207

[10] Kassassir H, Siewiera K, Sychowski R, Watała C. Can the antiplatelet effects of cangrelor be reliably studied in mice under in vivo and in vitro conditions using flow cytometry? Pharmacological Reports. 2013;65:870–883.

[11] Nemzek JA, Bolgos GL, Williams BA, Remick DG. Differences in normal values for murine white blood cell counts and other hematological parameters based on sampling site. Inflammation Research. 2001;50:523–527. DOI: 10.1007/PL00000229

[12] Unsworth AJ, Smith H, Gissen P, Watson SP, Pears CJ. Submaximal inhibition of protein kinase C restores ADP-induced dense granule secretion in platelets in the presence of Ca2+. The Journal of Biological Chemistry. 2011;286:21073–21082. DOI: 10.1074/jbc.M110.187138

[13] Cornelissen I, Palmer D, David T, Wilsbacher L, Concengco C, Conley P, et al. Roles and interactions among protease-activated receptors and P2ry12 in hemostasis and

thrombosis. Proceeding of the National Academy of Sciences of the United States of America. 2010;107:18605–18610. DOI: 10.1073/pnas.1013309107

[14] Jirouskova M, Shet AS, Johnson GJ. A guide to murine platelet structure, function, assays, and genetic alterations. Journal of Thrombosis and Haemostasis. 2007;5:661–669. DOI: DOI: 10.1111/j.1538-7836.2007.02407.x

[15] Armstrong PC, Kirkby NS, Zain ZN, Emerson M, Mitchell JA, Warner TD. Thrombosis is reduced by inhibition of COX-1, but unaffected by inhibition of COX-2, in an acute model of platelet activation in the mouse. PLoS One. 2011;6:e20062. DOI: 10.1371/journal.pone.0020062

[16] Bhavaraju K, Lakhani PR, Dorsam RT, Jin J, Hitchcock IS, Sanjay A, Kunapuli SP. G(12/13) signaling pathways substitute for integrin αIIbβ3-signaling for thromboxane generation in platelets. PLoS One. 2011;6:e16586. DOI: 10.1371/journal.pone.0016586

[17] Massberg S, Gawaz M, Grüner S, Schulte V, Konrad I, Zohlnhöfer D, et al. A crucial role of glycoprotein VI for platelet recruitment to the injured arterial wall in vivo. The Journal of Experimental Medicine. 2003;197:41–49. DOI: 10.1084/jem.20020945

[18] Renné T, Pozgajová M, Grüner S, Schuh K, Pauer HU, Burfeind P, et al. Defective thrombus formation in mice lacking coagulation factor XII. The Journal of Experimental Medicine. 2005;202:271–281. DOI: 10.1084/jem.20050664

[19] Stalker TJ, Traxler EA, Wu J, Wannemacher KM, Cermignano SL, Voronov R, et al. Hierarchical organization in the hemostatic response and its relationship to the platelet-signaling network. Blood. 2013;121:1875–1885. DOI: 10.1182/blood-2012-09-457739

[20] Tomaiuolo M, Stalker TJ, Welsh JD, Diamond SL, Sinno T, Brass LF. A systems approach to hemostasis: 2. Computational analysis of molecular transport in the thrombus microenvironment. Blood. 2014;124:1816–1823. DOI: 10.1182/blood-2014-01-550343

[21] Jayakumar T, Chen WF, Lu WJ, Chou DS, Hsiao G, Hsu CY, et al. A novel antithrombotic effect of sulforaphane via activation of platelet adenylate cyclase: ex vivo and in vivo studies. Journal of Nutritional Biochemistry. 2013;24:1086–1095. DOI: 10.1016/j.jnutbio.2012.08.007

[22] Armstrong PC, Kirkby NS, Zain ZN, Emerson M, Mitchell JA, Warner TD. Thrombosis is reduced by inhibition of COX-1, but unaffected by inhibition of COX-2, in an acute model of platelet activation in the mouse. PLoS One. 2011;6:e20062. DOI: 10.1371/journal.pone.0020062

[23] Przygodzki T, Talar M, Blazejczyk A, Kalchenko V, Watala C. Quantification of the blood platelet reactivity in the ADP-induced model of non-lethal pulmonary thromboembolism in mice with the use of laser Doppler flowmetry. PLoS One. 2016;11:e0146346. DOI: 10.1371/journal.pone.0146346

[24] Rughetti A, Giusti I, D'Ascenzo S, Leocata P, Carta G, Pavan A. Platelet gel-released supernatant modulates the angiogenic capability of human endothelial cells. Blood Transfusions. 2008;6:12–17. DOI: 10.2450/2008.0026-07

[25] Wu CL, Lee SS, Tsai CH, Lu KH, Zhao JH, Chang YC. Platelet-rich fibrin increases cell attachment, proliferation and collagen-related protein expression of human osteoblasts. Australian Dental Journal. 2012;57:207–212. DOI: 10.1111/j.1834-7819.2012.01686.x

[26] Albanyan AM, Harrison P, Murphy MF. Markers of platelet activation and apoptosis during storage of apheresis- and buffy coat-derived platelet concentrates for 7 days. Transfusion. 2009;49:108–117. DOI: 10.1111/j.1537-2995.2008.01942.x

[27] Lichtenfels R, Biddison WE, Schulz H, Vogt AB, Martin R. CARE-LASS (calcein-release-assay), an improved fluorescence-based test system to measure cytotoxic T lymphocyte activity. Journal of Immunological Methods. 1994;172:227–239.

[28] Neri S, Mariani E, Meneghetti A, Cattini L, Facchini A. Calcein-acetyoxymethyl cytotoxicity assay: standardization of a method allowing additional analyses on recovered effector cells and supernatants. Clinical and Diagnostic Laboratory Immunology. 2001;8:1131–1135. DOI: 10.1128/CDLI.8.6.1131-1135.2001

[29] Breuer W, Epsztejn S, Millgram P, Cabantchik IZ. Transport of iron and other transition metals into cells as revealed by a fluorescent probe. The American Journal of Physiology. 1995;268:1354–1361

[30] Konijn AM, Glickstein H, Vaisman B, Meyron-Holtz EG, Slotki IN, Cabantchik ZI. The cellular labile iron pool and intracellular ferritin in K562 cells. Blood. 1999;94:2128–2134.

[31] Thomas F, Serratrice G, Béguin C, Aman ES, Pierre JL, Fontecave M, et al. Calcein as a fluorescent probe for ferric iron. Application to iron nutrition in plant cells. The Journal of Biological Chemistry. 1999;274:13375–13383. DOI: 10.1074/jbc.274.19.13375

[32] Heger M, Salles II, van Vuure W, Deckmyn H, Beek JF. Fluorescent labeling of platelets with polyanionic fluorescein derivatives. Analytical and Quantitative Cytology and Histology. 2009;31:227–232.

[33] Rywaniak J, Luzak B, Podsedek A, Dudzinska D, Rozalski M, Watala C. Comparison of cytotoxic and anti-platelet activities of polyphenolic extracts from Arnica montana flowers and Juglans regia husks. Platelets. 2015;26:168–176. DOI: 10.3109/09537104.2014.894970

[34] Johnson PC, Ware JA, Cliveden PB, Smith M, Dvorak AM, Salzman EW. Measurement of ionized calcium in blood platelets with the photoprotein aequorin. Comparison with Quin 2. The Journal of Biological Chemistry. 1985;260:2069–2076.

[35] Sage SO, Merritt JE, Hallam TJ, Rink TJ. Receptor-mediated calcium entry in fura-2-loaded human platelets stimulated with ADP and thrombin. Dual-wavelengths studies with Mn2+. The Biochemical Journal. 1989;258:923–926.

[36] Salzman EW, Ware JA. Ionized calcium as an intracellular messenger in blood platelets. Progress in Hemostasis and Thrombosis. 1989;9:177–202.

[37] Zhou Y, Abraham S, Andre P, Edelstein LC, Shaw CA, Dangelmaier CA, et al. Anti-miR-148a regulates platelet FcγRIIA signaling and decreases thrombosis in vivo in mice. Blood. 2015;126:2871–2881. DOI: 10.1182/blood-2015-02-631135

[38] NaveenKumar SK, Thushara RM, Sundaram MS, Hemshekhar M, Paul M, Thirunavukkarasu C. Unconjugated bilirubin exerts pro-apoptotic effect on platelets via p38-MAPK activation. Scientific Reports. 2015;5:15045. DOI: 10.1038/srep15045

[39] Rink TJ, Smith SW, Tsien RY. Cytoplasmic free Ca2+ in human platelets: Ca2+ thresholds and Ca-independent activation for shape-change and secretion. FEBS Letters. 1982;148:21–26. DOI: 10.1002/1873-3468.12034

[40] Weiss HJ, Lages B. Platelet prothrombinase activity and intracellular calcium responses in patients with storage pool deficiency, glycoprotein IIb-IIIa deficiency, or impaired platelet coagulant activity—a comparison with Scott syndrome. Blood. 1997;89:1599–1611

[41] Suttle AW, Powling MJ, Ritter JM, Hardisty RM. Effects of a monoclonal antibody to glycoprotein IIb/IIIa (P256) and of enzymically derived fragments of P256 on human platelets. Thrombosis and Heamostasis. 1991;65:432–437

[42] Valant PA, Adjei PN, Haynes DH. Rapid Ca2+ extrusion via the Na+/Ca2+ exchanger of the human platelet. The Journal of Membrane Biology. 1992;130:63–82.

[43] Davies TA, Drotts DL, Weil GJ, Simons ER. Cytoplasmic Ca2+ is necessary for thrombin-induced platelet activation. The Journal of Biological Chemistry. 1989;264:19600–19606.

[44] Xu J, Krüger B, Vernunft A, Löhrke B, Viergutz T. Platelet-activating factor-stimulated production of reactive oxygen species in ovarian granulosa cells from periovulatory follicles. Cytometry Part A. 2009;75:658–664. DOI: 10.1002/cyto.a.20749

[45] Takahashi A, Camacho P, Lechleiter JD, Herman B. Measurement of intracellular calcium. Physiological Reviews. 2009;79:1089–1125.

[46] Carron CP, Hwo SY, Dingus J, Benson DM, Meza I, Bryan J. A re-evaluation of cytoplasmic gelsolin localization. The Journal of Cell Biology. 1986;102:237–245. DOI: 10.1083/jcb.102.1.237

[47] Paredes RM, Etzler JC, Watts LT, Zheng W, Lechleiter JD. Chemical calcium indicators. Methods. 2008;46:143–151. DOI: 10.1016/j.ymeth.2008.09.025

[48] Lopez E, Berna-Erro A, Salido GM, Rosado JA, Redondo PC. FKBP25 and FKBP38 regulate non-capacitative calcium entry through TRPC6. Biochimica et Biophysica Acta. 2015;1853:2684–2696. DOI: 10.1016/j.bbamcr.2015.07.023

[49] McDonough PM, Button DC. Measurement of cytoplasmic calcium concentration in cell suspensions: correction for extracellular Fura-2 through use of Mn2+ and probenecid. Cell Calcium. 1989;10:171–180.

[50] Merritt JE, McCarthy SA, Davies MP, Moores KE. Use of fluo-3 to measure cytosolic Ca^{2+} in platelets and neutrophils. Loading cells with the dye, calibration of traces, measurements in the presence of plasma, and buffering of cytosolic Ca^{2+}. Biochemical Journal. 1990;269:513–519. DOI: 10.1042/bj2690513

[51] Pasquet JM, Dachary-Prigent J, Nurden AT. Calcium influx is a determining factor of calpain activation and microparticle formation in platelets. European Journal of Biochemistry. 1996;239:647–654. DOI: 10.1111/j.1432-1033.1996.0647u.x

[52] Packham MA, Rand ML, Perry DW, Ruben DH, Kinlough-Rathbone RL. Probenecid inhibits platelet responses to aggregating agents in vitro and has a synergistic inhibitory effect with penicillin G. Thrombosis and Haemostasis. 1996;76:239–244.

[53] Chung SH, Kim MJ, Lee JY, Chung JH. Effects of probenecid on platelet aggregation and cytotoxicity: drawbacks of the use of probenecid in monitoring intracellular calcium metabolism. Thrombosis Research. 1997;85:345–350. DOI: 10.1016/S0049-3848(97)00020-0

[54] Carpenter-Deyo L, Duimstra JR, Hedstrom O, Reed DJ. Toxicity to isolated hepatocytes caused by the intracellular calcium indicator, Quin 2. Journal of Pharmacology and Experimental Therapeutics. 1991;258:739–746.

[55] Carpenter-Deyo L, Reed DJ. Involvement of calcium and iron in Quin 2 toxicity to isolated hepatocytes. Journal of Pharmacology and Experimental Therapeutics. 1991;258:747–752.

[56] Sedova M, Klishin A, Huser J, Blatter LA. Capacitative Ca2+ entry is graded with degree of intracellular Ca^{2+} store depletion in bovine vascular endothelial cells. The Journal of Physiology. 2000;523:549–559. DOI: 10.1111/j.1469-7793.2000.t01-3-00549.x

[57] Heusinkveld HJ, Westerink RH. Caveats and limitations of plate reader-based high-throughput kinetic measurements of intracellular calcium levels. Toxicology and Applied Pharmacology. 2011;255:1–8. DOI: 10.1016/j.taap.2011.05.020

[58] Assinger A, Volf I, Schmid D. A novel, rapid method to quantify intraplatelet calcium dynamics by ratiometric flow cytometry. PLoS One. 2015;10:e0122527. DOI: 10.1371/journal.pone.0122527

[59] Liedtke RJ, Kroon G, Batjer JD. Centrifugal analysis with automated sequential reagent addition: measurement of serum calcium. Clinical Chemistry. 1981;27:2025–2028.

[60] Liu K, Southall N, Titus SA, Inglese J, Eskay RL, Shinn P, et al. A multiplex calcium assay for identification of GPCR agonists and antagonists. Assay and Drug Development Technologies. 2010;8:367–379. DOI: 10.1089/adt.2009.0245

[61] do Céu Monteiro M, Sansonetty F, Gonçalves MJ, O'Connor JE. Flow cytometric kinetic assay of calcium mobilization in whole blood platelets using Fluo-3 and CD41. Cytometry. 1999;35:302–310.

[62] Vines A, McBean GJ, Blanco-Fernández A. A flow-cytometric method for continuous measurement of intracellular Ca(2+) concentration. Cytometry Part A. 2010;77:1091–1097. DOI: 10.1002/cyto.a.20974

[63] Davis KL, Martin E, Turko IV, Murad F. Novel effects of nitric oxide. Annual Review of Pharmacology and Toxicology. 2001;41:203–236. DOI: 10.1146/annurev.pharmtox.41.1.203

[64] Daff S. NO synthase: structures and mechanisms. Nitric Oxide. 2010;23:1–11. DOI: 10.1016/j.niox.2010.03.001

[65] Förstermann U, Sessa WC. Nitric oxide synthases: regulation. European Heart Journal. 2012;33:829–837. DOI: 10.1093/eurheartj/ehr304

[66] Friebe A, Koesling D. Regulation of nitric oxide-sensitive guanylyl cyclase. Circulation Research. 2003;93: 96–105. DOI: 10.1161/01.RES.0000082524.34487.31

[67] Geiger J, Nolte C, Walter U. Regulation of calcium mobilization and entry in human platelets by endothelium-derived factors. American Journal of Physiology. 1994;267:236–244.

[68] Subramanian H, Zahedi RP, Sickmann A, Walter U, Gambaryan S. Phosphorylation of CalDAG-GEFI by protein kinase A prevents Rap1b activation. Journal of Thrombosis and Haemostasis. 2013;11:1574–1582. DOI: 10.1111/jth.12271

[69] Jensen BO, Selheim F, Døskeland SO, Gear AR, Holmsen H. Protein kinase A mediates inhibition of the thrombin-induced platelet shape change by nitric oxide. Blood. 2004;104:2775 - 2782. DOI: 10.1182/blood-2004-03-1058

[70] Antl M, von Brühl ML, Eiglsperger C, Werner M, Konrad I, Kocher T, et al. IRAG mediates NO/cGMP-dependent inhibition of platelet aggregation and thrombus formation. Blood. 2007;109:552–559. DOI: 10.1182/blood-2005-10-026294

[71] Bredt DS. Nitric oxide signaling specificity—the heart of the problem. Journal of Cell Science. 2003;116:9–15. DOI: 10.1242/jcs.00183

[72] Radomski MW, Palmer RM, Moncada S. Endogenous nitric oxide inhibits human platelet adhesion to vascular endothelium. Lancet. 1987;330:1057–1058. DOI: 10.1016/S0140-6736(87)91481-4

[73] Gambaryan S, Tsikas D. A review and discussion of platelet nitric oxide and nitric oxide synthase: do blood platelets produce nitric oxide from L-arginine or nitrite? Amino Acids. 2015;47:1779–1793. DOI: 10.1007/s00726-015-1986-1

[74] Naseem KM, Riba R. Unresolved roles of platelet nitric oxide synthase. Journal of Thrombosis and Haemostasis. 2008;6:10–19. DOI: 10.1111/j.1538-7836.2007.02802.x

[75] Marjanovic JA, Stojanovic A, Brovkovych VM, Skidgel RA, Du X. Signaling-mediated functional activation of inducible nitric-oxide synthase and its role in stimulating platelet activation. The Journal of Biological Chemistry. 2008;283:28827–28834. DOI: 10.1074/jbc.M801646200

[76] Mehta JL, Chen LY, Kone BC, Mehta P, Turner P. Identification of constitutive and inducible forms of nitric oxide synthase in human platelets. The Journal of Laboratory and Clinical Medicine. 1995;125:370–377.

[77] Radomski MW, Palmer RM, Moncada S. Characterization of the L-arginine:nitric oxide pathway in human platelets. British Journal of Pharmacology. 1990;101:325–328. DOI: 10.1111/j.1476-5381.1990.tb12709.x

[78] Freedman JE, Loscalzo J, Barnard MR, Alpert C, Keaney JF, Michelson AD. Nitric oxide released from activated platelets inhibits platelet recruitment. The Journal of Clinical Investigation. 1997;100:350–356. DOI: 10.1172/JCI119540

[79] Dimmeler S, Fleming I, Fisslthaler B, Hermann C, Busse R, Zeiher AM. Activation of nitric oxide synthase in endothelial cells by Akt-dependent phosphorylation. Nature. 1999;399:601–605. DOI: 10.1038/21224

[80] Russo I, Doronzo G, Mattiello L, De Salve A, Trovati M, Anfossi G. The activity of constitutive nitric oxide synthase is increased by the pathway cAMP/cAMP-activated protein kinase in human platelets. New insights into the antiaggregating effects of cAMP-elevating agents. Thrombosis Research. 2004;114:265–273. DOI: 10.1016/j.thromres.2004.06.036

[81] O'Kane PD, Queen LR, Ji Y, Reebye V, Stratton P, Jackson G. Aspirin modifies nitric oxide synthase activity in platelets: effects of acute versus chronic aspirin treatment. Cardiovascular Research. 2003;59:152–159. DOI: 10.1016/S0008-6363(03)00323-7

[82] Gambaryan S, Kobsar A, Hartmann S, Birschmann I, Kuhlencordt PJ, Müller-Esterl W. NO-synthase-/NO-independent regulation of human and murine platelet soluble guanylyl cyclase activity. Journal of Thrombosis and Haemostasis. 2008;6:1376–1384. DOI: 10.1111/j.1538-7836.2008.03014.x

[83] Böhmer A, Gambaryan S, Tsikas D. Human blood platelets lack nitric oxide synthase activity. Platelets. 2015;26:583–588. DOI: 10.3109/09537104.2014.974024

[84] Marjanovic JA, Li Z, Stojanovic A, Du X. Stimulatory roles of nitric-oxide synthase 3 and guanylyl cyclase in platelet activation. Journal of Biological Chemistry. 2005;280:37430–37438. DOI: 10.1074/jbc.M506518200

[85] Williams RH, Nollert MU. Platelet-derived NO slows thrombus growth on a collagen type III surface. Thrombosis Journal. 2004;2:1–11. DOI: 10.1186/1477-9560-2-11

[86] Freedman JE, Sauter R, Battinelli EM, Ault K, Knowles C, Huang PL. Deficient platelet-derived nitric oxide and enhanced hemostasis in mice lacking the NOSIII gene. Circulation Research. 1999;84:1416–1421. DOI: 10.1161/01.RES.84.12.1416

[87] Momi S, Caracchini R, Falcinelli E, Evangelista S, Gresele P. Stimulation of platelet nitric oxide production by nebivolol prevents thrombosis. Arteriosclerosis, Thrombosis, and Vascular Biology. 2014;34:820–829. DOI: 10.1161/ATVBAHA.114.303290

[88] Brandes RP, Kim D, Schmitz-Winnenthal FH, Amidi M, Gödecke A, Mülsch A. Increased nitrovasodilator sensitivity in endothelial nitric oxide synthase knockout mice: role of soluble guanylyl cyclase. Hypertension. 2000;35: 231–236. DOI: 10.1161/01.HYP.35.1.231

[89] Tymvios C, Moore C, Jones S, Solomon A, Sanz-Rosa D, Emerson M. Platelet aggregation responses are critically regulated in vivo by endogenous nitric oxide but not by endothelial nitric oxide synthase. British Journal of Pharmacology. 2009;158:1735–1742. DOI: 10.1111/j.1476-5381.2009.00408.x

[90] Gupta A, Priya N, Jalal S, Singh P, Chand K, Raj HG. Specificity of calreticulin transacetylase to acetoxy derivatives of benzofurans: effect on the activation of platelet nitric oxide synthase. Biochimie. 2010;92:1180–1185. DOI: 10.1016/j.biochi.2010.06.011

[91] González-Trujano ME1, Alvarado-Vásquez N, Mendoza-Sotelo J, López G, Estrada-Camarena E, Martínez-Mota L, et al. Alterations on the morphology, nitric oxide synthesis and activity of platelets reproduced in rats as possible biomarkers for depression are reversed by fluoxetine. Pharmacology Biochemistry and Behavior. 2012;102: 349–356. DOI: 10.1016/j.pbb.2012.03.012

[92] Radomski MW, Palmer RM, Moncada S. An L-arginine/nitric oxide pathway present in human platelets regulates aggregation. Proceedings of the National Academy of Sciences of the United States of America. 1990;87:5193–5197. DOI: 10.1073/pnas.87.13.5193

[93] Chrapko W, Jurasz P, Radomski MW, Archer SL, Newman SC, Baker G, et al. Alteration of decreased plasma NO metabolites and platelet NO synthase activity by paroxetine in depressed patients. Neuropsychopharmacology. 2006;31:1286–1293. DOI: 10.1038/sj.npp.1300961

[94] Riba R, Sharifi M, Farndale RW, Naseem KM. Regulation of platelet guanylyl cyclase by collagen: evidence that Glycoprotein VI mediates platelet nitric oxide synthesis in response to collagen. Thrombosis and Haemostasis. 2005;94:395–403. DOI: 10.1160/TH05-01-0027

[95] Tsikas D, Sandmann J, Savva A, Luessen P, Böger RH, Gutzki FM. Assessment of nitric oxide synthase activity in vitro and in vivo by gas chromatography-mass spectrometry. Journal of Chromatography. 2000;742:143–153.

[96] Strijdom H, Muller C, Lochner A. Direct intracellular nitric oxide detection in isolated adult cardiomyocytes: flow cytometric analysis using the fluorescent probe, diaminofluorescein. Journal of Molecular and Cellular Cardiology. 2004;37:897–902. DOI: 10.1016/j.yjmcc.2004.05.018

[97] Schachnik NC, Peruhype-Magalhães V, Paula GM, Lucas F Jr, Freitas VM, Martins-Filho OA. Intracellular nitric oxide assessment in whole blood leukocytes by flow cytometry: optimization and applicability to monitor patients with chronic graft nephropathy. Journal of Immunological Methods. 2009;343:103–111. DOI: 10.1016/j.jim.2009.01.010

[98] Yamashita T1, Shoge M, Oda E, Yamamoto Y, Giddings JC, Kashiwagi S, et al. The free-radical scavenger, edaravone, augments NO release from vascular cells and platelets after laser-induced, acute endothelial injury in vivo. Platelets. 2006;17:201–206. DOI: 10.1080/09537100500444063

[99] Cortese-Krott MM, Rodriguez-Mateos A, Kuhnle GG, Brown G, Feelisch M, Kelm M. A multilevel analytical approach for detection and visualization of intracellular NO production and nitrosation events using diaminofluoresceins. Methods in Free Radical Biology and Medicine. 2012;53:2146–2158. DOI: 10.1016/j.freeradbiomed.2012.09.008

[100] Ku CJ, Karunarathne W, Kenyon S, Root P, Spence D. Fluorescence determination of nitric oxide production in stimulated and activated platelets. Analytical Chemistry. 2007;79:2421–2426. DOI: 10.1021/ac061572q

[101] Balcerczyk A, Soszynski M, Bartosz G. On the specificity of 4-amino-5-methylamino-2′,7′-difluorofluorescein as a probe for nitric oxide. Free Radical Biology and Medicine. 2005;39:327–335. DOI: 10.1016/j.freeradbiomed.2005.03.017

[102] Wardman P. Fluorescent and luminescent probes for measurement of oxidative and nitrosative species in cells and tissues: progress, pitfalls, and prospects. Free Radical Biology and Medicine. 2007;43:995–1022. DOI: 10.1016/j.freeradbiomed.2007.06.026

[103] György B, Szabó TG, Pásztói M, Pál Z, Misják P, Aradi B. Membrane vesicles, current state-of-the-art: emerging role of extracellular vesicles. Cellular and Molecular Life Sciences. 2011;68:2667–2688. DOI: 10.1007/s00018-011-0689-3

[104] Horstman LL, Ahn YS. Platelet microparticles: a wide-angle perspective. Critical Reviews in Oncology/Hematology. 1999;30:111–142. DOI: 10.1016/S1040-8428(98)00044-4

[105] Italiano JE Jr, Mairuhu AT, Flaumenhaft R. Clinical relevance of microparticles from platelets and megakaryocytes. Current Opinion in Hematology. 2010;17: 578–584. DOI: 10.1097/MOH.0b013e32833e77ee

[106] Ardoin SP, Shanahan JC, Pisetsky DS. The role of microparticles in inflammation and thrombosis. Scandinavian Journal of Immunology. 2007;66:159–165. DOI: 10.1111/j.1365-3083.2007.01984.x

[107] Nomura S. Function and clinical significance of platelet-derived microparticles. International Journal of Hematology . 2001;74:397–404 . DOI: 10.1007/BF02982082

[108] Cocucci E, Racchetti G, Meldolesi J. Shedding microvesicles: artefacts no more. Trends in Cell Biology. 2009;19:43–51. DOI: 10.1016/j.tcb.2008.11.003

[109] Freyssinet JM, Toti F. Formation of procoagulant microparticles and properties. Thrombosis Research. 2010;125:46–48. DOI: 10.1016/j.thromres.2010.01.036

[110] Jy W, Horstman LL, Jimenez JJ, Ahn YS, Biró E, Nieuwland R, et al. Measuring circulating cell-derived microparticles. Journal of Thrombosis and Haemostasis. 2004;2:1842–1843. DOI: 10.1111/j.1538-7836.2004.00936.x

[111] Ramacciotti E, Hawley AE, Farris DM, Ballard NE, Wrobleski SK, Myers DD Jr, et al. Leukocyte- and platelet-derived microparticles correlate with thrombus weight and tissue factor activity in an experimental mouse model of venous thrombosis. Thrombosis and Haemostasis. 2009;101: 605–794. DOI: 10.1160/TH08-09-0620

[112] Chen Y, Davis-Gorman G, Watson RR, McDonagh PF. Platelet CD62p expression and microparticle in murine acquired immune deficiency syndrome and chronic ethanol consumption. Alcohol and Alcoholism. 2003;38:25–30. DOI: 10.1093/alcalc/agg013

[113] Zumbach A, Marbet GA, Tsakiris DA. Influence of the genetic background on platelet function, microparticle and thrombin generation in the common laboratory mouse. Platelets. 2001;12:496–502. DOI: 10.1080/095371001317126392

[114] Schäfer A, Flierl U, Kobsar A, Eigenthaler M, Ertl G, Bauersachs J. Soluble guanylyl cyclase activation with HMR1766 attenuates platelet activation in diabetic rats. Arteriosclerosis, Thrombosis, and Vascular Biology. 2006;26:2813–2818. DOI: 10.1161/01.ATV.0000249407.92147.12

[115] López Andrés N, Tesse A, Regnault V, Louis H, Cattan V, Thornton SN, et al. Increased microparticle production and impaired microvascular endothelial function in aldosterone-salt-treated rats: protective effects of polyphenols. PLoS One. 2012;7: e39235. DOI: 10.1371/journal.pone.0039235

[116] Shah MD, Bergeron AL, Dong JF, López JA. Flow cytometric measurement of microparticles: pitfalls and protocol modifications. Platelets. 2008;19:365–372. DOI: 10.1080/09537100802054107

[117] Orozco AF, Lewis DE. Flow cytometric analysis of circulating microparticles in plasma. Cytometry A. 2010;77:502–514. DOI: 10.1002/cyto.a.20886

[118] van Ierssel SH, Van Craenenbroeck EM, Conraads VM, Van Tendeloo VF, Vrints CJ, Jorens PG. Flow cytometric detection of endothelial microparticles (EMP): effects of centrifugation and storage alter with the phenotype studied. Thrombosis Research. 2010;125:332–339. DOI: 10.1016/j.thromres.2009.12.019

[119] Horstman LL, Jy W, Jimenez JJ, Bidot C, Ahn YS. New horizons in the analysis of circulating cell-derived microparticles. The Keio Journal of Medicine. 2004;53:210–230. DOI: 10.2302/kjm.53.210

[120] Dey-Hazra E, Hertel B, Kirsch T, Woywodt A, Lovric S, Haller H, et al. Detection of circulating microparticles by flow cytometry: influence of centrifugation, filtration of

buffer, and freezing. Vascular Health and Risk Management. 2010;6:1125–1133. DOI: 10.2147/VHRM.S13236

[121] Yuana Y, Oosterkamp TH, Bahatyrova S, Ashcroft B, Garcia Rodriguez P, Bertina RM, et al. Atomic force microscopy: a novel approach to the detection of nanosized blood microparticles. Journal of Thrombosis and Haemostasis. 2010;8:315–323. DOI: 10.1111/j.1538-7836.2009.03654.x

[122] van der Pol E1, Hoekstra AG, Sturk A, Otto C, van Leeuwen TG, Nieuwland R. Optical and non-optical methods for detection and characterization of microparticles and exosomes. Journal of Thrombosis and Haemostasis. 2010;8:2596–2607. DOI: 10.1111/j.1538-7836.2010.04074.x

[123] van der Vlist EJ, Nolte-'t Hoen EN, Stoorvogel W, Arkesteijn GJ, Wauben MH. Fluorescent labeling of nano-sized vesicles released by cells and subsequent quantitative and qualitative analysis by high-resolution flow cytometry. Nature Protocols. 2012;7:1311–1326. DOI: 10.1038/nprot.2012.065

[124] Robert S, Lacroix R, Poncelet P, Harhouri K, Bouriche T, Judicone C, et al. High-sensitivity flow cytometry provides access to standardized measurement of small-size microparticles—brief report. Arteriosclerosis, Thrombosis, and Vascular Biology. 2012;32:1054–1058. DOI: 10.1161/ATVBAHA.111.244616

[125] Rousseau M, Belleannee C2, Duchez AC1, Cloutier N1, Levesque T, et al. Detection and quantification of microparticles from different cellular lineages using flow cytometry. Evaluation of the impact of secreted phospholipase A2 on microparticle assessment. PLoS One. 2015;10: e0116812. DOI: 10.1371/journal.pone.0116812

[126] Montoro-García S, Shantsila E, Orenes-Piñero E, Lozano ML, Lip GY. An innovative flow cytometric approach for small-size platelet microparticles: influence of calcium. Thrombosis and Haemostasis. 2012;108:373–383. DOI: 10.1160/TH12-02-0120

[127] Cloutier N, Tan S, Boudreau LH, Cramb C, Subbaiah R, Lahey L, et al. The exposure of autoantigens by microparticles underlies the formation of potent inflammatory components: the microparticle-associated immune complexes. EMBO Molecular Medicine. 2013;5:235–249. DOI: 10.1002/emmm.201201846

[128] Reid VL, Webster NR. Role of microparticles in sepsis. British Journal of Anaesthesia. 2012;109:503–513. DOI: 10.1093/bja/aes321

[129] Yuana Y, Bertina RM, Osanto S. Pre-analytical and analytical issues in the analysis of blood microparticles. Thrombosis and Haemostasis. 2011;105:396–408. DOI: 10.1160/TH10-09-0595

[130] Nantakomol D, Chimma P, Day NP, Dondorp AM, Combes V, Krudsood S, et al. Quantitation of cell-derived microparticles in plasma using flow rate based calibration. The Southeast Asian Journal of Tropical Medicine and Public Health. 2008;39:146–153.

[131] Logan DC. The mitochondrial compartment. Journal of Experimental Botany. 2006;57:1225–1243. DOI: 10.1093/jxb/erj151

[132] Kuznetsov AV, Margreiter R. Heterogeneity of mitochondria and mitochondrial function within cells as another level of mitochondrial complexity. International Journal of Molecular Sciences. 2009;10:1911–1929. DOI: 10.3390/ijms10041911

[133] Murphy MP. How mitochondria produce reactive oxygen species. The Biochemical Journal. 2009;417:1–13. DOI: 10.1042/BJ20081386

[134] Waldbaum S, Patel M. Mitochondria, oxidative stress, and temporal lobe epilepsy. Epilepsy Research. 2010;88:23–45. DOI: 10.1016/j.eplepsyres.2009.09.020

[135] Yamagishi SI, Edelstein D, Du XL, Brownlee M. Hyperglycemia potentiates collagen-induced platelet activation through mitochondrial superoxide overproduction. Diabetes. 2001;50:1491–1494. DOI: 10.2337/diabetes.50.6.1491

[136] Akkerman JW, Holmsen H. Interrelationships among platelet responses: studies on the burst in proton liberation, lactate production, and oxygen uptake during platelet aggregation and Ca^{2+} secretion. Blood. 1981;57:956–966.

[137] Barile CJ, Herrmann PC, Tyvoll DA, Collman JP, Decreau RA, Bull BS. Inhibiting platelet-stimulated blood coagulation by inhibition of mitochondrial respiration. Proceedings of the National Academy of Sciences of the United States of America. 2012;109:2539–2543. DOI: 10.1073/pnas.1120645109

[138] Tomasiak M, Stelmach H, Rusak T, Wysocka J. Nitric oxide and platelet energy metabolism. Acta Biochimica Polonica. 2004;51:789–803.

[139] Sjovall F, Morota S, Hansson MJ, Friberg H, Gnaiger E, Elmer E. Temporal increase of platelet mitochondrial respiration is negatively associated with clinical outcome in patients with sepsis. Critical Care. 2010;14:R214. DOI: 10.1186/cc9337

[140] Avila C, Huang RJ, Stevens MV, Aponte AM, Tripodi D, Kim KY, Sack MN. Platelet mitochondrial dysfunction is evident in type 2 diabetes in association with modifications of mitochondrial anti-oxidant stress proteins. Experimental and Clinical Endocrinology & Diabetes. 2012;120:248–251. DOI: 10.1055/s-0031-1285833

[141] Tang WH, Stitham J, Jin Y, Liu R, Lee SH, Du J, et al. Aldose reductase-mediated phosphorylation of p53 leads to mitochondrial dysfunction and damage in diabetic platelets. Circulation. 2014;129:1598–1609. DOI: 10.1161/CIRCULATIONAHA.113.005224

[142] Guo X, Wu J, Du J, Ran J, Xu J. Platelets of type 2 diabetic patients are characterized by high ATP content and low mitochondrial membrane potential. Platelets. 2009;20:588–593. DOI: 10.3109/09537100903288422

[143] Moreno J, Gaspar E, Lopez-Bello G, Juarez E, Alcazar-Leyva S, Gonzalez-Trujano E, et al. Increase in nitric oxide levels and mitochondrial membrane potential in platelets of

untreated patients with major depression. Psychiatry Research. 2013;209:447–452. DOI: 10.1016/j.psychres.2012.12.024

[144] Perales Villarroel JP, Figueredo R, Guan Y, Tomaiuolo M, Karamercan MA, Welsh J, et al. Increased platelet storage time is associated with mitochondrial dysfunction and impaired platelet function. Journal of Surgical Research. 2013;184:422–429. DOI: 10.1016/j.jss.2013.05.097

[145] Rottenberg H:. Proton electrochemical potential gradient in vesicles, organelles, and prokaryotic cells. Methods in Enzymology. 1989;172:63–84. DOI: 10.1016/S0076-6879(89)72008-5

[146] Cossarizza A, Salvioli S. Analysis of mitochondrial membrane potential with the sensitive fluorescent probe JC-1. Purdue Cytometry CD-ROM Series 1998;4:1–8. Available from: http://www.cyto.purdue.edu/archive/flowcyt/research/cytotech/apopto/data/cossar1/cossariz.htm [Accessed: 2016-01-29]

[147] Anderson CM, Norquist BA, Vesce S, Nicholls DG, Soine WH, Duan S, et al. Barbiturates induce mitochondrial depolarization and potentiate excitotoxic neuronal death. The Journal of Neuroscience. 2002;22:9203–9209.

[148] Emaus RK, Grunwald R, Lemasters JJ. Rhodamine 123 as a probe of transmembrane potential in isolated rat-liver mitochondria: spectral and metabolic properties. Biochimica et Biophysica Acta. 1986;850:436–448.

[149] Lemasters JJ, Ramshesh VK. Imaging of mitochondrial polarization and depolarization with cationic fluorophores. Methods in Cell Biology. 2007;80:283–295. DOI: 10.1016/S0091-679X(06)80014-2

[150] Rottenberg H. Flow cytometric analysis of mitochondria function. In: Lemasters J, Nieminen A-L, editors. Mitochondria in pathogenesis. New York: Springer US; 2002. pp. 3–20. DOI: 10.1007/0-306-46835-2_1

[151] Scaduto RC, Jr., Grotyohann LW. Measurement of mitochondrial membrane potential using fluorescent rhodamine derivatives. Biophysical Journal. 1999;76:469–477. DOI: 10.1016/S0006-3495(99)77214-0

[152] Eggeling C, Berger S, Brand L, Fries JR, Schaffer J, Volkmer A, et al. Data registration and selective single-molecule analysis using multi-parameter fluorescence detection. Journal of Biotechnology. 2001;86:163–180. DOI: 10.1016/S0168-1656(00)00412-0

[153] Kalyanaraman B. Oxidative chemistry of fluorescent dyes: implications in the detection of reactive oxygen and nitrogen species. Biochemical Society Transactions. 2011;39:1221–1225. DOI: 10.1042/BST0391221

[154] Kalyanaraman B, Darley-Usmar V, Davies KJ, Dennery PA, Forman HJ, Grisham MB, et al. Measuring reactive oxygen and nitrogen species with fluorescent probes: challenges and limitations. Free Radical Biology & Medicine. 2012;52:1–6. DOI: 10.1016/j.freeradbiomed.2011.09.030

[155] Dasgupta SK, Argaiz ER, Mercado JE, Maul HO, Garza J, Enriquez AB, et al. Platelet senescence and phosphatidylserine exposure. Transfusion. 2010;50:2167–2175. DOI: 10.1111/j.1537-2995.2010.02676.x

[156] Protti A, Lecchi A, Fortunato F, Artoni A, Greppi N, Vecchio S, et al. Metformin overdose causes platelet mitochondrial dysfunction in humans. Critical Care. 2012;16:R180. DOI: 10.1186/cc11663

[157] van der Wal DE, Gitz E, Du VX, Lo KS, Koekman CA, Versteeg S, et al. Arachidonic acid depletion extends survival of cold-stored platelets by interfering with the [glycoprotein Ibalpha-14-3-3zeta] association. Haematologica. 2012;97:1514–1522. DOI: 10.3324/haematol.2011.059956

[158] Wu Y, Dai J, Zhang W, Yan R, Zhang Y, Ruan C, et al. Arsenic trioxide induces apoptosis in human platelets via C-Jun NH2-terminal kinase activation. PLoS One. 2014;9:e86445. DOI: 10.1371/journal.pone.0086445

[159] Yamakawa K, Ogura H, Koh T, Ogawa Y, Matsumoto N, Kuwagata Y, et al. Platelet mitochondrial membrane potential correlates with severity in patients with systemic inflammatory response syndrome. Journal of Trauma and Acute Care Surgery. 2013;74:411–417. DOI: 10.1097/TA.0b013e31827a34cf

[160] Zhang S, Ye J, Zhang Y, Xu X, Liu J, Zhang SH, et al. P2Y12 protects platelets from apoptosis via PI3k-dependent Bak/Bax inactivation. Journal of Thrombosis and Haemostasis. 2013;11:149–160. DOI: 10.1111/jth.12063

[161] Bae ON, Lim KM, Noh JY, Chung SM, Kim SH, Chung JH. Trivalent methylated arsenical-induced phosphatidylserine exposure and apoptosis in platelets may lead to increased thrombus formation. Toxicology and Applied Pharmacology. 2009;239:144–153. DOI: 10.1016/j.taap.2008.12.020

[162] Wu F, Liu Y, Luo L, Lu Y, Yew DT, Xu J, et al. Platelet mitochondrial dysfunction of DM rats and DM patients. International Journal of Clinical and Experimental Medicine. 2015;8:6937–6946.

[163] Clarke MC, Savill J, Jones DB, Noble BS, Brown SB. Compartmentalized megakaryocyte death generates functional platelets committed to caspase-independent death. The Journal of Cell Biology. 2003;160:577–587. DOI: 10.1083/jcb.200210111

[164] Jayachandran M, Preston CC, Hunter LW, Jahangir A, Owen WG, Korach KS, et al. Loss of estrogen receptor beta decreases mitochondrial energetic potential and increases thrombogenicity of platelets in aged female mice. Age. 2010;32:109–121. DOI: 10.1007/s11357-009-9119-y

[165] Leytin V, Mykhaylov S, Starkey AF, Allen DJ, Lau H, Ni H, et al. Intravenous immunoglobulin inhibits anti-glycoprotein IIb-induced platelet apoptosis in a murine model of immune thrombocytopenia. British Journal of Haematology. 2006;133:78–82. DOI: 10.1111/j.1365-2141.2006.05981.x

[166] Liu C, Li J, Meng FY, Liang SX, Deng R, Li CK, et al. Polysaccharides from the root of Angelica sinensis promotes hematopoiesis and thrombopoiesis through the PI3K/AKT pathway. BMC Complement Altern Med. 2010;10:79. DOI: 10.1186/1472-6882-10-79.:79-10

[167] Ramsey H, Zhang Q, Wu MX. Mitoquinone restores platelet production in irradiation-induced thrombocytopenia. Platelets. 2015;26:459–466. DOI: 10.3109/09537104.2014.935315

[168] Cossarizza A. Measure of Mitochondrial Membrane Potential with the Fluorescent Probe JC-1. Purdue Cytometry 2007; 10: 1–15. Available from: http://www.cyto.purdue.edu/archive/flowcyt/research/cytotech/amfc/data/page13.htm [Accessed: 2016-01-29]

[169] Wu JY, Li M, Cao LJ, Sun ML, Chen D, Ren HG, et al. Protease Omi cleaving Hax-1 protein contributes to OGD/R-induced mitochondrial damage in neuroblastoma N2a cells and cerebral injury in MCAO mice. Acta Pharmacologica Sinica. 2015;36:1043–1052. DOI: 10.1038/aps.2015.50

[170] Chowdhury SR, Djordjevic J, Albensi BC, Fernyhough P. Simultaneous evaluation of substrate-dependent oxygen consumption rates and mitochondrial membrane potential by TMRM and safranin in cortical mitochondria. Bioscience Reports. 2015;36:e00286. DOI: 10.1042/BSR20150244

[171] Sukumar M, Liu J, Mehta GU, Patel SJ, Roychoudhuri R, Crompton JG, et al. Mitochondrial membrane potential identifies cells with enhanced stemness for cellular therapy. Cell Metabolism. 2016;23:63–76. DOI: 10.1016/j.cmet.2015.11.002

[172] Pecina P, Houstkova H, Mracek T, Pecinova A, Nuskova H, Tesarova M, et al. Noninvasive diagnostics of mitochondrial disorders in isolated lymphocytes with high resolution respirometry. Biochimica et Biophysica Acta Clinical. 2014;2:62–71. DOI: 10.1016/j.bbacli.2014.09.003

[173] Zhang X, Chen X, Liu J, Dong X, Jin Y, Tian Y, et al. Knockdown of WISP1 inhibit proliferation and induce apoptosis in ALL Jurkat cells. International Journal of Clinical and Experimental Pathology. 2015;8:15489–15496.

[174] Kumari S, Chaurasia SN, Nayak MK, Mallick RL, Dash D. Sirtuin inhibition induces apoptosis-like changes in platelets and thrombocytopenia. The Journal of Biological Chemistry. 2015;290:12290–12299. DOI: 10.1074/jbc.M114.615948

[175] Antony PM, Boyd O, Trefois C, Ammerlaan W, Ostaszewski M, Baumuratov AS, et al. Platelet mitochondrial membrane potential in Parkinson's disease. Annals of Clinical and Translational Neurology. 2015;2:67–73. DOI: 10.1002/acn3.151

[176] Jobe SM, Wilson KM, Leo L, Raimondi A, Molkentin JD, Lentz SR, et al. Critical role for the mitochondrial permeability transition pore and cyclophilin D in platelet

activation and thrombosis. Blood. 2008;111:1257–1265. DOI: 10.1182/blood-2007-05-092684

[177] Nicholls DG. Simultaneous monitoring of ionophore- and inhibitor-mediated plasma and mitochondrial membrane potential changes in cultured neurons. The Journal of Biological Chemistry. 2006;281:14864–14874. DOI: 10.1074/jbc.M510916200

[178] Perry SW, Norman JP, Barbieri J, Brown EB, Gelbard HA. Mitochondrial membrane potential probes and the proton gradient: a practical usage guide. Biotechniques. 2011;50:98–115. DOI: 10.2144/000113610

[179] Bossy-Wetzel E, Barsoum MJ, Godzik A, Schwarzenbacher R, Lipton SA. Mitochondrial fission in apoptosis, neurodegeneration and aging. Current Opinion in Cell Biology. 2003;15:706–716. DOI: 10.1016/j.ceb.2003.10.015

[180] Cossarizza A, Salvioli S. Flow cytometric analysis of mitochondrial membrane potential using JC-1. Current Protocols in Cytometry. 2001;9:9–14. DOI: 10.1002/0471142956.cy0914s13

[181] Leeksma CH, Cohen JA. Determination of the life human blood platelets using labelled diisopropylfluorophosphonate. Nature. 1955;175:552–553. DOI: 10.1038/175552b0

[182] Patel SR, Hartwig JH, Italiano Jr JE. The biogenesis of platelets from megakaryocyte proplatelets. Journal of Clinical Investigation. 2005;115:3348–3354. DOI: 10.1172/JCI26891

[183] Kerr JFR, Wyllie, AH, Currie, AR. Apoptosis: A basic biological phenomenon with wide-ranging implications in tissue kinetics. British Journal of Cancer. 1972;26:239–257.

[184] Brown SB, Clarke MCH, Magowan L, Sanderson H, Savill J. Constitutive death of platelets leading to scavenger receptor-mediated phagocytosis. A caspase-independent cell clearance program. Journal of Biological Chemistry. 2000;275:5987–5996. DOI: 10.1074/jbs.275.8.5987

[185] Thushara RM, Hemshekhar M, Kemparaju K, Rangappa KS, Devaraja S, Girish KS. Therapeutic drug-induced platelet apoptosis: an overlook issue in pharmacotoxicology. Archives of Toxicology. 2014;88:185–198. DOI: 10.1007/s00204-013-1185-3

[186] Tonon G, Luo X, Greco NJ, Chen W, Shi Y, Jamiesion GA. Weak platelet agonists and U46619 induce apoptosis-like events in platelets, in the absence of phosphatidyl exposure. Thrombosis Research. 2002;107:345–350. DOI: 10.1016/s0049-3848(02)00388-9

[187] Leytin V, Allen DJ, Mykhaylow S, Lyubimov E, Freedman J. Thrombin-triggered platelet apoptosis. Journal of Thrombosis and Haemostasis. 2006;4:2656–2663. DOI: 10.1111/j.1538-7836.2006.02200.x

[188] Leytin V, Allen D, Mutlu A, Gyualkhandanyan AV, Mykhaylov S, Freedman J. Mitochondrial control of platelet apoptosis: effect of cyclosporine A, an inhibitor of the

mitochondrial permeability transition pore. Laboratory Investigation. 2009;89:374–384. DOI: 10.1038/labinvest.2009.13

[189] Sener A, Ozsavaci D, Oba R, Demirel GY, Uras F, Yarimici KT. Do platelet apoptosis, activation, aggregation, lipid peroxidation and platelet-leukocte aggregate formation occur simultaneously in hyperlipidemia? Clinical Biochemistry. 2005;38:1081–1087. DOI: 10.1016/j.clinbiochem.2005.09.005

[190] Wang Z, Cai F, chen X, Luo M, Hu L, Lu Y. The role of mitochondria-derived reactive oxygen species in hyperthermia-induced platelet apoptosis. PLoS One. 2013;8:e75044. DOI: 10.1371/journal.pone.0075044

[191] Leytin V, Freedman J. Platelet apoptosis in stored platelet concentrations and other models. Transfusion and Apherosis Science. 2003;28:285–295. DOI: 10.1016/S1473-0502(03)00048-X

[192] Leytin V, Allen DJ, Mykhaylov S, Mis L, Lyubimov EV, Garvey B, et al. Pathologic high shear induces apoptosis events in human platelets. Biochemical and Biophysical Research Communications. 2004;320:303–310. DOI: 10.1016/j.bbre.2004.05.166

[193] Lin KH, Hsiao G, Shih ChM, Chou DS, Sheu JR. Mechanisms of resveratrol-induced platelet apoptosis. Cardiovascular Research. 2009;83:575–585. DOI: 10.1093/cvr/cvp139

[194] Wang Z, Wang J, Xie R, Liu R, Lu Y. Mitochondria-derived reactive oxygen species play an important role in doxorubicin-induced platelet apoptosis. International Journal of Molecular Sciences. 2015;16:11087–11100. DOI: 10.3390/ijtms160511087

[195] Liu G, Liu G, Chen H, Borst O, Gawaz M, Vortkamp A, et al. Involvement of Ca^{2+} activated Cl-channel Ano6 in platelet activation and apoptosis. Cellular Physiology and Biochemistry. 2015;37:1934–1944. DOI: 10.1159/000438554

[196] Gyulkhandanyan AV, Mutlu A, Freedman J, Leytin V. Markers of platelet apoptosis: methodology and applications. Journal of Thrombosis and Thrombolysis. 2012;33:397–411. DOI: 10.1007/s11239-012-0688-8

[197] Zhao Q, Li M, Chen M, Zhou L, Zhao L, Hu R, et al. Lovastin induces platelet apoptosis. Environmental Toxicology and Pharmacology. 2016;42:69–75. DOI: 10.1016/j.etap.2016.01.002

[198] Kroemer G1, Galluzzi L, Brenner C. Mitochondrial membrane permeabilization in cell death. Physiological Reviews. 2007;87:99–163. DOI: 10.1152/physrev.00013.2006

[199] Rong Y, Distelhorst CW. Bcl-2 protein family members: versatile regulators of calcium signaling in cell survival and apoptosis. Annual Review of Physiology. 2008;70:73–91. DOI: 10.1146/annurev.physiol.70.021507.105852

[200] Leytin V, Mykhaylov S, Starkey AF, Allen DJ, Lau H, Ni H, et al. Intravenous immunoglobulin inhibits anti-glycoprotein IIb-induced platelet apoptosis in a murine model

of immune thrombocytopenia. British Journal of Haematology. 2006;133:78–82. DOI: 10.1111/j.1365-2141.2006.05981.x

[201] Gao Q, xiang Y, Chen Z, Zeng L, Ma X, Zhang Y. ßy-CAT, a non-lens betagamma-crystallin and trefoil factor complex, induces calcium-dependent platelet apoptosis. Thormbosis and Haemostasis. 2011;105:743–932. DOI: 10.1160/TH10-10-0690

[202] Nayak MK, Dash A, Singh N, Dash D. Aspirin delimits platelet life span by proteasomal inhibition. PLoS One. 2014;9:e105049. DOI: 10.1371/journal.pone.0105049

[203] Klie BT. The role of the intrinsic apoptosis pathway in platelet life and death. Thrombosis and Haemostasis. 2009;7:214–217. DOI: 10.1111/j.1538-7836.2009.03366.x

[204] Li J, Xia Y, Bertino AM, Coburn JP, Kuter D. The mechanism of apoptosis in human platelets during storage. Transfusion. 2000;40:1320–1329. DOI: 10.1046/j.1537-2995.2000.40111320.x

[205] Schleicher RI, Reichenbach F, Kraft P, Kumar A, Lescan M, Todt F. Platelets induce apoptosis via membrane-bound FasL. Blood Journal. 2015;126:1483–1493. DOI: 10.1182.blood-2013-12-544445

[206] Tait JF, Gibson D. Phospholipid binding of annexin V: effects of calcium and membrane phosphatidylserine content. Archives of Biochemistry and Biophysics. 1992;298:187–191. DOI: 10.1016/0003-9861(92)90111-9

[207] Concha NO, Head JF, Kaetzel MA, Dedman JR, Seaton BA. Annexin V forms calcium-dependent trimeric units on phospholipid vesicles. FEBS Letters. 1992;314:159–162. DOI: 10.1016/0014-5793(92)80964-I

[208] Connor DE, Exner T, Ma DD, Joseph JE. Detection of the procoagulant activity of microparticle-associated phosphatidylserine using XACT. Blood Coagulation & Fibrinolysis. 2009;20:558–564. DOI: 10.1097/MBC.0b013e32832ee915

[209] Fox JE, Reynolds CC, Austin CD. The role of calpain in stimulus-response coupling: evidence that calpain mediates agonist-induced expression of procoagulant activity in platelets. Blood. 1990;76:2510 - 2519.

[210] Solum NO. Procoagulant expression in platelets and defects leading to clinical disorders. Arteriosclerosis, Thrombosis, and Vascular Biology. 1999;19:2841–2846. DOI: 10.1161/01.ATV.19.12.2841

[211] Wolfs JL, Wielders SJ, Comfurius P, Lindhout T, Giddings JC, Zwaal RF, et al. Reversible inhibition of the platelet procoagulant response through manipulation of the Gardos channel. Blood. 2006;108:2223–2228. DOI: 10.1182/blood-2006-01-009613

[212] Chang CP, Zhao J, Wiedmer T, Sims PJ. Contribution of platelet microparticle formation and granule secretion to the transmembrane migration of phosphatidylserine. The Journal of Biological Chemistry. 1993;268:7171–7178.

[213] Dachary-Prigent J, Freyssinet JM, Pasquet JM, Carron JC, Nurden AT. Annexin V as a probe of aminophospholipid exposure and platelet membrane vesiculation: a flow cytometry study showing a role for free sulfhydryl groups. Blood. 1993;81:2554–2565.

[214] Dachary-Prigent J, Pasquet JM, Freyssinet JM, Nurden AT. Calcium involvement in aminophospholipid exposure and microparticle formation during platelet activation: a study using Ca^{2+}-ATPase inhibitors. Biochemistry. 1995;34:11625–11634.

[215] Procházková R, Andrýs C, Hubácková L, Krejsek J. Markers of platelet activation and apoptosis in platelet concentrates collected by apheresis. Transfusion and Apheresis Science. 2007;37:115–123. DOI: 10.1016/j.transci.2007.03.015

[216] Bakry R, Sayed D, Galal H, Shaker S. Platelet function, activation and apoptosis during and after apheresis. Therapeutic Apheresis and Dialysis. 2010;14:457–464. DOI: 10.1111/j.1744-9987.2010.00842.x

[217] Vogler M, Hamali HA, Sun XM, Bampton ET, Dinsdale D, Snowden RT. BCL2/BCL-X(L) inhibition induces apoptosis, disrupts cellular calcium homeostasis, and prevents platelet activation. Blood. 2011;117:7145–7154. DOI: 10.1182/blood-2011-03-344812

[218] Liu G, Liu G, Chen H, Borst O, Gawaz M, Vortkamp A, et al. Involvement of Ca2+ Activated Cl- Channel Ano6 in Platelet Activation and Apoptosis. Cellular Physiology and Biochemistry. 2015;37:1934–1944 . DOI: 10.1159/000438554

[219] Watala C, Waczulikova I, Wieclawska B, Rozalski M, Gresner P, Gwozdziński K, et al. Merocyanine 540 as a fluorescent probe of altered membrane phospholipid asymmetry in activated whole blood platelets. Cytometry. 2002;49:119–133. DOI: 10.1002/cyto.10152

[220] Waczulikova I, Rozalski M, Rievaj J, Nagyova K, Bryszewska M, Watala C. Phosphatidylserine content is a more important contributor than transmembrane potential to interactions of merocyanine 540 with lipid bilayers. Biochimica et Biophysica Acta (BBA)—Biomembranes. 2002;1567:176–182. DOI: 10.1016/S0005-2736(02)00614-4

[221] Darzynkiewicz Z, Huang X, Okafuji M, King MA. Cytometric methods to detect apoptosis. Methods in Cell Biology. 2004;75:307–341.

[222] Shcherbina A, Remold-O'Donnell E. Role of caspase in a subset of human platelet activation responses. Blood. 1999;93:4222–4231.

[223] Leytin V. Apoptosis in the anucleate platelet. Blood Reviews. 2012;26:51–63. DOI: 10.1016/j.blre.2011.10.002

[224] Rand ML, Wang H, Bang KW, Poon KS, Packham MA, Freedman J. Procoagulant surface exposure and apoptosis in rabbit platelets: association with shortened survival and steady-state senescence. Journal of Thrombosis and Haemostasis. 2004;2:651–659. DOI: 10.1111/j.1538-7836.2004.00670.x

http://dx.doi.org/10.5772/63473

[225] Arachiche A, Kerbiriou-Nabias D, Garcin I, Letellier T, Dachary-Prigent J. Rapid procoagulant phosphatidylserine exposure relies on high cytosolic calcium rather than on mitochondrial depolarization. Arteriosclerosis, Thrombosis, and Vascular Biology. 2009;29:1883–1889. DOI: 10.1161/ATVBAHA.109.190926

Chapter 4

The Multiplexing of Assays for the Measurement of Early Stages of Apoptosis by Polychromatic Flow Cytometry

G. Warnes

Additional information is available at the end of the chapter

http://dx.doi.org/10.5772/60549

Abstract

The detection of apoptosis has been a stalwart application for flow cytometric analysis for decades and this review of flow cytometric methods to detect early stages of apoptosis includes the use of the pivotal assay to detect early and late apoptosis, the Annexin V assay which when multiplexed with biologically functional fluorescent dyes to measure mitochondrial function and Reactive Oxygen Species (ROS) generation allows further identification of functionally different subsets within apoptotic populations. Here we show how this polychromatic approach can be used to demonstrate which subset of cells show changes in mitochondrial function and when ROS is generated in a time dependent manner. This polychromatic approach to flow cytometry leads to the identification of over ten sub-populations of cells during classic apoptosis or programmed cell death (PCD).

Keywords: DNA dyes, Annexin V, MitoTracker, ROS, Polychromatic

1. Introduction

Apoptosis can be defined as 'gene-directed cellular self-destruction'; or 'programmed cell death' (Type I PCD) [1-4], although this is really a phenomenon where cells are programmed to die at a particular point during the normal function of those cells e.g. during embryonic development [5]. The term 'cell necrobiology' is an encompassing term for all modes of cell death and can be defined as "various modes of cell death: the biological changes, which predispose, precede and accompany cell death; as well as the consequences and tissue response

to cell death" [2, 3]. The term necrobiology thus includes all the many forms of apoptosis besides 'classic' PCD, including Caspase independent apoptosis-like PCD, autophagy or Type II PCD, mitotic catastrophe, necrosis-like PCD, necrosis or oncosis defined as accidental cell death and cell senescence [2, 3].

Apoptosis can be activated by two pathways, the first the 'extrinsic pathway' which is mediated via the Cell Death Receptor pathway. This pathway is typically activated by TNF binding to the Death Receptor, FAS Associated Death Domain or FADD [6]. This results in cleavage of Caspase 8 which then cleaves pro-Caspase 3 to release active Caspase 3 resulting in the final stages of apoptosis with DNA fragmentation and cell shrinkage by nuclear and cytoplasmic condensation and fragmentation, membrane blebbing and the formation of apoptotic bodies [1-3]. The second pathway, the 'Intrinsic pathway' can be induced by a variety of drugs, including Staurosporine (STS) and Etoposide (ETOP), UV-B irradiation, γ-irradiation, and reactive oxygen and is mediated via mitochondrial responses to such cellular insults with resulting mitochondrial membrane depolarization. This depolarization causes the release of cytochrome *c* from the inner mitochondrial membrane into the cytosol where it binds to Apaf-1 recruiting pro-caspase-9 in an ATP dependent manner, this complex activates Caspase 9 which in turn activate effector Caspases [7].

There are a plethora of flow cytometry assays for the study of apoptosis several hours after induction, by the use of dual fluorescent DNA binding dyes, Annexin V binding, activation of Caspases, depolarization of the mitochondrial membrane potential, cytochrome *c* release from the inner mitochondrial membrane through to cell death as measured by permeability of the plasma membrane to fluorescent DNA binding dyes and DNA fragmentation in the form of estimations of Sub G_1 [8]. Early apoptosis can be measured by the use of fluorescent DNA dyes such as Hoechst 33342 (Ho33342) or YO-PRO-1 and propidium iodide (PI) which identifies live (non-stained), early apoptosis (single positive), late apoptosis and dead cells (double positive). This assay is based upon the fact that cells undergoing apoptosis have a varying permeability to Hoechst 33342, while only late apoptotic and dead cells are permeable to PI [9-11].

The now classic Annexin V assay, includes the use of this protein, a vascular anti-coagulant which binds in a calcium dependent manner to externalised phospholipid, phosphatidylserine (PS) located on the outer leaflet of the plasma membrane. This when combined with a fluorescent viability dye, show the presence of live, apoptotic and necrotic cells in a similar manner to that observed by dual DNA dye assays [9-11]. The Annexin V binding assay can be used as a pivot point to differentiate between early and late apoptotic events. A polychromatic approach can then be applied by the multiplexing of various live cell functional fluorescent dyes to the Annexin V assay. These include the measurement of mitochondrial membrane potential and ROS dyes allowing the identification of further subsets of the live and early apoptotic cell populations [12-20]. There are a range of such fluorescent dyes, such as TMRE, JC-1/9, a range of carbocyanine and rhodamine chemical based dyes, $DiOC_6$, $DiIC_1(5)$ and rhodamine 123. All these dyes record the level of mitochondrial membrane potential, with the higher the fluorescence the more polarized the inner mitochondrial membrane potential (except JC-1/9 were a colour change occurs) [16]. While little fluorescence indicates depolari-

http://dx.doi.org/10.5772/60549

zation of the inner mitochondrial membrane and the presence of dysfunctional mitochondria within the cell [12-16].

Further multiplexing with Annexin V binding and mitochondrial membrane potential measurements can also be studied with measurement of ROS by the use of dihydroethidium (HE) which preferentially measures superoxide produced by the cell during apoptosis [17-20]. This allows the identification of multiple subsets within live and early apoptotic populations in terms of mitochondrial function and generation of ROS. The mode of action of a variety of chemicals and treatments to induce apoptosis, including UV-irradiation, Staurosporine (STS), Etoposide (ETOP), Curcumin [20] and Chloroquine (CQ) [21] can then be compared in a more complex fashion. To this end a time course study of STS induction of apoptosis from 1-30 h employing the multiplexing of Annexin V-FITC, DAPI for cell viability and mitotracker $DiIC_1(5)$ showed not only the changes in apoptotic culture dynamics but also that mitochondrial dysfunction occurs in live cells (Annexin V^{-ve}/$DAPI^{-ve}$) within an hour of treatment with STS and sequentially reduced over the time course [13-20].

More recently a non-calcium dependent plasma membrane dye F2N12S violet ratiometric asymmetry probe or 4'-N, N-diethylamino-6-(N, N, N-dodecyl-methylamino-sulfopropyl)-methyl-3-hydoxyflavone has been employed to measure the change in the outer surface charge of the plasma membrane which occurs when PS is flipped to the outer leaflet of the plasma membrane [22]. F2N12S does so by, after violet excitation (405 nm) emitting two fluorescence's at 530 and 585 nm (green and orange) were the ratio of orange/green fluorescence is high when the cells are alive and low when apoptotic.

Thus a polychromatic flow cytometric approach employing a range of assays can be achieved by the multiplexing of numerous assays allows the simultaneous analysis of the changes in functionality of cells as the apoptotic cascade is initiated, progresses to early apoptosis and eventually to cell death via late apoptosis.

2. Materials and methods

2.1. Cell lines

Jurkat T-cells were grown in RMPI-1640 with L-Glutamine (Life Technologies) supplemented with 10% Foetal Bovine Serum (FBS, Life Technologies) and penicillin and streptomycin (Life Technologies) in the presence of 5% CO_2 at 37°C.

2.2. Induction of apoptosis

Jurkat cells were treated with UV-irradiation, 1 μM Staurosporine (STS), 10 μM Curcumin, 75 μM Chloroquine (CQ), or 10 μM Etoposide (ETOP) for up to 30h to induce apoptosis (Sigma Chemicals). Time points analysed were 0, 1, 2, 3, 4, 5, 20, 24, 30h, (n=3) see cell labelling section below.

2.3. Labelling with DNA dyes

After the induction of apoptosis cells were labelled with by incubation of Hoechst 33342 (25 μg/ml) and PI (1 μg/ml) for 30 minutes on ice. Ho33342 was excited by UV or 405 nm lasers and emission collected at 440/40 nm and PI was excited at 488 nm and emission collected at 610/20 nm with 30, 000 events collected.

2.4. Annexin V labelling

After the induction of apoptosis cells resuspended in 100 μl calcium-rich buffer with Annexin-AF-647 or FITC (2.5 μl) (Life Technologies, Becton Dickinson). Cells were then incubated at Room Temperature (RT) for 15 min. DNA viability dyes, DAPI (200 ng/ml) (Sigma Chemicals) was added just before flow cytometric analysis. DRAQ7 (Biostatus, UK) was incubated at 5 μM for 10 min at 37^0C. Annexin V-FITC was excited at 488 nm and emission collected at 530/30 nm; Annexin V-AF-647 was excited at 633 nm and emission collected at 660/20 nm; DAPI was excited by UV or 405 nm lasers and emission collected at 440/40 nm; DRAQ7was excited at 633 nm and emission collected at 780/60 nm with 30, 000 events collected.

2.5. Dihydroethidium and Mitotracker dye loading

After the induction of apoptosis cells were loaded with 5 μM dihydroethidium (HE, Invitrogen) for 30 min at 37^0C and either carbocyanine dyes $DiOC_6(3)$ or $DiIC_1(5)$ at 40nM, (Invitrogen) by incubating cells with dyes for 15 minutes at 37^0C. Cells were then washed in PBS and resuspended in 100 μl calcium-rich buffer with Annexin-AF-647 or FITC (2.5 μl). Cells were then incubated at Room Temperature (RT) for 15 min. DNA viability dyes, DAPI (200 ng/ml) was added just before flow cytometric analysis. Annexin V-FITC or $DiOC_6(3)$ was excited at 488 nm and emission collected at 530/30 nm; Annexin V-AF-647 or $DiIC_1(5)$ was excited at 633 nm and emission collected at 660/20 nm; HE was excited at 488 nm and emission collected at 610/20 nm; DAPI was excited by UV or 405 nm lasers and emission collected at 440/40 nm with 30, 000 events collected. After gating on Annexin V and viability dye to define, live, early apoptotic, late apoptotic and dead cells, analysis of mitochondrial function +ve or -ve cells and HE +ve or -ve cells was determined by gating on the live cell population. The position of the vertical and horizontal axis can be placed to show low levels of ROS with the vertical axis and little mitochondrial dysfunction with the horizontal axis.

2.6. Violet Ratiometric Membrane Asymmetry Probe

After the induction of apoptosis cells resuspended in 100 μl calcium-rich buffer with Annexin-FITC (2.5 μl). Cells were then incubated at Room Temperature (RT) for 15 min. Violet Ratiometric Membrane Asymmetry Probe F2N12S (100 nM, Invitrogen) was then incubated for 10 mins at RT with DNA viability dye, PI (5 μg/ml). Annexin V-FITC was excited at 488 nm and emission collected at 530/30 nm; PI was excited at 488 nm and emission collected at 610/20 nm; F2N12S was excited by 405 nm laser and emission collected at 530/30 nm (Green) and 610/20 nm (Orange) with a Ratio set with Green as the denominator and Orange as the numerator with 30, 000 events collected. Live cells have a high orange signal with low green

http://dx.doi.org/10.5772/60549

channel signal and thus have a high ratio of orange/green fluorescence. While dead cells have a high green and orange signal and thus have a low ratio of orange/green fluorescence, which are confirmed by back-gating on viability dye positive cells.

3. Results

3.1. Use of DNA binding dyes to detect apoptosis

Prior to the introduction of the Annexin V binding assay, fluorescent DNA binding dyes were used as a means to identify apoptotic cells in live cultures. With late apoptotic cells which have undergone DNA fragmentation being detected in fixed cells by measurement of cells 'Sub G_1' to the G_1 cells when analysing cells for their cell cycle [8]. Hoechst 33342 and propidium iodide (PI) was originally used to determine the presence of apoptotic cells by the nature of the selective permeability of live, apoptotic and dead cells to the fluorescent DNA binding dye, Hoechst 33342; while PI is only fully permeable to dead cells. This use of the dual DNA binding dye assay was the assay of choice to detect early apoptotic cells, with sub G_1 analysis of the cell cycle for the detection of late apoptotic cells commonly used in fixed cell preparations [8-11].

See the example confirming that Ho33342-PI labels the same cell populations as the Annexin V assay (Figure 1). Resting live cells are double negative for Ho33342^{-ve}/PI^{-ve}, while early apoptotic cells are Ho33342^{+ve}/PI^{-ve} and dead cells double positive Ho33342^{+ve}/PI^{+ve} see Figure 1A. The same resting cells were also labelled with Annexin V-FITC (Figure 1B) and were the same percentages were shown by Ho33342/PI are shown as double negative live cells in the Annexin V assay as AnnexinV^{-ve}/PE^{-ve}, early apoptotic are AnnexinV^{+ve}/PE^{-ve} and dead cells as double positive AnnexinV^{-ve}/PE^{+ve}. Likewise STS treated cells undergoing apoptosis as shown by Ho33342/PI labelling showed a greater level of cell death than resting cells (Figure 1C). Gated Ho33342^{+ve}/PI^{-ve} cells (Figure 1C) are shown to be AnnexinV^{+ve}/PE^{-ve} in Figure 1D.

3.2. Use of Annexin V assay to detect apoptosis

The advent of the Annexin V binding assay largely replaced the methodology above and identifies apoptotic cells by virtue that phosphatidylserine normally present in the internal leaflet of the plasma membrane which is externalised in apoptotic cells to which Annexin V binds (as well as phosphatidylethanolamine), [12]. After Annexin V labelling (with a fluorescent tag of choice), a range of fluorescent DNA dyes can be employed to determined viability, these commonly include PI, DAPI, 7-ADD and DRAQ7. Quadrants show live cells as not labelled or Annexin-V^{-ve}/viability dye^{-ve}, early apoptotic cells as Annexin-V^{+ve}/viability dye^{-ve}, late apoptotic and dead cells as Annexin-V^{+ve}/viability dye^{+ve} or Annexin-V^{-ve}/viability dye^{+ve}.

Figures 2 A-C shows the employment of Annexin V-AF-647 with DAPI after UV-irradiation and STS treatment for 24 and 3h respectively. This demonstrates that different inducers of apoptosis have very different times at which early apoptosis is detected, with both samples displaying a similar degree of cell death. Highlighted in Figures A is an intermediate area

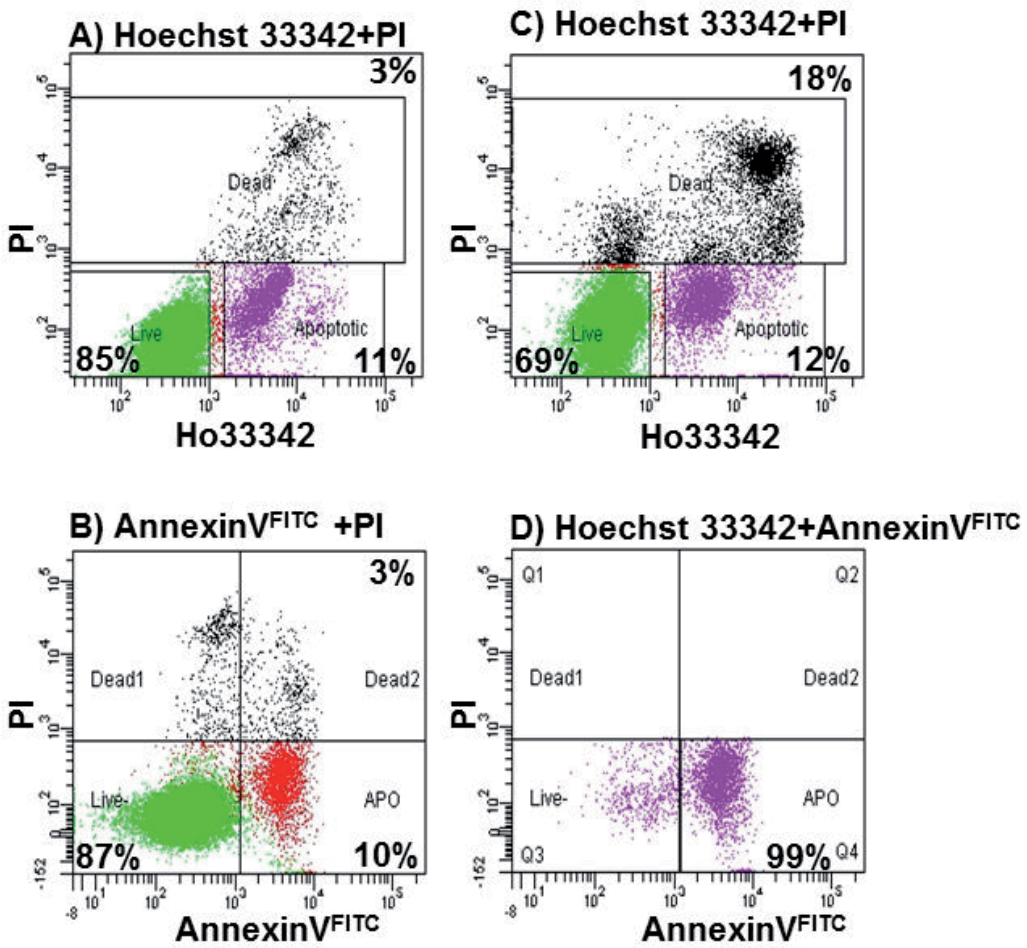

Figure 1. Jurkat T-cells (untreated) were incubated with B) Annexin V^{FITC} and PI with apoptosis at 10%. These cells were then incubated with 25 µg/ml Ho33342 for 30 min on ice to show apoptotic cells as $Ho33342^{+ve}PI^{-ve}$ at 11% A). STS treated cells showed a similar level of apoptotic cells (12%) when labelled with Ho33342 and PI C) but with more dead cells 18%. Back gating the apoptotic cells from C) shown in D) are apoptotic cells and are labelled with annexin V. Live, apoptotic (APO) and dead cells are shown in the quadrants, $AnnexinV^{-ve}/PI^{-ve}$, $AnnexinV^{+ve}/PI^{-ve}$, $AnnexinV^{+ve}/PI^{+ve}$ $AnnexinV^{-ve}/PI^{+ve}$ respectively.

between live and early apoptotic cells in which cells are starting the process of binding annexin V, moving minutes/hours later to the main $Annexin\text{-}V^{+ve}$/viability dye^{-ve} population. Later these cells start to become permeable to the viability dye and show a low degree of DAPI positivity. This population is classed as late apoptotic, with the fully DAPI labelled cells been necrotic or dead by the process of apoptosis.

Likewise Annexin V-FITC with DAPI can be used in a similar manner to that discussed above were Curcumin and ETOP has been employed for 24 h before labelling with Annexin V (Figure 2 D, E, F). A higher degree of apoptosis and cell death are shown in Figure 2 E, F than that produced by UV-irradiation and several hours of treatment with STS (Fig 2B, C).

http://dx.doi.org/10.5772/60549

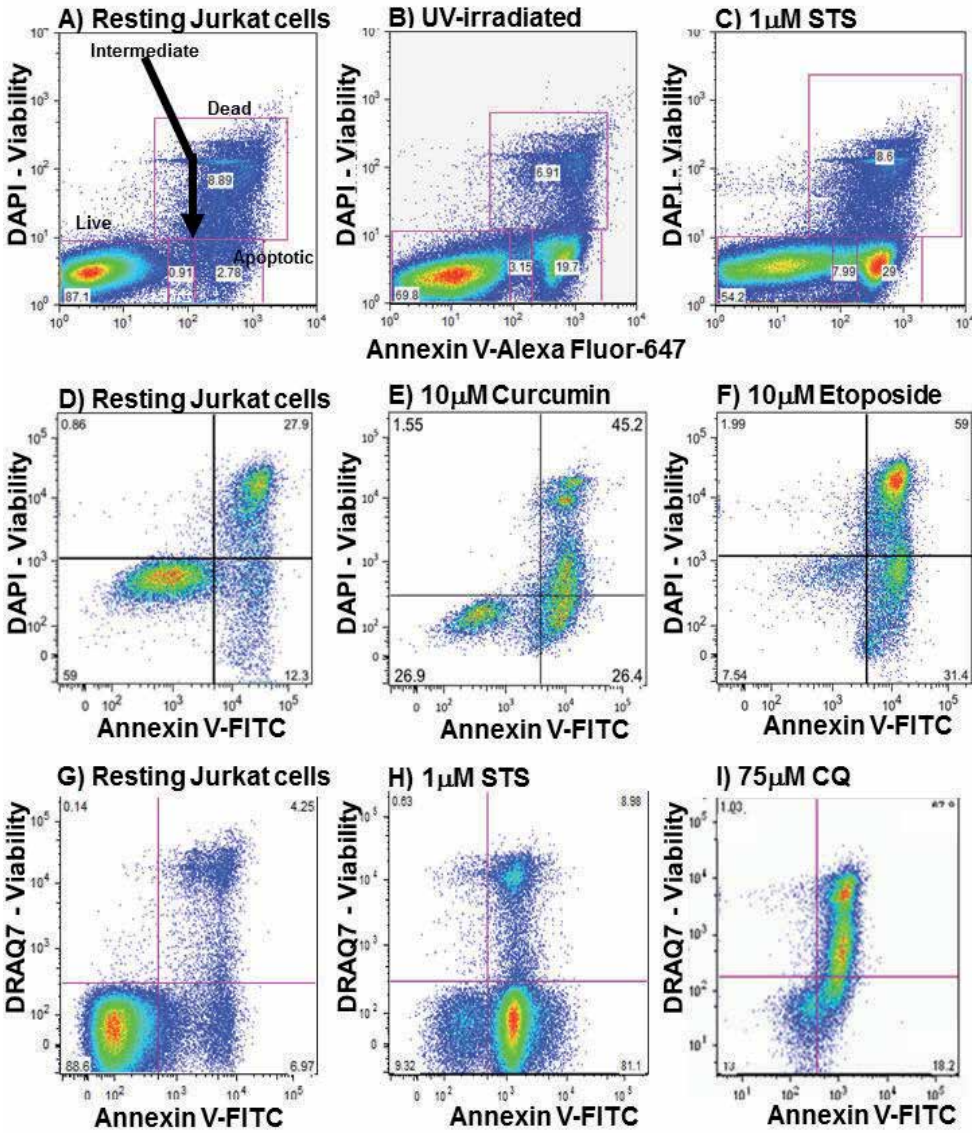

Figure 2. After induction of apoptosis cells were labelled with annexin V and a viability dye, A), and D) show resting cells labelled with Annexin V-647 or FITC and DAPI. Cells were UV-irradiated and labelled after 24 h B), while C) show cells treated with STS for 3 h; E) cells treated with Curcumin (Turmeric) for 24 h, and F) cells treated with ETOP for 24 h. Resting cells were also labelled with Annexin V-FITC and DRAQ7 G), and labelled likewise after H) STS treatment 6 h, and I) CQ treatment after 24 h. Live, apoptotic (APO) and dead cells are shown in the quadrants, AnnexinV^{-ve}/DAPI or DRAQ7^{-ve}, AnnexinV^{+ve}/DAPI or DRAQ7^{-ve}, AnnexinV^{+ve}/DAPI or DRAQ7^{+ve} AnnexinV^{-ve}/DAPI or DRAQ7^{+ve} respectively.

Also shown is the use of the new viability dye DRAQ-7 (Biostatus) with annexin V-FITC after STS and CQ treatment after 6 and 24 h respectively (Figure 2 G, H, I). Here a higher degree of cell death is shown in response to CQ and STS compared to after 3 h (Figure 2 C) [23].

3.3. Time course dynamics of apoptosis

The Annexin V assay gives the researcher a snap-shot of what is happening to a cell population for a particular time point (Figures 1, 2). The researcher should therefore use the Annexin V assay at multiple time points to get a fuller picture of the time maximal apoptosis is reached in any given experimental design. Figure 3 shows a 30 h time course of Jurkat STS induced apoptosis. At each time point (n=3) after the induction of apoptosis has been initiated the incidence of the live cell population showed a clear linear decline over time falling to 20% after 5 h. While the incidence of dead cells from 0-5 h remained constant at approximately 10% and only rose after the live population fell to 20% after 5 h of STS treatment. The dynamic population was the Annexin-V^{+ve}/viability dye^{-ve} cells which rapidly rose after 1 h <10% to over 60% at the 5 h time point which then declined as the incidence of the dead cell population rose and both live and apoptotic population fell from 20-30 h [13-20].

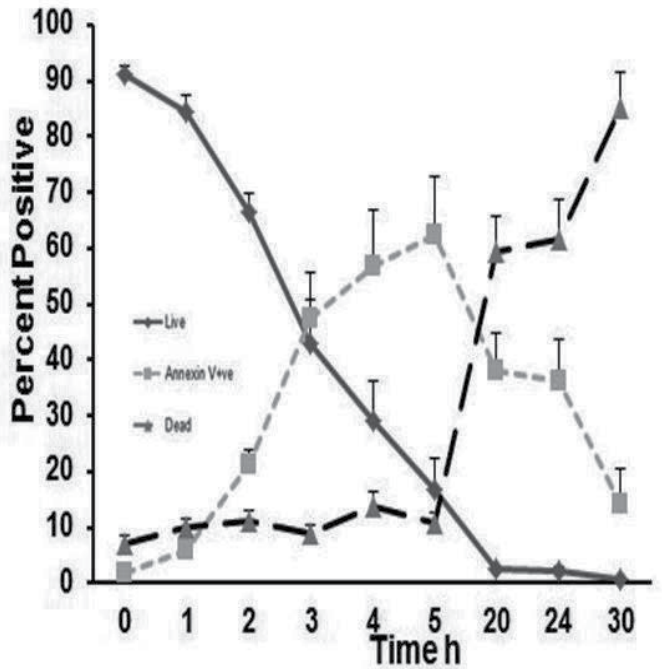

Figure 3. After induction of apoptosis cells with STS were labelled with annexin V-FITC and a DAPI at time points 0-30 h, with live, early apoptotic and dead cell populations plotted over this time, n=3, error bars, SEM. The population dynamics of apoptosis was shown to peak after 5 h and start to decline by 20 h at the same time the dead cell population significantly increased after 5 h. The live cell population systematically decreased over time.

3.4. Multiplexing other cell functions with the Annexin V assay

The multiplexing of fluorescent probes that measure functional or end products of biological processes with the standard Annexin V assay has allowed the researcher to further define the early events of apoptosis. The use of mitotracker carbocyanine dyes, $DiOC_6(3)$ or $DiIC_1(5)$,

http://dx.doi.org/10.5772/60549

which measure the functionality or the polarization state of the inner mitochondrial membrane in cell cultures undergoing apoptosis, leads to the identification of live and early apoptotic cell populations with or without mitochondrial function. This can then be multiplexed with for example dihydroethidium (HE) to detect ROS allowing the further identification of more subsets within live, apoptotic and dead cell populations when used together with a mitotracker dye and the Annexin V assay [13-20].

UV-irradiated Jurkat cells after 3 h showed a high degree of early apoptosis (21%), a small amount of cell death (7%) and 71% of cells shown to be alive or Annexin-V^{-ve}/viability dye^{-ve} (Figure 4A). These live cell (or double negative events) can be divided into four sub-populations (Figure 4B), which include those with functional mitochondria $DiOC_6(3)^{+ve}/HE^{-ve}$ with no ROS production (86%). Those live cells with functional mitochondria $DiOC_6(3)^{+ve}/HE^{+ve}$ and ROS production (1.6%). Also live cells with no mitochondrial function or ROS production $DiOC_6(3)^{-ve}/HE^{-ve}$ (12%). Lastly live cells with no mitochondrial function with ROS production or $DiOC_6(3)^{-ve}/HE^{+ve}$ (0.1%) (Figure 4 B).

Likewise early apoptotic cells can be divided into four sub-populations (Figure 4C) which include those with functional mitochondria $DiOC_6(3)^{+ve}/HE^{-ve}$ with no ROS production (1.4%); those early apoptotic cells with functional mitochondria $DiOC_6(3)^{+ve}/HE^{+ve}$ and ROS production (1%). As well as early apoptotic cells with no mitochondrial function or ROS production $DiOC_6(3)^{-ve}/HE^{-ve}$ (55%), and lastly early apoptotic cells with no mitochondrial function with ROS production or $DiOC_6(3)^{-ve}/HE^{+ve}$ (42.6%) (Figure 4C).

Lastly late apoptotic and dead cells can be divided into four sub-populations (Figure 4D) which included those with functional mitochondria $DiOC_6(3)^{+ve}/HE^{-ve}$ with no ROS production (3%). Those late apoptotic and dead cells with functional mitochondria $DiOC_6(3)^{+ve}/HE^{+ve}$ and ROS production (4%), and those with no mitochondrial function or ROS production $DiOC_6(3)^{-ve}/HE^{-ve}$ (45%). Lastly late apoptotic and dead cells with no mitochondrial function with ROS production or $DiOC_6(3)^{-ve}/HE^{+ve}$ (48%) (Figure 4D).

In a further study employing STS and ETOP to induce apoptosis AnnexinV-FITC and DAPI was used in combination with the red mitotracker dye $DiIC_1(5)$ and HE (ROS) which showed a significantly different outcome in the distribution of cell subsets within live, early, late and dead cell populations compared to the previous example (Figure 5). Untreated cells showed a relatively high degree of apoptosis and cell death (20%, Figure 5A). However the live control cell population had a high degree of functional mitochondria (80%) and little ROS production (6%, Figure 5B). The STS and ETOP treated live cells had varying degrees of $AnnexinV^{-ve}/DAPI^{-ve}$ events (80 and 8% respectively, Figure 5E, I). However these live cell populations had similar incidence of cells with functional mitochondria 48 and 56% (without ROS production) respectively (Figure 5F, 5J). The different drugs also showed a very different degree of ROS production in that the functioning mitochondria in live cells treated with ETOP produced ROS to a high degree (17%, Figure 5J) compared to low levels in STS treated cells (3%, Figure 5F).

Early apoptotic cell populations after STS and ETOP treatment had a very different incidence of cells with functional mitochondria 18 and 1% (without ROS production) respective-

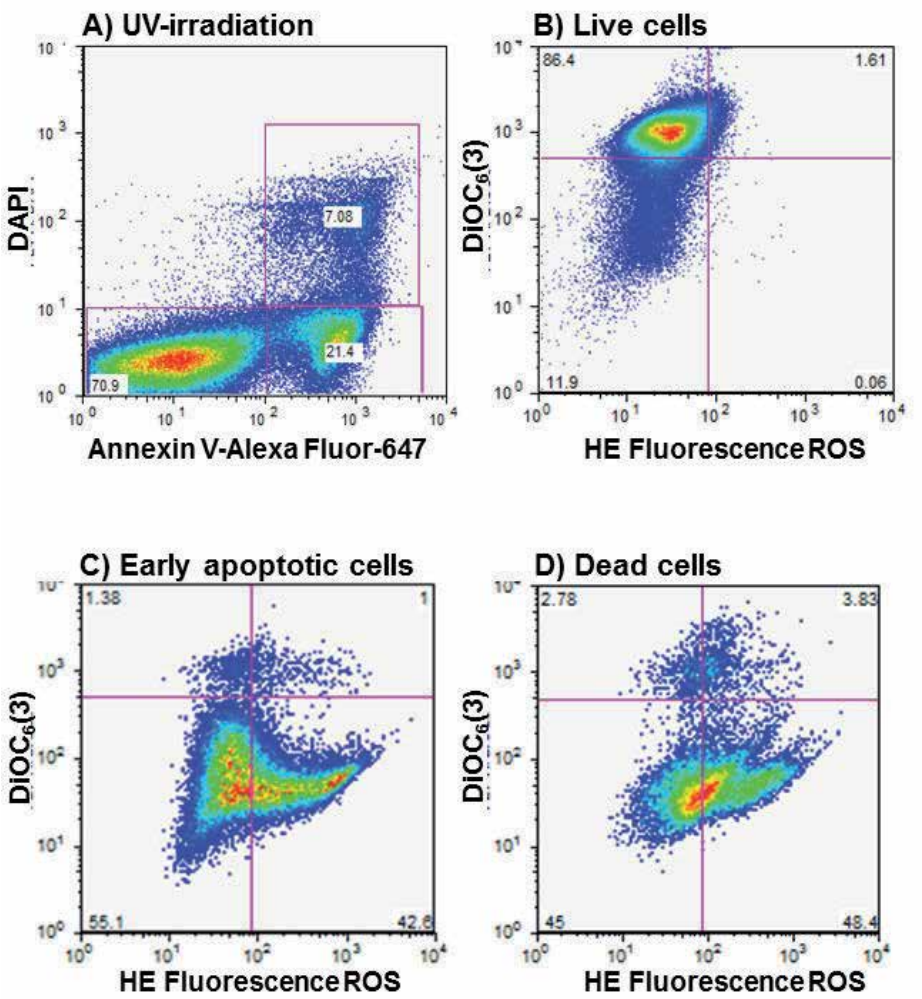

Figure 4. UV-irradiated Jurkat cells were labelled with HE, $DiOC_6(3)$ and Annexin V-FITC and DAPI after 3 h. The Annexin V and viability marker allows the live, apoptotic and dead cell populations to be determined A). Live B), apoptotic C) and dead D) populations were then analysed for mitochondrial function and ROS levels by plotting $DiOC_6(3)$ v HE parameters. $DiOC_6(3)^{+ve}/HE^{-ve}$ populations have fully functioning mitochondria, while $DiOC_6(3)^{+ve}/HE^{+ve}$ are functioning mitochondria with ROS generation. While $DiOC_6(3)^{-ve}/HE^{-ve}$ are cells with dysfunctional mitochondria and $DiOC_6(3)^{+ve}/HE^{+ve}$ are cells with dysfunctional mitochondria that have produced ROS.

ly (Figure 5G, 5K). The two drugs again also showed a very different degree of ROS production in that the cells with dysfunctional mitochondria treated with STS or ETOP produced ROS with an incidence of 17 and 54% respectively (Figure 5G, 5K). While late apoptotic and dead cells from both treatments show little or no mitochondrial function with most ROS+ve (86 and 79%, Figure 5H, 5L).

Following on from the observation that different drugs show varying affects upon the functionality of live and early apoptotic cell populations a time course study can reveal

http://dx.doi.org/10.5772/60549

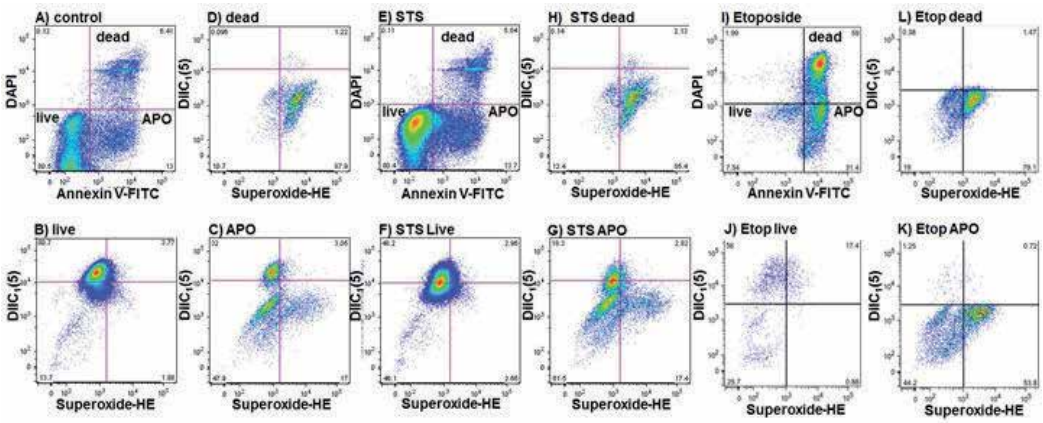

Figure 5. Untreated, STS (2 h) or ETOP (24 h) treated Jurkat cells were labelled with HE, $DiIC_1(5)$, Annexin V-FITC and DAPI. The Annexin V and viability dyes allow live, apoptotic and dead cell populations to be determined for untreated cells, STS or ETOP treatments A), E), I). Live B), F), J), apoptotic C), G), K), and dead D), H), L), populations were then analysed for mitochondrial function and ROS levels by plotting $DiIC_1(5)$ v HE parameters. $DiIC_1(5)^{+ve}/HE^{-ve}$ populations have fully functioning mitochondria, while $DiIC_1(5)^{+ve}/HE^{+ve}$ are functioning mitochondria with ROS production. While $DiIC_1(5)^{-ve}/HE^{-ve}$ are cells with dysfunctional mitochondria and $DiIC_1(5)^{+ve}/HE^{+ve}$ are cells with dysfunctional mitochondria that have produced ROS.

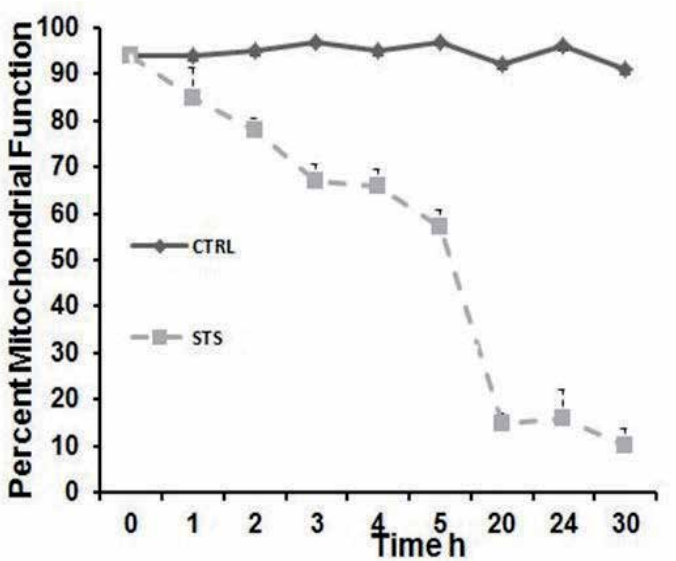

Figure 6. Jurkat cells were untreated or incubated with STS (1 μM) for 0, 1, 2, 3, 4, 5, 20, 24 and 30 h. Cells were loaded with $DiIC_1(5)$ to determine mitochondrial function and Annexin V-FITC and DAPI. Mitochondrial function was maintained throughout the assay in untreated cells but not in STS, n=3, error bar denote SEM.

interesting changes in these dynamics cell functions (*e.g.* mitochondrial function). A time course of live cell mitochondrial function can be plotted over 30 h after incubation with STS over this time course. After labelling with $DiIC_1(5)$ and Annexin V-FITC and DAPI the live cell

mitochondrial function can be plotted over time with the percentage of live cells with functioning mitochondria systematically decreasing over the 30 h with 40% of cells showing no function after 5 h (Figure 6) [13-17].

3.5. Use of Violet Ratiometric Membrane Asymmetry Probe

F2N12S, the violet ratiometric membrane asymmetry probe can also be used to measure apoptosis without the need for high calcium and is also not reversible unlike Annexin V binding to PS [22]. The use of the violet parameters, allows the blue and red laser parameters to be used for immunophenotyping without the need for separate labelling conditions as required for annexin V binding thus making a more flexible approach for labelling of samples. Here we compare F2N12S probe to Annexin V–PI labelling in untreated and STS treated cells, see Figure 7. Control cells labelled with Annexin V-FITC and PI are shown in Figure 7A with

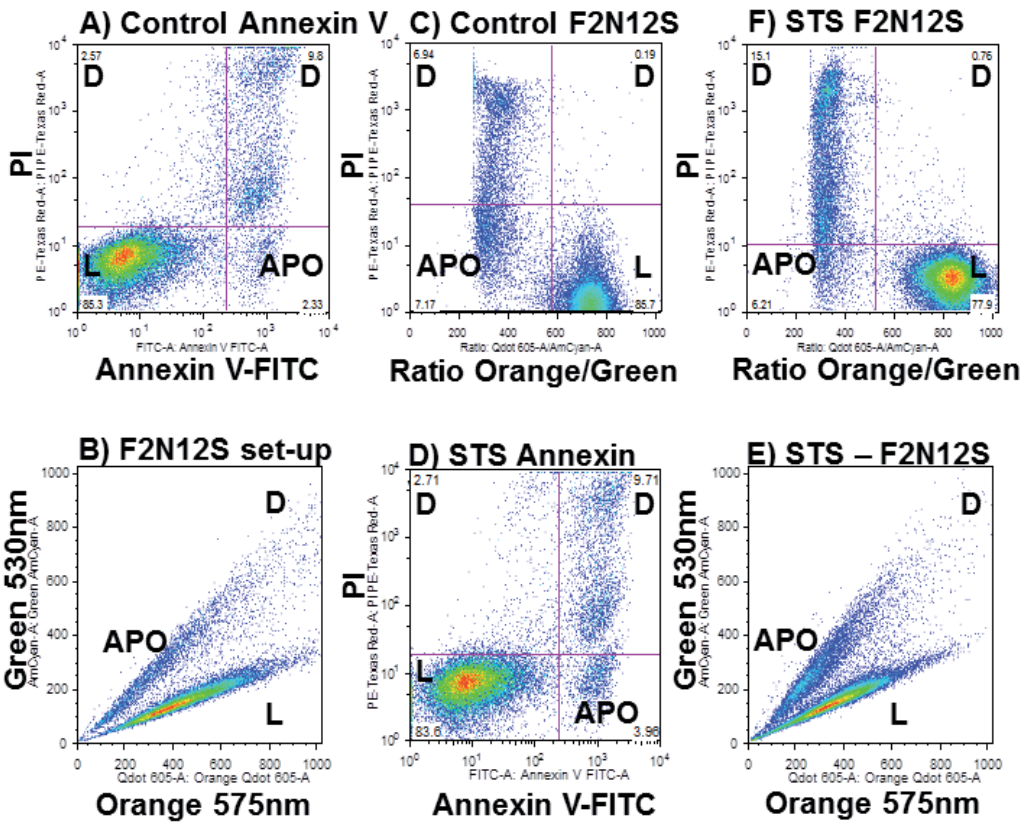

Figure 7. Jurkat cells were untreated or treated with 1 μM STS for 4 h and labelled with annexin V-FITC, the violet ratiometric membrane asymmetry probe, F2N12S and PI. A), D) show control and apoptotic cell cultures labelled with Annexin V-FITC and PI, L denotes live cells, APO apoptotic cells, and D denotes dead cells. B) and E) show the green and orange signals from F2N12S with live (L), apoptotic (APO) and (D) dead cells (confirmed by back-gating on PI positive events. Finally the F2N12S ratio signal of Orange/Green v PI indicates position of the live, apoptotic and dead cells for control and STS treated cells, C) and F).

http://dx.doi.org/10.5772/60549

live cells indicated by (L), early apoptotic (APO) and dead cells (D). Jurkat cells loaded with F2N12S give orange (575nm) signals in live cells and green (530nm) signals in early, late and dead cell populations (Figure 7B). The electronic ratioing of the Orange/Green signals with the BD FACSDiva software allows the researcher to plot the Ratio v PI to give a dot-plot showing the presence of live cells (Ratio orange/green high), early apoptotic cells (APO, Ratio orange/green low), with dead cells being PI^{+ve} and Ratio orange/green low (Figure 7C). Likewise STS treated cells are shown labelled with Annexin V-FITC-PI (Figure 7D) and F2N12S with orange and green signals displayed in a dot-plot (Figure 7E) with the corresponding Ratio orange/green parameter vs PI in Figure 7D).

Acknowledgements

I would like to thank Dr Barry Wilbourn, GSK, UK for the Etoposide work included in this chapter.

Author details

G. Warnes

Address all correspondence to: g.warnes@qmul.ac.uk

Flow Cytometry Core Facility, The Blizard Institute, Barts and The School of Medicine and Dentistry, Queen Mary London University, London, UK

References

[1] Kerr JF, Wyllie AH, Currie AR. Apoptosis: a basic biological phenomenon with wide-ranging implications in tissue kinetics. Br J Cancer 1972 Aug;26(4):239-257.

[2] Darzynkiewicz Z, Juan G, Li X, Gorcyzya W, Murakami T, Traganos F. Cytometry in cell necrobiology: Analysis of apoptosis and accidental cell death (necrosis). Cytometry 1997;27:1–20.

[3] Wlodkowic D, Skommer J, Darzynkiewicz Z. Cytometry in cell necrobiology revisited. Recent advances and new vistas. Cytometry A 2010;77A:591–606.

[4] Fink SL, Cookson BT. Apoptosis, pyrotosis and necrosis: mechanistic description of dead and dying eukaryotic cells. Infect Immun 2005;73:1907–1916.

[5] Jacobson MD, Weil M, Raff MC. Programmed cell death in animal development. Cell 1997 Feb 7;88(3):347-354.

[6] Yonehara S, Ishii A, Yonehara M. A cell-killing monoclonal antibody (anti-Fas) to a cell surface antigen co-down regulated with the receptor of tumor necrosis factor. J Exp Med 1989 May 1;169(5):1747-1756.

[7] Martinou JC, Youle RJ. Mitochondria in apoptosis: Bcl-2 family members and mitochondrial dynamics. Dev Cell 2011 Jul 19;21(1):92-101.

[8] Umansky SR, Korl BA Nelipovich PA. In vivo DNA degradation in thymocytes of gamma-irradiated or hydrocortisone treated rats. Biochem Biophys Acta 1981;655(1): 9-17.

[9] Pollack A, Ciancio G. Cell cycle phase-specific analysis of cell viability using Hoechst 33342 and propidium iodide after ethanol preservation. Methods Cell Biol 1990;33:19–24.

[10] Ormerod MG, Sun XM, Snowden RT, Davies R, Fearnhead H, Cohen GM. Increased membrane permeability of apoptotic thymocytes: a flow cytometric study. Cytometry 1993;14:595–602.

[11] Belloc F, Dumain P, Boisseau MR, Jalloustre C, Reiffers J, Bernard P, Lacombe F. A flow cytometric method using Hoechst 33342 and propidium iodide for simultaneous cell cycle analysis and apoptosis determination in unfixed cells. Cytometry 1994;17:59–6.

[12] Vermes I, Haanen C, Steffens-Nakken H, Reutelingsperger C. A novel assay for apoptosis: Flow cytometric detection of phosphatidylserine expression on early apoptotic cells using fluorescein labeled annexin V. J Immunol Methods 1995;184:39–51.

[13] Rasola A, Geuna M. A flow cytometric assay simultaneously detects independent apoptotic parameters. Cytometry A 2001;45A:151–157.

[14] Lugli E, Troaino L, Ferraresi R, Roat E, Prada N, Nasi M, Pinti M, Cooper EL, Cossaizza A. Characterization of cells with different mitochondrial membrane potential during apoptosis. Cytometry A 2005;68A:28–35.

[15] Poot M, Pierce RH. Detection of changes in mitochondrial function during apoptosis by simultaneous staining with multiple fluorescent dyes and correlated multiparameter flow cytometry. Cytometry 1999;35:311–317.

[16] Troiano L, Ferraresi R, Lugli E, Nemes E, Roat E, Nasi M, Pinti M, Cossarizza A. Multiparametric analysis of cells with different mitochondrial membrane potential during apoptosis by polychromatic flow cytometry. Nat Protoc 2007;2;2719-27.

[17] Lizard G, Fournel S, Genestier L, Dhedin N, Chaput C, Flacher M, Mutin M, Panaye G, Revillard JP. Kinetics of plasma membrane and mitochondrial alterations in cells undergoing apoptosis. Cytometry 1995;21:275–283.

[18] Yaffe, PB, Doucette CD, Walsh M, Hoskin DW. Piperine impairs cell cycle progression and causes reactive oxygen species-dependent apoptosis in rectal cells. Exp Mol Pathol 2013;94:109-114.

[19] Al-Mehdi AB, Shuman H, Fisher AB. Intracellular generation of reactive oxygen species during nonhypoxic lung ischemia. Am J Physiol 1997;272:L294-300.

[20] Thayyullathil F, Chathoth S, Hago A, Patel M, Galadari S. Rapid reactive oxygen species (ROS) generation induced by curcumin leads to caspase-dependent and –independent apoptosis in L929 cells. Free Radic Biol Med 2008;45:1403-12.

[21] Zhan L, Yang Y, Ma TT, Huang C, Meng XM, Zhang L, Li J. Mol Cell Biochem 2015; Epub DOI 10.1007/s11010-014-2298-6.

[22] Shynkar VV, Klymchenko AS, Kunzelmann C, Duportail G, Muller CD, Demchenko AP, Freyssinet JM, Mely Y. Fluorescent biomembrane probe for ratiometric detection of apoptosis. J Am Chem Soc 2007;129(7):2187-93.

[23] Vossenkamper A, Marches O, Fairclough PD, Warnes G, Stagg AJ, Lindsay JO, Evans PC, Luong LA, Croft NM, Naik S, Frankel G, McDonald TT. Inhibition of NF-kB signalling in human dendritic cells the enterpathogenic *Escherichia coli* effector protein NIeE .*J Immunol 2010*185: 4118-4127.

Chapter 5

Effects of WF10 on Glycosaminoglycan Sulphation in Proinflammatory Monocytes and Macrophages

Maria Schönberg, Denise Schlorke and Jürgen Arnhold

Additional information is available at the end of the chapter

http://dx.doi.org/10.5772/60862

Abstract

The chlorite-based drug solution WF10 has been successfully applied to dampen strong inflammatory disease states and to improve wound healing processes. However, the molecular mechanisms of this drug are not well understood. This study is directed to investigate how WF10 and its components affect the expression of surface markers and sulphated proteoglycans and glycosaminoglycans in proinflammatory-stimulated monocytes and macrophages.

Human blood-derived macrophages were cultivated from monocytes in the presence of 50 U/ml granulocyte-macrophage colony-stimulating factor and activated by a mixture of 100 ng/ml lipopolysaccharide (LPS) and 10 ng/ml interferon γ (IFNγ). These cells were identified and characterised by their specific cell-surface receptors CD14, CD16, CD80, CD86, CD163, and CD206 using flow cytometry approaches. The sulphation level of proteoglycans and glycosaminoglycans was assessed by the Blyscan™ dye-binding assay. The expression of the surface marker CD44, a proteoglycan with sulphated glycosaminoglycan side chains, was followed by antibodies against CD44. The binding of fluorescence-labelled hyaluronan to CD44 was also investigated by flow cytometry. All analyses were performed after incubation of monocytes and macrophages with WF10 or with its main components chlorite and chlorate.

The drug substance WF10 inhibited the activation of LPS/IFNγ-stimulated human monocyte-derived macrophages. Among them are the diminished expression of proinflammatory surface markers, the inhibition of the expression of the hyaluronan receptor CD44, and the binding of hyaluronan to CD44. Further, the overall amount of sulphated proteoglycans and glycosaminoglycans was down-regulated by WF10. These *in vitro* experiments indicate that WF10 is able to inhibit the proinflammatory activation of macrophages. The results suggested that chlorite is the active principle in WF10 as chlorite caused principally the same changes in targets as WF10. The WF10 component chlorate inhibited only the overall sulphation level of proteoglycans and glycosaminoglycans and the binding of hyaluronan to CD44.

To sum up, WF10 is a promising tool to inhibit proinflammatory states of immune cells. The inhibition of activation processes in monocytes and macrophages by WF10 coincides well with the results about clinical application of WF10.

Keywords: Inflammation, Macrophages, Hyaluronan, Sulphation, WF10

1. Introduction

Macrophages are key players during inflammatory immune response. At inflammatory loci, they not only efficiently remove damaged tissue components, apoptotic cells, and cell debris but also secrete numerous cytokines and growth factors that either further promote the inflammatory process or terminate the attraction of immune cells as well as initiate proliferative activities. On murine macrophages, several patterns of macrophage activation such as M1 (classically activated) and M2 (alternatively activated) macrophages and their subsets are distinguished on the basis of gene expression profiles, the appearance of cell surface markers, and the release of cytokines and other mediators [1]. Despite clear differences in immunological relevant characteristics between man and mouse [2], most properties of this polarisation pattern can also be transferred to human macrophages.

Macrophages express on their surface several proteins bearing sulphated glycosaminoglycan side chains. These sulphated proteoglycans are responsible for the interaction with cytokines, growth factors, and other mediators of inflammation as well as for the interaction with components of the extracellular matrix [3,4]. One of the cell-surface glycoproteins is CD44, which is known to function as receptor for the nonsulphated glycosaminoglycan hyaluronan [5]. After the onset of inflammation, large amounts of hyaluronan are secreted by endothelial cells, fibroblasts, and other cells at inflammatory loci. Due to the high water binding capacity, hyaluronan secretion contributes to oedema formation, changes in vascular permeability, and leukocyte recruitment [6]. Hyaluronan is thereby fixed to the surface of macrophages and tissue cells by CD44. This interaction is among others regulated by carbohydrate sulphation of the receptor [7,8].

Many strong disease scenarios are accompanied by an uncontrolled activation of the immune system and long-lasting inflammatory states. The worst-case scenario is the development of a sepsis syndrome accompanied by multiple organ failure [9].

Among the therapeutic approaches against inflammatory diseases is the intravenous infusion of the chlorite-based immunomodulatory drug solution WF10. This drug solution and the more diluted form Oxoferin have been successfully applied to dampen strong inflammatory states and to improve wound healing processes in patients [10–13]. However, the fine mechanism of the action of WF10 remains unknown. WF10 is a tenfold diluted aqueous solution of the drug substance OXO-K933 (NUVO Research Inc., Mississauga, Canada) that is composed of chlorite (4.25%), chloride (1.9%), chlorate (1.5%), and sulphate (0.7%) with sodium as cationic component [11].

http://dx.doi.org/10.5772/60862

Chlorite is known to interact preferentially with haem proteins affecting their catalytic cycles [14–16]. Furthermore, the chlorite component of WF10 converts oxyhemoglobin and ferryl hemoglobin into methemoglobin, which is also inactivated by chlorite/WF10 [17]. Chlorate is used as an inhibitor of the 3′-phosphoadenosine 5′-phosphosulphate (PAPS) synthase [18]. This enzyme is responsible for the production of PAPS, a common sulphur donor for all biological sulphation reactions that are catalysed by various sulphotransferases [19,20].

Here we addressed the question which effects WF10 and its components exhibit on human blood-derived monocytes and macrophages, which were stimulated by tumour necrosis factor α (TNFα) or a mixture of lipopolysaccharide (LPS) and interferon γ (IFNγ). In particular, we examined how WF10 influenced the expression of CD44 in these cells and the interaction of CD44 with hyaluronan. We demonstrated that WF10 inhibited the expression of surface markers in LPS/IFNγ-activated macrophages, diminished the global expression of sulphated proteoglycans and glycosaminoglycans (GAGs), and interfered with the binding of hyaluronan to CD44.

2. Materials and methods

2.1. Chemicals

Blyscan™ sulphated glycosaminoglycan assay was obtained from Biocolor Ltd., Carrickfergus, United Kingdom. Monocyte isolation Kit II and MACS® separation columns were purchased from Miltenyi Biotec GmbH, Bergisch Gladbach, Germany. Biocoll separating solution was obtained from Biochrome AG, Berlin, Germany. RPMI 1640 medium and recombinant human granulocyte-macrophages colony-stimulating factor (GM-CSF) were purchased from Life Technologies GmbH, Darmstadt, Germany. Human recombinant interferon γ (IFNγ) and tumour necrosis factor-alpha (TNFα) were supplied from Biomol, Hamburg, Germany. Lipopolysaccharide (LPS), papain from Papaya latex, foetal bovine serum (FBS), and penicillin/streptomycin were obtained from Sigma-Aldrich, Taufkirchen, Germany. Bovine serum albumin (BSA) was obtained from PAA Laboratories GmbH, Pashing, Germany. Hyaluronan conjugated with fluorescein isothiocyanate (FITC) was purchased from Calbiochem, Darmstadt, Germany. Antibodies conjugated with phycoerythrin (PE) and with PE-cyanine 5 (Cy5) for flow cytometry analysis were supplied from eBioscience, Frankfurt, Germany.

WF10 and special WF10 solutions free of either chlorate or chlorite were provided by NUVO Manufacturing GmbH, Wanzleben, Germany. In undiluted WF10, concentrations of chlorite and chlorate are 62.9 mM and 18 mM, respectively. In the chlorate-free WF10 solution (in the text mentioned as chlorite), chlorate was replaced by the equimolar amount of chloride. The same holds for the chlorite-free WF10 solution (named as chlorate).

2.2. Preparation and stimulation of monocytes and macrophages

Monocytes of human blood of healthy volunteers were isolated and purified by density gradient centrifugation followed by magnetic bead separation using the monocyte isolation

kit II and MACS® separation columns according to manufacturer's protocols. Monocytes (10^6 were cultivated in tissue culture dishes in RPMI medium containing 10% FBS, 2 mM L-glutamine, and 1% penicillin/streptomycin at 37 °C and 5 vol.% CO_2. The differentiation of monocytes towards macrophages was induced by addition of 100 ng/ml GM-CSF for 6 days followed by addition of a mixture of 100 ng/ml LPS and 10 ng/ml IFNγ with or without WF10, chlorate, and chlorite for 24 h at 37 °C and 5 vol.% CO_2.

Monocytes were stimulated with 2 ng/ml TNFα in the absence or presence of WF10, chlorate, and chlorite for 18 h at 37 °C and 5 vol.% CO_2.

2.3. Determining of cell-surface marker expression by flow cytometry

Cells were harvested by washing with PBS at room temperature followed by incubation with ice-cold PBS supplemented with 2.5 mM EDTA for 20 min. Cells rounded up and could be scraped off using a cell scraper. After centrifugation for 5 min (400×*g*), cells were incubated with PBS supplemented with 1% BSA and fluorescence-labelled antibodies (antiCD1a-PE, antiCD14-PE, antiCD16-PE, antiCD80-PE, antiCD86-PE, antiCD163-PE, antiCD206-PE, and antiTLR-4-PE), and the corresponding isotype controls for 30 min in the dark. Thereafter, cells were washed by centrifugation (400×*g*, 5 min) and fluorescence intensity of the cells was detected by flow cytometry using a FACSCalibur (Becton Dickinson, Franklin Lakes, USA) with a laser excitation wavelength of 488 nm (PE detection in channel FL-2). Ten thousand events were analysed for each measurement using Flowing Software 2.4.1 by Perttu Terho.

2.4. CD44-hyaluronan-binding assay

The expression of the surface marker CD44 and the binding of its ligand hyaluronan were determined using a flow cytometry assay. Harvested cells were either dissolved in PBS supplemented with 1% BSA and incubated with antibodies against CD44 (anti-CD44-PE-Cy5, eBioscience) for 30 min in the dark or dissolved in PBS supplemented with 2% FBS, 2 mM EDTA, and 10 μg FITC-labelled hyaluronan. Cells were washed with PBS (400×*g*, 5 min), and the fluorescence intensity of the cells was detected using a FACSCalibur (Becton Dickinson, Franklin Lakes, USA) with a laser excitation of 488 nm (FITC detection in channel FL-1, PE-Cy5 in channel FL-3). Ten thousand events were analysed for each measurement using Flowing Software 2.4.1 by Perttu Terho.

2.5. Blyscan dye staining of sulphated proteoglycans and glycosaminoglycans

The analysis of the total amount of sulphated proteoglycans and glycosaminoglycans (GAGs) was performed using the Blyscan™ dye-binding assay (Biocolor Ltd., Carrickfergus, United Kingdom) according to the manufacturer's protocol. Sulphated GAGs of the cells were extracted using a papain extraction reagent in 0.2 M sodium phosphate buffer (Na_2HPO_4–NaH_2PO_4), pH 6.4, containing 0.1 mg/ml papain at 65 °C for 3 h. After centrifugation at 10000×*g* for 10 min, supernatant was added to the Blyscan dye reagent and incubated in a mechanical shaker for 30 min. After centrifugation (12000×*g*, 10 min), addition of a dissociation reagent, and further centrifugation (12000×*g*, 10 min) the absorbance at 656 nm was

http://dx.doi.org/10.5772/60862

measured. The content of sulphated GAG can be calculated using a standard curve with known concentrations.

3. Results

3.1. Effects of WF10 on the expression of surface markers in LPS/IFNγ-stimulated macrophages

Macrophages were differentiated from peripheral blood-derived monocytes in the presence of the granulocyte-macrophage colony-stimulating factor (GM-CSF). These cells were stimulated by a mixture of LPS/IFNγ for 24 h to obtain macrophages with proinflammatory properties corresponding to M1-type macrophages. The activation pattern of these macrophages was assessed by the expression of selected surface markers (Figure 1).

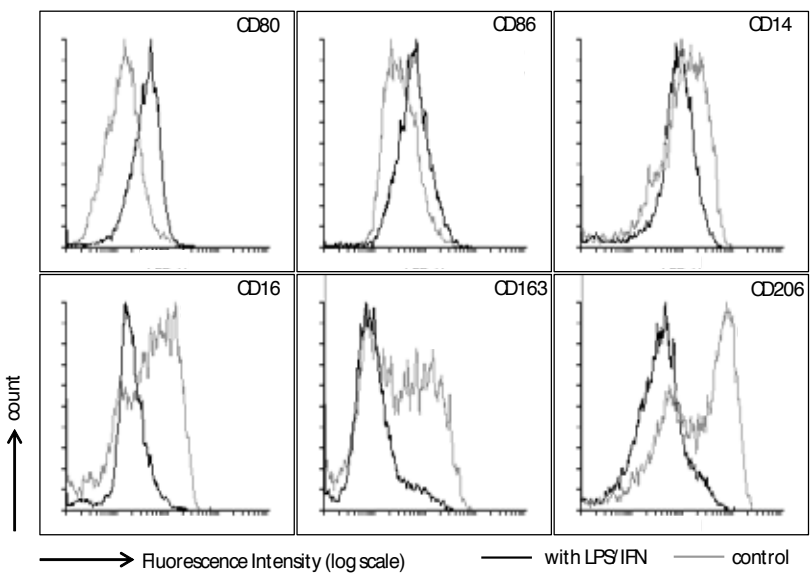

Figure 1. Profile of selected cell-surface markers of LPS/IFNγ-stimulated macrophages. Whereas the markers for M1 activation (CD80 and CD86) were up-regulated, the markers for M2 activation (CD14, CD16, CD163, and CD206) were down-regulated after stimulation with LPS/IFNγ. Representative examples of the fluorescence intensity of LPS/IFNγ-stimulated macrophages (black) are given in comparison to the control samples (silver) without LPS/IFNγ. Data were obtained from at least four different macrophage preparations.

As expected, there was an increased expression of the surface proteins CD80 and CD86 (Figure 1) upon exposure of macrophages to LPS/IFNγ. We analysed also the flow cytometry pattern of surface markers that are known to be up-regulated by alternative activation but down-regulated in the sole presence of LPS/IFNγ. The LPS/IFNγ-induced down-regulation of CD14, CD16, CD163, and CD206 is clearly demonstrated in Figure 1.

Next, the expression of several receptors was measured upon LPS/IFNγ-mediated stimulation of macrophages in the presence of WF10 (Figure 2). There was a concentration-dependent decrease of CD80 expression by WF10. At a 1:100 dilution of WF10 corresponding to a final chlorite concentration of 629 μM, only 40% ± 8% of the original amount of receptors could be detected. A similar pattern of receptor decrease was also observed for CD86, CD14, and the toll-like receptor 4 (TLR4). This indicates that WF10 exhibits a general effect on the proinflammatory activation mechanism of macrophages. These effects are caused by the WF10 component chlorite, as shown in experiments replacing WF10 by chlorite. The exposure of LPS/IFNγ-stimulated macrophages to chlorate does not cause any changes in the expression of surface markers (data not shown).

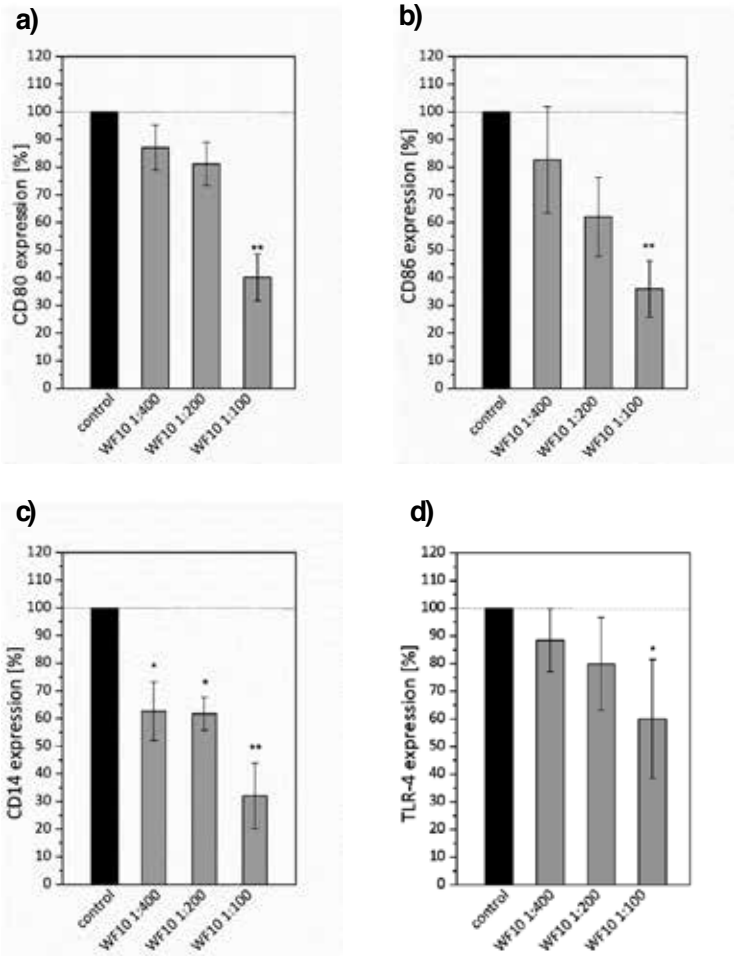

Figure 2. Regulation of selected cell-surface markers of macrophages by WF10. LPS/IFNγ-stimulated macrophages were incubated with or without (control) different concentrations of WF10 for 24 h. WF10 reduced the expression of CD80 (a), CD86 (b), CD14 (c), and TLR-4 (d) in a concentration-dependent manner. Fluorescence intensities (means ± standard deviation) are given as a function of the content of WF10. Fluorescence of samples without WF10 (control) was set to 100%. Data from three independent experiments are given. *$p \leq 0.05$, **$p \leq 0.01$.

http://dx.doi.org/10.5772/60862

3.2. Binding of hyaluronan to CD44 in the presence of WF10

The binding of fluorescence-labelled hyaluronan to CD44 is well described [7,8]. WF10 exposure diminished the binding of hyaluronan to LPS/IFNγ-stimulated macrophages and TNFα-stimulated monocytes in a concentration-dependent manner (Figure 3). At the highest applied WF10 concentration (1:100 dilution), the binding of hyaluronan was decreased by 41.2% ± 3% in macrophages and 22.6% ± 6% in monocytes. Chlorite (applied as chlorate-free WF10) caused a similar inhibition of hyaluronan binding as WF10. Chlorate (applied as chlorite-free WF10) diminished also the binding of this nonsulphated GAG. Thus, both chlorite and chlorate are involved in inhibition of the interaction between hyaluronan and CD44.

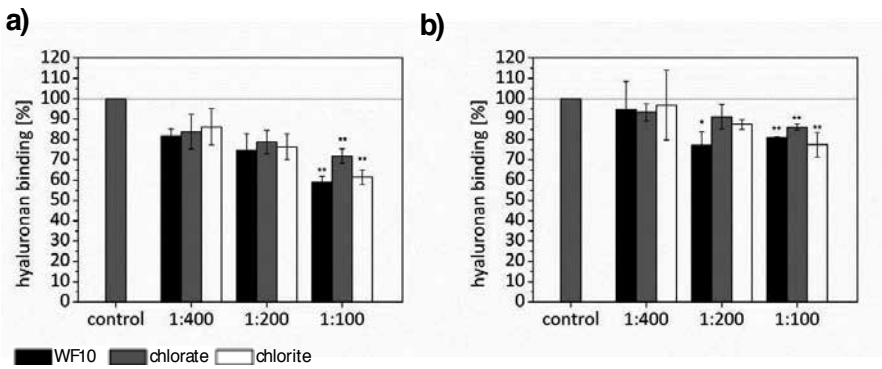

Figure 3. Binding of fluorescence-labelled hyaluronan to the surface of macrophages (a) and monocytes (b). LPS/IFNγ-stimulated macrophages and TNFα-stimulated monocytes were incubated for 24 or 18 h, respectively, with or without (control) different concentrations of WF10/chlorate/chlorite. In these experiments, the applied concentrations of chlorite or chlorate were the same as in WF10. WF10, chlorate, and chlorite reduced the binding of hyaluronan to monocytes and macrophages. Fluorescence intensities (means ± standard deviation) are given as a function of the content of WF10. Fluorescence of samples without WF10 (control) was set to 100%. Data from three independent experiments are given. $*p \leq 0.05$, $**p \leq 0.01$.

In addition, the expression of CD44 was assessed with anti-CD44 antibodies. The expression of CD44 was also significantly decreased by WF10 in both macrophages and monocytes (Figure 4). In both cell types, the WF10 effect coincides well with the application of chlorite. In monocytes, chlorate did not cause any changes in fluorescence values of CD44. In macrophages, the expression of CD44 was slightly decreased at the highest applied concentration of chlorate. However, this diminution was not significant.

3.3. Effects of WF10 on the sulphation of glycosaminoglycans

Due to the strong effects of WF10 on the activation pattern and binding of hyaluronan, we next investigated which effects exhibit WF10 on the total formation of sulphated proteoglycans and GAGs in monocytes and macrophages. After activation of macrophages with LPS/IFNγ or monocytes with TNFα, the total amount of sulphated GAGs was analysed in cell extracts by the Blyscan assay. This reagent interacts with sulphated proteoglycans and GAGs yielding a blue-coloured complex.

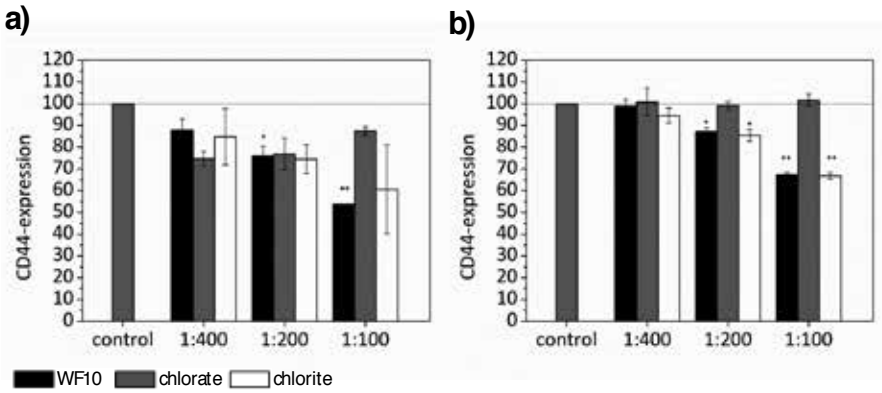

Figure 4. CD44 expression of macrophages (a) and monocytes (b) on cell surface. LPS/IFNγ-stimulated macrophages and TNFα-stimulated monocytes were incubated for 24 h or 18 h, respectively, with or without (control) different concentrations of WF10/chlorate/chlorite. WF10 and chlorite reduced the CD44 expression in a concentration-dependent manner. Fluorescence intensities (means ± standard deviation) are given as a function of the content of WF10. Fluorescence of samples without WF10 (control) was set to 100%. Data from three independent experiments are given. $*p \leq 0.05$, $**p \leq 0.01$.

WF10 considerably diminished the amount of sulphated proteoglycans and GAGs in macrophages and also in monocytes (Figure 5). Again, chlorite caused the same effects as WF10. A strong inhibition of the total sulphation degree was also observed for chlorate both in monocytes and macrophages. However, chlorate was less efficient than chlorite.

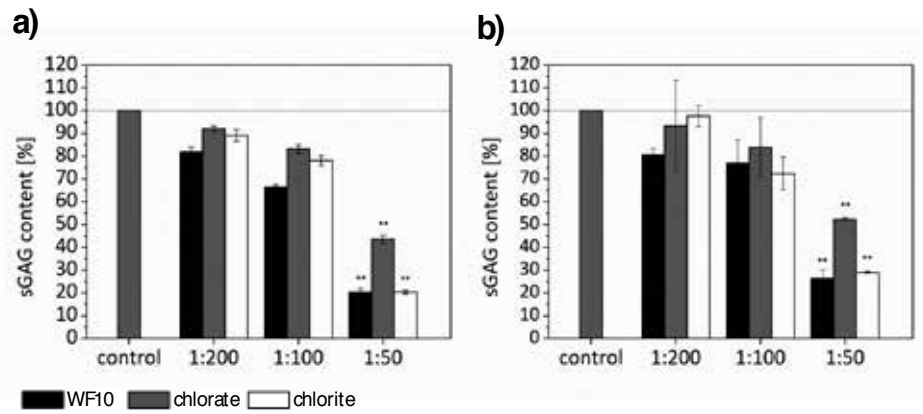

Figure 5. Effects of WF10 on the sulphation of glycosaminoglycans in macrophages (a) and monocytes (b). LPS/IFNγ-stimulated macrophages and TNFα-stimulated monocytes were incubated for 24 h or 18 h, respectively, with or without (control) different concentrations of WF10/chlorate/chlorite. WF10, chlorate, and chlorite reduced the sGAG content in a concentration-dependent manner. Absorbance values for sulphated GAGs are given as a function of the content of WF10, chlorite or chlorate. Absorbance of the control samples (without WF10 or components) was set to 100%. Data from at least three independent experiments are shown. $*p \leq 0.05$, $**p \leq 0.01$.

http://dx.doi.org/10.5772/60862

4. Discussion

The drug substance WF10 inhibits the activation of LPS/IFNγ-stimulated human monocyte-derived macrophages. Among them are the diminished expression of proinflammatory surface markers, the inhibition of the expression of the hyaluronan receptor CD44, and the binding of hyaluronan to CD44. Further, the overall amount of sulphated proteoglycans and GAGs was down-regulated by WF10. These *in vitro* experiments indicate that WF10 is able to inhibit the proinflammatory activation of the M1-type in macrophages.

These data are in line with other WF10 effects observed on monocytes, macrophages, and the interaction of these cells with fibroblasts and T-cells. In macrophages, WF10 is known to decrease the expression of TNFα [11], to diminish the antigen presentation that diminishes T-cell proliferation [21,22], and to enhance the interaction with fibroblasts [11]. WF10 inactivates AIDS viruses [10,23], enhances the cytotoxicity of natural killer cells [24], and prolongs cardiac graft survival in a rodent xenotransplantation model [25]. Further, the application of WF10 attenuates the disease state in radiation-associated tissue damage [12,26,27], in diabetic foot ulcera [13], and in wound healing [28,29].

The experimental data suggest that chlorite is the active principle in WF10 and in the more diluted form Oxoferin as chlorite caused principally the same changes in targets as WF10 [30]. In our experiments, a chlorate-free preparation of WF10 showed the same results as WF10 confirming the fact that chlorite is the active component. Chlorate was insensitive in all experiments concerning the expression of surface proteins in macrophages. Only the binding of hyaluronan to CD44 and the formation of sulphated proteoglycans and GAGs responded to chlorate. In experimental cell biology, chlorate is usually used as an inhibitor of sulphation reactions [18,31] because it inhibits the formation of the common sulphur transfer reagent PAPS. As chlorate and sulphate share a similar geometry concerning the arrangement of oxygen–chlorine and oxygen–sulphur bonds, respectively, chlorate reversibly blocks the sulphate-binding side in PAPS synthase [32]. The stronger impact of chlorite over chlorate on the total amount of sulphated proteoglycans and GAGs can be explained by the fact that chlorite inhibits important signalling pathways in proinflammatory cells that apparently affect also sulphation reactions. A 50% inhibition of PAPS production by PAPS synthase occurs by 0.11 mM chlorate in the presence of physiological relevant concentrations of ATP and sulphate [32].

In leukocytes, the binding of hyaluronan to CD44 is tightly regulated by additional glycosylation, sulphation and sialysation [8]. Upon stimulation of blood-derived monocytes with TNFα, the overall degree of CD44 sulphation increased [7,33]. This increased sulphation of CD44 in TNFα- or IFNγ-stimulated monocytes correlates well with the enhanced binding of hyaluronan that is inhibited by chlorate [7].

Our observation about the inhibition of hyaluronan binding and overall sulphation in stimulated monocytes and macrophages by WF10 can only partially be explained by the chlorate effect, as a chlorate-free preparation of WF10 exhibited the same inhibitory efficiency as the complete WF10 solution. Thus, the chlorite component of WF10 should preferential-

ly act on upstream targets of signalling pathways in stimulated leukocytes. In the result of this activity, not only the induction of PAPS synthase will be dampened but also other signalling cascades that induce the expression of proinflammatory receptors as well as the secretion of cytokines and other inflammatory mediators.

At the moment, we can only speculate about the molecular targets for chlorite in signalling cascades of macrophages. As a redox-active component, chlorite is well known to interact with the porphyrin iron in haem proteins [14–16, 34–37]. In monocytes and macrophages, a number of different cytochromes and other haem proteins are involved in signalling pathways. In human macrophages, IFNγ is a strong inducer of indoleamine-2,3-dioxygenase, a haem protein that catalyses the oxidation of the amino acid tryptophan to kynurenine [38]. Contrary to this, IFNγ up-regulates the expression of the haem protein inducible nitric oxide synthase in murine macrophages [39]. There are also several redox-sensitive elements in signalling cascades that respond to changes in oxidative homeostasis [40]. Different effects of WF10 on monocytes and THP-cells have been reported such as inhibition of translocation of the transcription factor NFAT to the nucleus or the activation of AP1 and NFκB signalling [22].

5. Conclusions

Taken together, WF10 is a promising tool to inhibit proinflammatory states of immune cells. By general inhibition of macrophage activation in the presence of inflammatory mediators, WF10 affects not only the activation state of these key immune cells but also the interaction of macrophages with T-cells, fibroblasts, and other cells at inflammatory sites [11,21,22,24]. Many diseases are accompanied by long-lasting chronic inflammations with disturbed processes of immune regulation. In a number of cases, the application of WF10 improved the disease state of these patients [10–13, 25–28]. Thus, our data about the inhibition of activation processes in monocytes and macrophages by WF10 coincide well with the results about clinical application of WF10.

The molecular mechanisms of the action of WF10 components are only poorly understood at present. Despite clear effects of chlorate on the overall sulphation in monocytes and macrophage, the chlorite component is the main active principle of WF10. Chlorite caused principally the same effects as WF10. Many efforts are necessary to deepen our knowledge about the cellular and tissue targets for chlorite, to understand how this WF10 component affects signalling pathways in inflamed tissues, and to give an answer on the question how WF10 contributes to resolution of chronic inflammatory states.

Acknowledgements

The authors gratefully acknowledge the financial support provided by the Sächsische Aufbaubank from a funding of the European Regional Development Fund (ERDF) (SAB

Project Nr: 100116526) and the German Federal Ministry of Education and Research (BMBF 1315883).

Author details

Maria Schönberg[1,2*], Denise Schlorke[1,2] and Jürgen Arnhold[1,2]

*Address all correspondence to: maria.schoenberg@medizin.uni-leipzig.de

1 Translational Centre of Regenerative Medicine Leipzig, University of Leipzig, Leipzig, Germany

2 Institute of Medical Physics and Biophysics, University of Leipzig, Leipzig, Germany

References

[1] Murray PJ, Wynn TA. Protective and pathogenic functions of macrophage subsets. Nat Rev Immunol. 2011;11:723–737. DOI: 10.1038/nri3073.

[2] Zschaler J, Schlorke D, Arnhold J. Differences in innate immune response between man and mouse. Crit Rev Immunol. 2014;34:433–454. DOI: 10.1615/CritRevImmunol. 2014011600

[3] Park PJ, Reizes O, Bernfield M. Cell surface heparin sulfate proteoglycans: selective regulators of ligand-receptor encounters. J Biol Chem. 2000;275:29923–29926. DOI: 10.1074/jbc.R000008200.

[4] Parish CR. The role of heparin sulphate in inflammation. Nat Rev Immunol. 2006;6:633–643. DOI: 10.1038/nri1918.

[5] Lesley J, Hyman R. CD44 structure and function. Front Biosci 1998;3:616–630. DOI: 10.2741/A306

[6] Bollyky PL, Bogdani M, Bollyky J, Hull R, Wight TN. The role of hyaluronan and the extracellular matrix in islet inflammation and immune regulation. Curr Diab Rep. 2012;12:471–480. DOI: 10.1007/s11892-012-0297-0.

[7] Brown KL, Maiti A, Johnson P. Role of sulfation in CD44-mediated hyaluronan binding induced by inflammatory mediators in human $CD14^+$ peripheral blood monocytes. J Immunol. 2001;167:5367–5374. DOI: 10.4049/jimmunol.167.9.5367.

[8] Delcommenne M, Kannagi R, Johnson P. TNF-α increases the carbohydrate sulfation of CD44: induction of 6-sulfo N-acetyl lactosamine on N- and O-linked glycans. Glycobiology 2002;12:613–622. DOI: 10.1093/glycob/cwf080.

[9] Doi K, Leelahavanichkul, Yuen KS, Star RA. Animal models of sepsis and sepsis-induced kidney injury. J Clin Invest. 2009;119:2868–2878. DOI: 10.1172/JCI39421.

[10] Raffanti SP, Schaffner W, Federspiel CF, Blackwell RB, Ching OA, Kuhne FW. Randomized, double-blind, placebo-controlled trial of the immune modulator WF10 in patients with advanced AIDS. Infection 1998;26:202–207. DOI: 10.1007/BF02962364.

[11] McGrath MS, Kahn JO, Herndier BG. Development of WF10, a novel macrophage-regulating agent. Curr Opin Investig Drugs. 2002;3:365–373.

[12] Veerasarn V, Boonnuch W, Kakanaporn C. A phase II study to evaluate WF10 in patients with late hemorrhagic radiation cystitis and proctitis. Gynecol Oncol. 2006;100:179–184. DOI: 10.1016/j.ygyno.2005.08.014.

[13] Yingsakmongkol N, Maraprygsavan P, Sukosit P. Effect of WF10 (Immunokine) on diabetic foot ulcer therapy: a double-blind, randomized, placebo-controlled trial. J Foot Ankle Surg. 2011;50:635–640. DOI: 10.1053/j.jfas.2011.05.006.

[14] Schempp H, Reim M, Dornisch K, Elstner E. Chlorite-hemoprotein interaction as key role for the pharmacological activity of the chlorite-based drug WF10. Drug Res. 2001;51:3–11. DOI: 10.1055/s-0031-1300079

[15] Jakopitsch C, Spalteholz H, Furtmüller PG, Arnhold J, Obinger C. Mechanism of reaction of horseradish peroxidase with chlorite and chlorine dioxide. J Inorg Biochem. 2008;102:293–302. DOI:10.1016/j.jinorgbio.2007.09.002.

[16] Jakopitsch C, Pirker KF, Flemmig J, Hofbauer S, Schlorke D, Furtmüller PG, Arnhold J, Obinger C. Mechanisms of reaction of chlorite with mammalian heme peroxidases. J Inorg Biochem. 2014;135:10–19. DOI: 10.1016/j.jinorgbio.2014.02.010.

[17] Piechert A, Arnhold J. Interaction of the chlorite-based drug WF10 and chlorite with hemoglobin, methemoglobin and ferryl hemoglobin. Arch Biochem Biophys 2015; 585:82-89. DOI: 10.1016/j.abb.2015.09.009.

[18] Baeuerle PA, Huttner WB. Chlorate—a potent inhibitor of protein sulfation in intact cells. Biochem Biophys Res Commun. 1986;141:870–877. DOI: 10.1016/S0006-291X(86)80253-4.

[19] Leyh TS. The physical biochemistry and molecular genetics of sulfate activation. Crit Rev Biochem Mol Biol. 1993;28:515–542. DOI: 10.3109/10409239309085137.

[20] Venkatachalam KV. Human 3′-phosphoadenosine 5′-phosphosulfate (PAPS) synthase: biochemistry, molecular biology and genetic deficiency. IUBMB Life 2003;55:1–11. DOI: 10.1080/1521654031000072148.

[21] McGrath MS, Benike C, Kühne FW, Engleman E. Effect of WF10 (TCDO) on antigen presentation. Transplant Proc. 1998;30:4200–4204. DOI: 10.1016/S0041-1345(98)01393-1.

[22] Giese T, McGrath MS, Stumm S, Schempp H, Elstner E, Meuer S. Differential effects on innate versus adaptive immune responses by WF10. Cell Immunol. 2004;229:149–158. DOI: 10.1016/j.cellimm.2004.08.001.

[23] Ennen J, Werner K, Kühne FW, Kurth R. Inactivation of HIV infectivity by the chlorite-oxygen reaction product tetrachlordecaoxygen. AIDS. 1993;7:1205–1212. DOI: 10.1097/00002030-1993909000-00009.

[24] Kühne L, Konstandin M, Samstag Y, Meuer S, Giese T, Watzl C. WF10 stimulates NK cell cytotoxicity by increasing LFA-1-mediated adhesion to tumor cells. J Biomed Biotechnol 2011;e436587:1–6. DOI: 10.1155/2011/436587.

[25] Hansen A, Kemp K, Kemp E, Bouchelouche K, Bouchelouche P, Dieperink H, Horn T, Larsen S. High-dose stabilized chlorite matrix WF10 prolongs cardiac xenograft survival in the hamster-to-rat model without inducing ultrastructural or biochemical sings of cardiotoxicity. Pharmacol Toxicol. 2001;89:92–95. DOI: 10.1034/j.1600-0773.2001.d01-141.x.

[26] Mason KA, Murphy S, Milas L. Stimulation of haematopoietic cell recovery by tetrachlorodecaoxide in sublethally irradiated mice. Radiat Res 1993;136:229–235. DOI: 10.2307/3578615.

[27] Veerasarn V, Khorprasert C, Lorvidhaya V, Sangruchi S, Tantivatana T, Narkwong L, Kongthanarat Y, Chitapanarux I, Tesavibul C, Panichevaluk A, Puribhat S, Sangkittipaiboon S, Sookpreedee L, Lertsanguansinchai P, Phromratanapongse P, Rungpoka P, Trithratipvikul S, Lojanapiwat B, Ruangdilokrat S, Ngampanprasert P. Reduced recurrence of late hemorrhagic radiation cystitis by WF10 therapy in cervical cancer patients. A multicenter, randomized, two-arm, open-label trial. Radiother Oncol. 2004;73:179–185. DOI: 10.1016/j.radonc.2004.05.007.

[28] Hinz J, Hautzinger H, Stahl KW. Rationale for and results from a randomised, double-blind trial of tetrachlorodecaoxygen anion complex in wound healing. Lancet. 1986;825–828. DOI: 10.1016/S0140-6736(86)90939-6.

[29] Wolin MS, Kleber E, Mohazzab KM, Elstner E. Tetrachlorodecaoxygen, a wound healing agent, produces vascular relaxation through hemoglobin-dependent inactivation of serotonin and norepinephrine. J Cardiovasc Pharmacol. 1994;23:664–668. DOI: 10.1097/00005344-199404000-00022.

[30] Habermann E, Müller B. Oxoferin und Natriumchlorit—ein Vergleich. Klin Wochenschr. 1989;67:20–25. DOI: 10.1007/BF01736530

[31] Humphries DE, Silbert JE. Chlorate: a reversible inhibitor of proteoglycan sulfation. Biochem Biophys Res Commun. 1988;154:365–371. DOI: 10.1016/0006-291X(88)90694-8

[32] Landson EB, Fisher AJ, Segal IH. Human 3′-phosphoadenosine 5-phosphosulfate synthetase (isoform I, brain): kinetic properties of the adenosine triphosphate sulfur-

ylase and adenosine 5′-phosphosulfate kinase domain. Biochemistry. 2004;43:4356–4365. DOI: 10.1021/bi049827m.

[33] Maiti A, Maki G, Johnson P. TNF-α induction of CD44-mediated leukocyte adhesion by sulfation. Science. 1998;282:941–943. DOI: 10.1126/science.282.5390.941.

[34] Youngman RJ, Wagner GR, Kühne FW, Elstner EF. Biochemical oxygen activation as the basis for the physiological action of tetrachlorodecaoxide (TCDO). Z Naturforsch. 1985;40c:409–414.

[35] Bercz JP, Jones L, Garner L, Murray D, Ludwig DA, Boston J. Subchronic toxicity of chlorine dioxide and related compounds in drinking water in the nonhuman primate. Environm Health Persp. 1982;46:47–55. DOI: 10.1289/ehp.824647.

[36] Langlois CJ, Calabrese EJ. The interactive effect of chlorine, copper and nitrite on methemoglobin formation in red blood cells of Dorset sheep. Human Exp Toxicol. 1992;11:223–228. DOI: 10.1177/096032719201100311.

[37] French CL, Yaun SS, Baldwin A, Leonard DA, Zhao XQ, Calabrese EJ. Potency ranking of methemoglobin-forming agents. J Appl Toxicol. 1995;15:167–174. DOI: 10.1002/jat.2550150306.

[38] Roshick C, Wood H, Caldwell HD, McClarty G. Comparison of gamma interferon-mediated antichlamydial defense mechanisms in human and mouse cells. Infect Immun. 2006;74:225–38. DOI: 10.1128/IAI.74.1.225-238.2006.

[39] Barish GD, Downes M, Alaynick WA, Yu RT, Ocampo CB, Bookout Al, Mangelsdorf DJ, Evans RM. A nuclear receptor atlas: macrophage activation. Mol Endocrinol. 2005;19:2644–2477. DOI: 10.1210/me.2002-0529.

[40] Brigelius-Flohé R, Flohé L. Basic principles and emerging concepts in the redox control of transcription factors. Antioxid Redox Signal. 2011;15:2325–2381. DOI:10.1089/ars.2010.3534.

Chapter 6

Immunophenotyping of Acute Leukemias – From Biology to Clinical Application

Francesco Mannelli

Additional information is available at the end of the chapter

http://dx.doi.org/10.5772/62332

Abstract

Immunophenotyping is an essential part of the modern diagnostic workup of acute leukemias and thus for an appropriate treatment of these complex and heterogeneous diseases. It provides a lot of useful information in this setting that transfers directly from laboratory to clinical management of patients. Lineage definition is the first goal leading to proper initial therapy. Some phenotypic patterns define specific subsets correlating with poor (mixed phenotype, dendritic cell neoplasm) or favorable (cortical T-lymphoblastic leukemia) outcome, thus guiding the application of treatment modalities. An advanced analysis of phenotypic data can address specific issues, such as the still debated role of multilineage dysplasia. The quality of response to chemotherapy is monitored by the detection of minimal residual disease and peripheral blast clearance during chemotherapy delivering. That allows a sharp discrimination of prognosis and again can drive the intensity of therapies proportionally to the disease chemosensitivity.

Keywords: Acute myeloid leukemia, acute lymphoblastic leukemia, diagnosis, prognosis, chemosensitivity, minimal residual disease

1. Introduction

1.1. Definition and clinical picture

Acute leukemias (AL) are hematological neoplasms featured by altered proliferation and/or differentiation of hematopoietic progenitors, leading to accumulation of immature cells in bone marrow (BM) and peripheral blood (PB). The clinical consequences are thus due to BM failure and infiltration of extra-hematological sites by leukemic cells, possibly causing organ function impairment. BM failure and related reduction in peripheral mature elements are responsible for the majority of clinical signs and symptoms at disease onset, that is, fatigue,

skin pallor, tachycardia (due to anemia), infections (due to neutropenia and/or T-cell deficiency), and hemorrhage (due to thrombocytopenia and/or coagulopathy). The clinical spectrum can be very wide, ranging from complete lack of manifestations to life-threatening ones. As such, a correct diagnosis is the first step for the right management of patients affected by AL.

1.2. Principles of treatment

Overall, treatment of AL goes through two main phases: induction and consolidation. The primary target of induction phase is the achievement of a complete remission (CR), which is defined by the decrease of immature cells below 5% of global BM cells at morphologic evaluation [1]. The benchmark of induction is chemotherapy, with different drugs, dosages, and schedules, depending on lineage definition and further on subclassification within different lineages. Some specific subsets [i.e., acute promyelocytic leukemia, Philadelphia-positive acute lymphoblastic leukemia (ALL)] benefit from the application of therapies targeted toward their unique underlying molecular pathways of leukemogenesis. Once more, the delivery of an appropriate treatment from the outset strictly depends upon AL's precise diagnostic definition. CR attainment is a prerequisite for long-term survival; once obtained, the consolidation phase deals with lowering the risk of relapse. Consolidation strategies include allogeneic hematopoietic stem cell transplantation (HSCT), providing the highest impact on relapse risk, chemotherapy, or autologous transplant. The use of allogeneic HSCT is generally reserved to patients with high relapse risk or with refractory disease, given the relevant treatment-related toxicity and mortality. The appraisal of prognosis at disease onset and during treatment phases is a dynamic and challenging process, with many potential predictors in turn characterized by different effectiveness in different contexts. Again, this process is the driver of important clinical decisions involving the application of highly toxic therapies.

1.3. Role of immunophenotype

Immunophenotyping is an essential part of the modern diagnostic workup and prognostic stratification of AL and thus for an appropriate treatment of these complex and heterogeneous diseases. It provides a lot of useful information in this setting that transfers directly from laboratory to clinical management of patients.

2. Diagnosis

According to the World Health Organization (WHO), ALs are defined as hematological neoplasms featured by the presence of 20% or more immature cells (blasts) with respect to PB or BM total cells [2, 3]. This benchmark threshold refers to morphology, which allows to recognize blasts by specific immature properties of nucleus and cytoplasm. Similarly, immunophenotyping permits to identify immature cells based on some immunological characteristics and, specifically, a dim expression of CD45 with low/intermediate side scatter signal [4]. Once identified, blasts are analyzed as regards the expression of a group of core

http://dx.doi.org/10.5772/62332

antigens. The phenotypic profile of blasts is thus related to normal hematopoietic counterpart, to define main lineage of differentiation and subclassification.

2.1. AL lineage definition

The first and main purpose of AL immunophenotyping is lineage definition of blasts, as myeloid or lymphoid, and in the latter case as B or T lymphoid. Lineage definition is based on similarities in antigenic expression patterns to normal myeloid, B-lymphoid progenitors, or T-lymphoid progenitors. With this respect, some "key" antigens have been defined for each lineage based on early and exclusive expression within them. However, it was immediately evident that in some AL forms, there was no clear-cut distinction and cross-lineage expression was quite frequent. As such, the first systematic attempt to regulate these findings was based on the concept that different antigens had a different weight for lineage attribution and was done by European Group for Immunological Classification of Leukemia (EGIL) [5] (Table 1). Although rigid by definition, as any such classification, it had the fundamental merit of creating a common reference for AL diagnosis. Recently many efforts have been tried to ameliorate and fine-tune the basic concept of EGIL classification. On the one side, the core group of lineage antigens has remained substantially the same: the interpretation of their pattern for lineage attribution has been updated by the WHO 2008 Classification [6]. On the other side, main efforts have been pursued to overcome the mere application of thresholds of antigen positivity, based on scarce biologic plausibility, and to attain a higher level of standardization. On this regard, the EuroFlow group has obtained amazing results toward sample handling, optimization on combinations of monoclonal antibodies, and even data analysis, possibly heading to go beyond dependence on operator [7].

Score	Myeloid	B lymphoid	T lymphoid
2	cyMPO	CD22, CD79a, cyIgM	cyCD3, TCR
1	CD13, CD33, CD117, CD65	CD19, CD10, CD20	CD2, CD5, CD8, CD10
0.5	CD14, CD15, CD64	CD24, TdT	TdT, CD7, CD1a

Abbreviations: MPO, myeloperoxidase; TdT, terminal deoxynucleotidyl transferase; cy, cytoplasmic; TCR, T-cell receptor.

More than 2 points are required to assign a lineage.

Table 1. Classification of European Group for Immunological Classification of Acute Leukemias

2.2. Diagnosis in challenging contexts

For an immediate diagnostic assessment, in the majority of cases, morphology is already able to assign myeloid lineage mainly by revealing granules, Auer bodies, or monocytic features. However, in several circumstances, immunophenotyping is absolutely essential for diagnostic workup:

- Morphologically undifferentiated blasts: when clear myeloid features are absent in PB- or BM-stained slides, immunophenotyping is the cornerstone of AL diagnosis. That pro-

vides the basis for definition of myeloid or lymphoid leukemia, a definition leading to completely different treatment strategies. In turn, within lymphoid lineages, phenotypic pattern is the basis for subclassification, according to the expression of selected key antigens in parallel with the maturation process in normal lymphopoiesis (Figure 1).

- Atypical presentation: ALs sometimes have atypical behavior, making hard to get a diagnosis and thus adequate therapy. These relatively rare circumstances are as follows: cases with low peripheral blast count and *punctio sicca* at BM aspiration; aplastic onset of T-lymphoblastic leukemia; BM necrosis reported to be associated with ALL or NPM1-mutated acute myeloid leukemia (AML) [8].
- Neoplasm of precursors of plasmacytoid dendritic cells: it is a novel subset in the WHO classification of myeloid neoplasms, with heterogeneous clinical presentation and variable extra-hematological infiltration. The normal counterpart of this tumor resides in the plasmacytoid dendritic cell lineage and as such its diagnosis depends on revealing a dendritic cell–related phenotype [9, 10]. The typical phenotypic profile consists of positivity for CD4, CD56, and CD123, together with intense expression of HLA-DR and negativity for main lineage antigens. In this setting, the phenotype provides an important piece of clinical information since this disease has a dismal outcome with chemotherapy consolidation and allogeneic transplantation seems to provide better chances of cure [11].

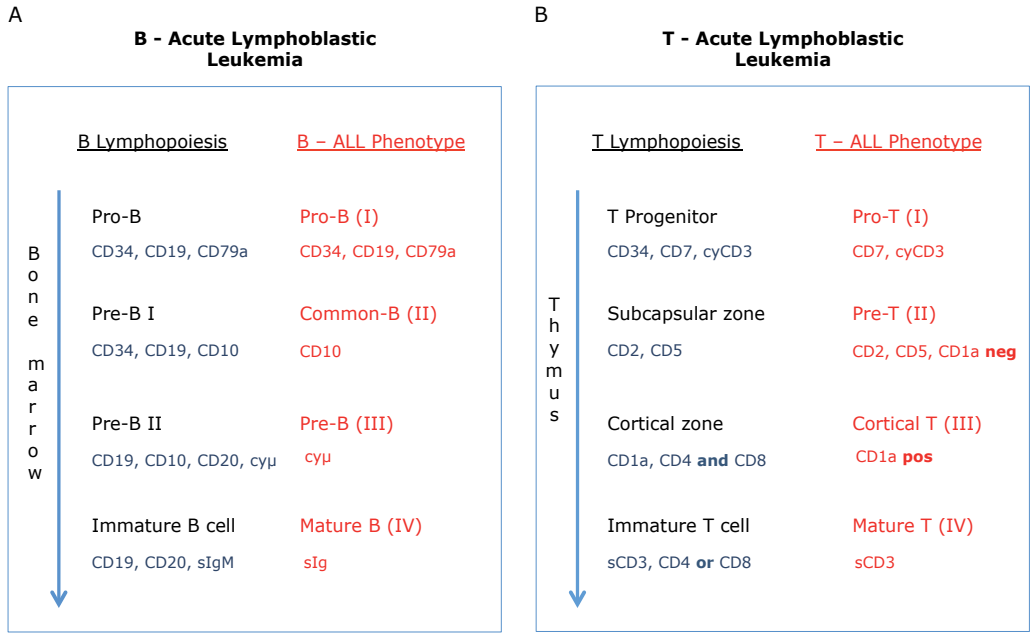

Figure 1. Subclassification of acute lymphoblastic leukemia in parallel to normal lymphopoiesis. Acute lymphoblastic leukemia of B lineage (panel A) and of lineage T (panel B) is classified according to phenotypic profile of blasts and its similarity to the stages of physiological lymphopoiesis.

http://dx.doi.org/10.5772/62332

2.3. Immunotherapy of AL

The application of immunotherapy is an emerging treatment approach in the field of AL. The basic concept is the killing of leukemic cells by direct attack to molecules on the cell surface. B-lineage antigens, CD19 and CD22, are effectively targeted by rituximab and inotuzumab, respectively, in B-ALL. Gemtuzumab ozogamicin is directed to pan-myeloid antigen CD33 and it is used in AML. More recently, immunological therapies based on the activation of T lymphocytes directly against blasts have been developed in B-ALL. This approach relies on bispecific T-cell engager antibodies, such as blinatumomab [12], or on autologous T lymphocytes engineered with chimeric activating receptors (CAR) [13] and represents one of the most promising strategies in the therapy of this disease. It is obvious that the application of immunotherapy relies on revealing the expression of the target antigens on the membrane of pathologic cells and thus on proper immunophenotyping.

3. Correlation phenotype–genotype

Karyotype and molecular genetics still represent the cornerstone of prognostic stratification of patients affected by AL. This information commonly drives the application of treatment. In AL bearing recurrent cytogenetic abnormalities, leukemic cells often display shared antigenic patterns usually able to predict the underlying genotype. Generally, this association is strong when few and relevant genetic events are responsible for leukemogenesis [i.e., CBF-AML, t(15;17), Philadelphia chromosome], whereas it is weaker with higher genetic heterogeneity (i.e., normal/intermediate karyotype with NPM1, FLT3, CEBPA, DNMT3A, IDH1-2 gene mutations). The definition of such "predictive" profiles is based on entire phenotypic patterns of blasts rather than on single antigen expression [14].

t(8;21): AML with t(8;21) is typically featured by maturation asynchrony, that is, high expression of CD34 together with mature antigens as CD15 and myeloperoxidase. Most cases display a cross-lineage co-expression of "dim" CD19. TdT and CD56 are common aberrancies on blasts. Maturing neutrophil compartment often shows phenotypic abnormalities (lack of CD10, expression of CD56) as well, due to its belonging to leukemic clone.

inv(16): often associated with eosinophilia, blasts of this AML subset show co-expression of immature antigens concomitantly to markers of granulocyte (CD15, CD65) or monocyte differentiation (CD14, CD4). In approximately half of cases, a cross-lineage expression of CD2 is observed.

NPM1: AML with mutations in the NPM1 gene usually shows monocytic differentiation. When detectable, myeloid blasts are often featured by negativity or dim expression for CD34 [15]. Typically, monocytic cells display immature phenotypic profile.

t(15;17): acute promyelocytic leukemia has two main characteristics: life-threatening coagulopathy and sensitivity to a differentiating treatment consisting of all-trans retinoic acid. Both of them prompt the urgency of a correct suspect and consequent diagnosis. In this light, the interpretation of the phenotypic profile of blasts is crucial. Leukemic promyelocytes typical-

ly have the phenotype of their normal counterpart (i.e., high side scatter signal with intense expression of CD33 and CD64, heterogeneous expression of CD13, negativity for HLA-DR) but with dim/negative CD15 [16]. Cross-lineage expression of CD56 can occur, with debatable prognostic meaning. A population of basophils with extremely high side scatter signal (SSC) can also be revealed.

t(9;22): this chromosomal aberration causes a chimeric fusion gene called BCR/ABL, a crucial event in leukemogenesis. Within ALs, the majority of cases bearing this translocation are B-precursor ALL and, frequently, are featured by CD10 expression. Moreover, most cases display several aberrant features. Among them, the expression of myeloid antigens (CD13 and/or CD33) is frequent as well as the expression of CD25 (interleukin-2 receptor alpha chain). Rather than a single aberration, the whole phenotype of blasts can reliably predict an underlying t(9;22), as reported by Tabernero et al. [17].

In the field of genotype prediction, a novel application of flow cytometry (FC) based upon an immunobead assay has been developed. This kind of test is able to detect the presence of chimeric proteins coded by relative fusion genes such as PML/RARalfa and BCR/ABL and, obviously, has the advantage to provide earlier results compared to PCR [18, 19].

Due to the capability to provide early results, immunophenotype is extremely useful to guide the analysis of karyotype and molecular genetics, aiding the application of the FISH method, for example. In this context, immunophenotyping can have a crucial role when karyotypic analysis results in lack of growth. The phenotypic profile can reliably channel genetic analyses toward most probable mutations, thus tuning an otherwise undefined prognostic assessment.

4. Prognostic value at baseline

As described above, immunophenotyping has mainly a diagnostic role in AL field. At any rate, there are some specific, less common subsets where FC assumes a significant prognostic weight, upon which clinicians can apply a proportional treatment strategy. These subsets are as follows:

4.1. Mixed Phenotype (MP) AL

The concomitance of expression of antigens belonging to different lineages has demonstrated to correlate with dismal prognosis. Consistently, the WHO classification considers these cases as a separate entity. The diagnostic criteria in the WHO 2001 classification adopted those previously defined by EGIL (see Table 1): a score >2 points for two or more lineages defined biphenotypic AL [5]. The WHO 2008 classification has established new criteria for the diagnosis of this subset, also renamed as MP-AL. Highly lineage-specific antigens are required for T- (cyCD3) and myeloid (myeloperoxidase and/or evident monocytic differentiation) lineage attribution. For B-lineage, one or three B-lineage markers have to be expressed depending upon intense or weak expression for CD19 [6]. MP-AL is usually associated with unfavorable karyotype, MLL/11q23 rearrangements, or BCR/ABL gene fusion. Patients

http://dx.doi.org/10.5772/62332

affected by MP-AL are characterized by unfavorable prognosis and should be considered for allogeneic HSCT once in CR [20].

4.2. Cortical T (EGIL T-III) acute lymphoblastic leukemia

This subset is defined by the expression of CD1a (see Figure 1). In a large multicenter prospective trial by UKALL and ECOG, a lower relapse risk and a longer overall survival were observed for this category of patients [21]. This immunological feature is often used for prognostic stratification of T-ALL.

4.3. Early T (ETP) ALL

A specific immature T phenotype, featured by absence of CD1a and CD8, weak CD5, and expression of one or more myeloid or stem cell-related antigens, has been associated with low response rate to chemotherapy and dismal prognosis [22]. However, the prognostic analyses within more modern clinical trials have shown survival similar to non-ETP ALL and the prognostic meaning of this subgroup is still under debate [23].

5. Advanced phenotypic analysis: assessment of multilineage dysplasia

Several papers have addressed the role of multilineage dysplasia (MLD) in AML leading to conflicting results, possibly because of technical and biological reasons [24, 25]. Technical reasons deal with morphological assessment of residual hematopoiesis at AML diagnosis, that is the standard criteria for defining MLD. Morphology is operator dependent; its specific application is even more complicated in this setting because residual nonblast cells are very few at diagnosis. Biologically, the MLD-related unfavorable prognosis would rely on clonal involvement at stem cell level or on pre-existing clonal hematopoiesis, conferring bad prognosis to AML. However, MLD might merely result from pathologic differentiation/maturation of the leukemic clone. We thus estimated MLD by FC, which is emerging as a useful method to study dysplasia, mainly by investigating the expression of key antigens throughout myeloid maturation. Our rationale was that an FC-based evaluation of dysplasia could get further insight into MLD actual significance. The application of FC to study BM maturing cell compartments in AML can provide many advantages compared to morphology: i) the amount of studied cells is much larger; ii) phenotypic parameters can be quantified and referred to control groups and, as such, reliably standardized; iii) phenotypic scores can be calculated, thus estimating accurately the extent of dysplasia; iv) there exists a capability to reveal dysplasia even in the absence of atypical morphology in MDS, as shown in a recent report [26]. Technically, the appraisal of MLD was based on a group of control BMs used to set normal phenotypic profile of maturing (i.e., neutrophil and erythroid) compartments; phenotypic abnormalities in AML were thus highlighted by reference to controls and the degree of dysplasia was appraised by a score proportional to deviation from normal phenotypic profile.

We focused our analysis on NPM1-mutated AML, for which a major controversy in the WHO classification exists. In fact, it is still under debate how to classify cases presenting with MLD

and a concomitant NPM1 mutation. This issue has relevant implications since NPM1-mutated status correlates with a relatively good prognosis (especially when FLT3-wt) [27].

Our study provided evidence that MLD, as assessed by immunophenotype, has no impact on clinical characteristics and outcome in NPM1+ AML. By investigating NPM1 status on separated cell compartments, we have established a correlation between MLD and belonging to AML clone [28] (Figure 2). Together with previous reports [29, 30], our findings further support MLD to be part of the spectrum of NPM1+ AML, without any relevant influence on major disease features and outcome. As such, these data strongly suggest the classification and the prognostic stratification of this category of patients should not be based upon MLD.

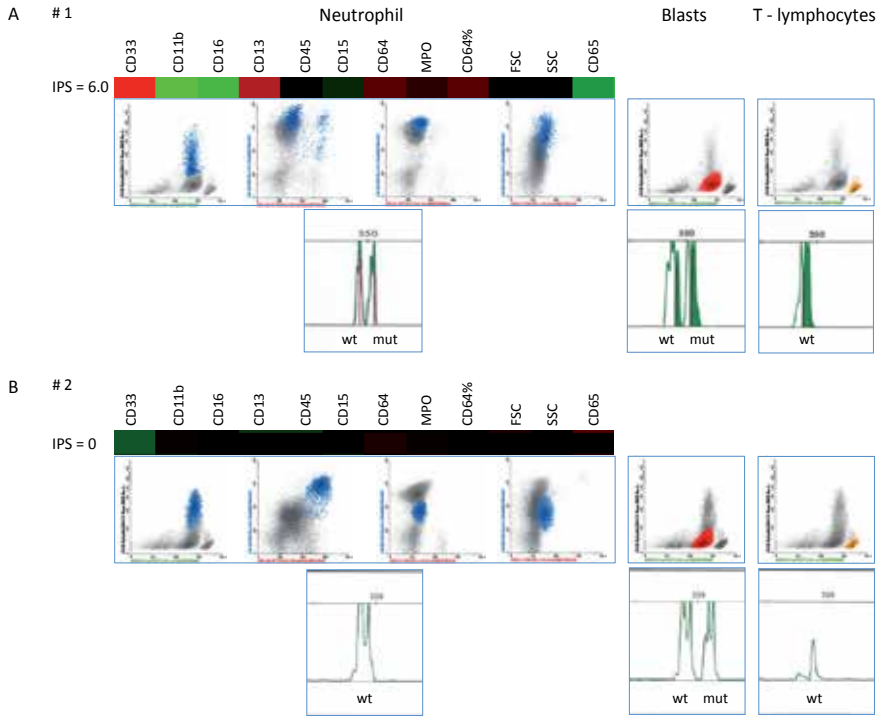

Figure 2. NPM1 mutational analysis on sorted cell fractions. Cell compartments are shown at the top; as concerns neutrophil compartment (left), the results of clustering analysis are depicted, together with phenotypic parameters and compartment's phenotypic score (IPS), appraising the extent of dysplasia. In the corresponding plots, the cell population is highlighted by color: blue for neutrophil cells, red for blasts, orange for T lymphocytes. The relative data from NPM1 mutational analysis are reported below. (A) Patient #1: neutrophil compartment showed several phenotypic abnormalities (as represented by clustering analysis and IPS = 6.0) and harbored NPM1 mutation; sorted blasts and T lymphocytes were NPM1-mutated and wild-type, respectively. (B) Patient #2: neutrophil compartment showed a preserved phenotypic profile (IPS = 0) and a NPM1 wild-type status. Sorted blasts and T lymphocytes were NPM1-mutated and wild-type, respectively. Clustering analysis was performed by R software. Dot plots were created by Infinicyt software. NPM1 mutational analysis: in order to discriminate NPM1 PCR products, we used 5'- end HEX dye-labeled reverse primer (M-Medical). The amplified products were separated with a capillary electrophoresis-based system using ABI PRISM 310 genetic analyzer (Applied Biosystems). The labeled fragment size corresponding to NPM1 wild-type gene was 347 bp. All NPM1-mutated samples were heterozygous, showing a double peak at positions 347 (wt) and 351 (mut).

http://dx.doi.org/10.5772/62332

6. Chemosensitivity assessment: minimal residual disease and peripheral blast clearance

Identification of AL patients who would have high likelihood to respond to standard induction therapy and those with low probability to do well and those who are candidates for more aggressive treatment is of major clinical importance. Most clinical and biological prognostic factors are based on characteristics of the patient and the disease at diagnosis and are surrogate for disease's chemosensitivity [31, 32]. In AML, the European Leukemia Net (ELN) stratification system is one of the most adopted systems and is based on cytogenetic/molecular abnormalities [31]. In fact, it allows to define patients' subgroups featured by high likelihood to achieve CR and long survival (ELN-favorable) and at the opposite a category with scarce response to chemotherapy and dismal prognosis (ELN-adverse). However, in the absence of genetic determinants, the ELN system merges patients with heterogeneous diseases (intermediate-1 and 2), where its clinical utility has major concerns. The same issue regards the field of ALL. The actual BM response to chemotherapy allows to refine the pretreatment risk stratification as it expresses the actual chemosensitivity resulting from killing leukemic cells.

6.1. Minimal Residual Disease (MRD)

Within responding patients, the detection of MRD beyond morphologic definition of CR is emerging as an accurate tool to refine risk category assignment, as initially established upon cytogenetic/genetic findings. FC allows to study MRD in the vast majority of patients (about 85% in AML, 90–95% in ALL), which is an advantage compared to molecular techniques.

The core concept of MRD by FC is the detection of one or more leukemia-associated aberrant immunophenotypes (LAIP), as phenotypic profiles that are absent or very rare on normal cells [33–35]. The sensitivity of MRD by FC ranges between 10^{-3} and 10^{-4}. MRD is usually estimated as the percentage of LAIP+ cells on global BM cells at certain time points. An alternative approach exploits logarithmic decrease of LAIP+ cells from diagnosis to BM assessment [36]. Conventionally, MRD is evaluated upon full recovery of PB counts after one and/or two chemotherapy cycles [33, 37]. An earlier BM morphologic and FC evaluation (7 days after completing induction) has been shown to correlate with CR achievement and survival [36]. Also at later time points in the treatment plan, for instance, before allogeneic HSCT, MRD confirms its prognostic weight [38].

In ALL, and especially in childhood, MRD by immunophenotype has been embedded within main clinical trials and is used to drive treatment strategy [39]. In AML, in spite of a clear prognostic meaning, MRD by FC has not found a defined place in clinical practice yet. The only published trial basing a clinical decision on MRD regarded the field of childhood AML [40]. Main reasons of this discrepancy between ALL and AML reside probably in a higher phenotypic heterogeneity of both normal and leukemic myeloid hematopoiesis compared to lymphopoiesis and ALL. Strictly linked to this subject, a substantial lack of standardization in method and data interpretation is still a major concern of FC in MRD setting, compared to molecular techniques.

6.2. Peripheral Blast Clearance (PBC)

Early response to treatment, and specifically to steroids, has been established as an important prognostic factor in ALL [41]. In modern therapy, this parameter is appraised by clinicians, but it is not generally considered *per se* as a driver of treatment modalities.

In AML, risk-oriented treatment exclusively concerns post-induction phase. As said before, the disease's characterization at diagnosis and the quality of response to therapy (estimated by MRD) are integrated to define a prognostic assessment that guides the consolidation phase. In fact, induction is delivered irrespectively of patient or AML features.

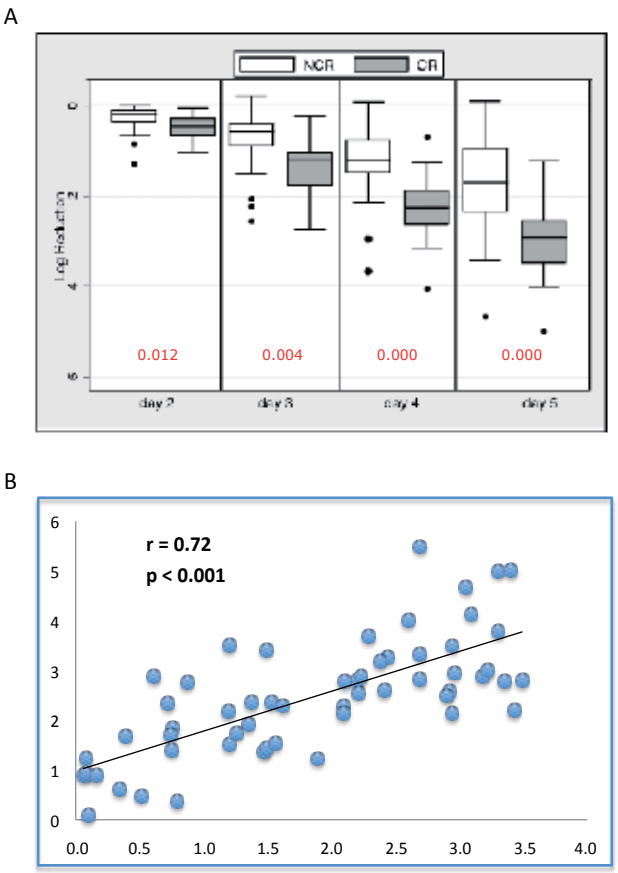

Figure 3. Relationship between peripheral blast clearance (PBC) during induction therapy and bone marrow response in AML. (A) PBC promptly resolves responders (CR) from nonresponder (NCR) patients. Log reduction is the ratio between baseline and daily absolute LAIP+ blast count converted to a logarithmic scale. The ranges of log reduction show minimal overlap between the two groups. Horizontal bars are medians, boxes are 25th percentiles, and whiskers are 75th percentiles. Dots are outliers. (B) Bone marrow blast clearance correlates with PBC. In this graph, the log decrease in bone marrow LAIP+ blasts (assessed by flow cytometry on day 14) is in linear relationship to log reduction of LAIP-positive blasts from peripheral blood at day 5 of induction treatment. In fact, a linear statistically significant correlation is found as from day 2.

To assess AML chemosensitivity in a relevant clinical time, we have evaluated the kinetics of leukemic cell reduction from PB during induction. To do this, we have quantified LAIP+ cell population on PB immediately before and daily during induction course. The ratio between absolute LAIP+ baseline and daily values converted to a logarithmic scale was defined as peripheral blast clearance (PBC).

We carried out a daily quantitative assessment of peripheral blasts during conventional "3+7" course in a cohort of 61 patients. We documented that PBC strictly correlated with the decrease of the overall leukemic burden in the patient. Specifically, we observed that PBC discriminated between responsive and refractory patients since day 2 of therapy [42, 43] (Figure 3). Being a very early and powerful predictor of CR achievement and outcome, PBC could allow to modulate the intensity of treatment since induction phase, providing an *in vivo* chemosensitivity assay in AML.

Author details

Francesco Mannelli*

Address all correspondence to: francesco.mannelli@unifi.it

University of Florence, Florence, Italy

References

[1] Cheson BD, Bennett JM, Kopecky KJ, Büchner T, Willman CL, Estey EH, et al. Revised recommendations of the International Working Group for diagnosis, standardization of response criteria, treatment outcomes, and reporting standards for therapeutic trials in acute myeloid leukemia. J Clin Oncol. 2003; 21(24): 4642–4649.

[2] Vardiman JW, Harris NL, Brunning RD. The World Health Organization (WHO) classification of the myeloid neoplasms. Blood. 2002; 100(7): 2292–2302.

[3] Gökbuget N, Hoelzer D. Recent approaches in acute lymphoblastic leukemia in adults. Rev Clin Exp Hematology. 2002; 6(2): 114–141; 200–202.

[4] Lacombe F, Durrieu F, Briais A, Dumain P, Belloc F, Bascans E, et al. Flow cytometry CD45 gating for immunophenotyping of acute myeloid leukemia. Leukemia. 1997; 11(11): 1878–1886.

[5] Bene MC, Castoldi G, Knapp W, Ludwig WD, Matutes E, Orfao A, et al. Proposals for the immunological classification of acute leukemias. European Group for the Immunological Characterization of Leukemias (EGIL). Leukemia. 1995; 9(10): 1783–1786.

[6] Borowitz M, Bene MC, Harris NL, Porwit A, Matutes E. Acute leukemias of ambiguous lineage. In: Swerdlow SH, Campo E, Harris NL, et al, eds. World Health Organization Classification of Tumours: Pathology and Genetics of Tumours of Haematopoietic and Lymphoid Tissues. Lyon, France: IARC Press; 2008: 150–155.

[7] van Dongen, Orfao, Consortium E. EuroFlow: Resetting leukemia and lymphoma immunophenotyping. Basis for companion diagnostics and personalized medicine. Leukemia. 2012; 26(9): 1899–1907.

[8] Badar T, Shetty A, Bueso-Ramos C, Cortes J, Konopleva M, Borthakur G, et al. Bone marrow necrosis in acute leukemia: Clinical characteristic and outcome. Am J Hematol. 2015; 90(9): 769–773.

[9] Chaperot L, Bendriss N, Manches O, Gressin R, Maynadie M, Trimoreau F, et al. Identification of a leukemic counterpart of the plasmacytoid dendritic cells. Blood. 2001; 97(10): 3210–3217.

[10] Martín-Martín L, Almeida J, Hernández-Campo PM, Sánchez ML, Lécrevisse Q, Orfao A. Immunophenotypical, morphologic, and functional characterization of maturation-associated plasmacytoid dendritic cell subsets in normal adult human bone marrow. Transfusion. 2009; 49(8): 1692–1708.

[11] Pagano L, Valentini CG, Pulsoni A, Fisogni S, Carluccio P, Mannelli F, et al. Blastic plasmacytoid dendritic cell neoplasm with leukemic presentation: An Italian multicenter study. Haematologica. 2013; 98(2): 239–246.

[12] Topp MS, Kufer P, Gökbuget N, Goebeler M, Klinger M, Neumann S, et al. Targeted therapy with the T-cell-engaging antibody blinatumomab of chemotherapy-refractory minimal residual disease in B-lineage acute lymphoblastic leukemia patients results in high response rate and prolonged leukemia-free survival. J Clin Oncol. 2011; 29(18): 2493–2498.

[13] Miller BC, Maus MV. CD19-targeted CAR T cells: A new tool in the fight against B cell malignancies. Oncol Res Treat. 2015; 38(12): 683–690.

[14] Hrusák O, Porwit-MacDonald A. Antigen expression patterns reflecting genotype of acute leukemias. Leukemia. 2002; 16(7): 1233–1258.

[15] Falini B, Mecucci C, Tiacci E, Alcalay M, Rosati R, Pasqualucci L, et al. Cytoplasmic nucleophosmin in acute myelogenous leukemia with a normal karyotype. N Engl J Med. 2005; 352(3): 254–266.

[16] Orfao A, Chillón MC, Bortoluci AM, López-Berges MC, García-Sanz R, Gonzalez M, et al. The flow cytometric pattern of CD34, CD15 and CD13 expression in acute myeloblastic leukemia is highly characteristic of the presence of PML-RAR alpha gene rearrangements. Haematologica. 1999; 84(5): 405–412.

[17] Tabernero MD, Bortoluci AM, Alaejos I, López-Berges MC, Rasillo A, García-Sanz R, et al. Adult precursor B-ALL with BCR/ABL gene rearrangements displays a unique

immunophenotype based on the pattern of CD10, CD34, CD13 and CD38 expression. Leukemia. 2001; 15(3): 406–414.

[18] Weerkamp F, Dekking E, Ng YY, van der Velden VH, Wai H, Böttcher S, et al. Flow cytometric immunobead assay for the detection of BCR-ABL fusion proteins in leukemia patients. Leukemia. 2009; 23(6): 1106–1117.

[19] Dekking EH, van der Velden VH, Varro R, Wai H, Böttcher S, Kneba M, et al. Flow cytometric immunobead assay for fast and easy detection of PML-RARA fusion proteins for the diagnosis of acute promyelocytic leukemia. Leukemia. 2012; 26(9): 1976–1985.

[20] Matutes E, Pickl WF, Van't Veer M, Morilla R, Swansbury J, Strobl H, et al. Mixed-phenotype acute leukemia: Clinical and laboratory features and outcome in 100 patients defined according to the WHO 2008 classification. Blood. 2011; 117(11): 3163–3171.

[21] Marks DI, Paietta EM, Moorman AV, Richards SM, Buck G, DeWald G, et al. T-cell acute lymphoblastic leukemia in adults: Clinical features, immunophenotype, cytogenetics, and outcome from the large randomized prospective trial (UKALL XII/ECOG 2993). Blood. 2009; 114(25): 5136–5145.

[22] Coustan-Smith E, Mullighan CG, Onciu M, Behm FG, Raimondi SC, Pei D, et al. Early T-cell precursor leukaemia: A subtype of very high-risk acute lymphoblastic leukaemia. Lancet Oncol. 2009; 10(2): 147–156.

[23] Woods BL, Winter SS, Dunsmore KP, et al. T-lymphoblastic leukemia (T-ALL) shows excellent outcome, lack of significance of the early thymic precursor (ETP) immunophenotype, and validation of the prognostic value of end-induction minimal residual disease (MRD) in Children's Oncology Group (COG) Study AALL0434[abstract]. Blood. 2014; 124(21). Abstract 1.

[24] Miesner M, Haferlach C, Bacher U, Weiss T, Macijewski K, Kohlmann A, et al. Multilineage dysplasia (MLD) in acute myeloid leukemia (AML) correlates with MDS-related cytogenetic abnormalities and a prior history of MDS or MDS/MPN but has no independent prognostic relevance: A comparison of 408 cases classified as "AML not otherwise specified" (AML-NOS) or "AML with myelodysplasia-related changes" (AML-MRC). Blood. 2010; 116(15): 2742–2751.

[25] Wandt H, Schäkel U, Kroschinsky F, Prange-Krex G, Mohr B, Thiede C, et al. MLD according to the WHO classification in AML has no correlation with age and no independent prognostic relevance as analyzed in 1766 patients. Blood. 2008; 111(4): 1855–1861.

[26] Kern W, Haferlach C, Schnittger S, Alpermann T, Haferlach T. Serial assessment of suspected myelodysplastic syndromes: Significance of flow cytometric findings validated by cytomorphology, cytogenetics, and molecular genetics. Haematologica. 2013; 98(2): 201–207.

[27] Schlenk RF, Döhner K, Krauter J, Fröhling S, Corbacioglu A, Bullinger L, et al. Mutations and treatment outcome in cytogenetically normal acute myeloid leukemia. N Engl J Med. 2008; 358(18): 1909–1918.

[28] Mannelli F, Ponziani V, Bonetti M, Bencini S, Cutini I, Gianfaldoni G, et al. Multilineage dysplasia as assessed by immunophenotype has no impact on clinical-biological features and outcome of NPM1-mutated acute myeloid leukemia. Exp Hematol. 2015; 43(10): 869–879.

[29] Falini B, Macijewski K, Weiss T, Bacher U, Schnittger S, Kern W, et al. Multilineage dysplasia has no impact on biologic, clinicopathologic, and prognostic features of AML with mutated nucleophosmin (NPM1). Blood. 2010; 115(18): 3776–3786.

[30] Díaz-Beyá M, Rozman M, Pratcorona M, Torrebadell M, Camós M, Aguilar JL, et al. The prognostic value of multilineage dysplasia in de novo acute myeloid leukemia patients with intermediate-risk cytogenetics is dependent on NPM1 mutational status. Blood. 2010; 116(26): 6147–6148.

[31] Döhner H, Estey EH, Amadori S, Appelbaum FR, Büchner T, Burnett AK, et al. Diagnosis and management of acute myeloid leukemia in adults: Recommendations from an international expert panel, on behalf of the European LeukemiaNet. Blood. 2010; 115(3): 453–474.

[32] Moorman AV, Harrison CJ, Buck GA, Richards SM, Secker-Walker LM, Martineau M, et al. Karyotype is an independent prognostic factor in adult acute lymphoblastic leukemia (ALL): Analysis of cytogenetic data from patients treated on the Medical Research Council (MRC) UKALLXII/Eastern Cooperative Oncology Group (ECOG) 2993 trial. Blood. 2007; 109(8): 3189–3197.

[33] San Miguel JF, Martinez A, Macedo A, Vidriales MB, Lopez-Berges C, Gonzalez M, et al. Immunophenotyping investigation of minimal residual disease is a useful approach for predicting relapse in acute myeloid leukemia patients. Blood. 1997; 90(6): 2465–2470.

[34] Venditti A, Buccisano F, Poeta DG, Maurillo L. Level of minimal residual disease after consolidation therapy predicts outcome in acute myeloid leukemia. Blood. 2000; 96(12): 3948–3952.

[35] Coustan-Smith E, Ribeiro RC. Clinical significance of residual disease during treatment in childhood acute myeloid leukaemia. Br J Haematol. 2003; 123: 243–252.

[36] Kern W, Voskova D, Schoch C, Schnittger S, Hiddemann W, Haferlach T. Prognostic impact of early response to induction therapy as assessed by multiparameter flow cytometry in acute myeloid leukemia. Haematologica. 2004; 89(5): 528–540.

[37] Buccisano F, Maurillo L, Spagnoli A, Del Principe MI, Fraboni D, Panetta P, et al. Cytogenetic and molecular diagnostic characterization combined to post consolida-

tion minimal residual disease assessment by flow cytometry improves risk stratification in adult acute myeloid leukemia. Blood. 2010; 116(13): 2295–2303.

[38] Walter R, Gooley T, Wood B, Milano F, Fang M, Sorror M, et al. Impact of pretransplantation minimal residual disease, as detected by multiparametric flow cytometry, on outcome of myeloablative hematopoietic cell transplantation for acute myeloid leukemia. J Clin Oncol. 2011; 29(9): 1190–1197.

[39] Basso G, Veltroni M, Valsecchi MG, Dworzak MN, Ratei R, Silvestri D, et al. Risk of relapse of childhood acute lymphoblastic leukemia is predicted by flow cytometric measurement of residual disease on day 15 bone marrow. J Clin Oncol. 2009; 27(31): 5168–5174.

[40] Rubnitz JE, Inaba H, Dahl G, Ribeiro RC, Bowman WP, Taub J, et al. Minimal residual disease-directed therapy for childhood acute myeloid leukaemia: Results of the AML02 multicentre trial. Lancet Oncol. 2010; 11(6): 543–552.

[41] Hoelzer D, Thiel E, Löffler H, Büchner T, Ganser A, Heil G, et al. Prognostic factors in a multicenter study for treatment of acute lymphoblastic leukemia in adults. Blood. 1988; 71(1): 123–131.

[42] Gianfaldoni G, Mannelli F, Baccini M, Antonioli E, Leoni F, Bosi A. Clearance of leukaemic blasts from peripheral blood during standard induction treatment predicts the bone marrow response in acute myeloid leukaemia: A pilot study. Br J Haematol. 2006; 134(1): 54–57.

[43] Gianfaldoni G, Mannelli F, Bencini S, Leoni F, Baldini S, Bosi A. Peripheral blood blast clearance during induction therapy in acute myeloid leukemia. Blood. 2008; 111(3): 1746–1747.

Chapter 7

Detection of Anti-HLA Antibodies by Flow Cytometer

Tülay Kılıçaslan Ayna and Aslı Özkızılcık Koçyiğit

Additional information is available at the end of the chapter

http://dx.doi.org/10.5772/62553

Abstract

Lives of patients with solid organ failure depend physically, emotionally, and economically on others. Improvement in organ transplantation is one of the most important medical breakthroughs of the twenty-first century. Being healthy upon organ transplantation is the second chance to live the life. This is frequently observed in heart-, lung-, and liver-transplanted patients. For instance, upon kidney transplantation, dialysis dependence terminates and life quality of the patients increases. The major difficulty in organ transplantation is the low number of organ donation. Thus, the number of patients in the waiting list for the cadaveric transplantation increases day by day. Under these limited circumstances, required conditions should be further provided for the long survival rates of recipients with allogeneic graft without any problem. Human leukocyte antigen (HLA) tissue typing and anti-HLA antibodies produced before and after the transplantation adversely affect the graft survival and thus the survival of an individual. Investigation of pretransplantation immune status of recipients is significant. Particularly, donor-specific anti-HLA antibodies determine early and long-term graft survival. Flow cytometer is one of the most important devices used in anti-HLA antibody detection and also for other clinical and scientific purposes. Compared to conventional methods, it supports transplantation clinics due to its high sensitivity and specificity. The use of flow cytometer dependent methods in transplantation field increases progressively.

Keywords: solid organ transplantation, HLA, flow cytometer, cross match, panel reactive antibody

1. Introduction

Transplantation can be defined as the transfer of cells, tissue, or organ from one body to another. Solid organ transplantation is the replacement of the ablated organ or a part of it from a donor to the recipient instead of his/her damaged or absent organ [1]. There are two important organ

resources in transplantation: related donors and deceased donors. Although there have been many studies aiming to increase the number of deceased donors in various countries, the number of patients in the waiting list for the transplantation increases every passing year due to low ratio of organ donation. Currently, there are 122,403 patients waiting for organ transplantation in the United States. Of these patients, 101,189 of them are waiting for kidney transplantation (as of 8 October 2015). The average waiting time for the first kidney transplantation is 3.6 years, and it depends on the health, compatibility, and availability of organs. Of 17,105 kidney transplants in the United States, it was reported that 11,570 of them were cadaver transplants and 5535 of them were related transplants in 2014. However, 3000 new recipients are currently included in the waiting list every month and 12 patients die each day while waiting for kidney transplantation [2]. It was reported that totally 70,000, 8500, 3850, 2200, 1600, and 70 patients were, respectively, waiting for kidney, liver, heart, lung, pancreas, and small bowel transplants in European Union countries such as Iceland, Norway, as well as Turkey, on 31 December 2013. It was also estimated that 6000 recipients died in 2013 while they were waiting to be transplanted in Iceland, Norway, and Turkey [3].

During eighteenth century, researchers tried to achieve organ transplantation in animals and humans. Despite failures, the first successful kidney transplantation was performed between monozygotic twins by Murray in 1954. Solid organ transplantation that is performed between genetically identical individuals, such as monozygotic twins, is called "syngeneic transplantation." In syngeneic transplants, graft would not undergo rejection. Consecutive syngeneic transplantation of more than 30 kidneys led to the consideration of patient treatment with end-stage kidney disease by transplantation. It was understood that tissue and organ transplantations can be performed between genetically non-identical individuals of the same species by the developments in immunosuppressive therapy. This type of transplantation is called allogeneic transplantation [4–6]. Currently, liver, heart, pancreas, lung, and intestine, as well as kidney, transplantations are commonly performed in this way. The most transplanted organ is kidney because there are double kidneys in an individual and one of them is sufficient for a healthy life. In recent years, increasing number of successful solid organ transplantations has been performed between genetically non-identical individuals [7].

Human leukocyte antigen (HLA) and ABO blood group compatibilities and detection of donor-specific anti-HLA antibodies (DSA) in recipients are important for the success of the organ transplantations as well as for the immunosuppressive therapy [8]. As it is well known, acceptance or rejection of a tissue or an organ is under the control of proteins encoded by HLA genes. The immunizations of recipients against HLAs due to pregnancy and blood transfusions are important. Also, previous transplantations are also important for the sake of the success of the organ transplantation. Hyper acute rejections can be observed in this kind of transplants [9, 10].

2. Human leukocyte antigen (HLA)

HLA genes reside on the short arm of sixth chromosome. It contains more than 200 genes. The region is in four centimorgan in length and is about 4 Mb in size [11]. HLA contains loci of

genes that encode proteins present on various cells. These proteins play critical roles in the graft rejection. Thus, they are also termed as "transplant antigens" [12].

In 1958, Dausset, Snell, and Rappaport found HLA antigens in human leukocytes for the first time. In the same year, van Rood et al. reported the production of antibodies against leukocytes in sera of multitransfused individuals and multiparous women [13]. These antigenic structures were defined as HLAs because they were first identified on leukocytes. It was observed that these antigens were present not only on leukocytes but also on tissue cells [11, 14, 15].

In the mid-1930s, Gorer and Snell determined that HLA antigens played an important role in the rejection of the allograft. HLA molecules are expressed co-dominantly in each individual and in three groups of gene regions (class I HLA, class II HLA, and class III HLA) were identified in major histocompatibility complex (MHC) (**Figure 1**) [16, 17].

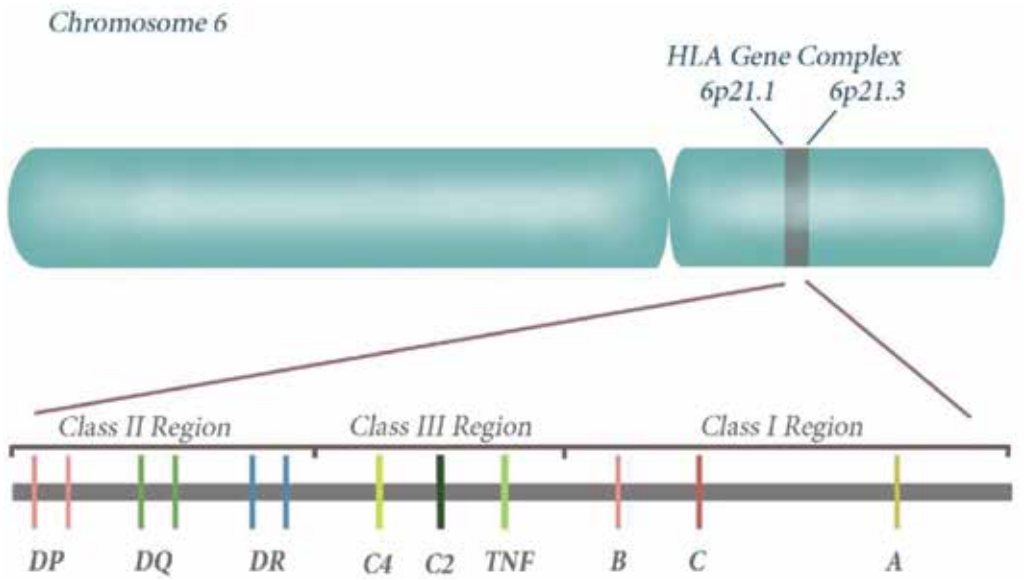

Figure 1. Gene map of HLA region on chromosome 6.

2.1. HLA class I molecules

HLA class I molecules are present in all nucleated cells in human. This region includes HLA-A, -B, -C, -E, -F, -G, -H, -J, and HLA-X loci. HLA-A, HLA-B, and HLA-C loci are polymorphic and functional classical class I loci. The rest of HLA loci are known as non-classical loci. These loci are pseudogenes and they do not encode proteins. HLA class I molecules contain two different polypeptide chains (α-chain and β_2-microglobulin) that are bound non-cova-

lently. The α-polypeptide chain is 44 kDa and consists of three loops that are 338 amino acids (aa), and they are bound to each other by disulfide bonds. This molecule is divided into three parts: extracellular hydrophilic region (1–281 residue), transmembrane hydrophobic region (282–306 residue), and intracellular hydrophilic region (307–338 residue). Extracellular parts of heavy chain (α_1 and α_2) are located on distal membrane and they constitute peptide binding region of the molecule. These regions are encoded by second and third exons and the variability is determined by them. The other part (α_3) on proximal membrane carries interaction region for CD8 molecule on T cells [16–18]. β_2-microglobulin, which is encoded by a gene on fifteenth chromosome, is a 12-kDa subunit. Non-polymorphic β_2-microglobulin is associated with HLA class I heavy chains without the membrane binding. It was shown that peptides that bound to HLA class I molecules were not longer than 8–9 amino acids, and they were exogenous peptides. β_2-microglobulin is required for heavy chain and antigenic peptide association. This molecule stabilizes heavy chain connection (**Figure 2A**) [17–19].

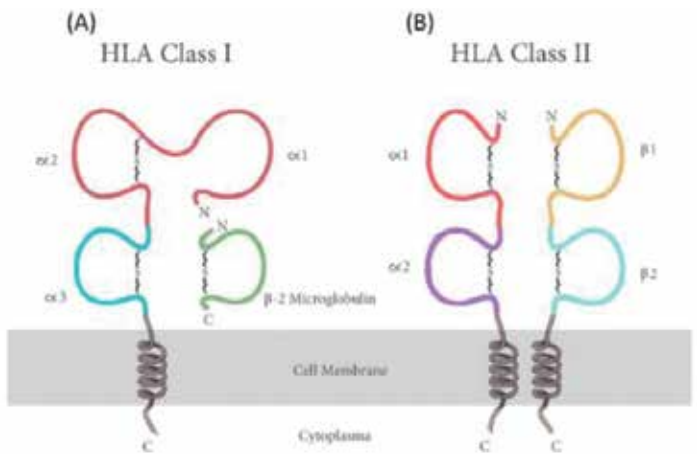

Figure 2. (A) The structure of class I HLA molecule. (B) The structure of class II HLA molecule.

2.2. HLA class II molecules

HLA class II molecules are located on B lymphocytes, macrophages, dendritic cells, endothelial cells, and active T cells. They consist of six different loci (HLA-DM, DN, DO, DP, DQ, and DR). DM, DN, and DO loci are pseudogenes and they do not encode proteins. They are type I integral membrane proteins with heterodimer structure. HLA class II molecules have two polypeptide chains (α, β), which bound non-covalently to each other. The α-chain is 24–32 kDa and β chain is 29–32 kDa. Second exons of α and β chains (α_1 and β_1) encode the variable peptide-binding region. This variable region is formed by two distinct chains. It can bind to peptides that are more than 11 amino acids in length in order to present them to $CD4^+$ T_H cells (**Figure 2B**) [17–19].

Foreign HLA molecules can be presented to immune cells by two ways (**Figure 3**):

http://dx.doi.org/10.5772/62553

A. Direct presentation: When unprocessed foreign HLA molecules and recipient HLA molecules are structurally similar, direct presentation occurs. Antigen presenting cells (APCs) of donors on the graft and migrant leukocytes are transported to lymphoid system of the patient. This activates T lymphocytes of the patient (**Figure 3A**)

B. Indirect presentation: Donor HLA molecules are processed, and peptides are presented by HLA molecules of the recipient (**Figure 3B**) [20, 21].

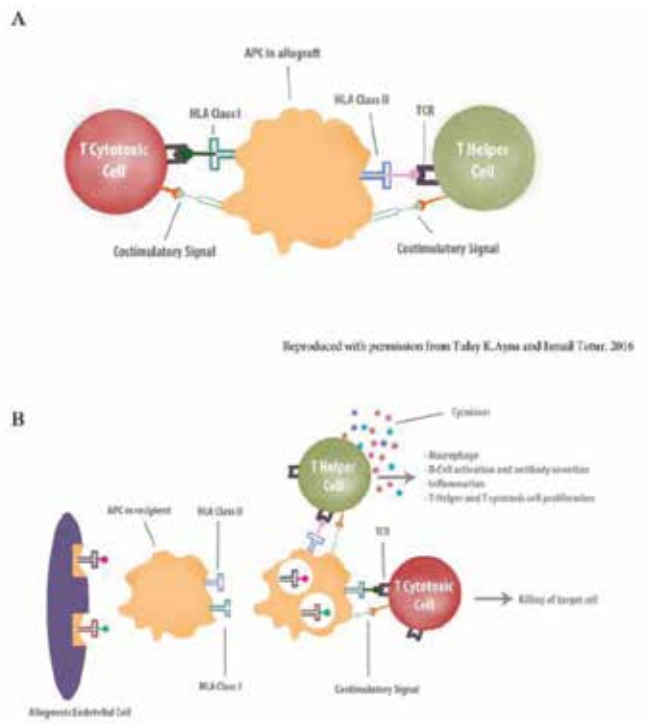

Figure 3. (A) Direct and (B) indirect recognition in allogeneic transplantation.

$CD4^+$ T cells usually develop by indirect presentation. Foreign antigens are processed and obtained by APCs through endosomal vesicular pathway, and HLA class II molecules present these antigens at the end of pathway. In addition, some antigens derived from graft cells are presented by HLA class I molecules and they are recognized indirectly by $CD8^+$ T cells. HLA similarity is not sufficient alone for the acceptance of the graft. When a graft is transplanted between genetically non-identical individuals, there is always a rejection risk; even if they have similar HLA antigens. The reason is the variability in minor histocompatibility loci. HLA antigens can be directly recognized by helper and cytotoxic T cells. This is called alloreactivity. However, minor histocompatibility antigens can be recognized only if they are presented by their own HLA molecules. Graft rejections due to major histocompatibility differences are stronger than rejections that are developed by minor histocompatibility differences. Graft rejection phenomena may be divided into phases: sensitization and effector [22, 23].

2.2.1. Sensitization phase

Foreign major and minor histocompatibility antigens that are expressed on graft cells can be recognized. Helper and cytotoxic T cells proliferate when they recognize these molecules. Even though a response against minor histocompatibility antigens is generally weak, combined response against numerous minor histocompatibility antigens may be stronger. Both HLA molecules and the peptide ligand in HLA cleft are recognized during the response. Peptides in the peptide-binding groove of HLA class I molecule are derived from proteins synthesized by foreign cells. On the other hand, peptides in the peptide-binding groove of HLA class II molecule are processed by foreign APCs via endocytic pathway [22, 23].

Under some conditions, fragments of foreign HLA class I molecule can be presented by class II HLA molecule. Costimulation signal by APC is required for the T-cell activation in recipients. Patient's APCs may migrate to the graft and take foreign antigens by endocytosis. They also present foreign peptides and minor/major histocompatibility molecules, which are processed by their HLA molecules [22, 23].

It was reported that donor APC populations (called as passenger leukocytes) migrated to lymph nodes. These cells are dendritic cells that express class II HLA molecules and they are common in majority of mammalian tissues except brain. Passenger leukocytes activate T cells in lymph nodes since they express foreign HLA antigens and thus they are recognized as foreign [22, 24].

Another type of APCs is endothelial cells. They are present in Langerhans islets and blood vessels. They can express HLA class I and II molecules [24].

Lymphocytes are transported to spleen and localized in lymph nodes to generate effector cells. When effector cells are generated, these cells are transferred back to the graft. The recognition of foreign antigens activates T-helper cells. Upon activation, T cells proliferate. It is considered that activated T cells have an important role in the initiation of various rejection mechanisms [22, 24].

2.2.2. Effector phase

The most common effector mechanisms are graft failure by delayed type hypersensitivity (DTH) and cytotoxicity developed by $CD8^+$ T cells (CTL). T cells and macrophages located in the graft lead to the graft rejection. Foreign class I HLA molecules are recognized by cytotoxic T cells of the patient, and this may lead to cell death by CTL. In some situations, when helper T cells bind to class II HLA molecule, they may function as cytotoxic T cells and lead to graft rejection [25].

Graft is rarely injured by antibody-dependent cell cytotoxicity (ADCC). These antibodies are immunoglobulin (IgG) isotypes. IgGs can be divided into four groups (IgG1, IgG2, IgG3, and IgG4) according to their hinge size, place, and the number of disulfide bonds between two heavy chains. There are 2, 4, 11, and 2 disulfide bonds in IgG1, IgG2, IgG3, and IgG4, respectively. Even though IgG2 and IgG4 have the same number of disulfide bonds, IgG heavy chain components are different. The relationship between IgG1 and IgG3 activates the comple-

ment system. This activation is initiated by C1 protein binding to CH2 or CH3 region on Fc area of IgG. This induces another complement protein cascade. As a result, pores are formed on the cell membrane, and thus cell lysis occurs [26, 27].

IgG2 and IgG4 are complement-independent antibodies, which play roles in ADCC. Some cells with cytotoxic activity express receptors specific for Fc region of the antibody on their membranes. Thus, these cells (natural killer cells, macrophage, monocyte, and eosinophil) can bind to target cell in case the antibody binds to the target cell. This leads to lysis of the target cell due to the release of lytic substances (such as tumor necrosis factor (TNF) and perforin) by cytotoxic cells from their lysosomes and granules [26, 27].

3. Anti-HLA antibodies

3.1. Panel reactive antibodies

Anti-HLA antibodies are generally defined as panel reactive antibody (PRA). They are one of the immunological factors affecting the graft survival. In recent studies, researchers have assessed the pretransplant incidence of anti-HLA antibodies and their clinical significance. Numerous studies reported that post-transplant anti-HLA antibody detection was associated with high rejection ratio [28–31]. Anti-HLA antibodies can directly recognize undamaged foreign HLA molecules on the cell surface. Thus, these antibodies play a critical role in solid organ transplantation and also in hematopoietic stem cell transplantation (HSCT). The humoral response directed against foreign HLA molecules can be because of encountering them during pregnancies, blood transfusions, and/or previous transplantations. Transplant candidates are tested for these anti-HLA antibodies by different techniques, such as PRA test. HLA laboratories perform PRA tests routinely (once in 3 months) in patients waiting for solid organ transplantation. Physicians can measure probability of the negative cross-matched donor [32, 33]. Earliest studies determined class I and II anti-HLA antibodies with complement-dependent lymphocytotoxic techniques (CDC). However, antibodies at low levels cannot be detected using this technique. In addition, only complement-dependent antibodies (IgG1, IgG3, and partly IgG2) can be detected by this method. Over the years, other analytical methods have become available, such as flow cytometer and solid-phase flow methods. It was observed that flow cytometer methods were more sensitive compared to CDC methods. All of IgG subtypes (IgG1, IgG2, IgG3, and IgG4) can also be detected by flow cytometry. The first flow cytometric PRA test experiment was reported by Cicciarelli et al. in 1992 [34, 35].

Complement-dependent cytotoxic crossmatch (CDCXM) and flow cytometric crossmatch (FCXM) are the two main crossmatch methods used nowadays, and they are used for the detection of donor-specific antibodies in most of transplant centers. It has been accepted that crossmatch (CM) and antibody screening methods should have similar sensitivity. Thus, a flow cytometric PRA would be suitable for the laboratories that use FCXM method for crossmatching [36–38].

There are two different flow cytometer PRA methods:

1. Cell-based method: It is used to estimate the percentage of PRA by incubating the patient serum with a panel of HLA-typed lymphocytes. In other words, a cell pool is generated from 10 healthy donors whose HLA class I and II tissue types are identified by serological or molecular methods. This cell pool should include HLA antigen variability in population. The cells from the pool are added onto negative, positive, and patient sera samples. If there is antibody specific to HLA antigens expressed on cells in the pool, they can be detected by fluorescence-labeled secondary antibody (FITC- or PE-labeled anti-human IgG). Anti-HLA class I antibodies can be detected by this cell-based method, because most of the cells in peripheral blood are T cells and they express HLA class I molecules. Lymphocytes are gated on FSC/SSC dot plot during the analysis by flow cytometer instrument. Anti-human IgG fluorescence density is detected depending on these cells [29]. The percentage of positive cells is identified by median channel shift considering the negative control serum [39]. This method is not very applicable because of the additional test requirements for antibody specificity determination. In addition, anti-HLA class I and II antibodies should be analyzed simultaneously (**Figure 4**) [32, 33, 40].
2. Based on bead method: These kits (PRA kits) were developed including beads coated with specific HLA antigens (HLA-A, HLA-B, Cw, DR, DQ, and DP) (**Figure 5A** and **Figure 5B**). Then, single antigen beads (SABs) were coated with only one HLA antigen (**Figure 5C**). This method allows identification of PRA specificity and definition of acceptable mismatches in hypersensitive patients. It is possible to differentiate anti-HLA antibodies from

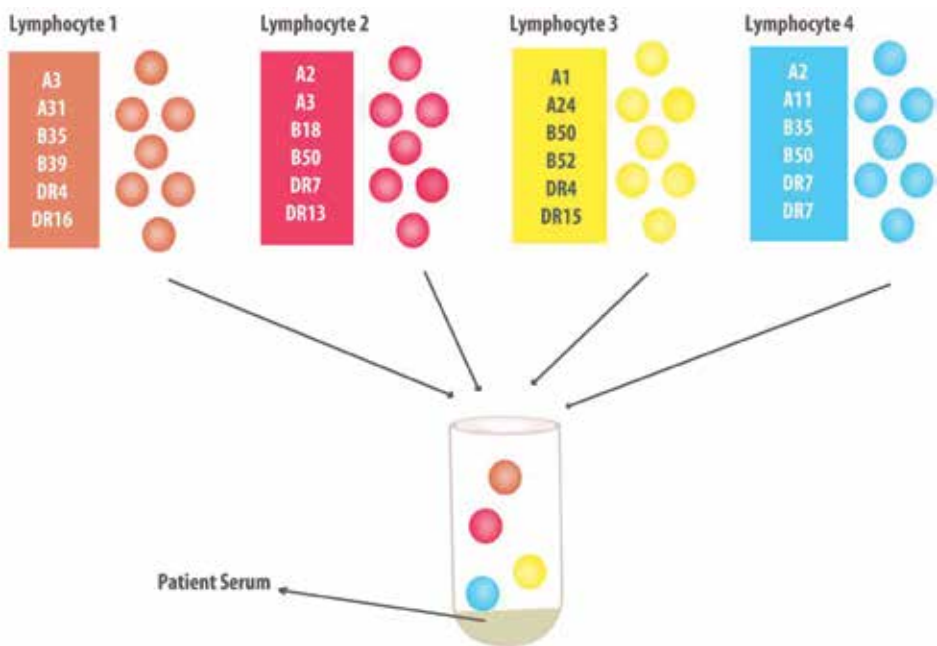

Figure 4. Cell-based PRA method by flow cytometer.

http://dx.doi.org/10.5772/62553

HLA antibodies because only HLA antigens are available on the commercially prepared beads.

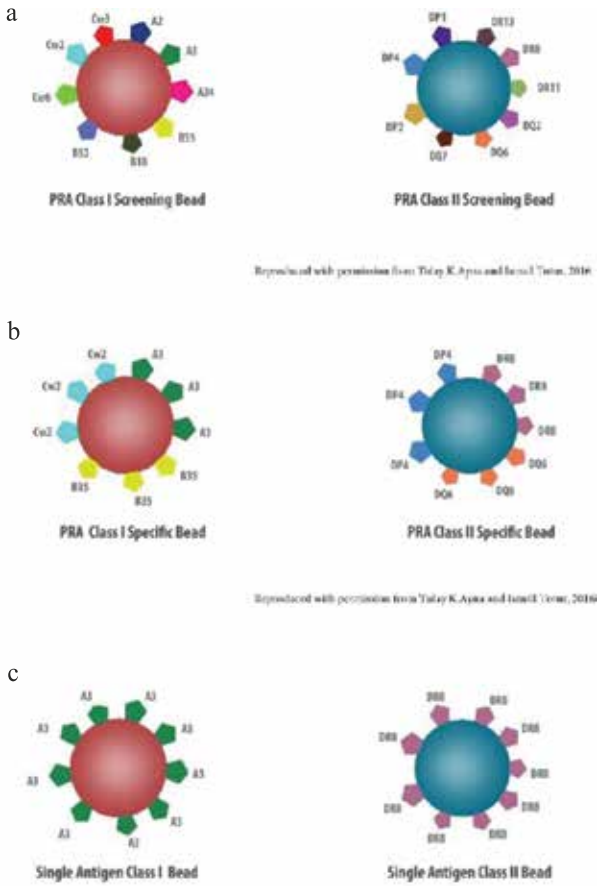

Figure 5. Bead-based PRA method by flow cytometer. (A) PRA screening beads. (B) PRA identification beads. (C) Single antigen beads.

Class I and II HLA antigens were isolated from B cell lines, which were transformed by an Epstein-Barr virus, and used for coating PRA beads. When the number of cells is increased in a culture medium, HLA molecules are released from these cells. Then, HLA antigens are kept on affinity columns. Class I and/or II HLA antigens are isolated from these columns. These antigens are accepted as "natural proteins" because of their expression on the cell surface. However, SABs are coated with only one HLA antigen. These HLA antigens are obtained by recombinant DNA technology. Thus, these HLA antigens can be defined as "recombinant proteins" instead of "natural HLA antigens".

PRA screening, identification, and SAB assays have similar test principle consisting of two main incubation steps. Primarily, patient and control sera are incubated with appropriate beads, while fluorescence-conjugated anti-human secondary antibodies are added during the

second incubation step. At the end of the assay, a fluorescence peak is generated, which indicates a positive result (binding of antibody to HLA antigens on the beads). We will now examine each of these tests [19].

3.1.1. PRA screening

PRA screening tests can be used for the first evaluation of anti-HLA antibodies and PRA percentage in recipient serum. Two pools of micro beads are coated with class I or II HLA antigens, each of them containing 30 different bead preparations, which represent all common antigens as well as rare HLA alleles (**Figure 5A**) [31, 33]. HLA class I antigen frequencies in PRA class I screening beads are shown in **Table 1**, and HLA class II antigen frequencies in PRA class II screening beads are shown in **Table 2**.

Specif icity	Number in panel	Speci ficity	Number in panel	Specif icity	Number in panel	Specif icity	Number in panel
A1	4	A80	2	B51	2	B75	1
A2	5	B7	2	B52	1	B78	1
A3	5	B8	2	B53	1	B81	2
A11	5	B13	2	B54	1	Bw4	18
A23	3	B18	2	B55	2	Bw6	26
A24	4	B27	2	B56	1	Cw1	6
A25	2	B35	2	B57	2	Cw2	6
A26	2	B37	2	B58	2	Cw4	4
A29	2	B38	1	B59	1	Cw5	1
A30	3	B39	1	B60	2	Cw6	7
A31	2	B41	2	B61	2	Cw7	9
A32	3	B42	1	B62	2	Cw8	5
A33	3	B44	2	B63	1	Cw9	2
A34	2	B45	1	B64	1	Cw10	4
A36	2	B46	1	B65	1	Cw12	1
A66	3	B47	2	B67	1	Cw14	2
A68	2	B48	2	B71	1	Cw15	3
A69	1	B49	1	B72	2	Cw16	2
A74	2	B50	1	B73	1	Cw17	3
PRA I screening Lot 017-One Lambda						Cw18	3

Table 1. Frequencies of HLA class I antigens in PRA class I screening beads.

Specificity	Number in panel	Specificity	Number in panel	Specificity	Number in panel	Specificity	Number in panel	Specificity	Number in panel
DRB1*01	4	DRB5*(51)	8	DQB1*02	8	DPB1*01	8	DPB1*20	0
DRB1*0103	2	DRB3*(52)	20	DQB1*04	8	DPB1*02	9	DPB1*21	0
DRB1*04	3	DRB4*(53)	9	DQB1*05	16	DPB1*03	4	DPB1*40	0
DRB1*07	5			DQB1*06	6	DPB1*04	15		
DRB1*08	4			DQB1*0301 (7)	8	DPB1*05	5		
DRB1*09	3			DQB1*0302 (8)	1	DPB1*08	0		
DRB1*10	3			DQB1* (9)	6	DPB1*09	0		
DRB1*11	3					DPB1*10	0		
DRB1*12	4					DPB1*11	1		
DRB1*13	5					DPB1*13	1		
DRB1*14	4					DPB1*14	3		
DRB1*15	4					DPB1*17	1		
DRB1*16	5					DPB1*18	2		
DRB1*0301 (17)	4					DPB1*19	1		
DRB1*0302 (18)	3					DPB1*105	1		

PRA II screening Lot 020-One Lambda.

Table 2. Frequencies of HLA class II antigen in PRA class II screening beads.

PRA screening test has two beneficial applications. First, the percentage of PRA may give an idea about the CM results. Second, analysis of PRA reactivity in detail can lead us to predict HLA antigens that are targets for antibodies. PRA screening test results give us the clue about which tests should be performed next. Targeted HLA antigens are determined in sera samples with low levels of PRA detected by PRA identification test, whereas these antigens are detected by SAB method in hypersensitized patients (PRA screening result >80%) [41, 42]. Therefore, unnecessary cost, time, and labor losses are prevented.

PRA screening test kit includes micro particle beads with diameter of approximately 2–4 μm. Concurrent analysis of HLA class I and II beads can be performed because class I beads are non-fluorescent, whereas class II beads are stained with a fluorochrome similar to phycoerythrin (PE) [43].

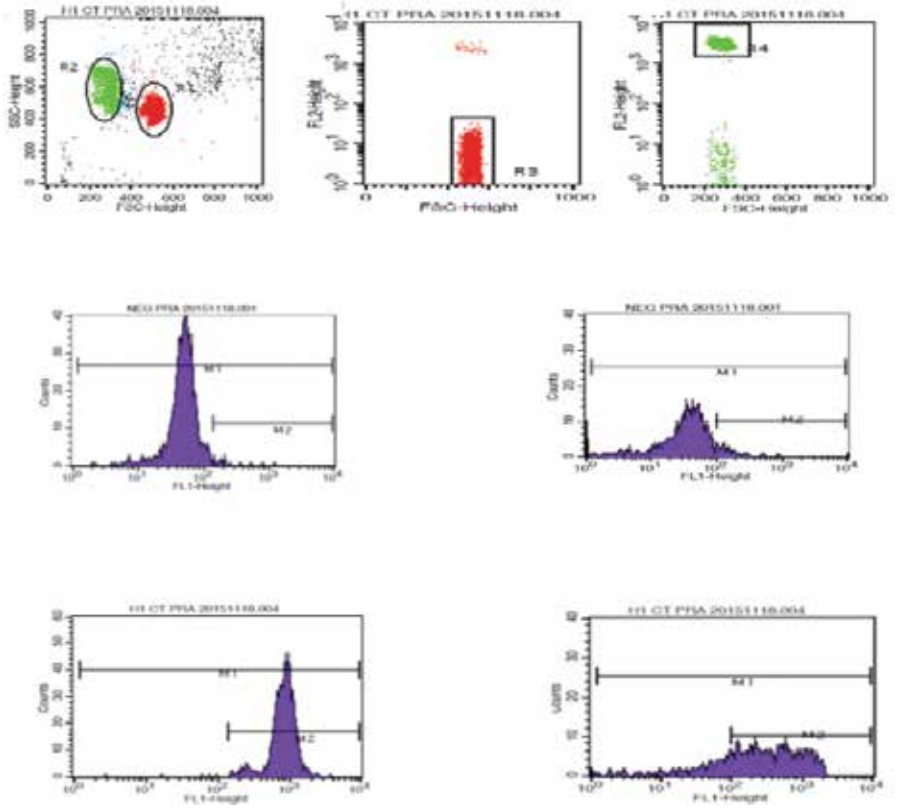

Figure 6. Class I and II PRA screening beads on SSC/FSC dot plot (A). Class I beads on PE/FSC dot plot (B). Class II beads on PE/FSC dot plot (C). Anti-human IgG-FITC staining with a negative control serum (D: class I, E: class II). Anti-human IgG-FITC staining with a patient serum (F: class I, G: class II). The results are the original results from our laboratory.

Class I and II beads are added into the control and patient tubes. Negative control serum does not have any anti-HLA antibody, and it is commercially available. It is important for the evaluation of positive results. Positive control sera are important for the evaluation of secondary antibody activity and observation of test performance. Sera are added onto the beads and incubated at room temperature. After incubation, the samples are washed and fluorescent-labeled anti-human IgG secondary antibody is added on the samples. After the samples are washed, beads are gated on a forward scatter (FSC)/side scatter (SSC) dot blot during the analysis by flow cytometer (**Figure 6**). Class I and II beads are gated on a PE/FSC dot blot. HLA class II beads stained with fluorochrome dye are indicated in **Figure 6C**, whereas the beads represent non-fluorescent HLA class I coated beads are shown in **Figure 6B**. The PRA ratio (%) can be estimated by determining positively reacting bead ratio (%). It is considered that if there is an antibody against a single antigen, fluorescence percentage will increase more than 3% because there are 30 different beads in the pool (100/30=3.3). Sera without antibody have single homogenous peak and its positivity ratio is under 3%. Sera antibodies have multiple peaks which represent heterogeneous population [41–43].

http://dx.doi.org/10.5772/62553

3.1.2. PRA specific assay

PRA identification test kit is composed of micro particle bead pools with diameter of 2–4 μm. Each of class I and II PRA test kit consists of a 32-bead panel coated with purified different class I and II antigens. Class I beads are coated with HLA-A, HLA-B, and HLA-C antigens, whereas class II beads are coated with HLA-DR, HLA-DQ, and HLA-DP antigens. This 32-

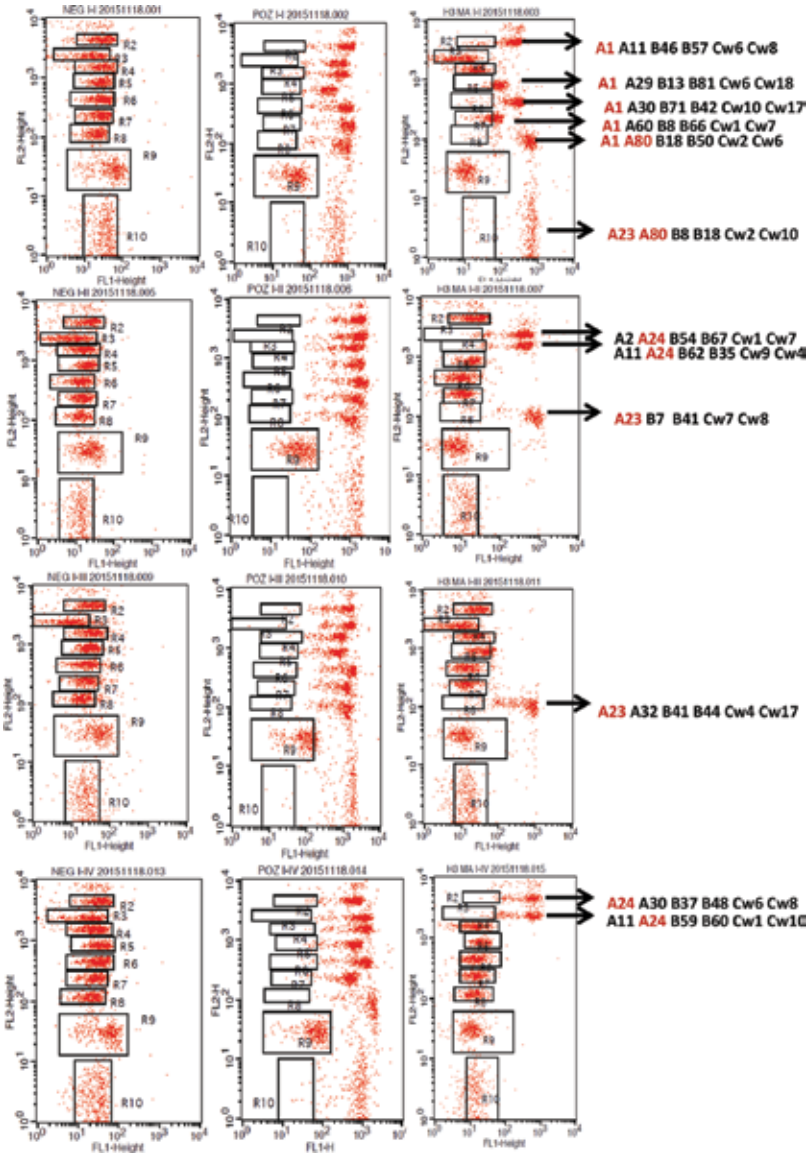

Figure 7. Evaluation of class I PRA identification tests (including negative, positive, and patient sera). PRA screening result is 31% positive. The results are the original results from our laboratory.

bead panel is divided into four HLA groups with eight antigens in each group. There is also a control bead group without HLA antigen in four groups. A serum sample should be tested with each group of beads in order to complete 32-bead panel analysis of HLA class I and II antibodies. During the procedure, each group of beads is incubated with the patient and control sera. Upon incubation, FITC-conjugated anti-human IgG secondary antibody is added [41–43]. During analysis, each group of beads is gated on FSC/SSC dot blot. A positive reaction has a FL1 channel shift when compared to negative control serum. Each of the eight beads has different FL2 channel shift. HLA specificity can be determined by analyzing the samples on FL1 vs. FL2 dot blot. The channel shifts over 50% are accepted as positive (Anti-HLA A1, A23, A24, A80 positive serum is shown in **Figure 7**). Results can be assessed by scoring the channel shifts on software program.

3.1.3. SAB assay

As mentioned before, PRA screening test gives an idea about the following analysis which is required for the fate of the transplantation. Targeted HLA antigens in sera samples with low level of PRA are determined by performing PRA identification test. However, anti-HLA antibody specificity cannot be detected in >80% positive sera samples by PRA identification test. These patients are termed as hypersensitive patients who have very low chance to find a CM negative donor. Testing the patient serum by using SABs is one of the best methods used for the detection of acceptable antigens (**Figure 5C**). When we compare studies in which virtual CM results are estimated by SAB technique and studies in which two important crossmatching methods are used before transplantations, the efficiency between virtual CM and CDCXM was 70–75%, whereas it was 85–95% between virtual CM and FCXM. Detection of clinical compatibility by the detection of anti-HLA antibodies and detection of donor-specific antibody compatibility increase the significance of SAB [44, 45]. Occasionally, there may be some incompatibilities between PRA screening and SAB results. For instance, if the copy number of the targeted antigen is low, a weak signal occurs even if there is a sufficient antibody titer in the serum and a positive fluorescence cannot be obtained. However, identical antibody level can be detected by SABs. If antibody level is limited in the serum, results may be negative due to the high antigen/epitope ratio. In this example, antibodies are dispersed over varied beads carrying the same epitope. In addition, new epitopes of HLA antigens may also occur as a result of the denaturation during SAB production. These new epitopes which are not present on cell surface *in vivo*, may lead to false positive results. Thus, HLA antibodies determined by SAB technique should be confirmed by cellular techniques [19, 33].

The test procedure of flow SAB test is similar to the procedure of PRA identification test. In this test kit, each of the bead group is coated with a single HLA allele. Class I SAB beads consist of 10 groups of beads. Each group is composed of eight different bead sets, and each bead has a single HLA-A, HLA-B, and HLA-C allele. The first four groups contain HLA-A, HLA-B, and HLA-C alleles, which are common in the population, whereas six groups have rare HLA alleles. Class II beads consist of five groups. The first four groups contain common HLA-DR, HLA-DQ, and HLA-DP alleles, whereas fifth group has rare alleles [43]. SAB results of a PRA class I screening (%100) positive patient is shown in **Figure 8**.

http://dx.doi.org/10.5772/62553

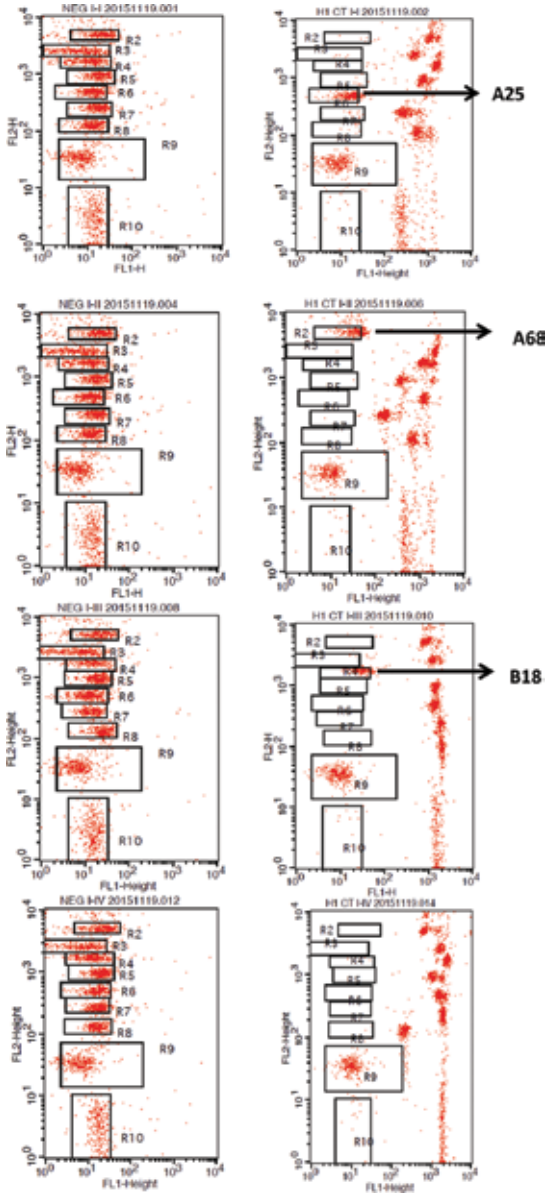

Figure 8. Class I SAB test result of the patient with 100% PRA class I screening. HLA type of patient is A*25, A*68, B*15, B*18, DRB1*11, and DRB1*16. Testing of negative control serum and patient serum with four bead groups. The results are the original results from our laboratory.

3.2. Donor specific antibody detection by flow cytometry

CM test is also performed in addition to tests mentioned above. It is a very important and common test in organ transplantation field, particularly in kidney, lung, heart, and intestine

transplantations. CM is a test system that shows the presence of DSA in the patient serum. The presence of anti-HLA antibodies in recipient is tested in PRA tests, whereas only the presence of DSA is tested in CM test. Detection of pretransplant antibodies provides an insight into the identification of transplants with high rejection risk [46, 47]. Lymphocytes are selected as target cells for the detection of DSAs because they express high levels of HLA antigens. If pre-existing anti-HLA antibodies in the recipient serum are specific to donor graft antigens, the graft is rejected very quickly [48]. These hyperacute rejection reactions can occur within the first 24 hours after transplantation. Acute rejection reactions generally begin in the first few weeks of transplantation, whereas chronic rejection reactions occur months to years after transplantation; as well as pre-existing DSAs, de novo DSAs produced after transplantation, are important for the graft survival. Thus, CM tests can be performed after transplantation in order to follow-up the immunological status of recipients [49, 50].

CDCXM test is the gold standard technique, which is frequently used for the detection of these antibodies. The significance of this test was shown in 1960s. This test is based on the detection of donor-specific anti-HLA antibodies in the patient serum. In 1980s, the ratio of early graft failure risk was 35–50% upon cadaveric kidney transplants. Since 1990, the risk has been decreased progressively. Introduction of more sensitive CM techniques, such as anti-human globulin (AHG) and FCXM plays an important role in this success. The very first experiments on FCXM method for transplants were initiated in 1983 by Goravay. Bray [19] had significant contributions to the development of multi-colored FCXM method [50–52].

Lymphocytes, which are used in FCXM test, can be isolated from peripheral blood, spleen, or lymph nodes. Cell viability should be >80%. For the test, totally $1–5\times10^5$ cells are sufficient. During the analysis in flow cytometer, it is sufficient to have 1000–2000 B cells and 9000–10,000 T cells. Monoclonal antibodies are used to determine the target cell population. To do this, anti-human-CD3 and anti-human-CD19/CD20 monoclonal antibodies are used for T and B cells, respectively. Indirect immunofluorescence is used for the determination of anti-HLA antibodies. Primarily, unlabeled antibody binds to the cells. Then, a second labeled antibody (anti-human IgG) is used for the analysis of unlabeled antibody-cell complexes. CD3-PE, CD19-PE/CD20-PE, and IgG-FITC are usually used for two colored analyses performed by flow cytometer. If three colored analysis is used, CD3-PerCP, CD19-PE, and IgG-FITC should be preferred (**Figure 9**). Secondary antibody should be specific to Fc region of the antibody, F(ab')2 fragment, and should not react with mouse and horse IgGs [19, 35].

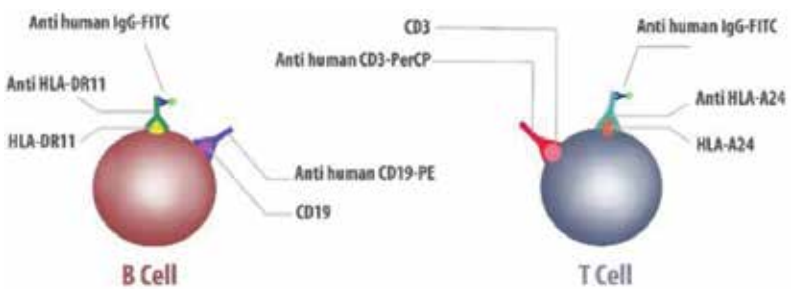

Figure 9. The principle of flow cytometric CM test.

http://dx.doi.org/10.5772/62553

Negative control should not have any alloimmunizations (pregnancy, blood transfusion, previous transplantations), should not be collected from an individual with autoimmune disease, and it should contain healthy sera with AB blood group.

In the FCXM protocol, the use of PBS control (wash buffer control), auto control, and diluted patient serum samples are important in addition to having negative and positive controls. Pretreatment of the serum may be useful before its use. Pretreatment includes high-speed or ultracentrifugation in order to remove large immune aggregates. Inactivation of complement proteins is also recommended [19, 26, 33].

A cut-off value should be determined for the evaluation of CM results. Negative serum and 20 different sera samples without anti-HLA antibodies, and at least 20 cell samples from healthy individuals should be tested. Once the cutoff value is determined, the FCXM test can then be performed. During FCXM protocol, donor cells and patient serum samples are incubated. Then, samples are again incubated with monoclonal and secondary antibodies. Results are analyzed and expressed as positive or negative according to the shift in the fluorescence intensities of samples compared to the results of the test serum (**Figure 10**). Laboratories can determine their own cutoff value by evaluating mean values, median values, and channel shift or fluorescence percentage values [19, 35].

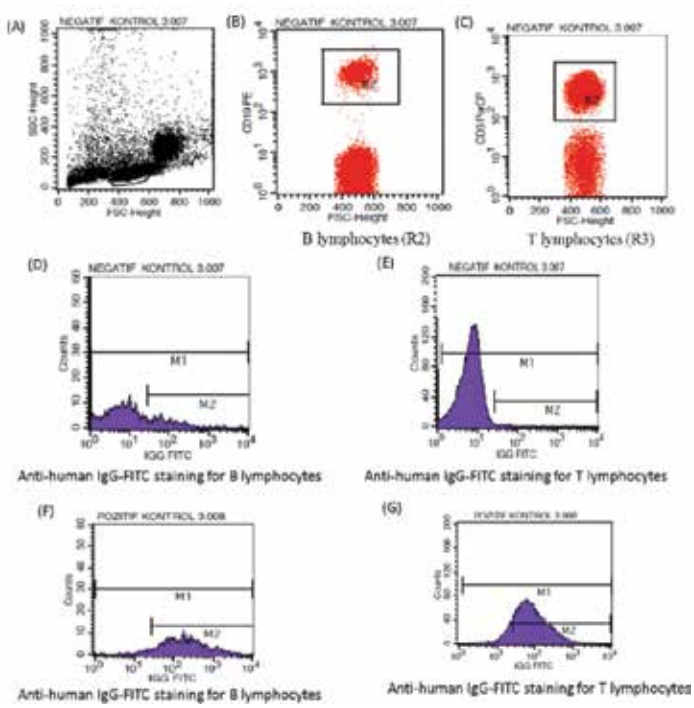

Figure 10. Flow cytometer CM test. Lymphocyte population gated on FSC/SSC dot plot (A). B and T lymphocytes on PE/FSC dot plot and PerCp-/FITC dot plot, respectively (B and C). Anti-human IgG-FITC staining with a negative control serum (D and E). Anti-human IgG-FITC staining with a positive control serum (F and G). The results are the original results from our laboratory.

3.2.1. T FCXM

FCXM is a more sensitive method compared to CDCXM test. Thus, DSAs that cannot be detected by CDCXM can be detected by FCXM technique. In this situation, the antibody concentration may be insufficient to generate hyperacute rejection. However, positive T FCXM and negative T CDCXM results indicate the high risk of graft failure. Positive FCXM may not affect the graft survival in non-sensitive patients who transplanted for the first time. Hypersensitive patients with previous transplantations and patients with positive FCXM would have shorter graft failure compared to patients with negative FCXM. Positive FCXM results obtained after previous transplantations can be due to the production of memory cells, their differentiation, and antibody production. If these antibodies recognize new HLA antigens during the new transplantation, they will lead to the rejection. Low levels of antibodies may indicate the memory cell activation [51, 53–55].

It has been also known that sensitive patients with positive FCXM are at high risk for the graft failure, even though they are going to be transplanted for the first time. This may occur because of IgG subgroups. If a patient has complement-independent antibodies, it cannot be detected by CDCXM and PRA tests [46, 54, 55].

3.2.2. B FCXM

Roles of class II anti-HLA antibodies in transplantation are contradictive. There are some reports indicating that when there is no class I HLA antibody and cytotoxicity, low levels of anti-HLA-DR and HLA-DQ antibodies are not harmful for the graft. However, high levels of antibodies may lead to hyperacute rejection.

Positive B FCXM is used for the class I and II antibody assessment. It is known that class I antigens are highly expressed on B cells compared to T cells. Thus, low level of class I antibody can be detected by B cell FCXM. However, false positive CM results can be obtained because B lymphocytes express immunoglobulin Fc receptors and anti-IgG antibodies can bind to these receptors non-specifically. In recent years, the proteolytic enzyme pronase has been used before FCXM test in order to remove Fc receptors from B lymphocytes [47, 52].

Although it is known that mostly DSAs lead to rejections, it has been reported that non-HLA antibodies can also be related to rejection. It was observed that antibodies produced against non-classical HLA molecules, such as MHC class I polypeptide-related sequence A (MICA) and B (MICB), also led to acute kidney rejection. It was shown that other antibodies such as anti-vimentin and anti-myosin were associated with long allograft survival in heart transplants. Some researchers reported that antibodies produced against vascular endothelial cells led to chronic rejection in heart and kidney transplantations. Therefore, endothelial precursor cells were isolated, and the antibody detection method was performed which was similar to FCXM [22, 53–55]. FCXM is important for clinical work due to its effect on graft and patient survival. If T/B FCXM is negative, it is generally considered that there is no DSA or DSA is at very low level. If T FCXM is negative and B FCXM is positive, then it is due to the presence of

strong class I antibody or class II antibody. If T FCXM is positive and B FCXM is negative; antibodies are most probably non-HLA antibodies.

In conclusion, transplantation can be performed if FCXM and CDCXM are negative. If CDCXM is positive and FCXM is negative, the patient cannot be transplanted due to the high risk of hyperacute rejection. Patient can be transplanted if FCXM result of a patient is positive without alloimmunizations and CDCXM is negative. Nevertheless, this patient should be considered as if he/she is at high risk for graft failure in case he/she has an alloimmunization.

Author details

Tülay Kılıçaslan Ayna* and Aslı Özkızılcık Koçyiğit

*Address all correspondence to: tulayayna@gmail.com

Faculty of Medicine, Medical Biology and Genetics Department, Izmir Tepecik Education and Research Hospital Tissue Typing Laboratory, Izmir Katip Çelebi University, Izmir, Turkey

References

[1] Kuby J. Transplantation Immunology. In: Kuby J editor. Immunology. 3rd ed. Freeman, Houston; 1997. pp. 481–499.

[2] Organ Donation and Transplantation Statistics [Internet] 2010. Available from www.kidney.org/news/newsroom/factsheets/Organ-Donation-and-Transplantation-Stats [Accessed: 22 December 2015].

[3] Journalist Workshop on Organ Donation and Transplantation [Internet] 2014. Available from http://ec.europa.eu/health/blood_tissues_organs/docs/ev_20141126_factsfigures_en.pdf [Accessed: 25 December 2015].

[4] Rood JJ van, Eernisse JG, Leeuwen A van. Leukocyte antibodies in sera pregnant women. Nature. 1958:181:1735–1736. doi: 10.1038/1811735a0

[5] Richet G. Hamburger's achievement with early renal transplants. Am J Nephrol. 1997:17:315–317.

[6] Murray JE, Merrill JP, Harrison JH. Renal homotransplantation in identical twins. 1955. J Am Soc Nephrol. 2001:12:201–204.

[7] Ayna TK, Soyöz M, Kurtulmuş Y, Doğan SM, Özyılmaz B, Tuğmen C, Pirim I. Comparison of complement-dependent cytotoxic and flow-cytometry crossmatch results before cadaveric kidney transplantation. Transplant Proc. 2013:45:878–880. doi: 10.1016/j.transproceed.2013.02.083.

[8] Terasaki PI,Cecka JM, Gjertson DW, Takemoto S. High survival rates of kidney transplants from spousal and living unrelated donors. N Engl J Med.1995:333:333–336. doi: 10.1056/NEJM199508103330601

[9] Peakman M, Vergani D. Basic and Clinical Immunology. 1st ed. Elsevier, UK; 1997.

[10] Geneugelijk K, Thus KA, Spierings E. Predicting alloreactivity in transplantation. J Immunol Res. 2014:2014:1–12. doi: 10.1155/2014/159479.

[11] Kurihara K, Kitada H, Miura Y, Terasaka S, Kaku K, Miyamoto K, Tsuchimoto A, Masutani K, Tanaka M. Impact of flow cytometry crossmatch B-cell positivity on living renal transplantation. Transplant Proc. 2013:45(8):2903–2906. doi: 10.1016/j.transproceed.2013.08.047.

[12] Abbas AK, Lichtman AH, Pober JS. Cellular and Molecular Immunology. 3rd ed. Saunders, Elsevier, Wallingford, UK; 1997.

[13] Abbas AK., Lichtman AH., Pober JS. Cellular and Molecular Immunology. 2nd ed. Saunders, Elsevier, Dunfermline, UK; 1994.

[14] Stites DP. Basic and Clinical Immunology. 8th ed. Mcgraw-Hill/Appleton & Lange, New York; 1994. pp. 237–255.

[15] Velez M, Johnson MR. Management of allosensitized cardiac transplant candidates. Transplant Rev (Orlando). 2009:23:235–247. doi: 10.1016/j.trre.2009.07.001.

[16] Hajeer AH. Panel reactive antibody test (PRA) in renal transplantation. Saudi J Kidney Dis Transplant. 2006:17:1–4.

[17] Gebel HM, Bray RA. HLA Antibody Detection with Solid Phase Assays: Great Expectations or Expectations Too Great? Am J Transpl. 2014:14:1964–1975. doi: 10.1111/ajt.12807.

[18] Dong II Won. Flow cytometry PRA using pooled lymphocytes for both HLA class I and II antibodies. Lab Med. 2011:42:17–24. doi: 10.1309/LM0MVD50JJGQUPVM

[19] Lobashevsky AL. Methodological aspects of anti-human leukocyte antigen antibody analysis in solid organ transplantation. World J Transplant. 2014:24:4(3):153–167. doi: 10.5500/wjt.v4.i3.153.

[20] Bray RA. Lymphocyte crossmatching by flow cytometry. Methods Mol Biol. 2013:1034:285–296. doi: 10.1007/978-1-62703-493-7_14.

[21] Delgado JC, Eckels DD. Positive B cell only flow cytometric crossmatch. Implications for renal transplantation. Exp Molecular Pathol. 2008:85:59–63.doi: 10.1016/j.yexmp.2008.03.009

[22] Angaswamy N, Tiriveedhi V, Sarma NJ, Subramanian V, Klein C, Wellen J, Shenoy S, Chapman WC, Mohanakumar T. Interplay between immune responses to HLA and

Non-HLA self-antigens in allograft rejection. Hum Immunol. 2013:74:1478–1485. doi: 10.1016/j.humimm.2013.07.002.

[23] Trivedi HL. Immunobiology of rejection and adaptation. Transplant Proc. 2007:39(3): 647–652.

[24] Carey JL, McCoy JP, Keren DF. Flow cytometry in Clinical Diagnosis. 4th ed. American Society for Clinical Pathology, Chicago, IL; 2007.

[25] Palomar R, López-Hoyos M, Pastor JM, Fernández-Fresnedo G, Rodrigo E, Ruiz JC, Cotorruelo JG, Valero R, Castañeda O, San Segundo D, Arias M. Impact of HLA antibodies on transplant glomerulopathy. Transplant Proc. 2005:37:3830–3832.

[26] Zhang Q1, Liang LW, Gjertson DW, Lassman C, Wilkinson AH, Kendrick E, Pham PT, Danovitch GM, Gritsch HA, Reed EF. Development of posttransplantantidonor HLA antibodies is associated with acute humoral rejection and early graft dysfunction. Transplantation. 2005:79:591–598.

[27] Müller-Steinhardt M, Fricke L, Kirchner H, Hoyer J, Klüter H. Monitoring of anti-HLA class I and II antibodies by flow cytometry in patients after first cadaveric kidney transplantation. Clin Transplant. 2000:14:85–89.

[28] Scornik JC, Brunson ME, Schaub B, Howard RJ, Pfaff WW. The crossmatch in renal transplantation. Transplantation. 1994:57:621–625.

[29] Bray RA, Gebel HM. Strategies for human leukocyte antigen antibody detection. Curr Opin Organ Transplant. 2009:14:392–397.

[30] Amico P, Hönger G, Steiger J, Schaub S. Utility of the virtual crossmatch in solid organ transplantation. Curr Opin Organ Transplant. 2009:14:656–661. doi: 10.1097/MOT. 0b013e328331c169.

[31] Pei R, Lee JH, Shih NJ, Chen M, Terasaki PI. Single human leukocyte antigen flow cytometry beads for accurate identification of human leukocyte antigen antibody specificities. Transplantation. 2003:75:43–49.

[32] Scornik JC. Detection of alloantibodies by flow cytometry: relevance to clinical transplantation Cytometry (Communications İn Clinical Cytometry) 1995:22:259–263.

[33] Ayna TK, Ciftci HS, Isitmangil G, Gurtekin M, Carin M. Flow cytometric crossmatching and panel-reactive antibodies in chronic renal failure patients. Transplant Proc. 2011:43(3):805–808. doi: 10.1016/j.transproceed.2010.11.021

[34] Cicciarelli J, Helstab K, Mendez R. Flow cytometry PRA, a new test that is highly correlated with graft survival. Clin Transplant. 1992:6(3 part 1):159–64.

[35] Kuby J. Major histocompatibility complex. In: Kuby J, editor. Immunology. 3rd ed. Freeman, Houston; 1997. pp. 224–246.

[36] Tinckam KJ, Chandraker A. Mechanisms and role of HLA and non-HLA alloantibodies. Clin J Am Soc Nephrol. 2006:1:404–414.

[37] Martin S, Dyer PA, Mallick NP, Gokal R, Harris R, Johnson RW. Posttransplantantidonorlymphocytotoxic antibody production in relation to graft outcome. Transplantation. 1987:44:50–53.

[38] Abbas AK, Lichtman AH, Pober JS. Cellular and Molecular Immunology.4th ed. Elsevier, USA; 2000. pp. 363–383.

[39] Piazza A, Poggi E, Borrelli L, Servetti S, Monaco P, Buonomo O, Valeri M, Torlone N, Adorno D, Casciani C. Impact of donor specific antibodies on chronic rejection occurrence and graft loss in renal transplantation: post-transplant analysis using flow cytometric techniques. Transplantation. 2001:71: 1106–1112.

[40] Haririan A, Nogueira J, Kukuruga D, Schweitzer E, Hess J, Gurk-Turner C, Jacobs S, Drachenberg C, Bartlett S, Cooper M. Positive cross-match living donor kidney transplantation: longer-term outcomes. Am J Transplant. 2009:9(3):536–542. doi: 10.1111/j.1600-6143.2008.02524.x.

[41] Rogers NJ, Lechler RI: Allorecognition. Am J Transplant. 2001:2:87-101.

[42] Gebel HM, Bray RA, Ruth JA, Zibari GB, McDonald JC, Kahan BD, Kerman RH. Flow PRA to detect clinically relevant HLA antibodies. Transplant Proc. 2001:33(1–2):477.

[43] Bray RA. Flow cytometry cross matching for solid organ transplantation. Methods Cell Biol. 1994:41:103–119.

[44] Thammanichanond D, Ingsathit A, Mongkolsuk T, Rattanasiri S, Kantachuvesiri S, Sakhonrat C, Leenanupan C, Worawichawongs S, Kitpoka P. Pre-transplant donor specific antibody and its clinical significance in kidney transplantation. Asian Pac J Allergy Immunol. 2012:30(1):48–54.

[45] Bryan CF, Baier KA, Nelson PW, Luger AM, Martinez J, Pierce GE, Ross G, Shield CF 3rd, Warady BA, Aeder MI, Helling TS, Muruve N. Long term graft survival is improved in cadaveric renal retransplantation by flow cytometric crossmatching. Transplantation. 1998:66:1827–1832.

[46] Ogura K, Terasaki PI, Johnson C, Mendez R, Rosenthal JT, Ettenger R, Martin DC, Dainko E, Cohen L, Mackett T, et al. The significance of a positive flow cytometry cross match test in primary kidney transplantation. Transplantation. 1992:56:294 – 298.

[47] Sağıroğlu T, Tozkır H, Kılıçarslan-Ayna T, Yağcı MA, Sezer A, Carin M. Is flow cytometry crossmatch analysis using sera with different dilutions important for pretransplant analysis? A case report. Transplant Proc. 2012:44(6):1767–1769. doi: 10.1016/j.transproceed.2012.04.019

[48] Filippone EJ, Farber JL. Humoral immune response and allograft function in kidney transplantation. Am J Kidney Dis. 2015:66(2):337–347. doi: 10.1053/j.ajkd.2015.03.033.

[49] Zachary AA, Ratner LE, Leffell MS. Low levels of HLA specific antibody; relevance, detection and treatment. Transplant Proc. 2001:33: 469–470. doi: 10.1016/S0041-1345(00)02096-0

[50] Scornik JC, Bray RA, Pollack MS, Cook DJ, Marrari M, Duquensoy R, Langley JW: Multicenter evaluation of the flow cytometry T-cell crossmatch. Transplantation. 1997:63:1440–1445.

[51] Patel R, Terasaki PI. Significant of the positive cross match test in kidney transplantation. N Engl J Med. 1969:280–735. doi: 10.1056/NEJM196904032801401.

[52] Kotb M, Russuel W, Ohman M, Hathaway D and Gaber AO. Clinical implications of flow cytometry B crossmatching in renal transplantation. Transplant Proc. 1997:29:1430–1432.

[53] Ball B, Mousson C, Ratignier C, Guignier F, Glotz D, Rifle G. Antibodies to vascular endothelial cells in chronic rejection of renal allografts. Transplant Proc. 2000:32:353–354.

[54] Ferry BL, Welsh KI, Dunn MJ, Law D, Proctor J, Chapel H, Yacoub MH, Rose ML. Anti-cell surface endothelial antibodies in sera from cardiac and kidney transplant recipients: association with chronic rejection. Transpl Immunol. 1997:5:17–24.

[55] Holgersson J, Elsheikh E, Grufman P, Sumitran-Holgersson S, Tydén G. A case of acute vascular rejection caused by endothelial-reactive non-HLA antibodies. Clin Transpl. 2006:535–538.

Edited by Ingrid Schmid

Flow cytometry - Select Topics is a collection of chapters that illustrate the constantly evolving application of flow cytometry to diverse areas of research or clinical investigations. It includes chapters on the utilization of flow cytometry in the fields of human reproduction and fertility, platelet function, apoptosis, inflammation research, leukemia immunophenotyping, and transplantation.

ISBN 978-953-51-5445-7

Photo by fotojog / iStock

IntechOpen